ISSN 0515-9628

ՀԱՅԱՍՏԱՆԻ ՔԻՄԻԱԿԱՆ ՀԱՆԴԵՍ

Химический журнал Армении

Chemical Journal of Armenia

“Химический журнал Армении” реферируется в “Chemical Abstracts” (США) и РЖХим (Россия).

http://chemjournal.sci.am

www.flib.sci.am

АЙАСТАНИ КИМИАКАН АНДЕС

“Химический журнал Армении” является органом Национальной Академии наук Армении. В нем публикуются результаты теоретических и экспериментальных исследований, проводимых в научно-исследовательских институтах, вузах и лабораториях промышленных предприятий Армении и других республик в области общей, физической, неорганической, аналитической, органической и биоорганической химии, химической физики и химической технологии.

Выходит 4 раза в год.

Редакционная коллегия журнала просит направлять статьи по адресу: Республика Армения, 0019, Ереван, пр. Маршала Баграмяна, 24г, тел: 56-08-31.

Address: Chemical Journal of Armenia
24g, Marshal Baghramyan Ave., 0019, Yerevan, Republic of Armenia
Phone: (374 10) 56-08-31
E-mail: chemjournal@sci.am
Website: www.flib.sci.am

Компьютерная верстка Анаит Акопян

E-mail: anulyamour@rambler.ru

Адрес редакции
0019, Ереван, пр. Маршала Баграмяна, 24—г, II этаж, 2 к., тел. 56-08-31

Сдано в набор 20.10.2018. Подписано к печати 20.11.2018.
Бумага фирменная. Набор компьютерный.
Печ. листов 12,5. Тираж 150. Заказ №76.
Издательство Национальной Академии наук Республики Армения
0019, Ереван, пр. Маршала Баграмяна, 24—г.
Цена договорная.

GRAFICAL ABSTRACTS

Six-coordinate complexes of nitrosyl iron-porphyrins with trans-DMSO ligand

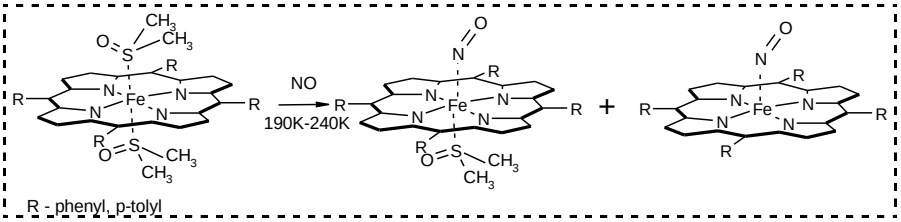

A. A. Hovhannisyan
A.V. Iretskii
T. S. Kurtikyan

Хим. ж. Армении, 2018, т. 71, №4, с. 464

DTA/TG study of NiO reduction by Mg+C combined reducer

M.K. Zakaryan
O.M. Niazyan
S.V. Aydinyan
S.L. Kharatyan

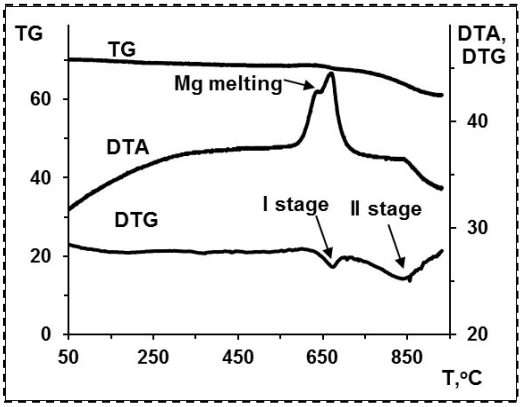

Хим. ж. Армении, 2018, т. 71, №4, с. 473

Photocatalyic oxidation of chlorinated phenylalkanes with dioxygen

L.A. Manucharova
R.A. Bakhtchadjian
L.A. Tavadyan

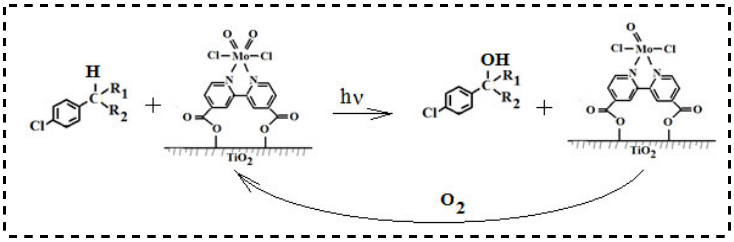

R_1=H, R_2=CH_3 for CEB; R_1=H, R_2=ClC_6H_4 for DDM; R_1=CCl_3 R_2= ClC_6H_4 for DDT

Хим. ж. Армении, 2018, т. 71, №4, с. 486

Hydrides of transition metals and their alloys as condensed hydrogen carriers

S. K. Dolukhanyan
A. G. Aleksanyan
G. N. Muradyan
V. Sh. Shekhtman
O. P. Ter-Galstyan
H. G. Hakobyan
N. N. Aghajanyan
N. L. Mnatsakanyan

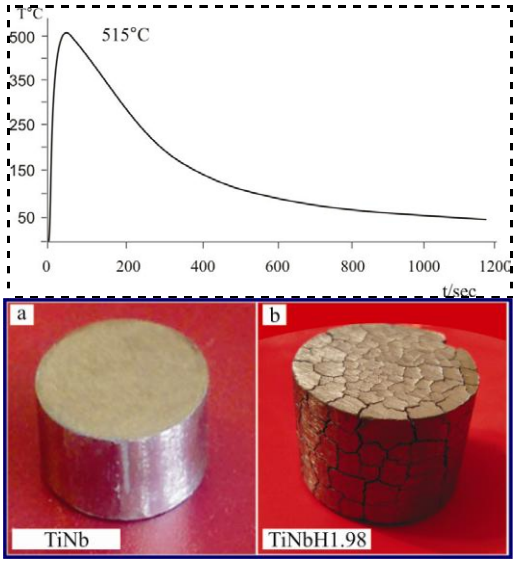

Хим. ж. Армении, 2018, т. 71, №4, с. 495

Barium silicates formation using silica hydrogel produced from serpentine minerals

A. M. Terzyan
S. A. Melikyan
H. A. Beglaryan
A. R. Isahakyan
N. H. Zulumyan

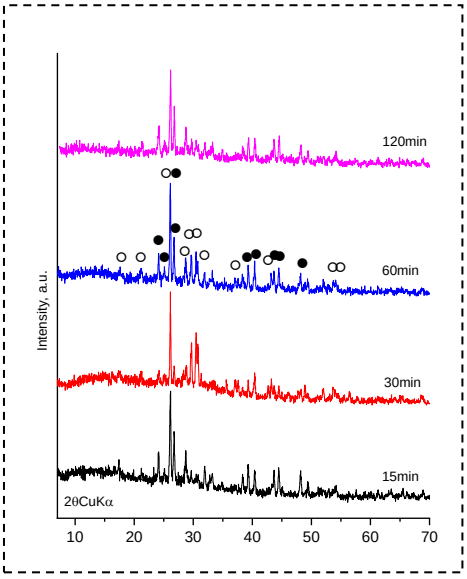

Хим. ж. Армении, 2018, т. 71, №4, с. 517

Advantages of the method of frontal polymerization in high technologies

A. O. Tonoyan
S. P. Davtyan

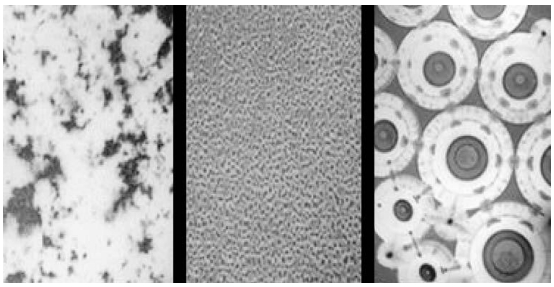

Хим. ж. Армении, 2018, т. 71, №4, с. 524

Synthesis and biological activity of new derivatives of pyrano[3-4-c][1,2,4]triazolo[4,3-a]pyridines

E. G. Paronikyan
Sh. Sh. Dashyan
N. S. Minasyan
A. G. Akopyan
H. M. Stepanyan

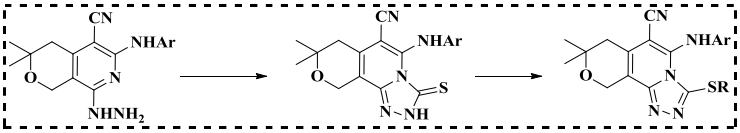

Хим. ж. Армении, 2018, т. 71, №4, с. 533

Synthesis of new achiral bis-alkylated analogs of glycine

Z. Z. Mardiyan
A. F. Mkrtchyan
A. S. Saghyan

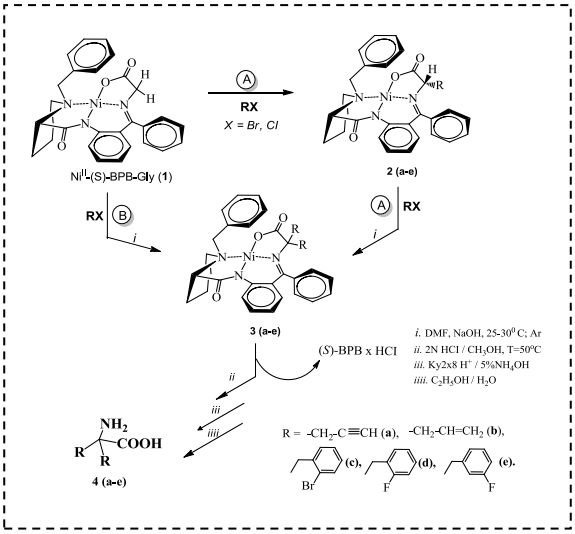

Хим. ж. Армении, 2018, т. 71, №4, с. 541

Evaluation of the dehydrating properties of some sililating agents in the synthesis of imidazole-5-one

V. O. Topuzyan
V. M. Ghazoyan
G. Sh. Hovhannisyan
A. A. Hovhannisyan

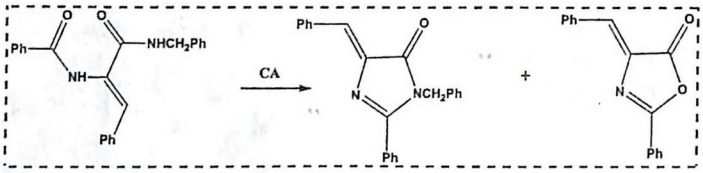

Хим. ж. Армении, 2018, т. 71, №4, с. 551

Synthesis of furfuryl derivatives of 4-allyl-1-(4-hydroxy-3-nitrobenzyl)-3-[2-(4-alkoxyphenyl)quinolin-4-yl]-4,5-dihydro-1H-1,2,4-triazol-5-thions and their cytotoxic action on human cancer cells

M. A. Iradyan
N. S. Iradyan
A. A. Hambardzumyan
H. A. Panosyan
C. Roussakis
V. A. Sakanyan

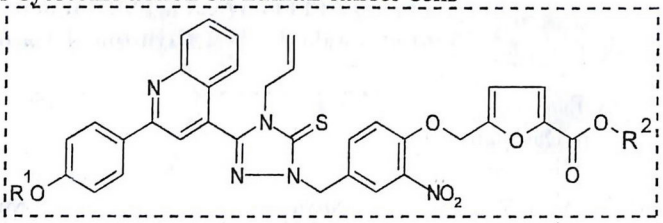

R^1= Alkyl, R^2= H, Ch_3

Хим. ж. Армении, 2018, т. 71, №4, с. 559

Targeted synthesis of 9-fluorenylmethyloxycarbonylglycyl-(s)-β-[4-allyl-3-propyl-5-thioxo-1,2,4-triazol-1-yl]-α-alanine and study of its effect on collagenase activity

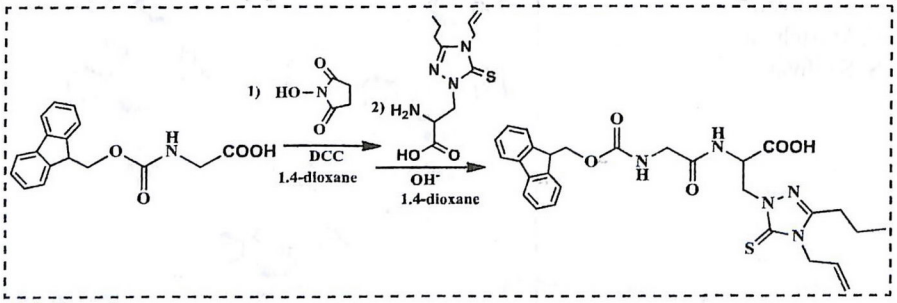

Yu. M. Danghyan
T. H. Sargsyan
S. M. Jamgaryan
A. S. Sargsyan
E. A. Gyulumyan
N. A. Hovhannisyan
A. M. Hovhannisyan
A. H. Tsaturyan
H. A. Panosyan
A. S. Saghyan

Хим. ж. Армении, 2018, т. 71, №4, с. 571

Syntheses and biological properties of benzo[4',5']imidazo[2',1': 6,1]pyrido[2,3-d]pyrimidines: mini-review

A. A. Harutyunyan

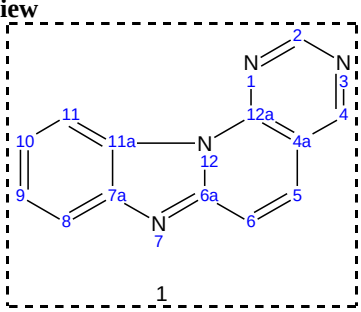

1

Хим. ж. Армении, 2018, т. 71, №4, с. 579

The peculiarities of interaction of some β,γ-unsaturated phosphonium salts with molecular bromine and dehydrobromination of resulted dibromoderivative compounds

M. Zh. Ovakimyan
G. Ts. Gasparyan
A. S. Bichakhchyan
A. S. Pogosyan
L. V. Derdzyan

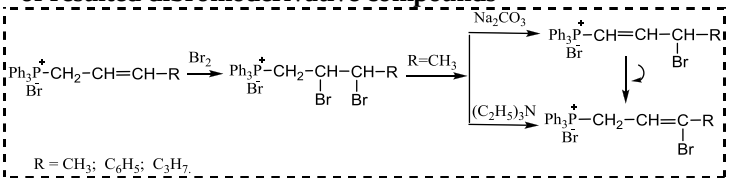

Хим. ж. Армении, 2018, т. 71, №4, с. 589

Synthesis and antitumor properties of 3-(2,2-dimethyltetrahydro-2H-pyran-4-yl)spiro[benzo[h]quinazoline-5,1'-cycloheptan]-4(6H)-ones

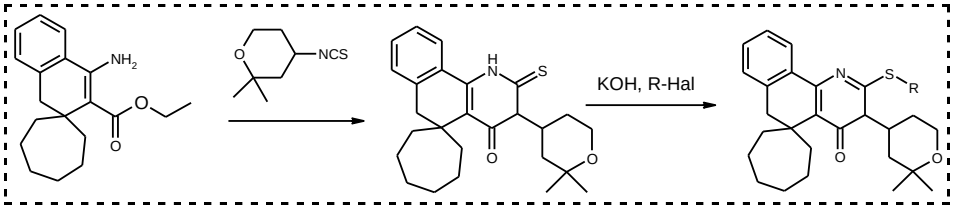

A. I. Markosyan
Kh. S. Hakopyan
A. S. Ayvazyan
S. S. Mamyan
A. G. Ayvazyan
R. A. Tamazyan
F. H. Arsenyan
J. A. Avakimyan

Хим. ж. Армении, 2018, т. 71, №4, с. 596

On the interaction of propagyl malonate with nucleophiles in the presence of mercury (II) acetate

N. G. Hobosyan
K. V. Balyan
H. S. Nersisyan
L. M. Ghalechyan
S. A. Hovakimyan
H. B. Sargsyan
Zh. A. Chobanyan

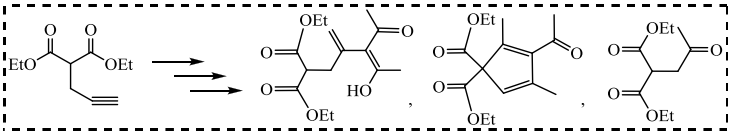

Хим. ж. Армении, 2018, т. 71, №4, с. 609

Synthesis of new amino derivatives of 9-(methylthio)thieno[3,2-d]pyrimidine and azide-tetrazole equilibrium

E. K. Hakobyan

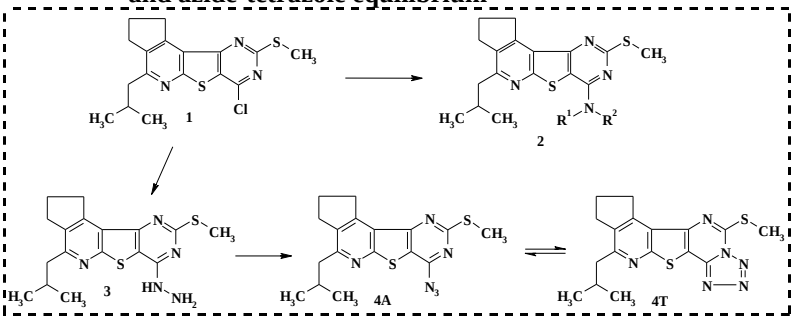

Хим. ж. Армении, 2018, т. 71, №4, с. 614

Round-leaved wintegreen (Pyrola Rotundifolia) as a valuable medicinal plant raw material

S. A. Dadayan
L. A. Stepanyan
A. S. Dadayan
M. B. Gasoyan
H. R. Petrosyan
A. S. Poghosyan
A. O. Tsaturyan

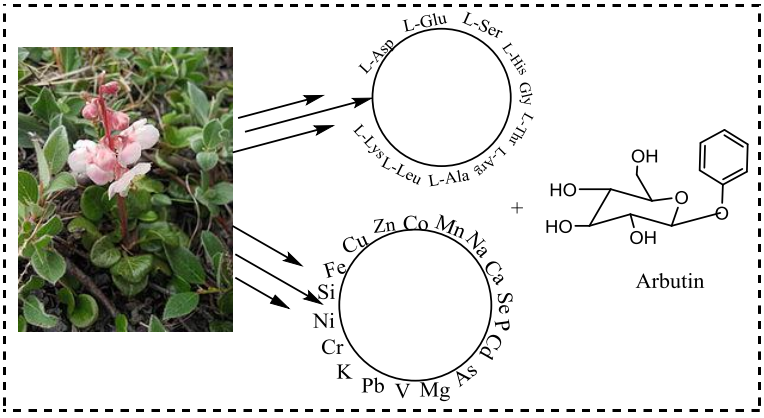

Хим. ж. Армении, 2018, т. 71, №4, с. 625

New three-dimensional heterocyclic cluster. Bis-benzo[4′,5′]imidazo[2′,1′: 6,1]pyrido[2,3-d]pyrimidines, symmetrically linked by a triarylmethane linker

A. A. Harutyunyan
H. A. Panosyan
G. T. Ghukasyan
G. G. Danagulyan

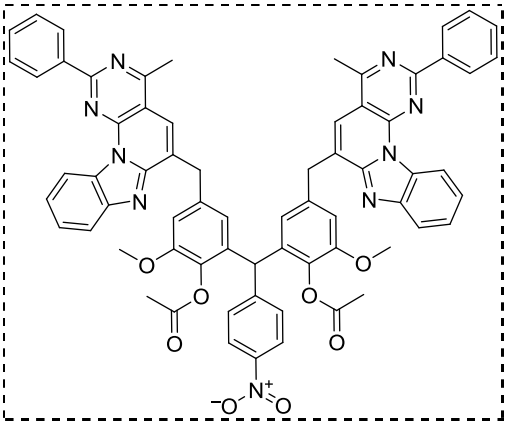

Хим. ж. Армении, 2018, т. 71, №4, с. 634

ՀԱՅԱՍՏԱՆԻ ՀԱՆՐԱՊԵՏՈՒԹՅԱՆ ԳԻՏՈՒԹՅՈՒՆՆԵՐԻ
ԱԶԳԱՅԻՆ ԱԿԱԴԵՄԻԱ

НАЦИОНАЛЬНАЯ АКАДЕМИЯ НАУК РЕСПУБЛИКИ АРМЕНИЯ
NATIONAL ACADEMY OF SCIENCES OF THE REPUBLIC OF ARMENIA

Հայաստանի քիմիական հանդես
Химический журнал Армении **71, №4, 2018** Chemical Journal of Armenia

UDC 947.973.733.543.22

SIX-COORDINATE COMPLEXES OF NITROSYL IRON-PORPHYRINS WITH *TRANS* DMSO LIGAND

A. A. HOVHANNISYAN[a], A.V. IRETSKII[b] and T. S. KURTIKYAN[a]

[a]Molecule Structure Research Centre (MSRC) of the Scientific Technological Centre of Organic and Pharmaceutical Chemistry NAS RA
26, Azatutyan Str., Yerevan 0014, Armenia
Fax: (+37410) 282267 E-mail: ahovhan@gmail.com
[b]Department of Chemistry, Lake Superior State University
Sault Sainte Marie, MI 49783 USA

By consecutive low-temperature reaction of DMSO and NO with sublimed microporous layers of Fe(Por) (Por - meso-tetraphenyl- and meso-tetra-p-tolyl-porphyrinato dianions) the mixed-ligand Fe(Por)(DMSO)(NO) complexes were partly obtained as was demonstrated by FTIR spectroscopy with supporting data provided by using ^{15}NO and DMSO-d_6 isotopomers. Formation of the Fe(Por)(DMSO)(NO) by the interaction of DMSO with Fe(Por)(NO) in low-temperature dichloromethane solution is almost quantitative. From the temperature dependence of the equilibrium constants thermodynamic parameters of complexation reaction were determined. FTIR data indicate coordination of DMSO through a sulfur atom, while DFT calculations performed with porphine at room temperature give some lower energy value for the O-bound species.

Figs. 5, tables 2, references 11.

The enormous physiological role of nitrogen oxide (NO) in many cases is connected to its interaction with *heme* proteins [1] including those with the *trans* methionine ligand. In the conditions of oxidative stress the oxidation of methionine to corresponding sulfoxide is possible. Therefore, it was of a great interest to examine whether the 6-coordinate nitrosyl complexes of Fe-porphyrins with *trans* dimethylsulfoxide ligand can exist and, if so, with which atom, sulfur or oxygen, it will be coordinated in these species [2]. In the complexes with transition metals both types of complexes are known. Moreover, in the same complex with two or more sulfoxides one of them may be bound through the sulfur atom while the other one through the oxygen atom [2, 3].

Sulfoxide group contains sigma S- and O-donor atoms as well as π-electrons that also can potentially enter into donor-acceptor interaction with transition metal.

While 6-coordinate Fe(II) porphyrin nitrosyl complexes with axial N-donors have been extensively studied as a model for an axial histidine ligation of hemoglobin and myoglobin [1], much less attention has been focused on the effect of axial S- and O-donor ligands. Ferrous NO adduct of myoglobin H93G cavity mutant ligated by thioether (THT) has been prepared by Dawson et al. [4], and studied by UV-vis and magnetic CD spectroscopy. The interaction of nitrosyl(protoporphyrin IX dimethyl esther)iron(II) with various sulfur and oxygen donor ligands was studied at low temperatures by Yoshimura using EPR spectroscopy [5]. The same technique was used recently by Lehnert et al. in examination of thiophenolates and thioether coordination to Fe(tetraphenylporphyrin)NO center [6]. The interaction of nitrosyl(*meso*-tetraphenyl)- and nitrosyl(*meso*-tetra-*p*-tolyl)-porphyrinato iron(II) with various sulfur and oxygen donor ligands was studied by Martirosyan et al. using low-temperature FTIR and optical absorption spectroscopy [7].

Experimental Section

The iron(II) porphyrinates Fe(Por) (Por – *meso*-tetraphenyl- and *meso*-tetra-*p*-tolyl- porphyrinato (TPP and TTP correspondingly) dianions) are very sensitive to oxygen and are readily oxidized. For this reason the more stable hexa-coordinate complexes $Fe(Por)(B)_2$ with nitrogen bases (B is Py or piperidine) were used as the precursors to prepare sublimed layers. The complexes $Fe(Por)(B)_2$ were synthesized according to published method [8].

Then, as done previously [7], the parent complexes were introduced into the Knudsen cell of the high vacuum system and heated at 490 K for ~2 *h* until the vacuum gauge indicated complete dissociation of the axial ligand. The resulting Fe(Por) was sublimed from the Knudsen cell at ~520 *K* and deposited on a KBr of the optical cryostat. NO (^{15}NO) was purified by passing it through KOH pellets and a cold trap (dry ice/acetone) to remove the higher nitrogen oxides and trace quantities of water. The purity was checked by IR measurements of the layer obtained by slow deposition of NO onto the cold substrate of the optical cryostat (77 *K*). The IR spectrum did not show the presence of N_2O, N_2O_3 or H_2O. ^{15}NO with 98.5% enrichment was purchased from the Institute of Isotopes, Republic of Georgia, and was purified by the same procedure. Sublimed layers of Fe(Por) were obtained on the cold (77 K) KBr support of an optical cryostat according to the published procedure [7]. Then the layer was warmed till 200 *K* under dynamic vacuum, DMSO was introduced into the cryostat and the layer was slowly warmed to the room temperature. FTIR spectra demonstrated the complete shifts of some of the porphyrin bands.

The interaction of DMSO with Fe(Por)(NO) in dichloromethane solution was carried out in the optical cryostat provided with the 0.05 *cm* CaF_2 cell. A measured quantity of Fe(Por)(NO) was fed into the airtight flask provided with septum. Known quantities of previously degassed solutions of DMSO in dichloromethane were transferred into this flask by vacuum techniques. The solutions thus prepared

were transferred to an IR cell using an airtight Hamilton syringe. The cell was then tightly closed and placed into the cryostat. The cell was then cooled using liquid nitrogen vapors and the FTIR spectra were taken at temperatures controlled by a thermocouple that was in close contact with the cell. By changing the flow rate of the liquid nitrogen it was possible to maintain the temperature of solution at a given temperature (±1 ^{o}C).

The FTIR spectra were acquired on a Nexus (Thermo Nicolet Corporation) in the spectral range of 400-4000 cm^{-1} with a resolution of 4 cm^{-1}. All density functional theory (DFT) calculations were performed at unrestricted TPSSTPSS/DGDZVP level of theory without symmetry constraints using Gaussian 09 package.

Results and discussion

In sublimed layers two types of experiments were carried out with the goal to obtain the mixed nitrosyl complex with *trans* sulfoxide ligand. In the first type of experiments the sulfoxide vapors were introduced into the cryostat containing the nitrosyl complexes of Fe(Por)(NO) that were obtained by interaction of NO gas with microporous layers of Fe(Por). Cooling of the layer does not lead to appearance of a new υ(NO) band that could be indicator of mixed complex formation. At low-temperatures when such a complex could be stable the mobility of DMSO in the layer is too low to provide the penetration of sulfoxide in the bulk of the layer.

In the second type of experiments the layers of iron-porphyrins were initially introduced under the vapors of DMSO. According to the changes in the FTIR spectra this procedure leads to the formation of iron-porphyrins 5- and 6-coordinate complexes Fe(Por)$(DMSO)_{1,2}$, in which 5-coordinate species are in the high-spin, while 6-coordinate complexes are in the low-spin state. In Fig. 1 the FTIR spectrum of Fe(TPP) is demonstrated before and after interaction with the very small quantities of DMSO vapors. This procedure leads to the appearance of new bands that are certainly associated with the presence of coordinated DMSO ligand. DMSO is ambidentate ligand and can be coordinated with the metal both through the oxygen and sulfur atom. IR spectroscopy is a powerful tool for distinguishing these two possibilities. Coordination through the oxygen atom leads to decreased frequency and coordination through the sulfur to the increased frequency of the sulfoxide bond relative to υ(S=O) of free ligand. As it is seen in Fig. 1 the new band at 1109 cm^{-1} appeared that is shifted to higher frequency in regard to the band of free ligand at ~1060 cm^{-1}.

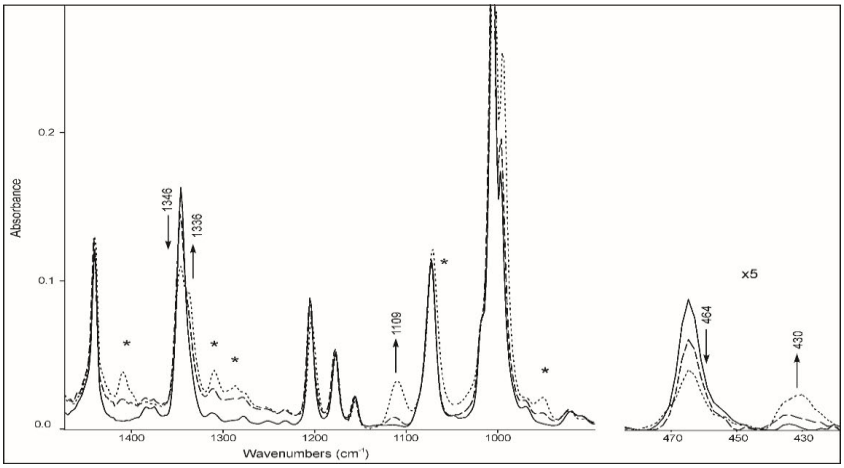

Fig. 1. FTIR spectral changes upon interaction of DMSO vapors (0,1 *torr*) with sublimed layers of Fe(TPP) (solid line) in temperature range 230-270 *K*.

The porphyrin vibrations provide additional insight into the electronic structure of the new complexes [9]. A band in the vicinity of 1350 cm^{-1} representing the porphyrin core mode corresponding to $\upsilon(C_a\text{-}C_m)$ mixed with some $\upsilon(C_m\text{-phenyl})$ lies at higher frequencies for low-spin complexes. Similarly, a low-energy porphyrin core deformation mode occurs in the range of 450 cm^{-1}. For the low-spin iron-porphyrin complexes it is located in the 460 cm^{-1} range while for high-spin species it shifts to 430 cm^{-1}. From Fig. 2 it is seen that the band at 1346 cm^{-1} that is characteristic for the intermediate state after interaction with more quantities of DMSO splits into 2 bands at 1350 and 1336 cm^{-1} (solid line). First one is observed in the range characteristic for the low-spin complexes and belongs to $Fe(TTP)(DMSO)_2$, while the second one at 1336 cm^{-1} is characteristic for the high-spin complex that should be the 5-coordinate Fe(TTP)(DMSO) complex.

Evacuation of the cryostat supports these assignments (Fig. 2, dashed and dotted spectra). Together with diminishing of the bands of coordinated and free DMSO, in the range of spin- sensitive bands the band at 1350 cm^{-1} loses intensity and undergoes some low-frequency shift while band at 1336 cm^{-1} grows in intensity. This is the evidence of $Fe(TTP)(DMSO)_2$ decomposition to Fe(TTP)(DMSO) and Fe(TTP).

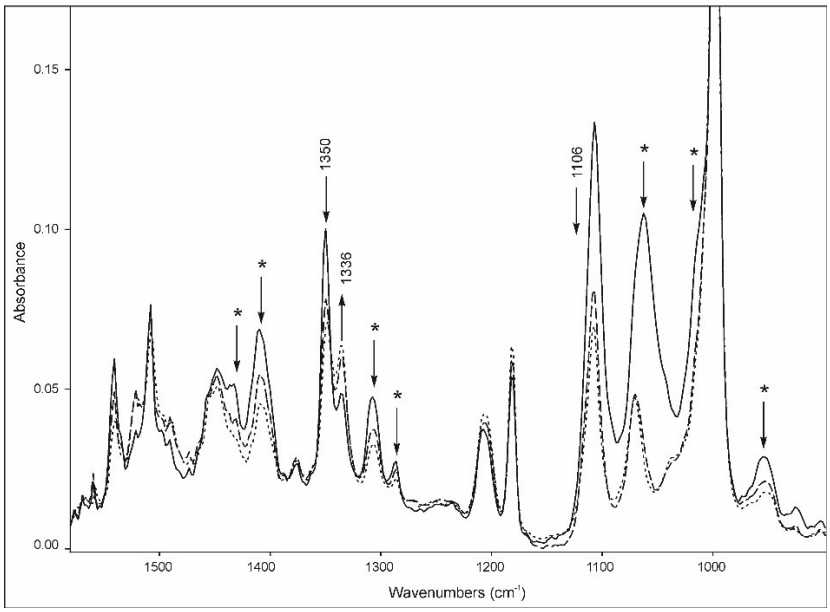

Fig. 2. FTIR spectral changes upon high-vacuum evacuation of DMSO for the layer containing mostly Fe(TTP)(S-DMSO)$_2$ (solid line) during 10 (dashed line) and 30 (dotted line) min.

Scheme 1

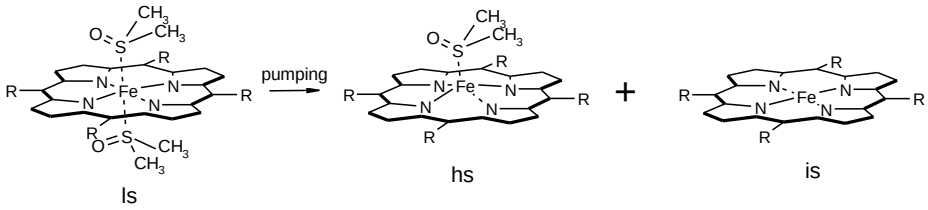

Addition of NO into the cryostat at 200 *K* leads to appearance of two new bands in the range of nitrosyl stretching frequencies (Fig. 3) that are summarized in Table 1 together with data for ^{15}NO species. The values of isotopic shifts certainly indicate that they belong to nitrosyl stretching υ(NO) of coordinated NO in iron-porphyrin complexes. Band at 1674 cm^{-1} belongs to 5-coordinate nitrosyl complex Fe(Por)(NO) while the band at 1637 cm^{-1} should be assigned to coordinated NO-group in 6-coordinate species with *trans* sulfoxide ligand, as is demonstrated in Scheme 2.

Table 1

υ(NO) (υ(^{15}NO)) in 5-coordinate nitrosyl complexes of Fe(Por) and 6-coordinate nitrosyl complex with *trans* dimethylsulfoxide ligand.

Complex	υ(NO)	υ(^{15}NO)
Fe(TPP)(NO)	1674	1645
Fe(TTP)(NO)	1676	1646
Fe(TPP)(NO)(DMSO)	1636	1607
Fe(TTP)(NO)(DMSO)	1637	1608

Table 2

DFT computations for iron-porphine dimethylsulfoxide-nitrosyl complexes coordinated through the S and O atoms in different spin-states

Complex	TPSSTPSS		B3LYP		3D model
	E, au	ΔE, kcal/mol	E, au	ΔE,kcal/mol	
Fe(P)(NO)(S-DMSO)_doublet Fe(P)(NO)(S-DMSO)_quartet Fe(P)(NO)(S-DMSO)_sextet	-2935,46974 -2935,43299	2 25	-2935,19158	3	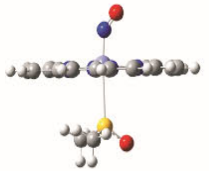
Fe(P)(NO)(O-DMSO)_doublet Fe(P)(NO)(O-DMSO)_quartet Fe(P)(NO)(O-DMSO)_sextet	-2935,47252 -2935,43264	0 25	-2935,19646	0	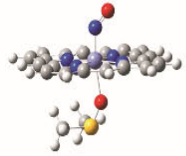

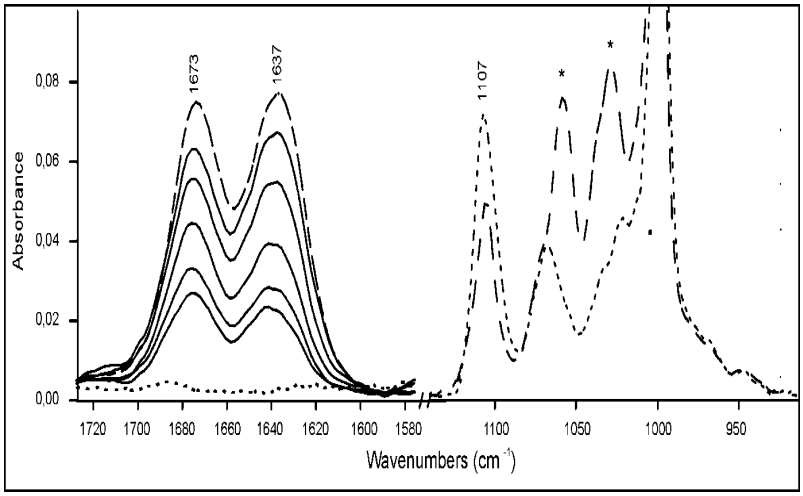

Fig. 3. FTIR spectral changes observed upon interaction of 3 torr NO with layer containing $Fe(TTP)(DMSO\text{-}d_6)_2$ in the temperature range 200-210 K.

Scheme 2

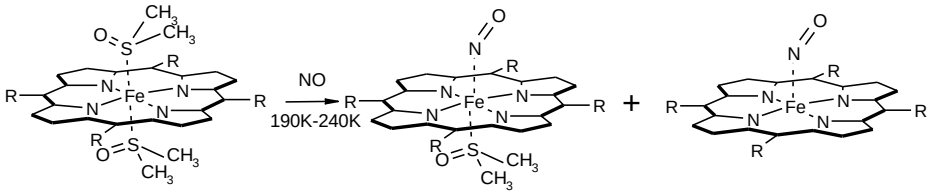

R - phenyl, p-tolyl

Hence NO can substitute DMSO ligand from $Fe(Por)(DMSO)_2$ to form Fe(Por)(NO)(DMSO) and Fe(Por)(NO). The attempt to obtain only 6-coordinate mixed ligand complex in the solid state was not successful. However, this complex almost quantitatively was possible to obtain in the solution upon decreasing its temperature (Fig. 4). In these experiments DMSO ligand was added to solution of Fe(Por)(NO) in dichloromethane and the temperature of solution was gradually decreased. This led to spectral changes represented in Fig. 4. At these conditions 5-coordinate complex Fe(Por)(NO) almost completely was transferred to the 6-coordinate mixed ligand complex Fe(Por)(NO)(DMSO). From these data the thermodynamic parameters and equilibrium constant of the reaction

$$Fe(Por)(NO) + DMSO \leftrightarrow Fe(Por)(NO)(DMSO)$$

were estimated, that in the case of Fe(TTP) are equal to $\Delta H = -11.3 \pm 0.2$ $kJ \cdot mole^{-1}$, $\Delta S = -66 \pm 2$ $J \cdot mole^{-1} \cdot K^{-1}$, $\Delta G = +8.6 \pm 0.2$ $kJ \cdot mole^{-1}$ and $K_{298} = 3 \cdot 10^{-2}$.

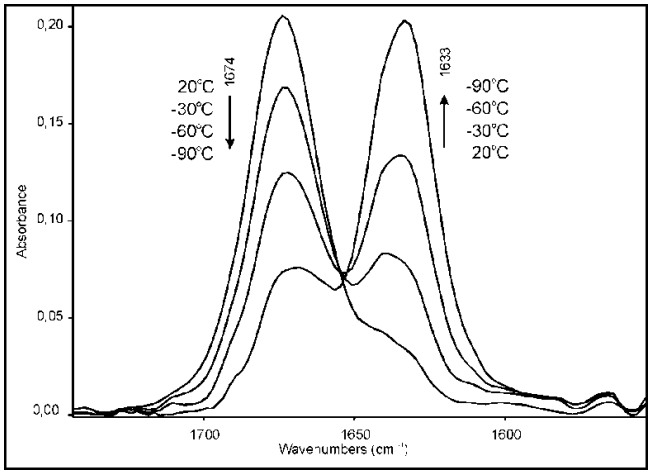

Fig. 4. Temperature dependence of the FTIR spectra in the υ(NO) range of the Fe(TTP)(NO) dissolved in the DMSO/CH_2Cl_2 solution.

DMSO is ambidentate ligand. In the 5- and 6-coordinate sulfoxide complexes of iron-porphyrins, as it was shown above, it is coordinated through the sulfur atom. The same is taking place in the mixed ligand Fe(Por)(NO)(DMSO) complexes. Since the rocking vibration of methyl group ρ(CH_3) [2] in DMSO is disposed in the range of 950 cm^{-1}, in which the υ(S=O) of O-coordinated sulfoxide is expected to occur, in order to be sure that there is no new band in this spectral range the experiments were performed also with DMSO-d_6. Rocking vibration of CD_3 groups is observed at much lower frequency and this spectral range is empty.

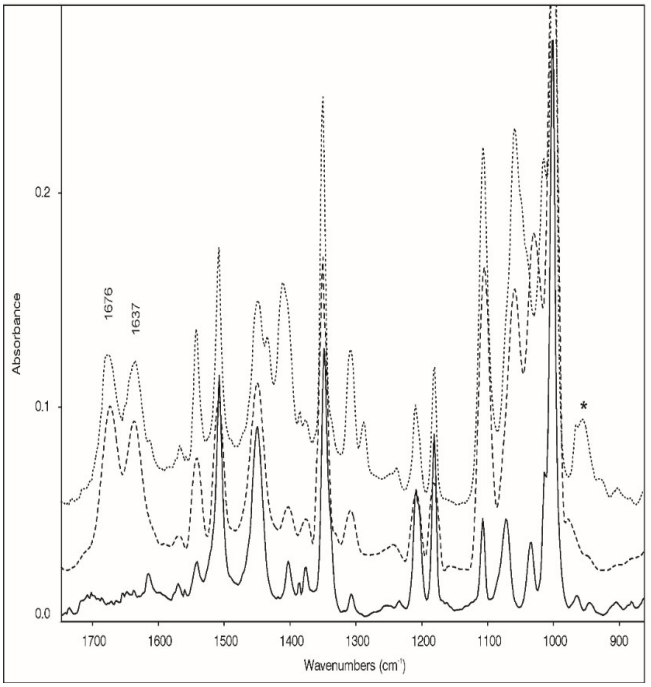

Fig. 5. FTIR spectra of the sublimed layer of Fe(TTP) (solid line), Fe(TTP)(DMSO-d_6)(NO) + Fe(TTP)(NO) (dashed line) and Fe(TTP)(DMSO)(NO) + Fe(TTP)(NO) (dotted line) at 205 K.

The absence of a new band in this spectral range upon formation of the mixed ligand Fe(Por)(NO)(DMSO) complexes (Fig. 5, dashed line) is an evidence that in this complex also sulfoxide is coordinated through the sulfur atom. Hence oxidation of methionine to sulfoxide both in complexes with sulfoxide and mixed ligand complexes with NO will leave sulfur atom coordinated with Fe(II). It means, that upon oxidation of proximal methionine to sulfoxide *heme* environment would not be subjected to significant changes.

It should be noted that computations give some lower energy for the O-coordinated DMSO ligand in the mixed ligand Fe(Por)(NO)(DMSO) complexes, so there is some discrepancy between experimental results and computations. However, it is necessary to stress that the computations were performed in the gas phase at room temperature. Calculation of both TPP and porphine (Table 2) 6-coordinate complexes favor O-coordinated DMSO by ~2 *kcal*/*mol*. Unfortunately, these compounds are not stable at room temperature and at this moment it seems rather difficult to evaluate the coordination mode of DMSO at 298 *K*. However, one must not rule out the possible isomerization following the increase in temperature.

In all cases warming of the layer to room temperature under high vacuum leads to slow elimination of the DMSO ligand. In the case of 5- and 6-coordinate DMSO complexes it results in the formation of the 4-coordinate Fe-porphyrin complexes, while in the case of mixed ligand Fe(Por)(NO)(DMSO) complexes it comes to the end with the formation of thermodynamically very stable nitrosyl complex Fe(Por)(NO).

Acknowledgment. The financial support of SCS (Project 18T-1D242) is gratefully acknowledged.

ՆԻՏՐՈՋԻԼ ԵՐԿԱԹ ՊՈՐՖԻՐԻՆՆԵՐԻ 6 -ԿՈՈՐԴԻՆԱՑՎԱԾ ԿՈՄՊԼԵՔՍՆԵՐԸ ՏՐԱՆՍ ԴԻՄԵԹԻԼՍՈՒԼՖՕՔՍԻԴԱՅԻՆ ԼԻԳԱՆԴԻ ՂԵՏ

Ա. Ա. ՂՈՎՀԱՆՆԻՍՅԱՆ, Ա. Վ. ԻՐԵՑԿԻ և Տ. Ս. ԿՈՒՐՏԻԿՅԱՆ

երկաթ-պորֆիրինների (Fe(Por), Por- մեզո-տետրաֆենիլ- և մեզո-տետրա-p-տոլիլ-պորֆիրինատո դիանիոն) միկրոծակոտկեն սուբլիմված թաղանթների հետ դիմեթիլ-սուլֆօքսիդի (DMSO) և ազոտի մոնօքսիդի (NO) հաջորդաբար փոխազդեցությամբ ցածր ջերմաստիճաններում մասնակիորեն ստացվել են խառը-լիգանդային Fe(Por)(DMSO)(NO) կոմպլեքսներ, ինչպես ցույց է տրված ՖՋԻԿ սպեկտրաչափության եղանակով, որոնք լրացուցիչ հիմնավորվում են 15NO և DMSO-d6 իզոտոպոմերների կիրառմամբ:

Fe(Por)(DMSO)(NO)-ի գոյացումը DMSO-ի փոխազդեցությամբ դիքլորմեթանում լուծված Fe(Por)(NO)-ի հետ գրեթե քանակական բնույթ է կրում: Հավասարակշռության հաստատունի ջերմաստիճանային կախվածությունից հաշվարկվել են կոմպլեքսագոյացման ռեակցիայի թերմոդինամիկ պարամետրերը: ՖՋԻԿ սպեկտրաչափական տվյալները խոսում են այն մասին, որ DMSO-ն կոորդինացիայի մեջ է մտնում երկաթի հետ ծծումբի ատոմի միջոցով: Միևնույն ժամանակ հաշվարկները կատարված խառնությունների փունկցիոնալ տեսության չրջանակներում գազ փազայում և սենյակի ջերմաստիճաններում քիչ ավելի խոր էներգիայի մինիմում են դրսևորում O-կապված իզոմերի համար:

ШЕСТИКООРДИНАЦИОННЫЕ НИТРОЗИЛЬНЫЕ КОМПЛЕКСЫ Fe-ПОРФИРИНОВ С *ТРАНС* ДИМЕТИЛСУЛЬФОКСИДНЫМ ЛИГАНДОМ

А. А. ОГАНЕСЯН[1], А. В. ИРЕЦКИЙ[2] и Т. С. КУРТИКЯН[1]

[1] Центр исследования строения молекулы Научно-технологического центра органической и фармацевтической химии НАН Республики Армения
E-mail: ahovhan@gmail.com
[2] Государственный университет Верхнего Озера, штат Мичиган, США

Последовательное взаимодействие DMSO и NO с микропористыми слоями Fe(Por) -ов (Por – *мезо*-тетра-фенил- и *мезо*-тетра-*p*-толил-порфиринато дианионы) при низких температурах ведет к частичному образованию смешанного комплекса Fe(Por)(DMSO)(NO), как об этом свидетельствуют Фурье-ИК-спектры, подкрепленные данными с изотопными ^{15}NO и DMSO-d_6. Образование при низких температурах Fe(Por)(DMSO)(NO) взаимодействием DMSO с растворенным в дихлорметане нитрозильным комплексом Fe(Por)(NO) носит почти количественный характер. Из температурной зависимости константы равновесия реакции комплексообразования вычислены термодинамические параметры этого процесса. Согласно данным Фурье-ИК-спектроскопии в смешанном комплексе DMSO координирован с железом через атом серы. В то же время расчеты по теории функционала плотности в газовой фазе и при комнатных температурах дают несколько более глубокий минимум для O-связанного изомера.

REFERENCES

[1] *Mc. Cleverty J.A.* // Chem.Rev., 2004, v. 104. p. 403.
[2] *Nakamoto K.* Infrared and Raman spectra of Inorganic and Coordination Compounds, 3rd Ed.; Wiley; New York, 1978; p. 244.
[3] *Diao T., White P., Guzei I., Stahl S.S.* // Inorg. Chem., 2012, v. 51, p. 11898.
[4] *Epstein M., Straub D.K., Maricondi C.* // Inorg. Chem., 1967, v. 6, p. 1720.
[5] *Kobayashi H., Yanagawa Y.* // Bull. Chem. Soc. Jpn., 1972, v. 45, 450.
[6] *Paulat F., Praneeth V.K.K., Nather C., Lehnert N.* // Inorg. Chem., 2006, v. 45, p. 2835.
[7] *Martirosyan G.G., Kurtikyan T.S., Azizyan A.S., Iretskii A.V., Ford P.C.* // J. Inorg. Biochem., 2013, v. 121, p. 129.
[8] *Perera R., Sono M., Sigman J.A., Pfister T.D., Lu. Y., Dawson J.H.* // Proc. Natl. Acad. Sci. USA, 2003, v. 100, p. 3641.
[9] *Yoshimura T.* // Inorg. Chim. Acta, 1982, v. 57, p. 99.
[10] *Oshio H., Ama T., Watanabe T., Kincaid J., Nakamoto K.* // Spectrochim. Acta, Part A, 1984, v. 40 A, 863.
[11] *Praneeth V.K.K., Haupt E., Lehnert N.* // J. Inorg. Biochem., 2005, v. 99, p. 940.

ՀԱՅԱՍՏԱՆԻ ՀԱՆՐԱՊԵՏՈՒԹՅԱՆ ԳԻՏՈՒԹՅՈՒՆՆԵՐԻ
ԱԶԳԱՅԻՆ ԱԿԱԴԵՄԻԱ
НАЦИОНАЛЬНАЯ АКАДЕМИЯ НАУК РЕСПУБЛИКИ АРМЕНИЯ
NATIONAL ACADEMY OF SCIENCES OF THE REPUBLIC OF ARMENIA

Հայաստանի քիմիական հանդես
Химический журнал Армении **71, №4, 2018** Chemical Journal of Armenia

UDC 542.971:546.74

DTA/TG STUDY OF NiO REDUCTION BY Mg+C COMBINED REDUCER

M. K. ZAKARYAN[1,2], O. M. NIAZYAN[2], S. V. AYDINYAN[3] and S. L. KHARATYAN[1,2]

[1]A.B. Nalbandyan Institute of Chemical Physics NAS RA
5/2, P. Sevak Str., Yerevan, 0014, Armenia
[2]Yerevan State University
1, A. Manoukyan Str., Yerevan, 0025, Armenia
[3]Tallinn University of Technology
5, Ehitajate tee, Tallinn, 19086, Estonia
E-mail: zakaryan526219@gmail.com

Kinetic parameters and reaction pathway for the reduction of nickel oxide with simultaneous utilization of magnesium and carbon were established to assess the feasibility of using combined reducers to produce powdered nickel from the NiO-Mg-C system. It was revealed that in this system the reduction of the metal oxide was initiated by Mg, followed by simultaneous action of magnesium and carbon, and at the end of the magnesiothermic process the second stage of the carbothermal reduction started. It was shown that relatively higher heating rates have beneficial influence on the reduction process of nickel oxide. The reduction of nickel oxide by the combined reducer (Mg+C) proceeds at a lower temperature as compared to separate binary mixtures, which evidences of the synergistic effect of combined reducers in the ternary mixture. The activation energy for the NiO+Mg+C reaction (117 $kJ{\cdot}mol^{-1}$) is lower than that of the binary NiO+C (291 $kJ{\cdot}mol^{-1}$) and NiO+Mg (178 $kJ{\cdot}mol^{-1}$) reactions. Thus, the utilization of Mg/C combined reducer allows to mitigate the reduction temperature of NiO, as well as the activation energy compared with the separate carbothermal and magnesiothermic reduction reactions.

Figs. 12, tables 5, references 29.

1. Introduction

Preparation of Ni-based alloys with refractory metals, such as tungsten or molybdenum, has been the subject of considerable interest during the past few years. Among such materials, Ni–W alloys exhibit distinguishing mechanical and tribological characteristics which provide enhanced performance for engineering applications. Owing to their superior strength and thermal stability, valuable electric and magnetic properties, high corrosion resistance Ni-W alloys have got increasing consideration in several applications, including protecting and covering coatings,

microelectromechanical systems, magnetic heads and powerful integral schemes. Alloys of tungsten with the metals of iron group (particularly with nickel) are considering as main substitute for hard chromium platings [1-3].

It is well known that alloys containing refractory metal (W, Mo) are inherently difficult to prepare using conventional powder metallurgy due to the large differences in melting points (1455°*C* and 3422°*C* for Ni and W, respectively) and limited mutual solubility. Hence, self-propagating high-temperature synthesis (SHS) or combustion synthesis (CS) has been suggested for the preparation of fine Ni-W composite material from oxide precursors by Mg/C combined reducers [4-5] using thermo-kinetic coupling approach [6-7]. However, it is highly challenging to monitor the interaction process in the WO_3-NiO-Mg-C system and to reveal the mechanism of combustion reaction due to its high velocity. One of the approaches to solve this issue is modeling the process under mild heating conditions (e.g., at low heating rates and tuning the process in time) using the DTA/TG method. By varying heating rates of reagents, it is possible to separate the main stages and analyze intermediate quenched compounds for the efficient exploration of interaction mechanism [8]. Moreover, performing the process with different heating rates allows to use various kinetic schemes developed for this purpose and to calculate kinetic parameters for separate stages.

The implementation of this research enables to obtain kinetic parameters and reduction pathway for the reduction processes of nickel oxide with simultaneous application of magnesium and carbon, with the aim of assessing the feasibility of using combined reducers to produce powdered nickel from the NiO-Mg-C system. Such approach will contribute to the preparation of Ni-W alloys from the NiO-WO_3-Mg-C system in the combustion mode.

Note that according to the available literature, the mechanism of NiO reduction by the combined Mg/C reducer has not been studied yet. In [9] the reduction of WO_3 was explored by means of combined reducers. The kinetics of nickel oxide reduction into nickel has been studied by using non-metallic reducers due to its practical importance as a catalyst in chemical industry [10-16]. Few kinetic studies have been reported where metals (magnesium or aluminium) were employed directly for the reduction of metal oxides. According to the literature data, high effective activation energy values were obtained for these thermite reactions (CuO+Mg, Ea = 424 ± 25 $kJ{\cdot}mol^{-1}$ [17]; Cu_2O+Al, Ea = 658 $kJ{\cdot}mol^{-1}$ [18]; MoO_3+Al, Ea = 209-373 $kJ{\cdot}mol^{-1}$ [19]; Ea = 312 $kJ{\cdot}mol^{-1}$ for the Al-30%Mg+Fe_2O_3 reaction [20]).

In our previous studies in the CuO-Mg-C [21], WO_3-Mg-C [9, 22], MoO_3-Mg-C [21, 23] systems at low and high heating rates the use of Mg+C reducing mixture was found attractive, especially due to the crucial influence of carbon addition on a reaction pathway with a lower effective activation energy.

This study is motivated by the need to investigate the interaction behavior and kinetic features of the NiO-Mg, NiO-C and NiO-Mg-C systems in non-isothermal conditions using DTA/TG method. Based on the data obtained interactions in the NiO-Mg-C system and in more complicated NiO-WO_3-Mg-C system can be

controlled allowing to fabricate powdered nickel or Ni-W alloys using the advanced combustion synthesis method.

2. Materials and methods

The experiments were carried out by differential thermal (DTA) and thermogravimetric (TG) analysis methods using Q-1500 instrument (Derivatograph Q1500 MOM, Hungary) which is linked to multichannel acquisition system, and output signals are recorded by a computer. The reactive powder mixture (30-200 *mg*) is placed into one of two crucibles. In the second crucible the Al_2O_3 powder is placed, which is used as a reference material. All measurements were conducted in nitrogen flow (100-120 $ml \cdot min^{-1}$). Heating rate was programmed to be 2.5, 5, 10, 20°C$\cdot min^{-1}$. In order to reveal the reaction mechanism, the process was terminated at preset temperatures, and the samples were cooled down in inert gas flow. Phase compositions of the intermediate and final products were analyzed by X-ray diffraction (XRD; D5005, Bruker, USA) using CuKα1 radiation (λ = 1.5406 Å) with a step of 0.02° (2θ) and a count time of 0.4 *s*.

As raw materials nickel (II) oxide (reagent grade, Russia, TU 6-09-4125-80), magnesium (MPF-3, Russia, pure, particle size 0.15 *mm*<μ<0.3 *mm*), carbon (P-803, Russia, μ<0.1 μm) were used in experiments.

3. Results and discussion

To clarify the interaction mechanism in the complex ternary (NiO-Mg-C) system, it was expedient firstly to explore the reaction pathways in the binary (NiO-Mg, NiO-C) systems in the identical conditions of linear heating.

3.1. NiO-Mg binary system

Fig. 1 depicts DTA/TG curves of the NiO+Mg stoichiometric mixture. It is clear that strong exothermic reduction starts before the melting point of magnesium (650°C), when temperature exceeds 630°C (heating rate: V_h = 10°C$\cdot min^{-1}$, m_o = 50 *mg*). A single stage process occurs and the maximum shift of the DTA curve appears at T_{max} = 648.3°C. It must be emphasized that no mass change was registered during the process. The latter is a clear fact that the reaction proceeds by solid+solid scheme (NiO + Mg = Ni + MgO) and no evaporation of reagents takes place (Fig. 1, TG curve).

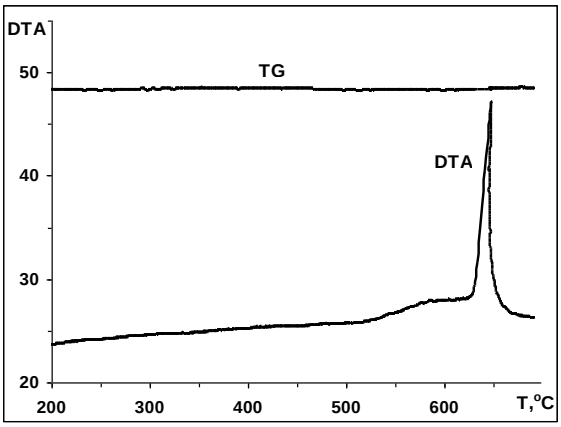

Fig. 1. DTA/TG curves of the NiO+Mg mixture, V_h = 10 $^oC{\cdot}min^{-1}$, m_o = 50 *mg.*

To reveal the influence of heating rate on the interaction mechanism, the DTA/TG studies were performed at heating rates from 2.5 up to 20°C$\cdot min^{-1}$. As it can be seen from the figure 2, with the increasing of heating rate, exothermic peaks of magnesiothermic reduction of nickel oxide shift to higher temperature area. In parallel, the intensity of DTA peaks increases. Thus, in the case of V_h = 2.5°C$\cdot min^{-1}$ it is weakly expressed, while peaks at V_h = 5, 10, 20°C$\cdot min^{-1}$ demonstrate the character of explosive reactions (Fig. 2; Table 1).

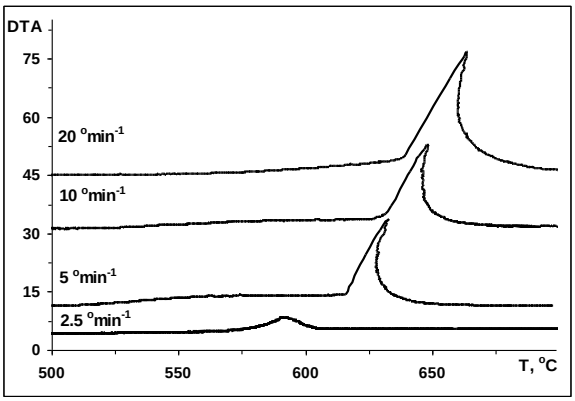

Fig. 2. DTA curves of the NiO+Mg mixture at various heating rates: V_h = 2.5; 5; 10; 20^{o}C$\cdot min^{-1}$.

Table 1

Influence of heating rate on the temperature range and T_{max} for the NiO+Mg system

Heating rate, °C $\cdot min^{-1}$	Reduction temperature range, °C	DTA_{max}, °C
20	635-715	663.7
10	630-670	648.3
5	615-652	631.7
2.5	570-610	593.3

In all cases, the main process predominately occurs before melting of Mg and the interaction takes place with a solid + solid mechanism. To some extent, the

reaction with relatively high heating rate ($20^oC \cdot min^{-1}$) deviates from this scheme (Table 1). In this case, the interaction begins with participation of solid Mg but lasts up to a temperature surpassing the melting point of Mg.

According to the results obtained at different heating rates, the latter phenomenon strictly affects the reduction degree. Thus, with increasing the heating rate, the intensity of Ni peaks in the XRD pattern (for the samples cooled down from 700^oC) noticeably increases; in parallel, the intensity of NiO peaks decreases (Fig. 3). Therefore, relatively higher heating rates have beneficial influence on the magnesiothermic reduction of nickel oxide.

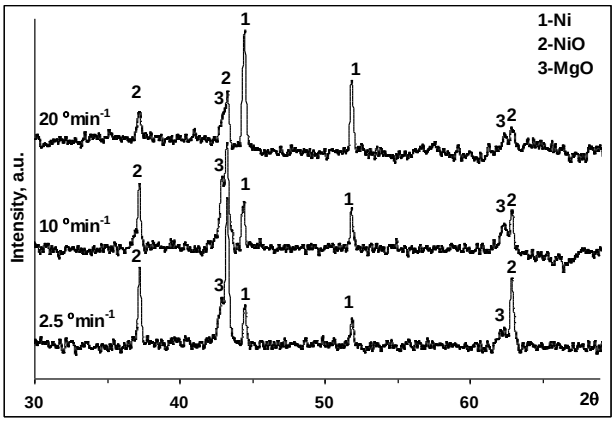

Fig. 3. XRD patterns of the NiO+Mg reaction products at various heating rates.

3.2. NiO-C binary system

Experiments in the NiO-C binary system reveal that at linear heating (V_h = $10^oC \cdot min^{-1}$, m_o = 200 *mg*) the stepwise carbothermal reduction is registered. Fig. 4 shows that there are no significant changes in the reactive mixture up to 750^oC. When the temperature exceeds 750^oC an endothermic reduction is registered with two sequential stages, which is simultaneously noticeable on DTA, TG and DTG curves. At that, the second stage is more intensive (Fig. 4). Note that in [24-26] was also reported that nickel oxide carbothermal reduction at high-temperature area occurred by two macroscopic stages.

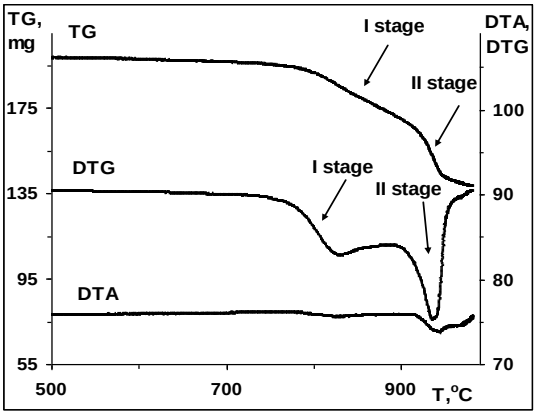

Fig. 4. DTA/TG/DTG curves of the NiO+C mixture, V_h = 10 $^oC \cdot min^{-1}$, m_o = 200 *mg.*

The mass change in the TG curve corresponds to the release of carbon dioxide or/and carbon monoxide either during the first or second stage of the process:

$$NiO + C \rightarrow Ni + CO/CO_2 \uparrow$$

According to mass loss calculations, the carbothermal reduction degree increases with the increase of the heating rate (Table 2). For example, according to the results shown in Fig. 4, the mass loss makes about 31% (according to the above reaction equation: 32.3%).

Table 2

Influence of heating rate on the initial mixtures' mass loss

Heating rate, $°C \cdot min^{-1}$	Mass loss by C, %
20	31.3
10	31.0
5	29.2
2.5	17.5

As can be seen from Fig. 5 (DTG curves), nickel oxide reduction by carbon proceeds at different temperature ranges depending on the heating rate. With the increase of the heating rate, the reduction process shifts to a higher temperature area (Table 3).

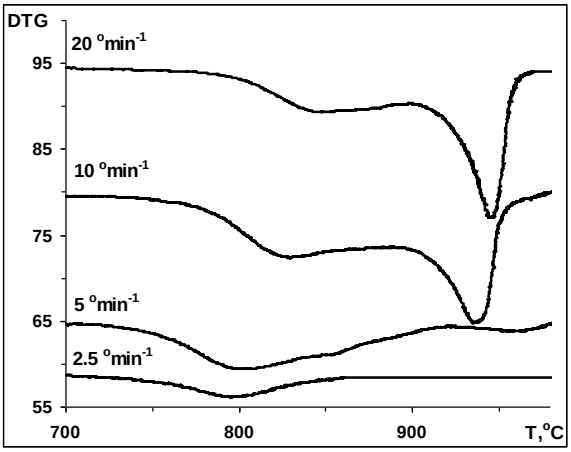

Fig. 5. DTG curves of the NiO+C mixture at various heating rates.

Table 3

Influence of heating rate on the temperature range and T_{max} for the NiO+C system

Heating rate, $°C \cdot min^{-1}$	Reduction temperature range, °C		(DTG_{min}), °C	
	I stage	II stage	I stage	II stage
20	780-900	905-985	843.4	948.1
10	750-890	900-970	829.5	943.3
5	730-930	935-990	808.6	966.2
2.5	715-860	–	782.6	–

As it was mentioned above, carbothermal reduction degree increases with the increase of the heating rate. This has been also proved by the results of XRD analysis of the reduction products at the end of the process (Fig. 6): with the increase of heating rate, the nickel oxide carbothermal reduction degree increases as it was in the case of magnesiothermic reduction.

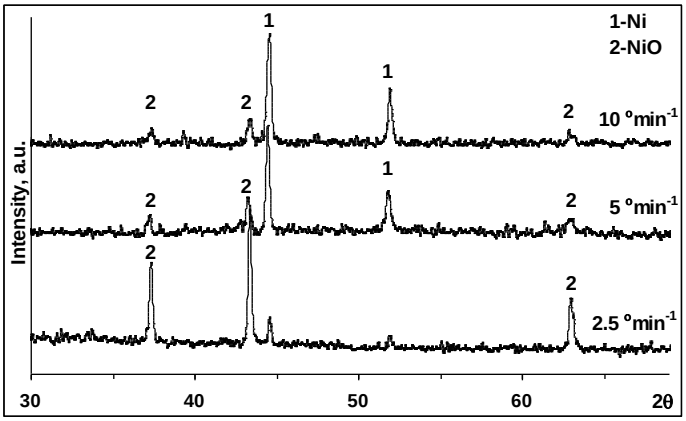

Fig.6. XRD patterns of the NiO+C reaction products at various heating rates.

3.3. NiO-Mg-C ternary system

Finally, thermal analysis in ternary NiO-Mg-C system was performed with the 2NiO+Mg+C stoichiometric mixture to distinguish carbon and magnesium reduction processes during the external heating. The DTA/TG curves in Figure 7 illustrate that first exothermic conversion proceeds at 590-740^{o}C (T_{max} = 673.5^{o}C), which corresponds to the NiO + Mg = Ni + MgO reaction (see Fig. 8). In the DTA curve, the endothermic process of magnesium melting is also observed. TG and DTG curves show the mass loss expressed in two different segments (Fig. 7) validating that the carbothermic reduction of nickel oxide is a double-stage process [24-26]. The first decline in the TG curve starts at 625^{o}C (DTG_{min} is observed at 684^{o}C), slightly later than the magnesiothermic process starts (590^{o}C). The second decline starts at 740^{o}C (DTG_{min} is observed at 853.7^{o}C), simultaneously with the end of the magnesiothermic process. This indicates that in the NiO-Mg-C system the reduction of the metal oxide is initiated by Mg (including magnesium melting zone), followed by simultaneous action of magnesium and carbon, and at the end of the magnesiothermic process, the second stage of the carbothermal reduction starts. The latter is additionally proved by XRD patterns of the samples cooled down at different temperatures (Fig. 8).

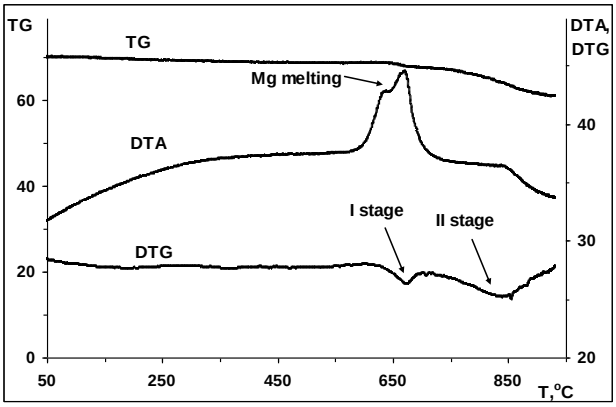

Fig. 7. DTA/TG/DTG curves of the 2NiO+Mg+C mixture, V_h = 20°C·*min*$^{-1}$, m_o = 70 *mg.*

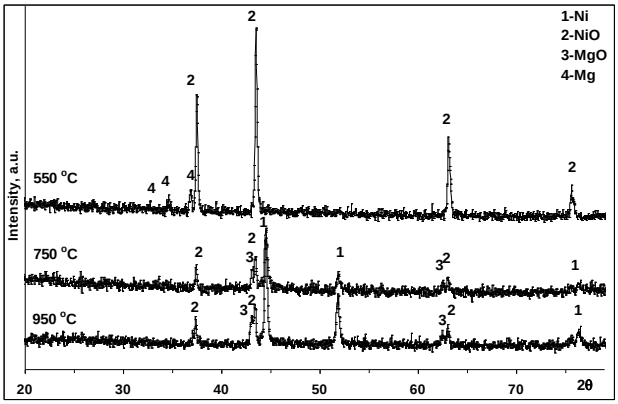

Fig. 8. XRD patterns of the 2NiO+Mg+C reaction products cooled down from different temperatures.

The results obtained during examinations of NiO reduction by combined Mg/C reducer are substantially different from the NiO reduction behavior by individual reducers. Here we deal with a typical example of the reactions kinetic coupling. According to the data obtained from individual reduction processes, the magnesiothermic reduction of nickel oxide (at V_h = 20°C·*min*$^{-1}$) proceeds at 635-715°C temperature range with DTA_{max} = 663.7°C. In the case of the same heating rate the carbothermal reduction occurs at 780-900 °C; 905-985°C temperature ranges (DTG_{mins} are observed at 843.4 and 948°C, respectively). So, the magnesiothermic reduction in the ternary system starts earlier by 50°C than in the NiO-Mg system, and the carbothermal two-stage reduction process moves to a low temperature area by 160 (I stage) and 60°C (II stage). Thus, the reduction of nickel oxide by the combined reducer (Mg+C) proceeds at lower temperatures as compared to separate binary mixtures, which evidences of the particular synergistic effect in the ternary mixture.

According to the mass loss calculations, the carbothermal reduction degree in the ternary system increases with the increase of the heating rate. Thus, according to the reaction equation (NiO + Mg + C → Ni + MgO + CO/CO_2↑), the maximum value of mass loss conditioned by carbothermal reduction process is 15.2%. On the

other hand, during the different heating rates in the reduction process the following percentages of weight loss were observed: 1.02% at 2.5°C·*min*$^{-1}$, 5.32% at 5°C·*min*$^{-1}$, 7.92% at 10°C·*min*$^{-1}$ and 11.76% at 20°C·*min*$^{-1}$. These results suggest that despite the degree of metal reduction increases with the increase of heating rate, carbon does not provide complete reduction of nickel oxide at least up to a temperature of 950°C (Fig. 9).

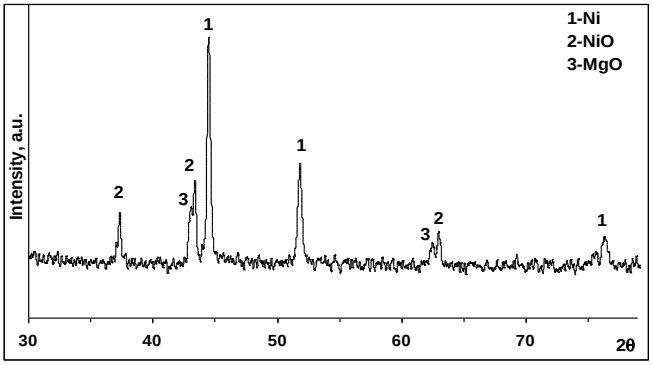

Fig. 9. XRD pattern of the 2NiO+Mg+C reaction product, T = 950°C, V_h = 20°C·*min*$^{-1}$

As in the case of binary systems, in the ternary NiO-Mg-C system exothermic peaks of nickel oxide magnesiothermic reduction also shift to the higher temperature area (Table 4, Fig. 10)

Table 4

Influence of heating rate on the temperature range and T_{max} for the 2NiO+Mg+C system

Heating rate, °C·*min*$^{-1}$	Reduction temperature range, °C	(DTA $_{max}$), °C
20	590-740	673.5
10	570-680	626.2
5	550-660	592.8
2.5	520-600	570.2

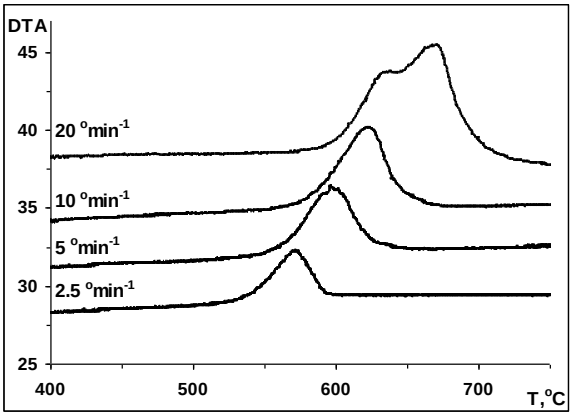

Fig. 10. IDTA curves of the 2NiO+Mg+C mixture at various heating rates.

3.4. Calculation of activation energy

Based on the results obtained by DTA/DTG/TG investigations the effective activation energy values were calculated for the reduction stages for all the studied reactions. There are several approaches for calculation of the effective activation energy in non-isothermal conditions. Among them are the well-known isoconversion methods formulated by Kissinger [27] and Ozawa [28]. Both methods are based on the shift of temperature corresponding to the maximum advance in the DTA (Kissinger) and DTG (Ozawa) curves depending on the heating rate kept constant. The methods are based on the Arrhenius equation corrected for the nonisothermicity of the reaction in such a way, that the temperature is a function of time.

The derived expression for determination of activation energy by Kissinger has the following form:

$$\ln\left(\frac{V_h}{\left(T_{\max}^{DTA}\right)^2}\right) = \ln A - \frac{E}{R}\left(\frac{1}{T_{\max}^{DTA}}\right)$$

and by Ozawa method the following form:

$$\ln\left(\frac{V_h}{\left(T_{\max}^{DTG}\right)^2}\right) = \ln A - \frac{E}{R}\left(\frac{1}{T_{\max}^{DTG}}\right)$$

where, A is a constant, E is the effective activation energy of the process, ($kJ{\cdot}mol^{-1}$), V_h is the heating rate ($K{\cdot}min^{-1}$), T_{max} is the reduction temperature corresponding to the maximum advance in the DTA/DTG curve (K), R is the universal gas constant.

3.4.1. Magnesiothermic and magnesiocarbothermal reduction of NiO (Kissinger method)

In Figure 11, experimental data for the reduction of nickel oxide by Mg (1) and Mg+C (2) mixture in appropriate coordinates are summarized. Based on these plots the values of effective activation energy are calculated. Thus, the activation energy for NiO + Mg reaction is 178 $kJ{\cdot}mol^{-1}$ and for NiO + (Mg+C) reaction - 117 $kJ{\cdot}mol^{-1}$ (refers to the magnesiothermic stage) (Fig. 11).

	NiO+Mg	NiO+Mg+C (I stage)
V_h, $^{o}min^{-1}$	T_{max}, ^{o}C	T_{max}, ^{o}C
20	664	674
10	648	626
5	617	593
2.5	593; 596	570

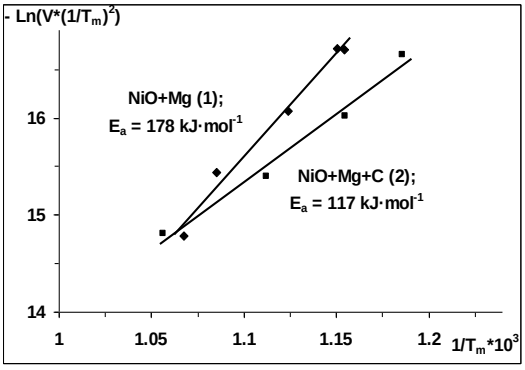

Fig. 11. Determination of activation energy values for NiO+Mg (1) and NiO+Mg+C (2) reactions by Kissinger method.

In comparison, according to [9], the activation energy for (WO_3+Mg) reaction is 153 $kJ{\cdot}mol^{-1}$ and for (WO_3+Mg+C) is 177 $kJ{\cdot}mol^{-1}$ (refers to the magnesiothermic reduction stage), while for (CuO+Mg) reaction is 424 $kJ.mol^{-1}$ [17] (Table 5).

3.4.2. Carbothermal reduction of NiO (Ozawa method)

In Figure 12 experimental data in appropriate coordinates for the reduction of nickel oxide by carbon are summarized. According to Figure 12, the activation energy for NiO reduction by carbon is 291 $kJ{\cdot}mol^{-1}$. In comparison, in [29] for nickel oxide carbothermal reduction the activation energy value was determined to be 299 $kJ{\cdot}mol^{-1}$ (Table 5).

	NiO+C
V_h, $^o min^{-1}$	T_{max}, ^{o}C
20	847
10	830
5	804
2.5	783

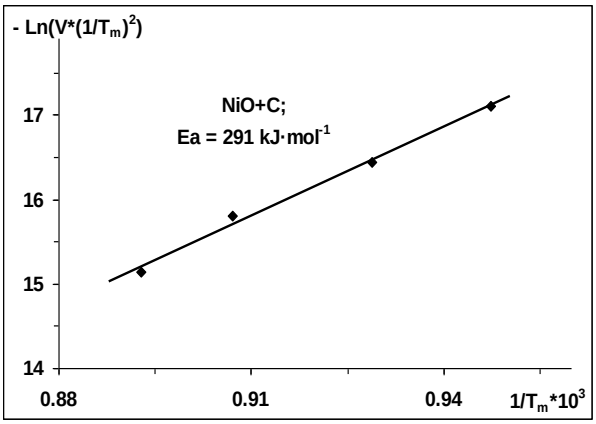

Fig. 12. Determination of activation energy for NiO+C reaction by Ozawa method.

Table 5

Comparison of the values of activation energies with reference data

Reaction	Activation energy, $kJ{\cdot}mol^{-1}$	Reference
WO_3 + Mg	153	[8]
CuO + Mg	424	[16]
WO_3 + Mg + C (for WO_3 + Mg)	177	[8]
NiO + C	299	[28]
NiO + Mg	178	[this work]
NiO + Mg + C (for NiO+Mg)	117	[this work]
NiO + C	291	[this work]

Furthermore, the activation energy of nickel oxide reduction by carbon is comparable with that of the same reaction determined from isothermal experiments (315 $kJ{\cdot}mol^{-1}$) [25].

Thus, the activation energy for the NiO+Mg+C reaction (117 $kJ{\cdot}mol^{-1}$) is lower than that of the binary NiO+C (291 $kJ{\cdot}mol^{-1}$) and NiO+Mg (178 $kJ{\cdot}mol^{-1}$) reactions.

The application of Mg/C combined reducer allows to decrease the activation energy of magnesiothermic reduction stage by about 1.5 times.

NiO-ի ՎԵՐԱԿԱՆԳՆՄԱՆ ՊՐՈՑԵՍԻ ՈՒՍՈՒՄՆԱՍԻՐՈՒԹՅՈՒՆԸ Mg+C ՀԱՄԱԿՑՎԱԾ ՎԵՐԱԿԱՆԳՆԻՉՈՎ ԴԵՐԻՎԱՑՈԳՐԱՖԻԱԿԱՆ ԵՂԱՆԱԿՈՎ

Մ. Կ. ԶԱՔԱՐՅԱՆ, Օ. Մ. ՆԻԱԶՅԱՆ, Ս. Վ. ԱՅԴԻՆՅԱՆ և Ս. Լ. ԽԱՌԱՏՅԱՆ

Սույն աշխատանքում ուսումնասիրվել են Mg/C համակցված վերականգնիչով նիկելի օքսիդի վերականգնման կինետիկական օրինաչափությունները դերիվատոգրա-ֆիական եղանակով գծային տաքացման պայմաններում: Բացահայտվել է, որ NiO-Mg-C համակարգում նիկելի օքսիդի վերականգնումն սկսվում է մագնեզիումով, շարունակվում է միաժամանակ մագնեզիումով և ածխածնով, իսկ մագնեզիումջերմային պրոցեսի ավարտին զուգահեռ սկսվում է ածխածնով վերականգնման երկրորդ փուլը: Հաստատվել է, որ տաքացման արագության մեծացումը բարենպաստ ազդեցություն ունի նիկելի օքսիդի վերականգնման աստիճանի վրա: Ցույց է տրվել, որ նիկելի օքսիդի վերականգնումը Mg/C վերականգնիչով տեղի է ունենում համեմատաբար ավելի մեղմ ջերմաստիճանային պայմաններում՝ համեմատած NiO+Mg և NiO+C բինար համակարգերի հետ, ինչը վկայում է սինէրգետիկական էֆեկտի մասին: Որոշվել են հետազոտված ռեակցիաների էֆեկտիվ ակտիվացման էներգիայի արժեքները, որոնք NiO+Mg+C, NiO+C և NiO+Mg ռեակցիաների համար համապատասխանաբար կազմել են 117, 291 և 178 կՋ·մոլ$^{-1}$:

ДТА/ТГ ИССЛЕДОВАНИЕ ВОССТАНОВЛЕНИЯ NiO КОМБИНИРОВАННЫМ ВОССТАНОВИТЕЛЕМ Mg+C

М. К. ЗАКАРЯН[1,2], О. М. НИАЗЯН[1], С. В. АЙДИНЯН[3] и С. Л. ХАРАТЯН[1,2]

[1] Институт химической физики им. А.Б. Налбандяна НАН Республики Армения
Армения, 0014, Ереван, ул. П. Севака, 5/2
[2] Ереванский государственный университет
Армения, 0025, Ереван, ул. А. Манукяна, 1
[3] Таллинский технологический университет
Эитайате ул. 5, Таллинн, 19086, Эстония
E-mail: zakaryan526219@gmail.com

В данной работе дериватографическим методом исследованы кинетические закономерности восстановления оксида никеля (II) комбинированным восстановителем Mg/C в условиях линейного нагрева. Установлено, что восстановление NiO начинается магнием, продолжается одновременно магнием и углеродом, а в конце магниетермического процесса наступает вторая стадия карботермического восстановления. Выявлено, что увеличение скорости нагрева оказывает благотворное влияние на степень восстановления окиси никеля. Показано, что восстановление оксида никеля (II) комбинированным восстановителем (Mg+C) происходит при более низких температурах по сравнению с отдельными бинарными смесями NiO+Mg и NiO+C, что свидетельствует о наличии синергетического эффекта. Определены значения эффективной энергии активации исследованных реакций: 117 *кДж·мол$^{-1}$* – для реакции NiO+Mg+C, 291 *кДж·мол$^{-1}$* – для NiO + C и 178 *кДж·мол$^{-1}$* – для NiO + Mg.

REFERENCES

[1] *Eliaz N., Sridhar T.M., Gileadi E.* // Electrochim. Acta, 2005, v. 50, p. 2893.
[2] *Younes O., Gileadi E.* // J. Electrochem. Soc., 2002, v. 149, №2, p. 100.
[3] *Aning A.O., Wang Z., Courtney T.H* // Acta Metall. Mater., 1991, v. 4, p. 165.
[4] *Merzhanov A.G.* // J. Mater. Chem., 2004, v. 14, p. 1779.
[5] *Varma A., Rogachev A.S., Mukasyan A.S., Hwang S.* // Adv. Chem. Eng., 1998, v. 24, p. 79.
[6] *Merzhanov A.G* // Int. J. SHS, 2011, v. 20, p. 61.
[7] *Kharatyan S.L., Merzhanov A.G* // Int. J. SHS, 2012, v. 21, p. 59.
[8] *Baghdasaryan A.M., Niazyan O.M., Khachatryan H.L., Kharatyan S.L* // Int. J. Refract. Met. Hard Mater., 2015, v. 451, p. 315.
[9] *Baghdasaryan A.M., Niazyan O.M., Khachatryan H.L., Kharatyan S.L* // Int. J. Refract. Met. Hard Mater., 2014, v. 43, p. 216.
[10] *Alizadeh R., Jamshidi E., Ebrahim H.A.* // Chemical Engineering & Technology, 2007, v. 30, №8, p. 1123.
[11] *Richardson J.T., Scates R., Twigg M.V.* // Applied Catalysis A: General, 2003, v. 246, №1, p. 137.
[12] *Szekely J., Evans J.W.* // Metall. Mater. Trans. B, 1971, v. 2, №6, p. 1699.
[13] *Evans J.W., Song S., Leon-Sucre C.E.* // Metall. Mater. Trans. B, 1976, v. 7, №1, p. 55.
[14] *Szekely J., Lin I.* // Metall. Trans., 1975, v. 7, №3, p. 493.
[15] *Rostrup-Nielsena. J.R.* // PCCP, 2001, v. 3, p. 283.
[16] *Gong M., Zhou W., Tsai M.C, Zhou J., Guan M., Lin M.C., Zhang B., Hu Y., Wang D.Y., Yang J., Pennycook S.J.* // Nature communications, 2014, v. 5, p. 4695.
[17] *Hosseini S.G., Sheikhpour A., Keshavarz M.H., Tavangar S.* // Thermochim. Acta, 2016, v. 626, p. 1.
[18] *Wang L.L., Munir Z.A., Maximov Y.M.* // J. Mater. Sci., 1993, v. 28, p. 3693.
[19] *Schoenitz M., Umbrajkar S., Dreizin E.L.* // J. Propul. Power, 2007, v. 23, №4, p. 683.
[20] *Wang Y., Jiang W., Zhang X., Liu H., Liu Y., Li F.* // Thermochim. Acta, 2011, v. 512, №1-2, p. 233.
[21] *Kirakosyan H., Minasyan T., Niazyan O., Aydinyan S., Kharatyan S*. // J. Therm. Anal. Calorim., 2016, v. 123, p. 35.
[22] *Aydinyan S.V., Nazaretyan Kh.T., Zargaryan A.G., Tumanyan M.E., Kharatyan S.L.* // J. Therm. Anal. Calorim., 2018, v. 133, №1, p. 261.
[23] *Manukyan Kh., Aydinyan S., Aghajanyan A., Grigoryan Y., Niazyan O., Kharatyan S.* // Int. J. Refract. Met. Hard Mater., 2012, v. 31, p. 28.
[24] *Sharma S.K., Vastola F.J., Walker P.L.* // Carbon, 1996, v. 34, №11, p. 1407.
[25] *Sharma S.K., Vastola F.J., Walker P.L.* // Carbon, 1997, v. 35, № 4, p. 529.
[26] *Sharma S.K., Vastola F.J., Walker P.L.* // Carbon, 1997, v. 35, № 4, p. 535.
[27]. *Kissinger H.E.* // Anal. Chem., 1957, v. 29, №11, p. 1702.
[28] *Ozawa T., Kato T.* // J. Therm. Anal., 1991, v. 37, p. 1299.
[29] *Grigoryan E.G., Niazyan O.M., Kharatyan S.L.* // Kinet. Catal., 2018, v. 48, p. 829.

ՀԱՅԱՍՏԱՆԻ ՀԱՆՐԱՊԵՏՈՒԹՅԱՆ ԳԻՏՈՒԹՅՈՒՆՆԵՐԻ
ԱԶԳԱՅԻՆ ԱԿԱԴԵՄԻԱ
НАЦИОНАЛЬНАЯ АКАДЕМИЯ НАУК РЕСПУБЛИКИ АРМЕНИЯ
NATIONAL ACADEMY OF SCIENCES OF THE REPUBLIC OF ARMENIA

Հայաստանի քիմիական հանդես
Химический журнал Армении **71, №4, 2018** Chemical Journal of Armenia

UDC 541.145

PHOTOCATALYIC OXIDATION OF CHLORINATED PHENYLALKANES WITH DIOXYGEN

L. A. MANUCHAROVA*, R. A. BAKHTCHADJIAN and L. A. TAVADYAN

*A. B. Nalbandyan Institute of Chemical Physics, NAS RA
5/2, P. Sevak Str., Yerevan, 0044, Armenia
E-mail: loriettam@yandex.ru

The photocatalytic oxidation of some chlorinated derivatives of the following mono- and biphenyl-substituted alkanes - 1-chloro-4-ethylbenzene (CEB); 4,4'-ichlorodiphenylmethane (DDM); 1,1,1-trichloro-2,2-bis(p-chlorophenyl)ethane (DDT) – with dioxygen in the presence of the photocatalyst – heterogenizied dioxo-Mo organometallic complex (dioxo-molybdenum(VI)-dichloro[4,4'-dicarboxylato-2,2'-bipyridine]) anchored on the photosensitive TiO_2 support under UV-irradiation (λ= 253.7 *nm*) has been investigated. The catalytic role of the anchored on Mo-metal-organic complex in the selective activation of the benzylic C-H bonds of these compounds with the formation of the corresponding oxygenated products in mild conditions has been shown.

The catalytic cycle consists of two successive stages, involving the oxidation of substrate by the oxo-atom transfer from dioxo-Mo(VI)-complex under UV-irradiation and regeneration of the reduced Mo(IV)-center by the oxidation with dioxygen in the dark. Experimentally, these two stages are separated in time. It has been shown that under these conditions even such a persistent pollutant as DDT can be selectively oxidized to dicofol, which is currently not available by other ways. The possible mechanism suggested for this group of reactions is discussed. It has been suggested that the formation of oxo-peroxo-Mo(VI) moieties, apparently, enhances the oxo-atom transfer from the Mo-complex to the substrate.

Figs. 3, table 1, references 11.

Introduction

Chlorinated derivatives of mono- and biphenyl-substituted alkanes are used as pesticides, dyestuffs; they are also used in various chemical syntheses [1]. The wide use of them causes different environmental problems [2,3]. One of the ways to neutralize these compounds is photocatalytic oxidation or oxidative destruction by air or oxygen. The existing methods for the transformation of these compounds to corresponding oxygenates in industrial scale are usually multistage complex

processes. For example, the transformation of DDT to dicofol (2,2,2-trichloro-1,1-*bis*-(4-chlorophenyl)ethanol) occurs as a four stages complex process [4].

Selective activation and functionalization of the benzylic C-H bonds of these compounds [5] permits directly to synthesize a great number of different halogenated derivatives of aromatic alcohols, ketones, carboxylic acids, etc.

In this work the oxidation of 1-chloro-4-ethylbenzene(chloroethylbezene (CEB)- 1), 4,4'-dichlorodiphenylmethane(dichlorodiphenylethane (DDM)-2) and 1,1,1-trichloro-2,2-bis(p-chlorophenyl)ethane (dichlorodiphenyltrichloroethane (DDT)- 3)

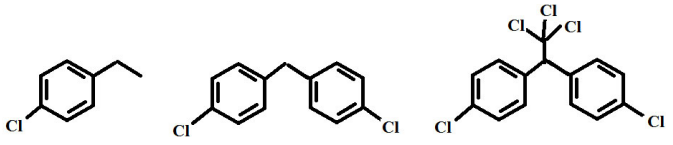

1 2 3

1- CEB; 2-DDM; 3-DDT.

with dioxygen was tested in the presence of the photocatalyst: dioxo-Mo(VI)-dichloro[4,4'-dicarboxylato-2,2'-bipyridine] complex, anchored on TiO_2 (Fig. 1) under UV-irradiation (λ= 253.7 *nm*). The catalytic activity of dioxo-molybdenum(VI) complexes in the presence of dioxygen was well known in oxidation reactions of the organic compounds, such as alkylarens, olefins, alcohols, phosphines, etc., in homogeneous conditions (in different solvents) [6,7]. The applied catalyst is a heterogenizied modification of a dioxo-Mo(VI) organometallic complex on the photosensitive material like TiO_2 [8].

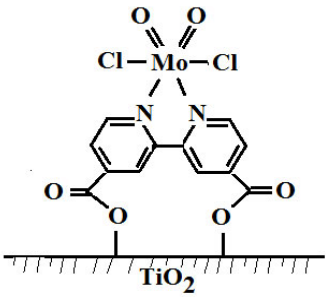

Fig. 1. Complex 1. Dioxo-Mo(VI)-dichloro[4,4'-dicarboxylato-2,2'-bipyridine] complex, anchored on TiO_2 surface.

Being a photosensitive material, TiO_2 promotes oxo-atom transfer reactions via enhanced electronic flux from support onto the molybdenum coordination sphere under UV or visible light irradiation [6-8].

The catalytic action of the anchored complex is based on the redox capacity of the Mo-active centers, performing catalytic cycle ($Mo^{VI} \leftrightarrows Mo^{IV}$) in the presence of dioxygen.

In the above context, the aim of this work is examination of the possibility of catalytic oxidation, or oxidative destruction of the mentioned chlorinated mono- and biphenyl-substituted alkanes, directly with the cheapest oxidant, like dioxygen, in

mild conditions, under UV-irradiation or visible light, using heterogenizied transition metal complexes on the photosensitive support.

Experimental Section

The experimental studies of the photocatalytic oxidation and oxidative destruction of 1-chloro-4-ethylbenzene (CEB); 4,4'-dichlorodiphenylmethane (DDM); 1,1,1-trichloro-2,2-bis (p-chlorophenyl)ethane (DDT) with dioxygen were performed in a reaction vessel (quartz, 30 *mL*) with a magnetic stirrer. The source of UV-irradiation was high pressure Hg-lamp DRT- 230. λ= 253.7 *nm* irradiation was applied. The experimental setup was described in previous works [9].

The dioxo-molybdenum(VI)-dichloro-[4,4'-dicarboxylato-2,2'-bipyridine] complex, anchored on the TiO_2 was synthesized by the transesterification of trimethylsilylated titania with the carboxylic ligand, giving trimethylsilanol (eliminated as hexamethyldisiloxane and water), then, the complexation was done by treating the anchored complex with a tetrahydrofuran solution, containing the calculated amount of MoO_2Cl_2 [10]. The method for the synthesis, as well as characterization of the obtained samples by a number of spectroscopic methods (^{13}C CAP NMR, FTIR and others) was also described in our previous works. The chemical and thermogravimetric analyses were performed for determination of the quantities of this complex on the surface of TiO_2.

The typical experiment was carried out by the following sequence of stages. The reaction mixture was exposed to UV-irradiation under stirring conditions and in the absence of dioxygen for 6-7 *h*. It was a suspension of the mentioned chlorinated alkanes (about $N\times10^{-5}$ *mol*) in acetonitrile, containing 10 *mg* of Complex 1. This was the first stage (period) of the experimental cycle. The second stage (period) was regeneration of the used catalyst in the presence of oxygen (2-2.5 *h*) in the dark. Before the beginning of every new experimental cycle, dioxygen was removed from the reaction medium and replaced by argon or helium. Identification and qualitative analyses of the reaction products were mostly carried out by gas-liquid chromatography and mass-spectrometry.

Results and Discussion

All observation tests of the consumption of substrates and formation of products in interactions of the chosen compounds with dioxygen, in the absence of the anchored complex, were negative in comparable experimental conditions. In the presence of "pure" TiO_2 (without anchored complex), as well as under UV-irradiation, the conversion of the initial substrates and detected products was quantitatively about two or three orders lower than in experiments with the anchored complex, with the exception of DDT. In the latter case, the conversion of DTT was no more than 5-7% in the time intervals comparable with the experiments with anchored complex.

In experiments with 1-chloro-4-ethylbenzene (CEB), in the first period of the first experimental cycle, the chromatographic and chemical analyses showed formation of Cl-C_6H_5, accompanied with small quantities of Cl-C_6H_4-CH(-OH)-CH_3 and Cl-C_6H_4-C(=O)-CH_3, traces of Cl-C_6H_4-CH(O-OH)-CH_3 and other chlorinated derivatives of the oxygen containing aromatic organic compounds, as well as CO_2, H_2O. No Cl–ions were found in the reaction zone. The time evolution profiles of some products in the first and consequent experimental cycles are presented in Fig. 2. The horizontal sections on the curve of the main reaction product, chlorobenzene, corresponding to the second time-periods ("dark" reaction) of the experimental cycles, the aim of which was re-oxidation of Mo(IV), formed in the first periods, into Mo(VI) with dioxygen, indicate practically the absence of the accumulation of the product. Contrarily, in the first periods of the second and consequent experimental cycles the amounts of the product permanently increase under UV irradiation in argon atmosphere.

The analyses showed that about 0.5 *mol* of CEB was transformed into products per 1 mol of the Mo-complex at the first period (about 7 *h* of experiment) of the first experimental cycle.

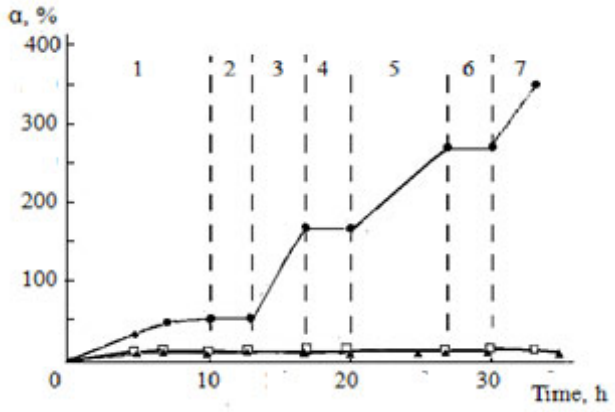

Fig. 2. Time evolution profiles of products: Cl-C_6H_5 (●), Cl-C_6H_4-C(O)-CH_3(□), Cl-C_6H_4-CH(OH)-CH_3 (▲) on oxidative decomposition of 1-chloro-4-ethylbenzene. 1; 3; 5; 7: periods under UV irradiation and argon; 2; 4; 6: periods of O_2 flow, in the dark. α = ([final product] *mmol*/[dioxo-Mo-complex] *mmol*)x100 (%).

The qualitative and quantitative analyses indicate the existence of the stoichiometric relations between the products in the following reaction:

$$p\text{-Cl-}C_6H_4\text{-}CH_2CH_3 + 3O_2 \xrightarrow{h\nu} \text{Cl-}C_6H_5 + 2CO_2 + 2H_2O$$

Thus, one of the main products of this reaction is chlorobenzene. Usually the main products of the oxidation of the aromatic hydrocarbons in the presence of Complex I correspond to alcohols or ketones [5-7,11].

Apparently, the formation of chlorobenzene is a result of the oxidative destruction of other intermediates, such as 4'-chloroacetophenone and 1-(4-

chlorophenyl)ethanol. This hypothesis has been verified by studying the photocatalytic decomposition of the 1-(4-chlorophenyl)ethanol in the same experimental conditions, under argon atmosphere, in the presence of Complex I. The following reaction may be written on the basis of the obtained data:

$$p\text{-Cl}(C_6H_4)\text{-C(O)-CH}_3 \xrightarrow{h\nu,\ 4[O]} \text{Cl}(C_6H_5) + 2CO_2 + H_2O$$

where [O] is oxo-atom in Complex 1. On the other hand, in analogous conditions, under visible light, ethylbenzene produces acetophenone, as a main product of the reaction [10, 11].

The multiple increase of the turnover number (ratio of [substrate] mmol/[anchored complex] *mmol*) in the second and consequent experimental cycles indicates that Complex 1 plays the role of a catalyst in the presence of dioxygen in oxidative destruction of CEB. Apparently, it occurs by the oxygen atom transfer to benzylic carbon by the formation of the chlorinated phenyl alcohol and ketone, which in their turn form all observed varieties of the decomposition products.

The oxidation of 4,4'-dichlorodiphenylmethane (DDM), in the same experimental conditions, showed analogous behavior, nearly repeating the form of the above presented time profile, obtained for CEB: the consumption of initial substrate and formation of reaction products in the first periods of the experimental cycles, and practically absence of the conversion of a substrate in the second periods. Composition of the products was relatively more complex for this compound than for CEB. The main reaction products were 4,4'-dichlorodiphenylmethanol, 4,4'-dichlorobenzophenon, chlorobenzene, as well as the products of complete oxidation, CO_2 and H_2O. Taking into account the results of all other experiments without anchored complex, on "pure" TiO_2, under UV-irradiation or in its absence, it may be concluded that the anchored complex plays the catalytic role in oxidative decomposition of DDM.

The reaction of DDT with oxygen was investigated in more detail, proceeding from its practical importance. The results obtained in 5 consecutive cycles are presented in Fig. 3. The curve (**b**) corresponds to the photochemical oxidation of DDT on the surface of "pure" TiO_2 (without anchored Complex 1), in the presence of dioxygen. Note, the amount of the "pure" TiO_2 in the reaction mixture was twice as much than that in experiments with Complex 1. The simple comparison of two curves indicates a significant increase of the consumption of DDT in the presence of the anchored complex (curve (**a**)), reaching 32% of the initial amount of the substrate. The post-reaction mixture, in this case, contains not only chlorinated products and Cl-ions, but also non-chlorinated organic compounds (C_1-C_{14}), CO_2, and H_2O. As the results show, the sum of a dozen dechlorinated products was about 53-57%. Correspondingly, other products (43-47%) were non-dechlorinated and partially dechlorinated compounds.

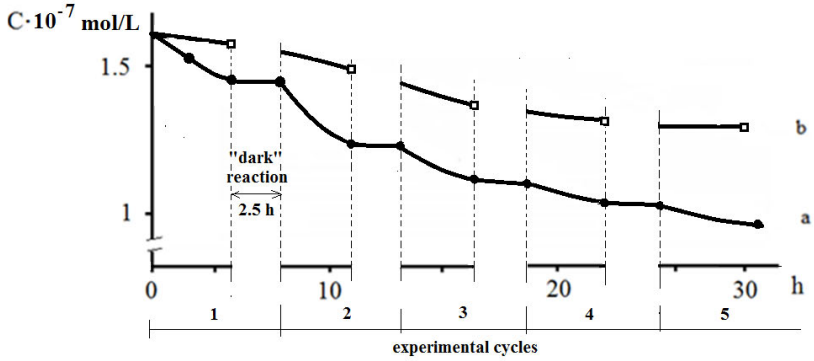

Fig. 3. Time profiles of the consumption of DDT($C\times10^{-7}$ mol/L), under UV-irradiation: (**a**) - in the presence of the anchored Complex (1); (**b**) - in the presence of the "pure" TiO_2 (in amounts 2 times more than Complex 1) with O_2.

The main product of the reaction dicofol (2,2,2-trichloro-1,1-bis(4-chlorophenyl)ethanol), (21 *mol* %), apparently, was also playing the role of an intermediate for the formation of a number of other chlorinated and non-chlorinated products. Note, under the same conditions, but in the absence of the anchored complex (on the "pure" TiO_2), the formation of dicofol was very slow, and the reaction gave a more complex mixture of other oxidative/reductive decomposition products, including the products of the complete degradation in small amounts.

The above results of the oxidation and oxidative destruction of CEB, DDM and DDT permit to conclude that the primary reaction in the interaction of Complex 1 with substrate is the formation of the corresponding oxygenated products, such as alcohols and often ketones, via photo-stimulated O-atom transfer from the anchored complex to substrate (reactions 1).

$$\text{Cl-C}_6\text{H}_4\text{-CHR}_1\text{R}_2 + \text{O=Mo(O)Cl}_2\text{L/TiO}_2 \xrightarrow{h\nu}$$
$$(\text{Cl-C}_6\text{H}_4)_x\text{-C(OH)R}_1\text{R}_2 + \text{Mo(O)Cl}_2\text{L/TiO}_2 \qquad (1)$$

where, R_1=H, R_2=CH_3 for CEB; R_1=H, R_2=ClC_6H_4 for DDM; R_1=CCl_3 R_2= ClC_6H_4 for DDT; L is 4,4′-dicarboxylato-2,2′-bipyridine ligand of Complex 1. For compounds R_1=H, the formation of ketenes may take place (reaction 2)

$$\text{Cl-C}_6\text{H}_4\text{-CH}_2\text{R}_2 + 2\text{O=Mo(O)Cl}_2\text{L/TiO}_2 \xrightarrow{h\nu}$$
$$(\text{Cl-C}_6\text{H}_4)_x\text{-C(O)R} + 2\text{Mo(O)Cl}_2\text{L/TiO}_2 + \text{H}_2\text{O} \qquad (2)$$
$$2\text{Mo(O)Cl}_2\text{L/TiO}_2 + \text{O}_2 \rightarrow 2\text{O=Mo(O)Cl}_2\text{L/TiO}_2 \qquad (3)$$

Correlation between the yield of dicofol and turnover number (Δ[DDT]/[anchored complex]) in experimental cycles, is presented in Table 1. The turnover number in the second cycle increases more than two times after the re-oxidation in the second period of the first cycle, becoming 2.13 from 0.63 (Table 1), while it could be no more than 2, or no more than 1 for only one cycle, taken

separately, in consideration that the reaction (1) is a predominant way of the consumption of DDT. In other words, the consumption of DDT quantitatively exceeds the initial stoichiometric quantities of the reaction (1), which proceeds under UV-irradiation, after the "dark" reaction, in the absence of dioxygen.

Table 1

Experimental data of the dependence of the turnover number (Δ[DDT]*mmol*/[anchored complex]*mmol*) and the yield of dicofol on the number of experimental cycles (the reaction time (*h*) is given in parentheses)

Number of the experimental cycles	1	2	3	4	5
Turnover number	0.63 (5)	2.13(11)	2.58(17)	3.38(23)	3.68(32)
Yield of dicofol (*mole* %)	9.5	13.5	15.4	18.2	21.0

It is noteworthy that the yield of dicofol also increases (about 1.42 times) with the increase of the consumed amount of DDT in the nearly the same reaction time interval in the first period of the second cycle. In further experimental cycles, apparently, the different reaction channels of oxidation and decomposition become more significant than the selective formation of dicofol by the reactions (1)-(3).

Nearly analogous situation can be observed in experiments of the oxidative destruction of CEB (Fig. 1). The accumulated amounts of the main product 4′-chlorobenzene in the first period of the second experimental cycle were more than possible stoichiometric amounts of the reactions (1)-(2).

These facts permitted to assume that in the second periods of the experimental cycles, the re-oxidation with dioxygen of the reduced Mo(IV) into Mo(VI) occured by the formation of the oxo-peroxo-Mo(VI) moiety in coordination sphere of the anchored complex.

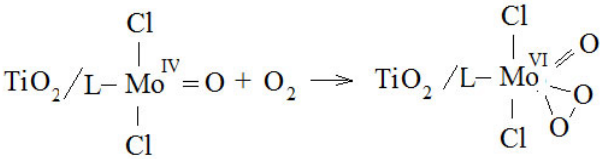

As a result, the capacity of Complex 1 in oxygen atom transfer reactions may be either doubled or, at least, noticeably increased. In this regard, the primary reaction in the first periods of the second and consecutive experimental cycles may be represented as:

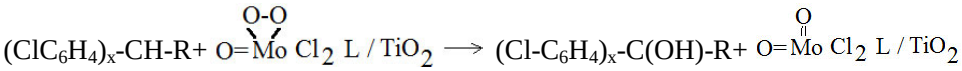

Although the main peculiarities of the photocatalytic oxidation or/and oxidative destruction by the applied catalyst for the mentioned three compounds, in general, are similar, the oxidation of DDT exhibits some important differences. For example, the post-reaction mixture also contains products of the reductive decomposition, such as DDE (1,1-dichloro-2,2-bis(p-chloro-phenyl)ethylene about 9%), DDD (1,1-

dichloro-2,2-*bis*-(p-chlorophenyl)ethane), DDM (2,2-*bis*-(p-chloropheny)methane, diphenylmethane), and others, summarily about 13-14%.

Conclusions

As it was shown on the given examples, in photocatalytic oxidation of the mentioned compounds, the main primary reaction occurs by the selective activation and functionalization with the anchored Complex 1 of the benzylic (or bibenzylic) C-H bond, producing alcohols or ketones via oxo-atom from transition-metal to substrates. Note that, in this case, the chlorophenyl fragments of the mentioned compounds may rest untouched in the formation of the main products of primary reaction.

In the aspects of the reaction mechanism, the observed acceleration of the reaction in the first periods of the second and consequent experimental cycles may be assigned to the formation of oxo-peroxo-Mo(VI) moieties in coordination sphere of the complex in the second periods, which, apparently, are more active in oxo-atom transfer reactions to benzylic carbon-atom.

ՔԼՈՐԱՑՎԱԾ ԱԼԿԱՆՆԵՐԻ ՖՈՏՈԿԱՏԱԼԻԶԱՅԻՆ ՕՔՍԻԴԱՑՈՒՄԸ ԹԹՎԱԾՆՈՎ

Լ. Ա. ՄԱՆՈՒՉԱՐՈՎԱ, Ռ. Ա. ԲԱԽՉԱՋԱՆ և Լ. Ա. ԹԱՎԱԴՅԱՆ

Ուսումնասիրվել է մոնո- և դիֆենիլտեղակալված ալկանների որոշ քլորացված ածանցյալների 1-քլոր-4-էթիլբենզոլ; 4,4'-դիքլորդիֆենիլմեթան; 1,1,1-եռքլոր-2,2-բիս (p-քլորֆենիլ)էթան ֆոտոկատալիզային օքսիդացումը թթվածնով, հետերոգենացված դիօքսո-Mo-մետաղօրգանական կոմպլեքս (դիօքսո-մոլիբդեն(VI)-դիքլոր[4, 4'-դիկարբոքսիլատո-2,2'-բիպիրիդին]) TiO_2 լուսազգայուն կրիչի վրա ֆոտոկատալիզատորի ներկայությամբ, ՈւՄ (λ = 253.7 նմ) ճառագայթման տակ: Ցույց է տրվել, որ այդ միացությունների բենզիլային C-H կապի ընտրողական ակտիվացման մեջ խարսխված Mo-մետաղօրգանական կոմպլեքսի կատալիտիկ դերը մեղմ պայմաններում համապատասխան օքսիդների առաջացմամբ: Քննարկվել են այս խմբի ռեակցիաների հնարավոր մեխանիզմները: Առաջարկվել է, որ օքսո-պերօքսո-Mo(VI) մասնիկների ձևավորումն, ըստ երևույթին, խթանում է օքսո-ատոմի փոխանցումը Mo-կոմպլեքսից դեպի սուբստրատ:

ФОТОКАТАЛИТИЧЕСКОЕ ОКИСЛЕНИЕ ХЛОРИРОВАННЫХ ФЕНИЛАЛКАНОВ КИСЛОРОДОМ

Л. А. МАНУЧАРОВА, Р. А. БАХЧАДЖЯН и Л. А. ТАВАДЯН

Исследовано фотокаталитическое окисление некоторых хлорированных производных моно- и дифенилзамещенных алканов:1-хлор-4-этилбензола; 4,4'-дихлордифенилметана; 1,1,1-трихлор-2,2-бис(p-хлорфенил)этана, молекулярным кислородом в присутствии фотокатализатора: гетерогенизированного диоксо-Mo органометаллического комплекса (диоксо-молибден(VI)-дихлоро[4,4'-дикарбоксилато-2,2'-бипиридин]), закрепленный на фоточувствительном носителе TiO_2, при УФ-облучении (λ= 253.7 *нм*). Показана каталитическая роль закрепленного на носителе Mo-металлорганического комплекса в селективной активации бензиль-

ных С-Н связей этих соединений с образованием соответствующих продуктов окисления в мягких условиях. Каталитический цикл состоит из двух последовательных стадий, включающих окисление субстрата посредством переноса оксо-атома от диоксо-Mo(IV)-комплекса при UV-облучении, и регенерации восстановленного Mo(IV)-центра окислением молекулярным кислородом в темноте. Показано, что в этих условиях даже такой устойчивый загрязнитель как ДДТ может быть селективно окислен до дикофола, что в настоящее время другими путями невозможно. Предложен возможный механизм для этой группы реакций. Очевидно, что формирование оксо-пероксо-Mo(VI) частиц способствует переходу оксо-атома от Mo-комплекса к субстрату.

REFERENCES

[1] *Gelfand S.* Chlorocarbons, hydrocarbons (toluene). In: Kirk, R. E.; Othmer, D.F. Eds. Encyclopedia of Chemical Technology, v.5, 3rd edition, NY: John Wiley and Sons, New York, 2004, p.896, pp. 819-827.

[2] O*rme-Zavaleta J., Connery J.* Eds. Drinking Water Health Advisory: Volatile Organic Compounds. US Environmental Protection Agency. Lewis Publishers, Chelsea, 1991, 259 p., p. 37.

[3] *Adrians P., Gruden C., McCormick M.L.* Biochemistry of halogenated hydrocarbons. pp. 511-540. In: Sherwood Lolla B. Ed**.** Environmental Geochemistry, v. 9, Holland H.D.; Turekian K.K. Exclusive Eds. Elsevier, Amsterdam, 2005, 631 p.

[4] *Srikumar K.* Chemical Process Technology and Simulation. PHI Leaming Private Limited, Dehli, 2013, 352 p., p. 127.

[5] *Sheldon R.A.* Allylic and benzylic oxidation. Chapter 9.4, pp. 519-526. In: Sheldon, R.A.; van Bekkum, H. Fine chemicals through heterogeneous catalysis. Eds. Wiley-VCH, Weinheim, Germany, 2001, 611 p.

[6] *Arzoumanian H.* Molibdenum-oxo and peroxo complexes in oxygen atom transfer processes with O_2 as a primary oxidant. Current Inorganic Chemistry, 2011, 1, 2, p. 140.

[7] *Arzoumanian H., Bakhtchadjian R.* Oxo-Atom transfer reactions of transition metal complexes in catalytic oxidation with O_2 on the light of some recent results in molybdenum-oxo chemistry. Chemical Journal of Armenia, 2012, 65, 2, p.168.

[8] *Paez C.A., Castellanos, N.J., Martınez F.O., Ziarelli F., Agrifoglio G., Paez-Mozo E.A., Arzoumanian H.* Oxygen atom transfer photocatalyzed by molybdenum(VI) dioxodibromo-(4,4′-dicarboxylate-2,2′-bipyridine) anchored on TiO_2. Catalysis Today, 2008, 133–135, p. 619.

[9] *Bakhtchadjyan R.A., Tsarukyan S.V., Manucharova L.A., Tavadyan L.A., Barrault J., Martinez F.O.* Photochemical oxidative decomposition of 1-chloro-4-ethylbenzene in the presence of dioxo-molybdenum(VI) complex anchored on the TiO_2. Chemical Journal of Armenia, 2011, 64, 1, p. 9.

[10] *Arzoumanian H., Castellanos N.J., Martınez F.O., Paez-Mozo E.A., Ziarelli F.* Silicon-assisted direct covalent grafting on metal oxide surfaces: Synthesis and Characterization of carboxylate N,N′-ligands on TiO_2. Europ. J. Inorganic Chemistry, 2010, 11, p.1633.

[11] *Castellanos N.J., Martınez F., Lynen F., Biswas, S., Van Der Voort P., Arzoumanian H.* Dioxygen activation in photooxidation of diphenylmethane by a dioxo-molybdenum(VI) complex anchored covalently onto mesoporous titania. Transition Metal. Chemistry, 2013, 38, p. 119.

ՀԱՅԱՍՏԱՆԻ ՀԱՆՐԱՊԵՏՈՒԹՅԱՆ ԳԻՏՈՒԹՅՈՒՆՆԵՐԻ
ԱԶԳԱՅԻՆ ԱԿԱԴԵՄԻԱ
НАЦИОНАЛЬНАЯ АКАДЕМИЯ НАУК РЕСПУБЛИКИ АРМЕНИЯ
NATIONAL ACADEMY OF SCIENCES OF THE REPUBLIC OF ARMENIA

Հայաստանի քիմիական հանդես
Химический журнал Армении **71, №4, 2018** Chemical Journal of Armenia

UDC 534.46:541.44.661.968

HYDRIDES OF TRANSITION METALS AND THEIR ALLOYS AS CONDENSED HYDROGEN CARRIERS

S. K. DOLUKHANYAN[*], A. G. ALEKSANYAN, G. N. MURADYAN[*], V. Sh. SHEKHTMAN[**], O. P. TER-GALSTYAN[*], H. G. HAKOBYAN[*], N. N. AGHAJANYAN[*] and N. L. MNATSAKANYAN[*]

[*]A. B. Nalbandyan Institute of Chemical Physics, NAS RA
5/2, P. Sevak Str., Yerevan, 0014, Armenia
[**] Institute of Solid State Physics of Russian Academy of Sciences
Chernogolovka, Moscow region, 142432, Russia
E-mail: seda@ichph.sci.am

The review of the work of the Laboratory of High-Temperature Synthesis and Technology of Inorganic Materials, ICP NAS of Armenia, is presented. For the first time, more than 200 binary and multicomponent hydrides and deuterides of metals and alloys were synthesized by the method of self-propagating high-temperature synthesis (SHS). These studies became the physico-chemical basis of SHS processes in Me-H systems and led to the formulation of technological works having huge industrial prospects. Hydrides of transition metals and alloys are of great value as condensed hydrogen carriers. Further studies of hydrides synthesized in the SHS regime made it possible to develop yet another fundamentally new method for the synthesis of alloys and intermetallides of transition metals, which we called the "Hydride cycle-HC" method. The method is based on reactions of interaction of two or more metal hydrides, for example, $xMe'H_2 + (1-x)Me''H_2 \rightarrow$ alloy $Me_xMe_{(1-x)} + H_2\uparrow$. It is shown that when a compacted mixture of two or more hydrides, as well as hydride and metal powder (for example, TiH_2 and Al) is heated, the removal of hydrogen from the compacted charge at temperatures slightly above the dissociation temperatures of the hydrides leads to the formation of strong, nonporous, compact binary, ternary alloys of these metals. More than 100 alloys and intermetallics in Ti-Zr systems were synthesized in the HC mode; Ti-Hf; Ti-Nb; Ti-V; Zr-Hf; Ti-Zr-Hf; Ti-Ni; Zr-Co; Ti-Al; Nb-Al, etc. Some of the obtained compact alloys without preliminary grinding interact with hydrogen in the SHS mode, forming hydrides with a high hydrogen content.

Figs. 18, tables 4, references 25.

1. Hydrides of transition metals

When the reserves of fossil fuels such as oil, natural gas and coal are depleted and disappear, they will be replaced by water decomposed to hydrogen and oxygen. Hydrogen is a fuel of the future. Although it was shown that hydrogen has a great future, its accumulation, storage and usage is dangerous. Gaseous hydrogen is stored in gas cylinders at a pressure of 150 *atm* with explosion hazard. Hydrogen is liquefied at temperatures between -253– -259°C and stored in special containers – tanks.

It is worth noting that at present, the modern technology offers a more advantageous way of hydrogen storage by incorporation it into a metal, storage without loss for a long time at ambient temperature and pressure, and extraction at a right time applying heating. The extracted hydrogen is of as high purity as 99.99% because at the temperature of its extraction no other gases or impurities are released from the metal. There is a huge literature devoted to metal-hydrogen compounds named hydrides. Actually, the term "hydrides" combines a very broad class of substances with cardinally different properties, chemical composition and type of inter-atomic bonds.

Fig. 1 shows the elementary crystal lattice of titanium hydride, TiH_2.

The hydrides of transition metals and alloys having "metallic bonds", the so-called metal hydrides, are the subject of the present article. Hydrogen, embedded in the metal can radically change the properties of the latter. The interaction of transition metals with hydrogen results in formation of structures, in which the hydrogen atoms are located in the interstices of the metal sublattice, for example, in tetrapores.

Hydrides of transition metals are of wide interest as a large class of compounds with unique physical and chemical characteristics. Table 1 presents some characteristics of several hydrides of transition metals and hydrogen containing materials.

Table 1

The most important characteristics of some transition metal hydrides and hydrogen containing materials

Compound	Atomic concentration of H_2, $N_H \times 10^{22}$ at. *H/cm*^{3}	Content of H_2, wt. %	Dissociation temperature, ^oC
ZrH_2	7.34	2.01	800-1000
TiH_2	9.5	4.02	600-800
MgH_2	6.7	7.6	
VH_2	11.4	3.78	
$ZrV_2H_{4.3}$	7.06	1.85	550-600
$ZrNiH_3$	7.73	1.96	250-350
$ZrCoH_3$	7.64	1.95	250-350
$TiFeH_2$	5.5	1.5	80
$LaNi_5H_7$	7.6	1.5	30-50
Mg_2NiH_4	5.9	3.8	200-250
Gaseous H_2 at 100 *atm*	0.65	–	–
Liquid H_2	4.2	–	–
H_2O	6.7	–	–
Lithium borohydride, $LiBH_4$	7.6	18.5	–
Polystyrene, $(C_8H_9)_n$	5.4	1.05	–

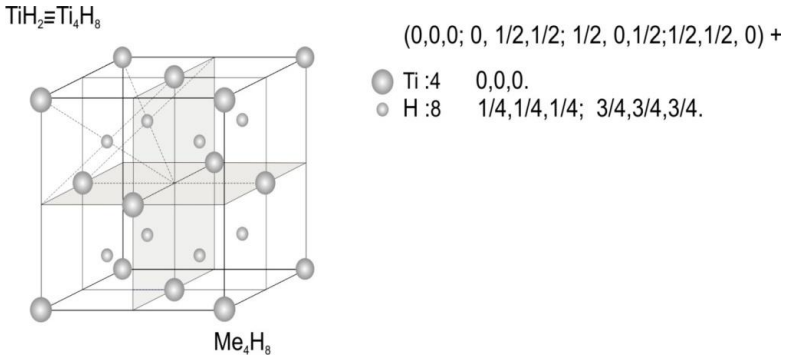

Fig. 1. Elementary crystal lattice of TiH_2.

The data in Table 1 show that the hydrogen content in a unit volume of metal hydride is much higher than in a unit volume of many hydrogen-containing materials including liquid hydrogen and water. Consequently, hydrides of transition metals and alloys are of great value as condensed hydrogen carriers.

The interest in hydrogen and metal hydrides is associated with two global problems: protection of environment and depletion of fossil carbon and hydrocarbon fuels. Metal hydrides are multifunctional materials. The range of application of hydrides of metals and alloys is very wide.

1. In hydrogen energy, the metal hydrides serve as hydrogen accumulators and are promising as components of environmentally pure fuel. In this sense, the hydrides with dissociation temperatures below 300°C are of particular interest [1].
2. In nuclear power, the metal hydrides are used as biological protection against ionizing radiation and fast neutron flux. The mass of hydrogen atom is closer to the mass of neutron than the mass of any other element; therefore, upon interaction with neutron, it exhibits a unique property: is the most effective absorber of neutron energy. The content of hydrogen atoms in volume unit, $N_H \times 10^{22}$ at. H/cm^3, is the most important characteristic determining the effectiveness of any protective material in slowing down neutron flux. The data in Table 1 show that this characteristic for metal hydrides is the best [2].
3. In powder metallurgy, the metal hydrides are used as most convenient compounds for dispersing the refractory metals. It is known that the introduction of hydrogen into the crystal lattice of a metal brings to its embrittlement [3]. The hydrides of transition metals can be easily ground to micron and submicron grain sizes, besides they consist of crystallites of nanoscale sizes. In metallurgy, the term "hydrogen fragility" is known. In steel and cast iron, this very undesirable phenomenon can appear due to the hydrogen impurity even not exceeding 0.1wt.%.
4. Metal hydrides can serve as sources of the purest hydrogen, ≈ 99.4444%.
5. Metal hydrides are successfully used as catalysts in the chemical industry.

Many other original and unexpected applications of metal hydrides have been described in the literature.

The current method of metal hydride producing consists in the heat treatment of metal at high temperature (~ 1000^{o}C) in inert atmosphere and stepwise cooling it in the hydrogen atmosphere. The process lasts from 10 to 40 *hours*, depending on the metal. For preparation of hydride of stoichiometric composition, multiple cycling, deep purification of hydrogen, etc. are required. The obvious difficulty of producing hydrogen rich, single-phase metal hydrides hinders their wide application in industry, studying their physical and chemical properties for finding new areas and expanding application fields [4].

The SHS method has appeared a perspective direction for the synthesis of metal hydrides.

The essence of SHS method consists in the usage of heat of exothermic reaction after local instantaneous initiation of combustion in a thin layer of non-heated mixture of metal and solid metalloid (C, B, Si), or metal and gaseous metalloid (N_2). The heat of the initiated exothermic reaction creates a front of high temperature, which propagates with a constant linear velocity through the mixture at the expense of transferring the heat from layer to layer. The process proceeds exclusively at the expense of heat of chemical reaction without input of external energy [5].

At the Institute of Chemical Physics of the AS of Armenian SSR in the Laboratory of high-temperature synthesis, the SHS processes in Me-H systems were predicted and implemented for the first time [6-9]. The study of metal combustion in hydrogen in the SHS mode resulted in the synthesis of hydrides of transition metals. Therefore, a promising SHS method for the synthesis of hydrides of transition metals and alloys was elaborated. The interaction of a transition metal with hydrogen occurs with release of significant heat. For example, $Ti + H_2 \leftrightarrow TiH_2 + Q$ (ΔH of TiH_2 formation is equal to 39 *kcal/mol*). The released heat ensures the propagation of the combustion front along the unheated metal tablet with constant linear velocity.

Fig. 2 shows the scheme of the exothermic reaction flow in the Ti-H_2 system.

Fig. 3 shows the photo of titanium hydride formed in SHS mode.

Fig. 4 shows the thermograms of combustion of zirconium, titanium and ZrCo intermetallic in hydrogen atmosphere at P = 3 *atm*.

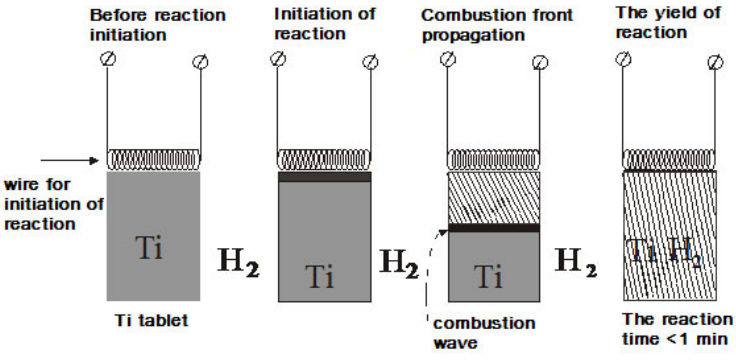

Fig. 2. Scheme of exothermic reaction in Ti-H_2 system.

Fig. 3. Photo of non-crushed SHS-synthesized TiH_2 sample.

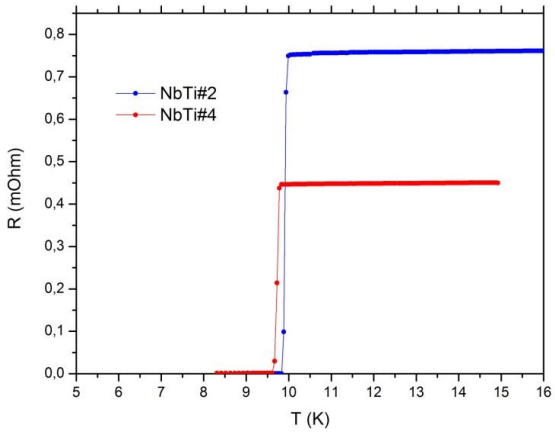

Fig.10. The dependences from the temperature of resistance of $Ti_{0.4}Nb_{0.6}$ and $Ti_{0.5}Nb_{0.5}$ alloys.

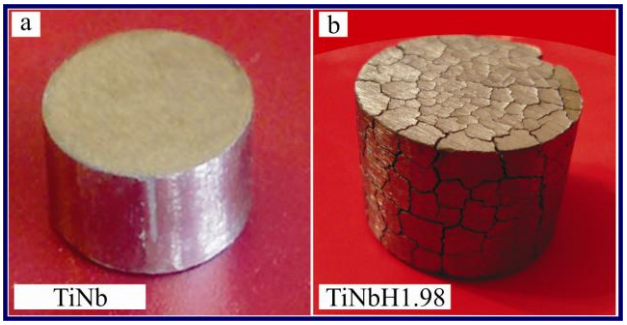

Fig. 12. The pictures of $Ti_{0.5}Nb_{0.5}$ alloy and its hydride.

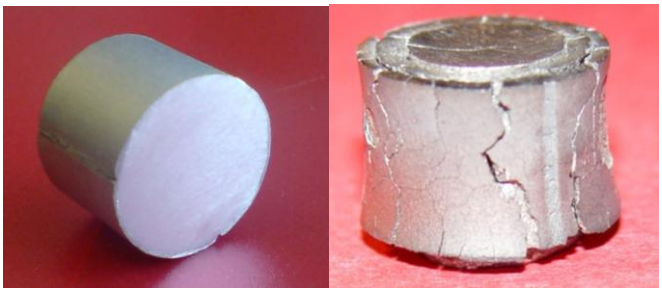

a b

Fig. 18. The pictures of: a – $Ti_{0.5}Al_{0.25}Nb_{0.25}$ alloy; b – its hydride.

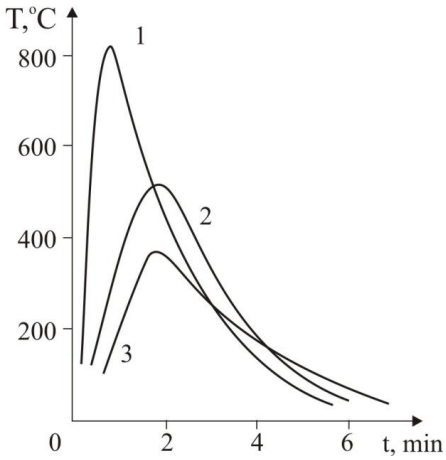

Fig. 4. The thermograms of combustion of zirconium (1), titanium (2) and ZrCo intermetallic (3) in hydrogen atmosphere at P = 3 *atm.*

Numerous hydrogen-containing systems, such as Me-H, Me-Me[1]-H, Me-nonmetal (C, N) - H have been investigated, including:

1. III, IV and V group and rare earth metals – hydrogen (or deuterium) [6];
2. IV and V group metals – carbon – hydrogen [7];
3. IV and V group metals – nitrogen – hydrogen [8];
4. Zr_2Ni, Zr_2Co, ZrNi, ZrCo, Ti_2Co and other intermetallics – hydrogen [9].

The implemented researches resulted in:

- synthesis of more than 200 compounds: binary hydrides and deuterides of III-V group transition metals and lanthanoides (TiH_2, ZrH_2, HfH_2, $NbH_{1.23}$, PrH_2, etc.), as well as of carbohydrides, hydridonitrides, hydrides of intermetallics, based on titanium, zirconium, nickel, cobalt, etc. [6, 9, 10];
- elucidation of the scientific basis for SHS processes proceeding in hydrogen atmosphere in various condensed systems [10];
- clarification of the factors, controlling the characteristics of combustion wave, velocity of its propagation, the temperature and completeness of combustion and other conditions demanded for production of compounds of given chemical and phase composition [11];
- proof of a two-stage mechanism of combustion and formation of hydrides in SHS: in the first stage, a solid solution of hydrogen in metal is formed in the combustion front; this stage is followed by the second stage, when a stoichiometric hydride is formed by saturation of sample with hydrogen (after-hydrogenation) [6-11];
- description ofthe physical and chemical characteristics of synthesized hydrides (heat resistance, dissociation kinetics, etc.) [6-11].

Fig. 5 shows the diffraction patterns of TiH_2, $NbH_{1.3}$, $TiC_{0.4}$ $H_{1.2}$ and $TiN_{0.21}H_{1.34}$ hydrides.

Fig. 6 shows the microstructure of synthesized in SHS mode niobium hydride.

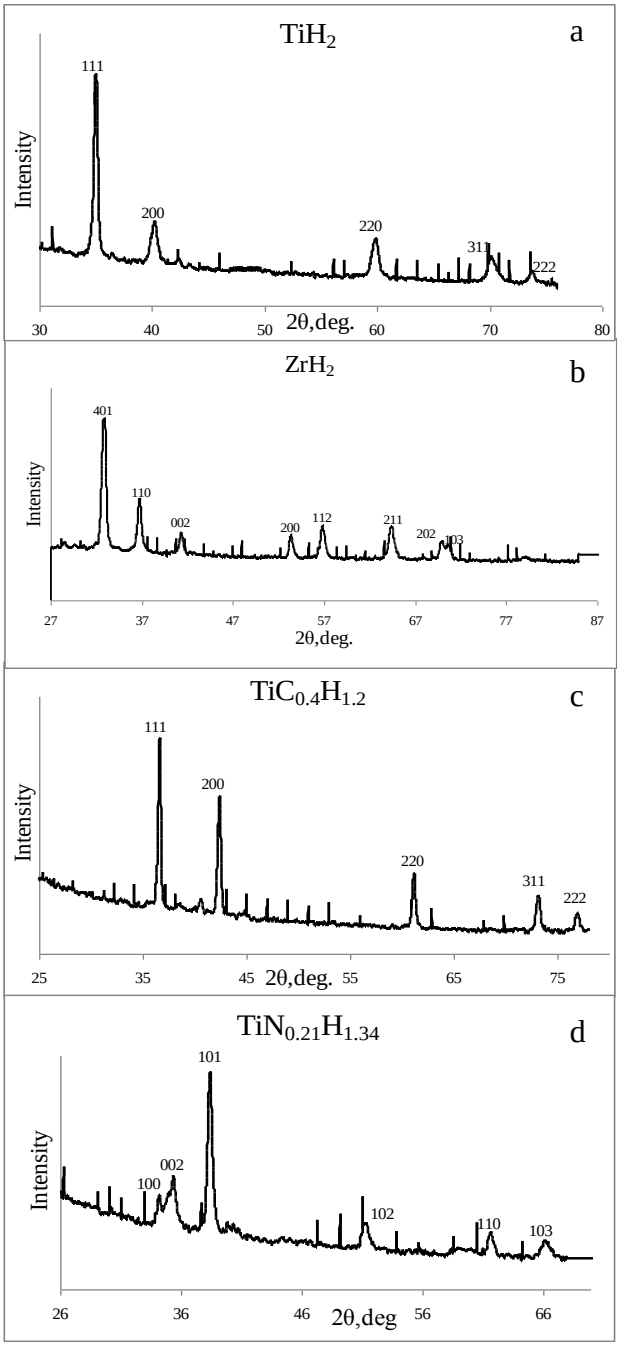

Fig. 5. X-ray patterns of SHS hydrides: a) TiH2, b) $NbH_{1.3}$, c) $TiC_{0.4}H_{1.2}$, d) $TiN_{0.21}H_{1.34}$.

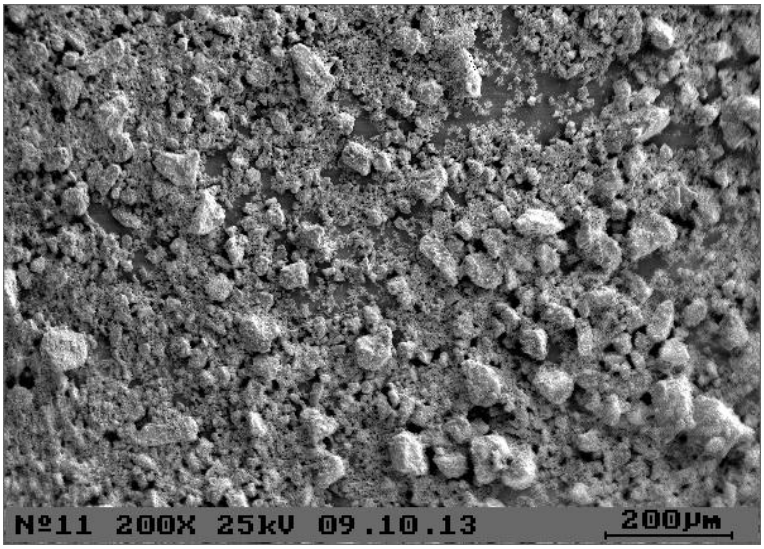

Fig. 6. Microstructure of SHS-synthesized niobium hydride, $NbH_{1.23}$.

Tables 2 and 3 show some characteristics of SHS-synthesized binary hydrides, deuterides, carbohydrides and hydridonitrides.

Table 2

Characteristics of SHS-synthesized binary hydrides and deuterides

Metal	H_2, D_2content, wt.%	Cristal structure	Lattice parameters, Å	Calculated formula
Sc	4.25	FCC	a=4.782	ScH_2
	3 .01	FCC	a =4.698	$ScD_{0,73}$
Y	3.255	HCP	a=3.661; c= 6.630	$YH_{2,9}$
	4.41	FCC	a= 5.197	$YD_{2,1}$
Ti	4.01	FCC	a= 4.460	TiH_2
	7.03	FCC	a =4.51	$TiD_{1,82}$
Zr	2.16	tetragonal	a= 3.527; c= 4.476	ZrH_2
	4.16	tetragonal	a= 3.520; c= 4.476	$ZrD_{1,96}$
Hf	1.09	tetragonal	a= 4.911; c= 4.405	HfH_2
	2.11	tetragonal	a= 4.911; c= 4.405	$HfD_{1,93}$
V	1.71	tetragonal	a= 3.310; c= 3.339	$VH_{0,8}$
Nb	0.95	orthorhombic	a=4.451; b=4.878; c=3.453	NbH
Nd	1.78	FCC	a=5.446	$NdH_{2,6}$
	3.61	FCC	a=5.364	$NdD_{2,5}$
Sm	1.87	HCP	a=3.771; c=6.782	SmH_3
Ho	1.78	HCP	a=3.653	HoH_3
Gd	1.79	HCP	a=3.373; c=6.71	$GdH_{2.88}$

Table 3

Characteristics of SHS-synthesized carbohydrides and hydridonitrides

Formula	Content, wt.%			Crystal structure and lattice parameters, Å	Dissociation temperature, °C
	H_2	C	N_2		
$TiC_{0.4}H_{1.2}$	2.2	8.45	–	HCP, a=3.09; c= 5.08	400-840
$TiC_{0.45}H_{0.5}$	0.95	10.08	–	FCC, a=4.296	380-840
$ZrN_{0.3}H_{1.52}$	1.52	–	3.81	HCP, a=3.27; c= 5.519	370-795
$TiN_{0.28}H_{1.33}$	2.2	–	7.6	HCP, a=3.044; c= 5.09	455-610
$Ti_{0.7}V_{0.3}C_{0.69}$	–	14.42	–	FCC, a=4.272	–
$Ti_{0.7}V_{0.3}C_{0.60}N_{0.30}$	–	12.65	6.78	FCC, a=4.205	–
$Ti_{0.7}V_{0.3}C_{0.7}H_{0.16}$	0.28	14.57	–	FCC, a=4.249	–
$Ti_{0.7}V_{0.3}N_{0.69}H_{0.2}$	–	14.39	3.35	FCC, a=4.252	–
$Ti_{0.7}V_{0.3}C_{0.7}N_{0.13}H_{0.1}$	0.17	14.42	3.1	FCC, a=4.249	–
$Zr_{0.5}Nb_{0.5}C_{0.42}N_{0.34}$	–	5.17	4.34	FCC, a=4.57	–

The study of combustion in hydrogen of various condensed systems permitted the elucidation of the physical and chemical basis of SHS process in metal-hydrogen systems and led to the carrying out technological researches having enormous industrial prospects. High-performance technological processes for the synthesis of various hydrides have been developed, which have no analogues in the world. The developed methods can provide production of large assortment of cheap high-quality hydrides. At the experimental plant "ArmNIItsvetmet" (Yerevan) more than 20 *tons* of titanium and zirconium hydrides were produced.

The SHS method for the synthesis of hydrides has several significant advantages over traditional methods: high productivity, high quality of hydrides, practically no energy consumption, ecological purity and safety of the process, etc. The SHS synthesis of hydrides excludes a number of laborious operations demanded in the traditional methods, such as preliminary activation of the metal, deep purification of hydrogen, fine dispersion of metal powders, etc.

A special advantage of SHS is the possibility of metal sponge, chips and other industrial waste utilization using them as raw material. It means that the SHS hydrogenation can be applied in the high-efficiency recycling of the waste of refractory metals (Ti, Zr, Hf, Nb, V, etc.) and alloys, formed in huge quantities during their mechanical processing. This is a very cheap way of synthesis of valuable hydrides of expensive metals.

2. Synthesis of alloys and intermetallics of transition metals by hydride cycle method

Further study of SHS synthesized hydrides of transition metals brought to the development of a fundamentally new, early unknown method for formation of the

alloys and intermetallics of transition metals, which we called the "Hydride cycle" (HC) method.

The hydrogen-rich metal hydrides are very plastic. It means that they can be effectively pressed (compacted). Fig. 7 shows the microstructures of the initial powder of titanium hydride and of the surface of the tablet compacted from TiH_2. The tablet has a very dense structure. The particles perfectly conform with one another.

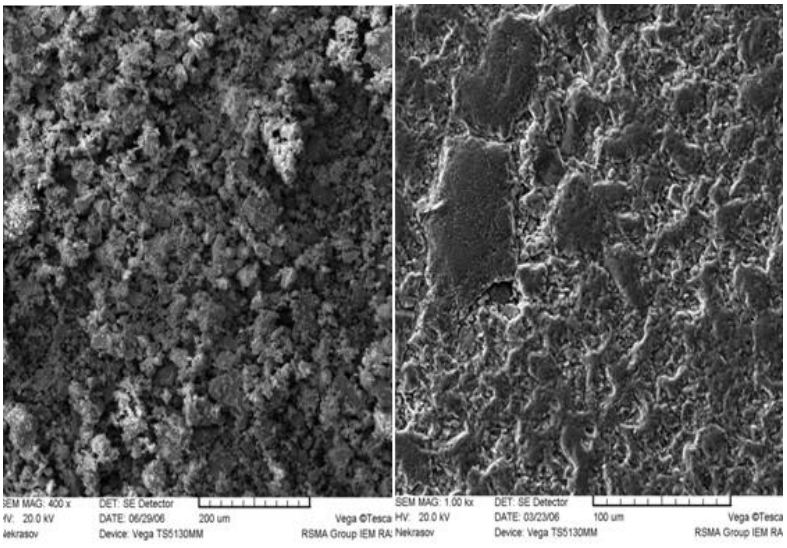

a b

Fig.7.The initial surface of titanium hydride powder (A) and the microstructure of surface of the pressed from it tablet (B).

We used the compatibility of hydrides for elaboration of method for the synthesis of alloys. It was shown that upon heating a compacted mixture of powders of two (for example, TiH_2 and ZrH_2, TiH_2 and NbH_X, TiH_2 and VHx, etc.) or more hydrides, as well as powders of a hydride and metal (for example, TiH_2 and Al, TiH_2 and Fe, TiH_2 and Re, ZrH_2 and Y, etc.), hydrogen was removed a little above the hydride dissociation temperature (far below the melting points of the used metals). This process brought to the formation of strong, nonporous, compact binary (or ternary) alloy of taken metals. In HC mode, more than 100 alloys and intermetallics were synthesized in Ti-Zr, Ti-Hf, Ti-Nb, Ti-V, Zr-Hf, Ti-Zr-Hf, Ti-Ni,Zr-Co and other systems [12-16], among them – the alloys with structure of α-, β-, γ- and ω-phases.

The HC process is based on the reactions:

1. The interaction of hydrides of two metals [12-15]:

$x\mathrm{Me'H_2} + (1\text{-}x)\mathrm{Me''H_2} \rightarrow \mathrm{Me'_xMe''_{(1\text{-}x)}alloy} + \mathrm{H_2}\uparrow$

For example, $TiH_2 + ZrH_2 \leftrightarrow TiZr + H_2\uparrow$ or $TiH_2 + NbH_X \leftrightarrow TiNb + H_2\uparrow$ etc. These reactions resulted in synthesis of $Ti_xZr_{(1\text{-}x)}$, $Ti_xHf_{(1\text{-}x)}$, $Zr_xHf_{(1\text{-}x)}$, $Ti_xNb_{(1\text{-}x)}$, $Ti_xV_{(1\text{-}x);}$ etc. binary alloys.

2. The interaction of hydrides of three metals [16]:

$x\text{Me}'\text{H}_2 + y\text{Me}''\text{H}_2 + z\text{Me}'''\text{H}_2 \rightarrow \text{Me}'_x\text{Me}''_y\text{Me}'''_z$ alloy + $\text{H}_2\uparrow$

For example, $\text{TiH}_2 + \text{ZrH}_2 + \text{HfH}_2 \rightarrow \text{Ti}_{0.66}\text{Zr}_{0.22}\text{Hf}_{0.12} + \text{H2}\uparrow$ ternary alloys formed

3. The interaction of hydride of any metal of *III, IV, V groups with any metal* of *III, VI, VII, VIII groups* [17-19]:

$x\text{Me}'\text{H}_2 + (1\text{-}x)\text{Me}'' \rightarrow \text{Me}'_x\text{Me}''_{(1-x)}$alloy + $\text{H}_2\uparrow$ (Me″ can be: Al, Mn, Co, Ni, Fe, Re).

For example, TiH_2 and Al, TiH_2 and Fe, TiH_2 and Re, ZrH_2 and Y, ZrH_2 and Co (Ni), ZrH_2 and Al, etc. These reactions resulted in formation of ZrCo, ZrNi, TiFe, TiAl, ZrAl, etc. intermetallics.

In [12-20], HC method is described and the experimental results of synthesis of alloys of IV-V group metals are presented. The influence on the characteristics (the crystal structure, density, adsorption properties, etc.) of the synthesized alloys and intermetallics of various parameters: ratio of metal hydride and metal in the reaction mixture; grain size in hydride powder (micro- and nanoscale); compaction pressure, conditions of dehydrogenation and sintering (temperature and rate of heating) was defined. Based on the experimental results, the following mechanism of HC-formation of alloys and intermetallics was suggested. During heating of the compacted mixture $x\text{Me}'\text{H}_2 + (1\text{-}x)\text{Me-H}_2$, due to breaking of the Me-H bonds at 800-1100°*C*, the metals become strongly activated. Simultaneously, hydrogen atmosphere reduced the oxide film, which usually exists on the surface of fine powders. The "open bonds" and the cleaned surface of the powders ensure the solid-phase diffusion of refractory metals at relatively low temperatures. For a more precise description and confirmation of the mechanism of formation of alloys and intermetallics in the HC, a differential thermal analysis (DTA) of the initial charge was carried out under conditions close to the HC. The comparison of these two processes clarified the nature of thermal effects at dissociation of hydrides and formation of alloys.

As starting powders, the metals of high purity were used: zirconium (98.9%), niobium (99.9%), titanium (98.9%), nickel (99.5%), cobalt (99.1%) and aluminum (99.7%). The hydrides of titanium (TiH_2, H_2 content 4.01 wt.%), zirconium (ZrH_2, H_2 content 2.0 wt.%) and niobium ($\text{NbH}_{1.23}$, H_2 content 1.31 wt.%) were synthesized and crushed down to <50 μm particles. In SHS hydrides of transition metals of III, IV, V and RE groups, the hydrogen content is very high, between 2-4 wt.% (60 at.%). As it was mentioned above, due to introducing of hydrogen into the crystal lattice, the metal becomes brittle, it can be easily crushed to micron, submicron grain sizes, consisting of nanoscale crystallites [21]. The powders of one (or more) hydride(s) of transition metals and the same with aluminum, nickel or cobalt were carefully mixed and pressed in collet molds into cylindrical tablet with a diameter of 22-25 *mm* and a height of 8-10 *mm* by hydraulic press, using pressing force between of 20000-45000 *kgf*.

The alloys were produced in a specially designed hermetic unit consisting of a quartz reactor, a furnace, and devices for monitoring the vacuum and temperature in the reactor. A tablet sample was placed into the reactor, evacuated and heated. The HC process was carried out at temperatures of 600÷1100°C. The samples were identified using the chemical, differential-thermal (Derivatograph Q-1500) and X-ray diffraction (Diffractometer DRON-0.5) methods. DTA was carried out by heating the samples up to 1000°C at a rate of 20°C per minute.

2.1. Synthesis of alloys in Ti-Nb system.

Synthesis of alloys in Ti-Nb system proceeds in accordance with the reaction:

$$x\mathrm{TiH_2} + (1\text{-}x)\mathrm{NbH_2} \rightarrow \mathrm{Ti_xNb_{(1\text{-}x)}alloy} + \mathrm{H_2}\uparrow$$

Fig. 8a shows the thermograms of HC-formation of $Ti_{0.6}Nb_{0.4}$ alloy [13]. At heating of 60%TiH_2 + 40%$NbH_{1.23}$ charge up to 1000°C, no thermal effect was registered on the HC thermogram. The sample was kept for about 30 *min* at this temperature, and the heater was turned off. According to XRD data, the sample, cooled down to the ambient temperature, represented a single-phase $Ti_{0.6}Nb_{0.4}$ alloy. Obviously, during heating to 1000°C, the TiH_2 and $NbH_{1.23}$ hydrides dissociated, but because of the high rate of heating, these processes were not reflected on the thermogram in Fig. 8a.

At the heating of the same charge at thermal analysis (Fig. 8b), DTA curve 2 shows three endo-effects at 130, 470 and 580°C, reflecting dissociation of titanium and niobium hydrides. No other thermal effects were registered at the temperature increasing up to 1000°C (8b, curve 1).

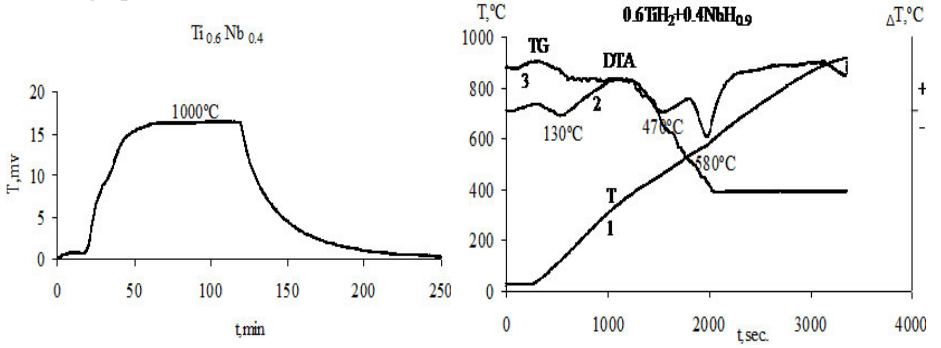

Fig. 8. (a) thermograms of HC-formation of TiNb alloy from TiH_2 + $NbH_{1,23}$; (b) DTA curves at heating of the same charge up to 1000°C.

Fig. 9 shows the diffraction patterns of TiH_2 + $NbH_{1,23}$ mixture, of two Ti-Nb based alloys and their hydrides.

The superconductivity of HC synthesized Ti-Nb-based alloys was investigated. Fig. 10 shows the dependences of reistance on the temperature of $Ti_{0.4}Nb_{0.6}$ and $Ti_{0.5}Nb_{0.5}$ alloys with BCC crystal lattice. In excellent accordance with the literature (Tc = 9.5-10.5*K*), the critical temperatures (transformation to overconductivity) of the studied alloys were registered at Tc = 9.8 and 9.9*K*.

$Ti_{0.5}Nb_{0.5}$-based alloys without preliminary crushing interacted with hydrogen in SHS mode and formed reversible hydrides. For example, $Ti_{0.5}Nb_{0.5} + H_2 \leftrightarrow Ti_{0.5}Nb_{0.5}H_{0.99}$. Fig. 11 shows the thermogram of combustion in hydrogen of $Ti_{0.5}Nb_{0.5}$ alloy.

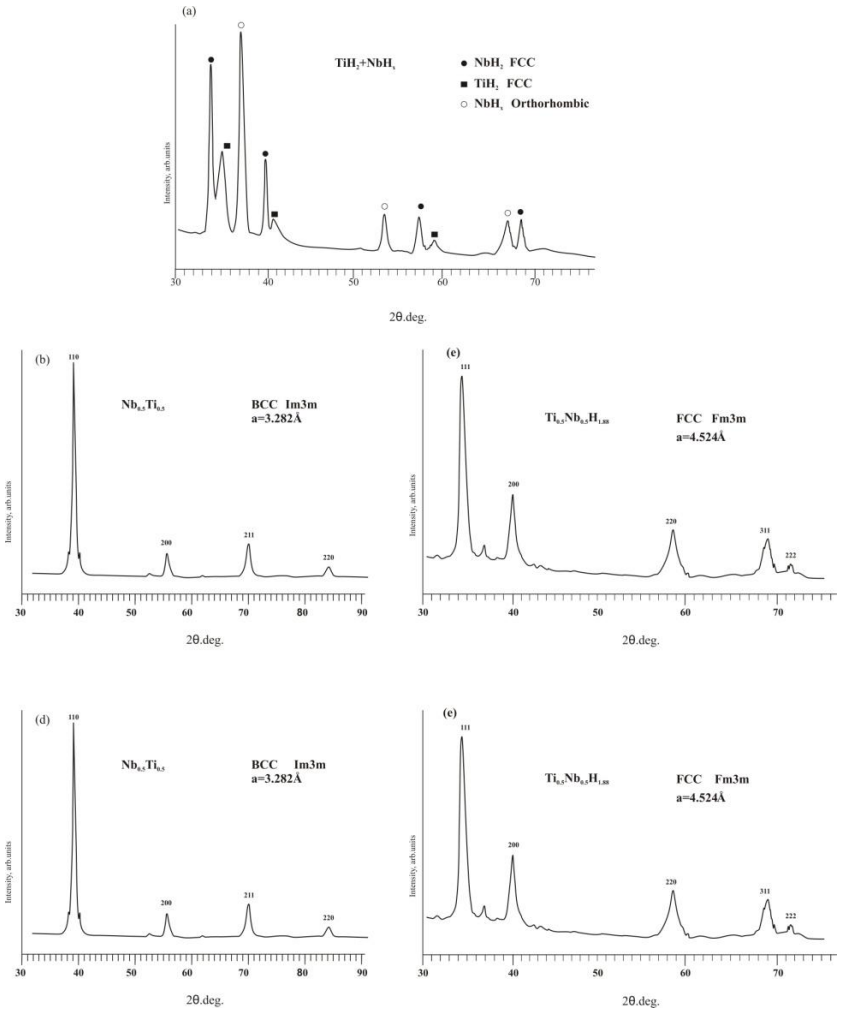

Fig. 9. Diffraction patterns of $TiH_2 + NbH_{1,23}$ mixture (a), two Ti-Nb based alloys (b, c), and the hydrides of these alloys (d, e).

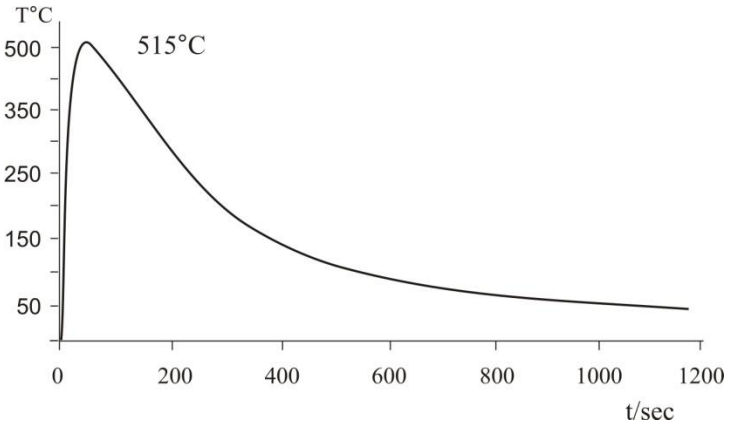

. Fig. 11. Thermogram of combustion in hydrogen of $Ti_{0.5}Nb_{0.5}$ alloy.

Fig. 12 shows the pictures of $Ti_{0.5}Nb_{0.5}$ alloy and its hydride.

Similarly, the alloys were formed in the systems: xTiH$_2$ - (1-x)ZrH$_2$; xTiH$_2$ - (1-x)HfH$_2$; xTiH$_2$-(1-x)VH$_{0.8}$; xTiH$_2$-yZrH$_2$-zHfH$_2$, etc., where the HC alloy formation takes place in solid phase mechanism, excluding melting [12-16]. Fig. 13 shows the diffraction pattern of HC synthesized $Ti_{0.2}Zr_{0.4}Hf_{0.4}$ alloy.

Fig. 14 shows the microstructure of Ti_2Zr alloy, taken on a thin section of flat surface of a sample by scanning electron microscope.

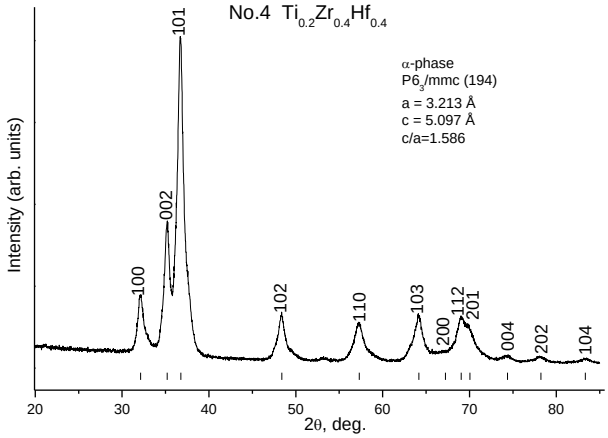

Fig. 13. Diffraction patterns of HC-synthesized alloys of $Ti_{0.2}Zr_{0.4}Hf_{0.4}$.

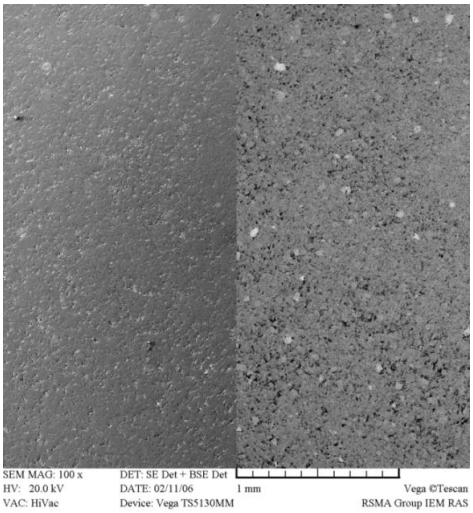

Fig. 14. Microstructure of Ti_2Zr alloy: *a* – surface relief (surveyed in secondary electrons); b – image of the surface in the phase contrast mode (surveyed in reflected electrons).

2.2. Investigation of HC processes in Ti-Al, Zr-Al and Nb-Al systems. Synthesis of Ti, Zr and Nb based aluminides

A distinctive feature of aluminum containing systems is that the formation of aluminides in HC proceeds via exothermic reactions. Fig. 15 shows the thermograms of HC formation of aluminides of titanium, zirconium, hafnium (a, b, c) and the DTA curves (d, e, f) registered upon heating up to 1000℃ of three compositions: 75 at.% TiH_2 + 25 at.% Al (Ti_3Al); 75 at.%ZrH_2 + 25 at.% Al (Zr_3Al) and 75 at.%$NbH_{1.3}$ + 25 at %Al (Nb_3Al).

On the HC thermograms of all three compositions in Fig. 15 a, b, c, the exo-effects are registered at the temperature interval of 670-940°C. The registration of these exo-effects indicates that the reactions of aluminide formation are exothermic. On the DTA curves (Fig. 15 d, e, f), in the temperature interval of 140-600°C, the endo-effects are registered at temperatures corresponding to the dissociation of titanium, zirconium and niobium hydrides. Only in the case of $3NbH_{1.3}$ + 25%Al system (Fig. 15f) on curve 2, the additional endo-effect is observed at 660℃ due to aluminum melting. Simultaneously, on the HC thermogram of the same composition (Fig. 15c), no endo-effects, corresponding to the dissociation of the initial hydrides and/or the aluminum melting were registered.

DTA curves 3 in Fig. 15 d, e, f manifest sharp loss of weight by all the samples due to the dissociation of hydrides and liberation of hydrogen. On the HC thermograms (Fig. 15 a, b, c) and DTA curves 2 (Fig. 15 d, e, f), the temperatures of the exo-effects due to interaction of aluminum with titanium, zirconium and niobium coincide for the same compositions (Fig.15 a and d, b and e, c and f).

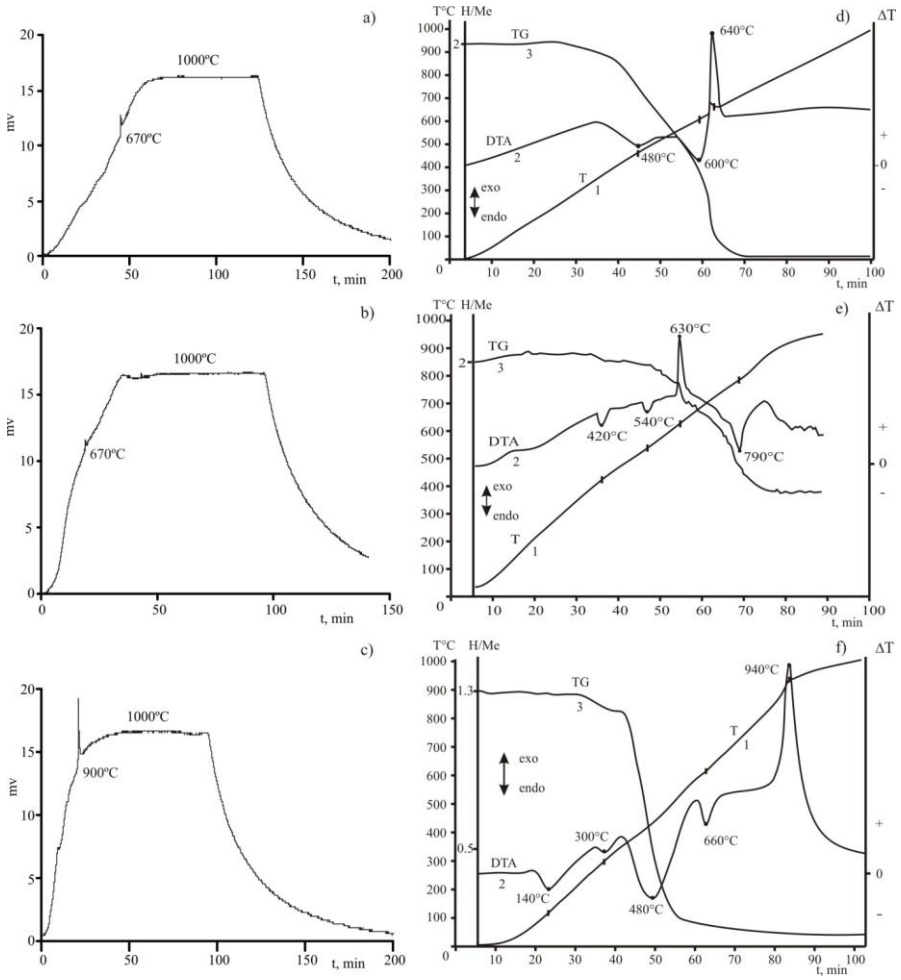

Fig. 15.The thermograms of HC-formation of aluminides (a, b, c) and DTA curves (d, e, f) upon heating up to 1000°C of three compositions: (a, d) – 75at.%TiH_2 + 25at.%Al(Ti_3Al), (b, e) – 75%ZrH_2 + 25%Al(Zr_3Al) and (c, f) – 3$NbH_{1.3}$ + 25%Al(Nb_3Al).

Each of the titanium, zirconium and niobium hydrides shows its own specific feature of interaction with aluminum. The process of titanium aluminide formation in HC (Fig. 15 a) upon heating the initial mixture can be described by:

$$75at.\%TiH_2 + 25at.\%Al \rightarrow 75at.\%Ti + 25at.\%Al + H_2\uparrow \rightarrow Ti_3Al$$

The dissociation of titanium hydride is reflected in the endo-effect at 600°C, which smoothly turns to the exoeffect at 640°C (DTA curve 2 in Fig. 15d) [17].

The behavior of ZrH_2 is different (Fig. 15e) [18]. When the temperature of the charge reaches 540°C (endoeffect on curve 2), the hydride partially decomposes to $ZrH_{1.5}$. A phase transition occurs: the tetragonal crystal lattice transforms to FCC lattice. The future temperature increase brings to the exo-effect at 630°C, indicating the formation of zirconium alumo-hydride. The latter decomposes at 790°C (reflected in the endo-effect), resulting in Zr_3Al formation.

$$3ZrH_2(FCT)+Al \xrightarrow{500^oC} 3ZrH_{1.5}(FCC)+Al + H_2 \xrightarrow{630^oC}$$
$$Zr_3AlH_{1.5}(FCC) \xrightarrow{790^oC} Zr_3Al+H_2\uparrow.$$

As it was noted above, only in the $3NbH_{1.3}$-25%Al system, beside the endo-effect due to dissociation of $NbH_{1.23}$, an endoeffect due to aluminum melting is observed at 660℃ (Fig. 15f). Then, on DTA curve 2, the exoeffect at 940℃ indicates the formation of Nb_3Al (proved by X-ray analyses) [19]. These results from the differences in the conditions of the HC and DTA processes.

Judging by the HC thermograms (Fig. 15 a, b, c) and the DTA curves (Fig. 15 d, e, f), the formation of binary and ternary aluminides of titanium, zirconium and niobium proceeds identical to the alloy formation in HC. At heating of corresponding charge in the reactor, the initial hydrides dissociate. As a result, the metals became activated and quickly interacted exothermically with aluminum in solid-phase mechanism, without aluminum melting. At first, regardless of the aluminum content, solid solution of aluminum in metal is formed. It is worth noting that, according to the phase diagrams, the melting points of aluminum solid solutions in titanium, zirconium and niobium are much higher, in the interval of 1680-2100℃. Hence, the temperatures registered as exo- endo-effects in the DTA curves do not reflect the aluminum melting. This is evidenced by the external view of the samples – no trace of melting is seen. An exception is $3NbH_{1.23}$-Al system (Fig.15 c), in which an endo-peak is observed on the DTA curve at 660℃ due to aluminum melting.

In the HC mode, more than 30 binary aluminides are synthesized: single-phase titanium aluminides: α_2-Ti_3Al, γ-TiAl and $TiAl_3$ [17]; solid solutions of aluminum in zirconium of Zr_3Al composition, accompanied by various zirconium aluminide phases (Zr_4Al_3, ZrAl and Zr_2Al_3); single-phase zirconium aluminides $ZrAl_2$; $ZrAl_3$ [18]; single-phase niobium aluminides $NbAl_3$, Nb_2Al and Nb_3Al, containing about 10% Nb_2Al [19]. Some of aluminides reacted with hydrogen in the SHS mode forming reversible hydrides.

2.3. The HC-formation of ternary aluminides

The processes of HC-formation of ternary aluminides were studied in the following systems: $xTiH_2+yAl+zNbH_{1.23} \rightarrow Ti_xAl_yNb_z+H_2\uparrow$ (where x+y+z=1) and $xTiH_2+(1-x)ZrH_2+Al$ (Al content between 25-75 at.%)

Depending on the $TiH_2/NbH_{1.23}$ and TiH_2/ZrH_2 ratios, single or double phase bimetallic aluminides formed with FCC ($D0_{23}$) and ($D0_{22}$), orthorhombic O-phase, BCC, β or B_2 structures. The experiments resulted in the synthesis of the following aluminides: $Ti_{0.35}Zr_{0.4}Al_{0.25}$; $Ti_{0.55}Zr_{0.2}Al_{0.25;}$ $Ti_{0.15}Zr_{0.1}Al_{0.75}$; $Ti_{0.1}Zr_{0.15}Al_{0.75}$; $Ti_{0.5}Al_{0.23}Nb_{0.27}$; $Ti_{0.33}Al_{0.34}Nb_{0.33}$; $Ti_{0.125}Al_{0.75}Nb_{0.125}$; $Ti_{0.52}Al_{0.15}Nb_{0.33}$; $TiAl_6Nb$; $Ti_{0.25}Al_{0.5}Nb_{0.25}$; $Ti_{0.45}Al_{0.28}Nb_{0.27}$; etc. [20, 22]. Fig. 16 shows the diffraction patterns of $Ti_{0.1}Zr_{0.15}Al_{0.75}$ (a) and $Ti_{0.2}Zr_{0.05}Al_{0.75}$ (b) three-aluminides.

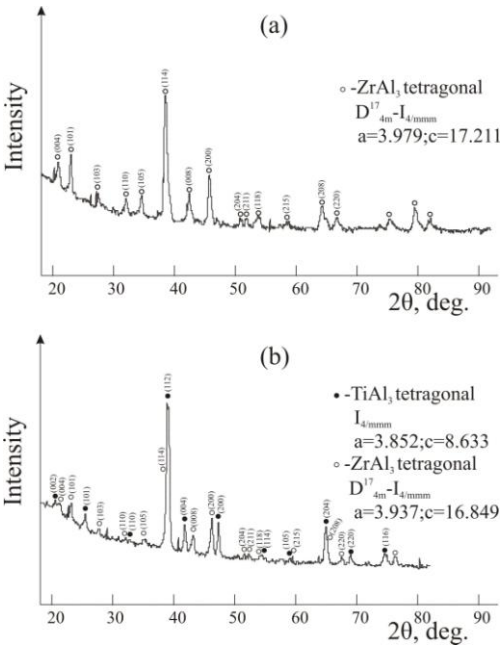

Fig.16.Diffraction patterns of: a – $Ti_{0.1}Zr_{0.15}Al_{0.75}$; b – $Ti_{0.2}Zr_{0.05}Al_{0.75}$.

Fig. 17 shows the diffraction patterns of $Ti_{0.5}Al_{0.23}Nb_{0.27}$, $Ti_{0.333}Al_{0.333}Nb_{0.334}$ and $Ti_{0.125}Al_{0.75}Nb_{0.125}$ aluminides.

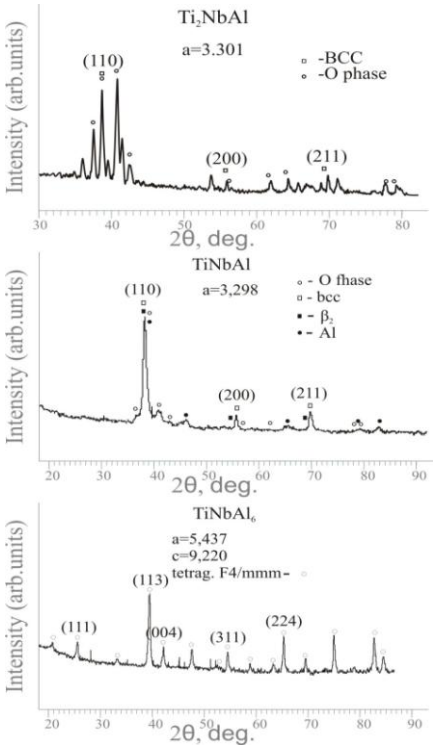

Fig. 17. Diffraction patterns of: a – $Ti_{0.5}Al_{0.23}Nb_{0.27}$; b – $Ti_{0.333}Al_{0.333}Nb_{0.334}$; c – $Ti_{0.125}Al_{0.75}Nb_{0.125}$ aluminides.

It was shown that some aluminides reacted with hydrogen in the SHS mode at P_H = 5-10 *atm* ($T_{comb.}$= 300-500℃), forming reversible hydrides, which dissociated with one endo-effect at ~300-380℃.

$$Ti_{0.375}Al_{0.25}Zr_{0.375} + H_2 \leftrightarrow Ti_{0.375}Al_{0.25}Zr_{0.375}H_{0.99}.$$

$$Ti_{0.5}Al_{0.25}Nb_{0.25} + H_2 \leftrightarrow Ti_{0.5}Al_{0.25}Nb_{0.25}H_{0.89}$$

Fig. 18 shows the pictures of $Ti_{0.5}Al_{0.25}Nb_{0.25}$ alloy and its hydride.

2.4. Synthesis of Ti, Zr and Ni, Co based aluminides

The other example of HC-process is the reaction of a metal (titanium or zirconium) hydride interaction with any metal of VII or VIII groups (Ni, Co, Mn) [23-25]: $TiH_2 + Ni \rightarrow TiNi + H_2\uparrow$; $ZrH_2 + Ni \rightarrow ZrNi + H_2\uparrow$; $TiH_2 + Co \rightarrow TiCo + H_2\uparrow$; $TiH_2 + ZrH_2 + Ni \rightarrow Ti_{44-52}Zr_{40-32}Ni_{16} + H_2\uparrow$; $TiH_2 + 1.2VH + 0.8Mn \rightarrow TiV_{1.2}Mn_{0.8} + H_2\uparrow$; etc. The synthesized compact intermetallics in the combustion (SHS) mode ($T_{comb.}$= 480-600℃) interacted without crushing with hydrogen at a pressure of 10-30 *atm*. These interactions brought to the formation of reversible hydrides of intermetallics with rather high hydrogen content (Table 2). For example:

$$TiNi+H_2 \leftrightarrow TiNiH_3;\ TiV_{1.2}Mn_{0.8} + H_2 \leftrightarrow TiV_{1.2}Mn_{0.8}H_{3.7}$$

Table 4

Characteristics of intermetallics and their hydrides

Compound	H_2content, wt.%	Crystal structure and lattice parameters, Å	Dissociation temperature, °C
Ti_2Co	–	Cubic, a = 11.31	–
Ti_2CoH_3	1.7	Cubic, a = 11.89	240 – 360
Zr_2Co	–	Tetragonal, a=6.387, c=5.542	–
Zr_2CoH_5	2.02	Tetragonal; a=6.906, c=5.55	190 - 360
ZrCo	–	Cubic, a= 3.197	–
$ZrCoH_3$	1.68	Orthorhombic, a= 3.37, b=10.57, c= 4.318	300
Zr_2Ni	–	Tetragonal, a=6,54, c=5.34	–
Zr_2NiH_5	2.08	Tetragonal, a=6,86, c=5.657	170-250
ZrNi	–	Orthorhombic, a= 3.29, b=9.998, c= 4.080	–
$ZrNiH_3$	1.96	Orthorhombic, a= 3.53, b=10.62, c= 4.328	220-260
Ti_2Co	–	Cubic, a= 11.31	–
Ti_2CoH_3	1.7	Cubic, a= 11.89	220-260
$Ti_{44-52}Zr_{40-32}Ni_{16}$	2.10-2.15	C14 hexagonal Laves phase	–
$Ti_{44-52}Zr_{40-32}Ni_{16}H_3$		–	170-260
$TiV_{1.2}Mn_{0.8}$	–	BCC, (HCP traces); a =3.039 (6)	–
$TiV_{1.2}Mn_{0.8}H_{3.67}$	2.36	BCT- monohydride, a = 3.069(6), c= 3. 510(5)	280; 330

2.5. The applications of alloys and intermetallics

Interest in alloys is associated with their numerous and important practical applications. They are used in the high-tech areas of nuclear and hydrogen power

engineering, aerospace, shipbuilding, chemical, automotive, metalworking, machine and machine tool industry, tool manufacturing, radio and electrical engineering, electronics, as composite materials in nuclear power plants, as biocompatible materials in medicine, etc. Particularly, the titanium- and zirconium-based alloys are interesting for the production of construction materials that can work in various chemically active environments (sea water, steam, gas turbines), at low temperatures (for example, in liquid oxygen). The main advantages of titanium alloys are lightness and corrosion resistance. Alloys of zirconium and hafnium are used in nuclear reactors.

In modern materials science, the problem of development of new light, heat-resistant alloys with operating temperatures higher than 550-600°C is acute. From this point of view, transition metal alloys and intermetallics are very promising construction materials. Their advantages are low density, high melting points, high mechanical strength, high heat and electrical conductivity, superconductivity, heat and corrosion resistance, etc. These characteristics condition their use in aerospace and ground engine construction, in the defense industry, in many branches of machine building, chemical and food industry, electronics, medicine, etc. Titanium aluminides are used in the first wall of thermonuclear reactor (TNR) as constructive materials. Aluminides of IV-V group metals are 3 times cheaper than such competing materials as, for example, nickel alloys. The aluminides are known as construction materials and can absorb high amounts of hydrogen and serve as hydrogen storage materials.

The current methods for producing binary and multicomponent alloys and intermetallics are based on melting (induction, electric arc, electron beam), powder metallurgy and mechano-chemistry. Each of these methods bears considerable laboriousness and instrumental complexity. The powder metallurgy methods are characterized by long-duration processes: the interaction of metals in the initial mixtures is mainly determined by the diffusion rates in the solid state. Specific difficulties in obtaining high-quality alloys and intermetallics are associated with the presence of a dense oxide film on the surface of refractory metal particles, which hinders the process of mutual diffusion. In the mechano-chemical methods of producing alloys and intermetallics, the initial components are mixed in drums for 10-40 *hours* or more, when the sticking of the reaction components to the drum wall can occur changing their ratio; besides, the contamination of the reaction mixture by the ball and drum materials can occur.

The differences in melting and evaporation temperatures, in densities of titanium, niobium, zirconium and aluminum also complicate the current technologies. Therefore, new effective methods for producing binary and multicomponent alloys with given physical and technical properties are urgently demanded in modern materials science. The described in the present work Hydride Cycle method can be such a promising technique.

The significant advantages of "Hydride Cycle" method over the above presented traditional methods are listed below.

1. The alloys and intermetallics are formed in lower temperatures (600-1200℃ instead of 1800-2600℃) and with a shorter duration (1.5-2 *hours* instead of tens of hours) processes. Because of alloy formation via solid-phase mechanism excluding melting, the energy consumption is low.

2. The binary and multicomponent alloys and intermetallics of the defined composition are produced in one technological stage.

3. The processes of formation of alloys and intermetallics are safe, wasteless and highly effective.

4. Instead of the expensive fine-dispersed powders of refractory metals demanded as starting materials, cheap SHS hydrides are used, formed in a highly efficient, low-energy technological process, utilizing the wastes appeared during machining of refractory metals.

5. More than 100 HC-synthesized alloys, intermetallics and their hydrides have been produced. Among them – the alloys with structure of α-, β-, γ- and ω-phases.

6. The elaborated method for synthesis of alloys and intermetallics of transition metals can be very attractive for industry and be of commercial interest. Hydrides of synthesized alloys and intermetallics potentially can serve as hydrogen storage materials.

ԱՆՑՈՒՄԱՅԻՆ ՄԵՏԱՂՆԵՐԻ ԵՎ ՆՐԱՆՑ ՀԱՄԱՁՈՒԼՎԱԾՔՆԵՐԻ ՀԻԴՐԻԴՆԵՐԸ ՈՐՊԵՍ ԽՏԱՑՎԱԾ ՋՐԱԾՆԻ ԿՐՈՂՆԵՐ

Ս. Կ. ԴՈԼՈՒԽԱՆՅԱՆ, Ա. Գ. ԱԼԵՔՍԱՆՅԱՆ, Գ. Ն. ՄՈՒՐԱԴՅԱՆ, Վ. Շ. ՇԵԽՏՄԱՆ, Օ. Պ. ՏԵՐ-ԳԱԼՍՏՅԱՆ, Ն. Գ. ՀԱԿՈԲՅԱՆ, Ն. Ն. ԱՂԱՋԱՆՅԱՆ և Ն. Լ. ՄՆԱՑԱԿԱՆՅԱՆ

ՀՀ ԳԱԱ ՔՖԻ բարձրջերմաստիճանային սինթեզի և անօրգանական միացությունների տեխնոլոգիայի լաբորատորիայում ԲԻՄ(Բարձրջերմաստիճանային ինքնատարածվող Սինթեզ) մեթոդով սինթեզվել են 200-ից ավելի մետաղների և համաձուլվածքների երկ- և բազմակոմպոնենտ հիդրիդներ և դեյտերիդներ: Հետազոտությունները Me-H համակարգերում ֆիզքիմիական հիմք դարձան ԲԻՄ պրոցեսների համար և հանգեցրին տեխնոլոգիական աշխատանքների կատարմանը: Մշակված են պրոցեսների բարձրարտադրողական տեխնոլոգիաներ ամենատարբեր հիդրիդների սինթեզի համար, որոնք կարող են ապահովել բարձր որակով էժան հիդրիդների մեծ տեսականու սինթեզ և արտադրություն: «ԱրմՆիիցվետմետ» փորձնական փոքրիկ գործարանում (ք. Երևան) արտադրվել է տիտանի և ցիրկոնիումի ավելի քան 20 տոննա հիդրիդներ: Անցումային մետաղների և նրանց համաձուլվածքների հիդրիդները՝ որպես կոնդենսված ջրածնի կրիչներ, մեծ արժեք են ներկայացնում: Մշակված է անցումային մետաղների համաձուլվածքների և միջմետաղական միացությունների սինթեզի ևս մեկ՝ սկզբունքորեն նոր մեթոդ, որն անվանվեց մեր կողմից «Հիդրիդային ցիկլի-ՀՑ» մեթոդ: Մեթոդի հիմքում ընկած են երկու և ավելի մետաղների հիդրիդների փոխազդեցության ռեակցիաները, ինչպես օրինակ՝ $xMe'H_2 + (1-x)Me''H_2 \rightarrow$ *համաձուլվածք* $Me'xMe''_{(1-x)} + H_2\uparrow$*: Ցույց է տրված, որ երկու և ավելի հիդրիդների սեղմված խառնուրդի, օրինակ՝* TiH_2 *և* ZrH_2*, ինչպես նաև հիդրիդի և մետաղական փոշու՝* TiH_2 *և Al, տաքացման դեպքում սեղմված սկզբնական խառնուրդից ջրածնի անջատումը հիդրիդների քայքայման ջերմաստիճաններից քիչ բարձր ջերմաստիճաններում բերում է նշված մետաղների ամուր, հոծ, կոմպակտ երկ- և եռկոմպոնենտ համաձուլվածքների առաջացման: ՀՑ ռեժիմում սինթեզվել են 100 և ավելի*

Համաձուլվածքներ և միջմետաղական միացություններ Ti-Zr; Ti-Hf; Ti-Nb; Ti-V; Zr-Hf; Ti-Zr-Hf; Ti-Ni; Zr-Co; Ti-Al; Nb-Al և այլ համակարգերում: Ստացված որոշ կոմպակտ համաձուլվածքները առանց նախնական մանրացման փոխազդում են ջրածնի հետ ԲԻՄ ռեժիմում առաջացնելով ջրածնի բարձր պարունակությամբ հիդրիդներ:

ГИДРИДЫ ПЕРЕХОДНЫХ МЕТАЛЛОВ И ИХ СПЛАВОВ КАК НОСИТЕЛИ КОНДЕНСИРОВАННОГО ВОДОРОДА

С. К. ДОЛУХАНЯН, А. Г. АЛЕКСАНЯН, Г. Н. МУРАДЯН, А. Г. АКОПЯН, Н. Н. АГАДЖАНЯН, Н. Л. МНАЦАКАНЯН и О. П. ТЕР-ГАЛСТЯН

Институт химической физики им. А.Б. Налбандяна НАН Республики Армения
Армения, 0014, Ереван, ул. П. Севака, 5/2
E-mail: seda@ichph.sci.am

Представлен обзор работ Лаборатории высокотемпературного синтеза и технологии неорганических материалов ИХФ НАН Армении. В первой части статьи описаны исследования процессов горения переходных металлов в водороде. Впервые методом СВС (самораспространяющегося высокотемпературного синтеза) было синтезировано более 200 бинарных и многокомпонентных гидридов и дейтеридов металлов и сплавав. Эти исследования стали физико-химической основой СВС процессов в системах Me-H и привели к постановке технологических работ, имеющих огромные промышленные перспективы. Разработаны не имеющие аналогов в мире высокопроизводительные технологические процессы синтеза различных гидридов, которые могут обеспечить синтез и производство большого ассортимента дешевых гидридов высокого качества. На опытном заводе АрмНИИцветмет (г. Ереван) было изготовлено более 20 *m* гидридов титана и циркония. Гидриды переходных металлов и сплавов представляют большую ценность как конденсированные носители водорода. Интерес к водороду и металлогидридам связан с двумя глобальными проблемами: охрана окружающей среды и истощение запасов ископаемого углеродного и углеводородного топлива. Спектр применения гидридов металлов и сплавов очень широк.

Дальнейшие исследования синтезированных в режиме СВС гидридов позволили разработать еще один, принципиально новый метод синтеза сплавов и интерметаллидов переходных металлов, названный нами методом «Гидридного цикла – ГЦ». Вторая часть работы посвящена исследованиям процесса формирования сплавов и интерметаллидов в ГЦ. В основе метода лежат *реакции взаимодействия двух и более гидридов металлов*, как например, $x\mathrm{Me'H_2} + (1\text{-}x)\mathrm{Me''H_2} \rightarrow$ сплав $\mathrm{Me'_xMe''_{(1-x)}} + \mathrm{H_2}\uparrow$. Показано, что при нагреве компактированной смеси двух и более гидридов, например $\mathrm{TiH_2}$ и $\mathrm{ZrH_2}$, а также гидрида и металлического порошка (например $\mathrm{TiH_2}$ и Al) удаление водорода из компактированной шихты при температурах чуть выше температур диссоциации гидридов приводит к образованию прочных, беспористых, компактных бинарных, тройных сплавов указанных металлов. В режиме ГЦ синтезировано более 100 сплавов и интерметаллидов в системах Ti-Zr; Ti-Hf; Ti-Nb; Ti-V; Zr-Hf; Ti-Zr-Hf; Ti-Ni; Zr-Co; Ti-Al; Nb-Al и др. Некоторые полученные компактные сплавы без предварительного измельчения взаимодействуют с водородом в режиме СВС, образуя гидриды с высоким содержанием водорода. Установлено влияние параметров – соотношения гидридов металлов и порошков металлов в реакционной смеси, размеров зерен порошков гидридов (микро- и наноразмеры), давления прессования при компактировании гидридов, а также режимов дегидрирования и спекания (температуры и скорости

нагрева) на характеристики полученных сплавов и интерметаллидов – кристаллическую структуру, плотность, адсорбционные свойства и др. Предложен механизм их формирования. Перспективы метода ГЦ для синтеза сплавов и интерметаллидов могут быть очень привлекательны для индустрии. Разработанные технологии по методу ГЦ могут представлять коммерческий интерес, поскольку имеют большие преимущества перед традиционными.

REFERENCES

[1] Metal Hydrides (Ed. Muller W. et al.). New York and London. Academic Press. 1968.
[2] *Antonova M.M*. Properties of metal hydrides. Directory. Naukova Dumka, 1975.
[3] *Samsonov G.V., Vinitsky I.M*. Refractory compounds. M., Metallurgy,1976.
[4] Hydrogen in metals. 2-volume, edited by Alefeld G., M., Мир, 1981.
[5] *Merzhanov A.G., Borovinskaya I.P.* // Doklady AN SSSR,1972, v. 204, №2, p.366.
[6] *Dolukhanyan S.K, Nersesyan M.D.* Nalbandyan A.B, Borovinskaya I.P., Merzhanov A.G. Doklady AN SSSR, 1976, v. 231, №3, p. 675.
[7] *Martirosyan N.N., Dolukhanyan S.K, Merzhanov A.G*. // Fizika goreniya i vzriva, 1981, №4, p.24.
[8] *Dolukhanyan S.K, Aleksanyan A.G., Seyranyan G.B., Aghajanyan N.N., Nalbandyan A.B.* // Doklady AN SSSR, 1984, v. 276, №1, p. 131.
[9] *Dolukhanyan S.K. J.* // Alloys Comp., 1997, v. 253-254, p. 10.
[10] *Dolukhanyan S.K.* «Self-Propagating High-Temperature Synthesis of Materials», Borisov A.A., De luca L and Merzhanov A.G., Eds., translated by Yu.B. Scheck, New York: Taylor and Francis, 2002, p. 219.
[11] *Dolukhanyan S.K., Aleksanyan A.G., ShekhtmanV.Sh., Hakobyan H.G., Mayilyan D.G, Aghajanyan N.N., Abrahamyan K.A., Mnatsakanyan N.L., Ter-Galstyan O.P.* // Intl. J. of Self-Propagating High-Temperature Synthesis, 2010, v.19, №2, p.85.
[12] *DolukhanyanS.K, Aleksanyan A.G., Ter-Galstyan O.P., ShekhtmanV.Sh, Sakharov M.K. Abrosimova G.E.* // Russian Journal of Physical Chemistry B, 2007, v. 2, №6, p. 563.
[13] *Aleksanyan A.G., Dolukhanyan S.K., ShekhtmanV.Sh., Khasanov S.S., Ter-Galstyan O.P., Martirosyan M.V.* // Int. J. Hydrogen Energy, 2012, №37, p. 14234.
[14] *Aleksanyan A.G., Dolukhanyan S.K., Shekhtman V.Sh., Huot J., Ter-Galstyan O.P., Mnatsakanyan N.L.* // J. Alloys Comp., 2011. *v*.509, p. 786.
[15] *Dolukhanyan S.K., Aleksanyan A.G., Shekhtman V.Sh., Mantashyan A.A., Mayilyan D.G, Ter-Galstyan O.P.* // Chemical J. of Armenia, 2007, v.60, №4, p. 545.
[16] *Aleksanyan A.G., Mayilyan D.G.,Dolukhanyan S.K., Shekhtman V.Sh., Ter-Galstyan O.P.* // Int. J. of Self-Propagating High-Temperature Synthesis, 2010, v. 19, №.1, p. 34.
[17] *Dolukhanyan S.K., Aleksanyan A.G., Ter-Galstyan O.P., Shekhtman V.Sh., Mnatsakanyan N.L*. // Int. J. of Self-Propagating High-Temperature Synthesis, 2014, v. 23, №2, p. 78.
[18] *Muradyan G.N.* // Chemical J. of Armenia, 2016, v.69, №4, p. 416.
[19] *Dolukhanyan S.K., Ter-Galstyan O.P., Aleksanyan A.G., Hakobyan A.G., Mnatsakanyan N.L., Shekhtman V. Sh.* // Russian J. of Physical Chemistry B, 2015, v. 9, №5, p 702.
[20] *Dolukhanyan S.K., Ter-Galstyan O.P., Aleksanyan A.G., Muradyan G.N, Mnatsakanyan N.L* // Russian J. of Physical Chemistry B**,** 2017, v. 11, №2, p. 272.
[21] *ShekhtmanV.Sh., Dolukhanyan S.K., Abrosimova G.E., Abrahamyan K.A., Aleksanyan A.G., Aghajanyan N.N., Ter-Galstyan O.P.* // Int.J. Hydrogen Energy, 2001, v.26, p. 435.
[22] *Мурадян Г.Н*. // Chemical J. of Armenia, 2017, v.70, №3, p. 323.
[23] *Hakobyan H.G., Aleksanyan A.G., Dolukhanyan S.K., Mnatsakanyan N.L.* // Int.J. of Self-Propagating High-Temperature Synthesis, 2010, v. 19, №1, p. 49.
[24] *Shekhtman V.Sh., Hakobyan H.G., Aleksanyan A.G., Dolukhanyan S.K., Ter-Galstyan O.P., Sakharov M.K.* // Int. J. Hydrogen Energy, 2011,v. 361, p. 206.
[25] *Aleksanyan A.G., Dolukhanyan S.K., Ter-Galstyan O.P., Mnatsakanyan N.L*. // Int. J. Hydrogen Energy, 2016,v. 41, p.13521.

ՀԱՅԱՍՏԱՆԻ ՀԱՆՐԱՊԵՏՈՒԹՅԱՆ ԳԻՏՈՒԹՅՈՒՆՆԵՐԻ
ԱԶԳԱՅԻՆ ԱԿԱԴԵՄԻԱ
НАЦИОНАЛЬНАЯ АКАДЕМИЯ НАУК РЕСПУБЛИКИ АРМЕНИЯ
NATIONAL ACADEMY OF SCIENCES OF THE REPUBLIC OF ARMENIA

Հայաստանի քիմիական հանդես
Химический журнал Армении **71, №4, 2018** Chemical Journal of Armenia

UDC 54.057: 546.284+546.43'284+549.671/.64 +544.344.016.2:543.572.3+543.442.2

BARIUM SILICATES FORMATION USING SILICA HYDROGEL PRODUCED FROM SERPENTINE MINERALS

A. M. TERZYAN[1], S. A. MELIKYAN[1], H. A. BEGLARYAN[1,2], A. R. ISAHAKYAN[1] and N. H. ZULUMYAN[1]

[1]Institute of General and Inorganic Chemistry of NAS RA
10, Lane 2, Argutyan Str., Yerevan, 0051, Armenia
Fax: (374-10) 231275, E-mail: Isahakyananna@yahoo.com
[2]Yerevan State University
1, A. Manoukyan Str., Yerevan, 0025, Armenia
Fax: (374-10) 231275 E-mail: Hayk_b@ysu.am

In the paper the interaction between silica hydrogel recovered from serpentines $(Mg(Fe))_6[Si_4O_{10}](OH)_8$, sodium hydroxide NaOH and barium chloride $BaCl_2$ in aqueous medium has been investigated. It has been revealed that depending on the stirring time of the boiling aqueous suspension prepared from the mentioned reagents in air at ambient pressure, species of either a hydrated barium silicate like $BaSiO_3 \cdot H_2O$ or BaH_2SiO_4 can be precipitated. Subsequent heat treatment of each of the precipitated intermediates to a temperature of 800 °C results in their crystallization into barium silicates, namely, barium meta- $BaSiO_3$ and orthosilicate Ba_2SiO_4.

Figs. 3, references 12.

Because of a structural variety, high thermal and chemical stability, congruent melting points, most barium silicate compounds are known by their wide use in the manufacture of phosphors. Particularly, Ba_2SiO_4, $BaSiO_3$, $Ba_2Si_3O_8$, $Ba_5Si_8O_{21}$ and $BaSi_2O_5$ are good host candidates for the preparation of scintillators and Ba_2SiO_4, $BaSiO_3$, $Ba_2Si_3O_8$, and $BaSi_2O_5$ doped with rare earth ions demonstrate luminescence under UV light and electron beams [1-9]. The rest of three barium silicates Ba_3SiO_5, $Ba_3Si_5O_{13}$ and high-pressure $BaSi_4O_2$, pure phase of which cannot be provided and which have incongruent melting points are not involved in luminescent materials manufacture.

One of the most popular synthetic methods for different barium silicate-based phosphors is high-temperature solid-phase synthesis (at 1200°C or higher) via annealing barium carbonate $BaCO_3$ with silicon dioxide SiO_2 for many hours [1-6]. Two-step methods including sol-gel process, where an intermediate solid is first

precipitated in a liquid medium via reacting an inorganic or organic barium salt ($Ba(NO_{3)2}$ or $BaCl_2$, barium acetate $Ba(CH_3COO)_2$) with a silica-containing reagent (silica gel, tetraethoxysilane, or sodium silicate $Na_2SiO_3 \cdot 9H_2O$) and then annealed are also suggested [7-10]. Very often a hydrothermal treatment is applied for intermediates prepararion [7, 8]. All these methods are either connected with technological difficulties or energy-consuming.

A new species of silica hydrogel containing up to 6% of amorphous silica SiO_2 has been produced from dehydrated serpentine minerals structure via a new approach to the acid treatment of serpentinites[1][11]. Unlike conventional silicon dioxide, this SiO_2 species, has a high chemical activity caused by a low dissociation energy of siloxane bonds in Si–O–Si bridges which is explained by the presence of unsaturated Si–O(Si) bonds in its structure [12, 13].

Can any intermediates be precipitated in the first stage and which barium silicate species can be produced from them via heat-treatment if this silica hydrogel is used as an initial reagent? – are questions of great interest.

In the present work, X-ray diffraction (XRD) study and differential thermal analysis (DTA) are involved to study the intermediates formed in the system SiO_2–$NaOH$–$BaCl_2$–H_2O and their thermal transformation using the silica hydrogel derived from serpentine minerals as a sourse of SiO_2.

Experimental Part

A serpentinite sample located in Shorja (Armenia) was used as a precursor for the silica hydrogel production using the method described in the work [11].

1.64 M sodium hydroxide solution was prepared by adding NaOH pellets (ACS reagent procured from Sigma-Aldrich) to distilled water. The solution was stirred for 15 *min*.

Barium chloride $BaCl_2$·(procured from Sigma-Aldrich) was used as a source of barium cations.

For the sol-gel procedure four samples were prepared by adding $BaCl_2$ salt to the sodium hydroxide solution with the SiO_2:NaOH:BaO molar ratios of 1:4:2. Each of the prepared samples was put into a vessel and stirred with a mechanical stirrer for a certain time (15, 30, 60, 120 *min*) in air at ambient pressure while being heated up to the temperature of 95°C (boiling point). Then each of the suspensions produced in the mixer was filtered. A gel-like mass remained on the filter was washed by distilled water and dried at the temperature of 100°C for 24 *h* in a dryer type KBC G – 100/250 manufactured by Premed (Warszawa, Poland). As a result, a white precipitate powder was produced.

Serpentinite is a rock largely composed of serpentine group minerals $(Mg(Fe))_6[Si_4O_{10}](OH)_8$[1].

Each of the four samples produced was studied in air by XRD analysis and two of them were selected for DTA from room temperature up to 1000°C.

Then all the four precipitate samples were annealed at 800°C for 2 *hours* and also subjected to XRD analysis.

X-ray powder diffraction (XRPD) measurements were made on a Dron-3 diffractometer (Russia) equipped with nickel filter, under the following conditions: CuKα-radiation; power supply 25 *kV*/10 *mA*; angular range 2θ=8°-70° at room temperature in air. The mass of each test specimen was 250 mg. All the reflections were identified and interpreted using the ICDD-JCPDS database of crystallographic 2004.

DTA, thermogravimetric (TG) and DTG (differential thermogravimetric) measurements were performed by using a Derivatograph Q–1500D equipment manufactured by the MOM company (Hungary) in air at a heating rate of 10°C min^{-1}. The samples of equal mass were investigated in platinum crucibles.

Results and Discussion

The XRPD patterns of the precipitate samples produced from the suspension with the SiO_2:NaOH:BaO molar ratio of 1:4:2 reveal that either barium silicate hydrate like $BaSiO_3$·H2O or BaH_2SiO_4 is precipitated depending on stirring time. The fifteen-minute stirring leads to the formation of $BaSiO_3·H_2O$ that is evidenced by the appearance of intensive diffraction peaks of $BaSiO_3·H_2O$ (Card №34–0016) (Fig. 1). The increase in stirring time up to 30 *min* provides the formation of BaH_2SiO_4 (Card №75–1429), lower intensity reflections of which are recorded in the diffraction patterns of the corresponding sample. Both the 60- and 120-*minute* treatment also result in BaH_2SiO_4 formation (Fig. 1).

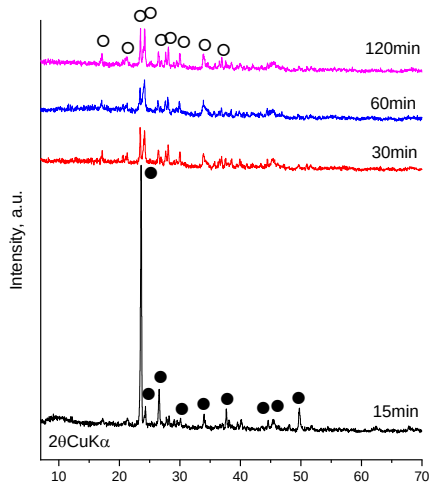

Fig. 1. XRPD patterns of the precipitate samples separated from the suspensions which were prepared from the silica hydrogel derived from serpentine minerals, NaOH and $BaCl_2$ with the SiO_2:NaOH:$BaCl_2$ molar ratio of 1:4:2 by stirring for different time. ●– $BaSiO_3·H_20$; O– BaH_2SiO_4

The DTA curves of the precipitate samples comprised of a-$BaSiO_3·H_2O$ and b-BaH_2SiO_4 prepared by stirring for 15 and 30 min, respectively, display a number of endothermic events of different intensities and minimum up to 700°C and the only

exothermic peak of a low intensity about the temperature of 700°C (Fig. 2). The trend of the TG curve shows that the endothermic processes are accompanied by mass loss whereas the exothermic process occurs without any mass change (Fig. 2). On the DTA curves of both samples two endotherms are recorded in the range of low temperatures 300–360°C, evidencing a stepwise release of bound water from the intermediates (Fig. 2). An endothermic event at 337°C in the form of shoulder is hardly traceable on the DTA curve of $BaSiO_3 \cdot H_2O$. Despite it, the intensive endothermic peak with minimum at 354°C points to the fact that most part of crystalline water is removed at this temperature. Also, the TG curve shows that this process involves a considerable weight loss and continues up to 400°C (Fig. 2). It should be noted that another exothermic event can be barely seen in the range of 600–650°C (Fig. 2). As for the BaH_2SiO_4 precipitate sample, the two endotherms are recorded on its DTA curve up to 400°C: the first one with minimum at 306°C C and the second one with minimum at 349°C. They must be caused by the removal of structural water and indicate that the water is driven off from the BaH_2SiO_4 sample in two stages (Fig. 2).

Taking into account the DTA data, all the four samples annealed at 800°C were subjected to XRD study in order to determine what causes the only exothermic peak on the DTA curve.

The XRPD patterns of the four samples comprised of either $BaSiO_3 \cdot H_2O$ or BaH_2SiO_4 exhibit that on heating up to 800°C both $BaSiO_3 \cdot H_2O$ and BaH_2SiO_4 transform into barium silicate species, namely barium metasilicate $BaSiO_3$ and orthosilicate Ba_2SiO_4. The intensive diffraction peaks of $BaSiO_3$ (Card №70–2112) and Ba_2SiO_4 (Card №77–0150) can be seen in the diffraction patterns of all the samples annealed at 800°C (Fig. 3). This is a good reason to think that the only exothermic effect up to 800°C on the DTA curve must be produced by the formation of $BaSiO_3$ and Ba_2SiO_4.

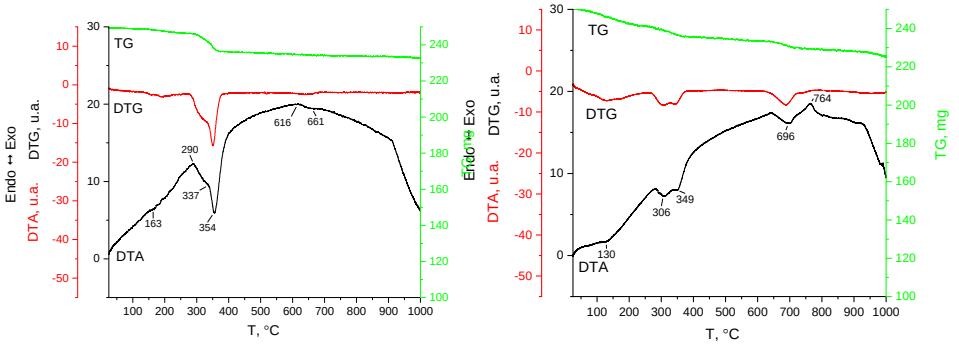

Fig. 2. Differential thermal curve for the precipitate sample comprised of a- $BaSiO_3 \cdot H_2O$ and b- BaH_2SiO_4**.** *TG* thermogravimetric or weight loss curve, *DTA* differential thermal analysis curve. *DTG* differential thermal thermogravimetric curve. The vertical axis label applies to the *DTA* curve.

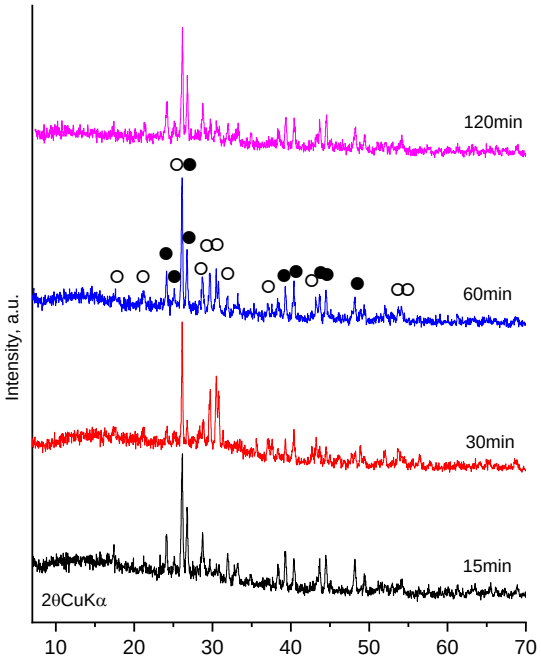

Fig. 3. XRPD patterns of the specimens produced by the heat-treatment at 800°C of the precipitate samples which were precipitated in the boiling suspensions prepared from the hydrosilixcagel derived from serpentine minerals, NaOH and $BaCl_2$ with the SiO_2:NaOH:$BaCl_2$ molar ratio of the 1:4:2 by stirring for different time. ○– $BaSiO_3$; ●– Ba_2SiO_4.

It is noticeable that the most intensive diffraction peaks of $BaSiO_3$ and Ba_2SiO_4 are fixed in the diffraction pattern of the sample comprised of $BaSiO_3 \cdot H_2O$, which was precipitated by fifteen-minute stirring. The XRPD patterns of the BaH_2SiO_4 samples prepared by stirring for 30, 60 and 120 *min* demonstrate $BaSiO_3$ and Ba_2SiO_4 refelctions of similar intensities. Hence, the increase in stirring time by more than 15 *min* does not essentially influence the yields of $BaSiO_3$ and Ba_2SiO_4.

Conclusions

The data derived from the experiments have allowed to conclude that in spite of the fact that the involvement of the silica hydrogel derived from serpentine minerals in the system SiO_2–NaOH–$BaCl_2$–H_2O as a source of silica is accompanied by either the participation of BaH_2SiO_4 or $BaSiO_3 \cdot H_2O$ depending on stirring time, the heat treatment of each of the synthesized intermediates to a temperature of 80°C is accompanied by their transformation into $BaSiO_3$ and Ba_2SiO_4.

This study is of great practical interest and futher research is needed to find optimal parameters for the development of efficient techniques for the production of $BaSiO_3$ and Ba_2SiO_4 and phosphors based on them.

Acknowledgments

This work was supported by the RA MES State Committee of Science, in the frames of the research project №16YR-1D025.

ՍԵՐՊԵՆՏԻՆԱՅԻՆ ՄԻՆԵՐԱԼՆԵՐԻՑ ՍՏԱՑՎԱԾ ՍԻԼԻԿԱԺԵԼԻ ՀԻՄԱՆ ՎՐԱ ԲԱՐԻՈՒՄԻ ՍԻԼԻԿԱՏՆԵՐԻ ՍՏԱՑՈՒՄԸ

Ա. Մ. ԹԵՐՋՅԱՆ, Ս. Ա. ՄԵԼԻՔՅԱՆ, Հ. Ա. ԲԵԳԼԱՐՅԱՆ, Ա. Ռ. ԻՍԱՀԱԿՅԱՆ և Ն. Հ. ԶՈՒԼՈՒՄՅԱՆ

Ուսումնասիրվել է սերպենտիններից ($(Mg(Fe))_6[Si_4O_{10}](OH)_8$) առաջացած հիդրոսիլիկաժելի, նատրիումի հիդրօքսիդի ($NaOH$) և բարիումի քլորիդի ($BaCl_2$) փոխազդեցությունը ջրային լուծույթում: Ցույց է տրված, որ մթնոլորտային ճնշման և եռման պայմաններում ջրային սուսպենզիայի խառնման տևողությունից կախված կարող են նստել կամ հիդրատացված բարիումի սիլիկատ՝ $BaSiO_3 \cdot H_2O$, կամ ստրոնցիումի դիհիդրոսիլիկատ՝ BaH_2SiO_4: Այս միջանկյալ միացությունների հետագա ջերմամշակումը մինչև 800°C բերում է բարիումի սիլիկատի բյուրեղացման, մասնավորապես, ստրոնցիումի օրթոսիլիկատի (Sr_2SiO_4) և ստրոնցիումի մետասիլիկատի ($SrSiO_3$) առաջացման:

ОБРАЗОВАНИЕ СИЛИКАТОВ БАРИЯ, ПРИМЕНЯЯ ГИДРОГЕЛЬ КРЕМНЕЗЕМА, ПОЛУЧЕННЫЙ ИЗ СЕРПЕНТИНОВЫХ МИНЕРАЛОВ

А. М. ТЕРЗЯН[1], С. А. МЕЛИКЯН[1], А. А. БЕГЛАРЯН[1,2], А. Р. ИСААКЯН[1] и Н. О. ЗУЛУМЯН[1]

[1] Институт общей и неорганической химии им. М.Г.Манвеляна НАН Республики Армения
Армения, 0051, Ереван, ул. Аргутяна 2-ой пер., д. 10
Факс: (374-10) 231275 E-mail: Hayk_b@ysu.am
[2] Ереванский государственный университет
Армения, Ереван, 0025, ул. А. Манукяна, 1

Исследовано взаимодействие в водной среде между гидрогелем кремнезема, выделенным из серпентинов $(Mg(Fe))_6[Si_4O_{10}](OH)_8$, гидроксидом натрия $NaOH$ и хлоридом бария $BaCl_2$. Установлено, что в зависимости от длительности перемешивания в условиях атмосферного давления кипящей водной суспензии, приготовленной из указанных реагентов, могут осаждаться или гидратированный силикат бария типа $BaSiO_3 \cdot H_2O$, или BaH_2SiO_4. Дальнейшая термообработка каждого осажденного интермедианта до температуры 800°C приводит к его кристаллизации в силикаты бария, а именно, в метасиликат бария $BaSiO_3$ и ортосиликат бария Ba_2SiO_4.

REFERENCES

[1] *Pires A.M., Davolos M.R., Malta O.L.* // J Lumin, 1997, 72-74, Supplement C, 244.
[2] *Streit H.C., Kramer J., Suta M., Wickleder C.* // Materials, 2013, 6, 8, 3079.
[3] *Ferracin L.C., Davolos M.R., Nunes L.A.O.* // J Lumin, 1997, 72-74, Supplement C, 185.
[4] *Park J.K., Lim M.A., Choi K.J., Kim C.H.* // Journal of Materials Science, 2005, 40, 8, 2069.
[5] *Herrmann A., Simon A., Rüssel C.* // 2012, 132, 215.
[6] *Mishra L., Sharma A., Vishwakarma A.K., Jha K., Jayasimhadri M., Ratnam B.V., et al.* // J Lumin, 2016, 169, Part A, 121.
[7] *Lu Z., Weng L., Song S., Zhang P., Luo X., Ren X.* // Ceram Int, 2012, 38, 6, 5305.
[8] *Han J.K., Hannah M.E., Piquette A., Talbot J.B., Mishra K.C., McKittrick J.* // J Lumin, 2015, 161, Supplement C, 20.
[9] *Yao Y., Zhou Z., Ye F.* // J Alloys Compd, 2017, 712, Supplement C, 213.
[10] *Kamei S., Kojima Y., Nishimiya N.* // J Lumin, 2010, 130, 11, 2247.

[11] *Zulumyan N.O., Isaakyan A.R., Ovsepyan T.A., Kazanchyan A.M., Terzyan A.M.,* Method for complex processing of serpentinit. RF patent 2 407 704 C2. 2010.
[12] *Isahakyan A.R., Beglaryan H.A., Pirumyan P.A., Papakhchyan L.R., Zulumyan N.H.* // Russ J Phys Chem A, 2011, 85, 1, 72.
[13] *Zulumyan N.O., Isaakyan A.R., Pirumyan P.A., Beglaryan A.A.* // Russ J Phys Chem A, 2010, 84, 4, 700.

ՀԱՅԱՍՏԱՆԻ ՀԱՆՐԱՊԵՏՈՒԹՅԱՆ ԳԻՏՈՒԹՅՈՒՆՆԵՐԻ
ԱԶԳԱՅԻՆ ԱԿԱԴԵՄԻԱ
НАЦИОНАЛЬНАЯ АКАДЕМИЯ НАУК РЕСПУБЛИКИ АРМЕНИЯ
NATIONAL ACADEMY OF SCIENCES OF THE REPUBLIC OF ARMENIA

Հայաստանի քիմիական հանդես
Химический журнал Армении **71, №4, 2018** Chemical Journal of Armenia

ADVANTAGES OF THE METHOD OF FRONTAL POLYMERIZATION IN HIGH TECHNOLOGIES

A. O. TONOYAN and S. P. DAVTYAN

National Polytechnic University of Armenia
105, Teryan Str., Yerevan, 0009, Armenia
E-mail: atonoyan@mail.ru

This paper is devoted to advantages and opportunities of frontal polymerization applied to nanotechnologies with the aim to obtain polymeric nanocomposites with a uniform distribution of nanoparticles in polymer matrix. It can also be used in the synthesis of high temperature superconducting polymer ceramic intercalated composites and superconducting electrically conductive polymer composites.

It has been shown that the frontal polymerization allows obtaining multifunctional, gradient materials due to the specificity of the propagation process of heat wave polymerization.

The frontal polymerization has a significant contribution to the synthesis of pure super absorbent hydrogels, in contrast to traditionally obtained, and many others.

Figs. 7, references 24.

Introduction

For a better assessment of the advantages of frontal polymerization, we would like to present a small comparison of exothermic radical polymerization in traditional technologies with frontal polymerization (FP), occurring in the mode of auto-wave propagation of thermal polymerization.

In the traditional methods after initial mixture is loaded into the reactor, it is heated to the temperature at which initiator decomposes to yield active radicals. From this moment, exothermic polymerization takes place with the formation of high-molecular polymer chains. A sufficiently large amount of heat is released. In order to avoid thermal explosion in the industry, cooling systems are installed around the reactor. To reduce the polymerization rate, respectively, to reduce the rate of released heat, inert solvents are often added to the initial mixture. At the end of the process, solvents are either released into the atmosphere polluting the environment or cleaned and reused (which complicates the process and makes it more expensive). It is one problem. From the point of view of non-isothermal processes in traditional technologies, there is also a problem.

The fact is that large-size products are generally produced with internal defects - during the process of solidification into the sample defects are formed [1,2]. Therefore, we began to study the reasons and opportunities to avoid defects and create a controlled production of these products. These studies led to the idea of FP. This was in the seventies of the last century. At that time, only our laboratory in the branch of the Moscow Institute of Physical Chemistry, in Chernogolovka, was engaged in the FP method; and up to the 90s we were the only ones engaged in the FP–monopoly [3–8].

Experiment and discussion

Fig. 1 shows a schematic polymerization in the conditions of FP [1]. The reaction ampoule is loaded with the initial mixture; the heat is supplied not to the entire reactive mass. In the FP method the process is carried out by local and short warm-up of the local part of the reactor (for example, one end of the tubular reactor) filled with the reacting mixture. The polymerization process is initiated at the site of heating. The heat evolved is transferred to the neighboring layer of unreacted reaction mixture. In this layer a new round of polymerization is initiated followed by the corresponding release of heat to warm the neighboring layer, and thus the polymerization process extends from one end of the reactor to another in the auto-wave mode. This process fixes properties of the composite, which are determined by the initial mixture.

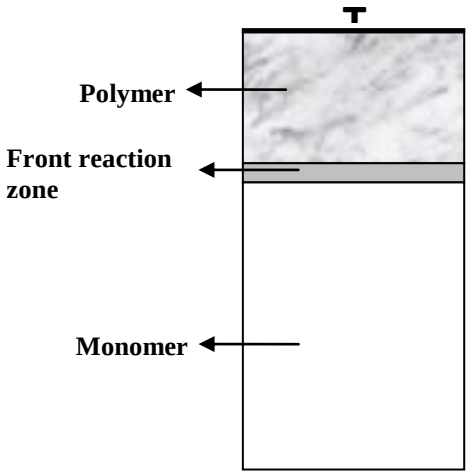

Fig. 1. Schematic polymerization in the conditions of the FP method

Unlike the traditional methods of synthesis, here we are interested in preserving this heat, so that it does not leave the walls of the reactor, but transfers to an adjacent layer. In FP it is necessary to keep the released heat, which is the initiator of the process and eliminates the need for heat removal, respectively, the use of solvents to reduce heat generation. This is the basis for the high productivity of FP and its

environmental safety. Currently FP is the most researched subject in the world Scientist Centers and Universities, because of its rationality [9–14].

Therefore, until recently the FP was considered as a high-performance technological method, but with the development of high technologies, it became clear that this method was indispensable in the synthesis of polymer superconducting composites, moreover it has serious advantages in the synthesis of polymeric nanocomposites with a uniform distribution of nanoparticles in the polymer matrix [15–18].

It is known that to obtain polymeric nanocomposites filled with nanoparticles, different methods of passivation (neutralization of high activity of nanoparticles) are used. These include plasma polymerization, polymerization under conditions of acoustic waves, the use of surface-active materials (SAMs) and others.

All these methods are designed to protect the nanoscale of the added nanoparticles. The fact is that due to high activity, nanoparticles are attracted to each other and stick together, losing their nano-scale properties.

Acoustic waves prevent the nanoparticles from sticking together in the melt or solution of the polymerizable monomer. SAMs envelop a nanoparticle with the formed micellar single-charged structures and thereby make the nanoparticles passive, preventing them from sticking together. However, a serious problem arises here. A strong surfactant reacts with a nanoparticle, neutralizing its activity and attractiveness of nanoscale. Weak surfactants during the polymerization depart from the surface of the particles and stick together.

We have performed a series of experiments with the addition of surfactant-treated nanoparticles to the monomeric medium by the FP method. We did the same without processing nanoparticles in different thermal regimes. Below are presented the microscopic photographs of the samples obtained in the adiabatic, isothermal and frontal regimes. You can see that by FP, the initial state is fixed; in this case the uniform distribution of nanoparticles in the polymer matrix takes place. Two factors work here: the effect of the auto-wave propagation of the polymerization, analogous to acoustic waves and fast fixation of the initial state, which does not allow the particles to agglomerate.

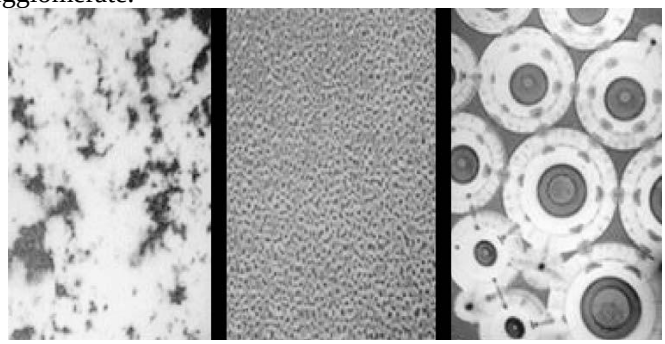

a b c

Fig. 2. (a) Initial reaction medium without surfactant, (b) in the presence of surfactant, and (c) at 30X magnification of the microscope. Surfactant-treated, untreated surfactants.

This Figure shows microscopic photographs of a solution of acrylamide complex with nanoparticles additives.

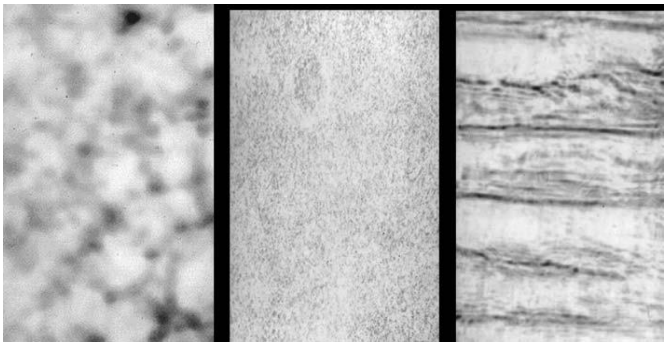

a b c

Fig. 3. Effect of the thermal mode of polymerization on the structure of nanocomposites based on PAAM: (a) adiabatic mode, (b) frontal stationary mode, and (c) frontal oscillating mode.

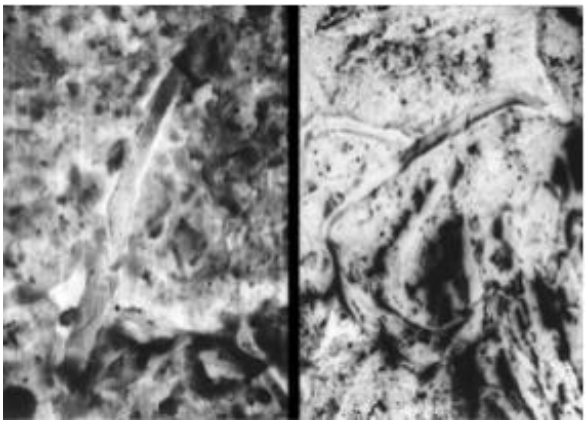

Fig. 4. The micrograph of polymer–ceramic nanocomposites with the UHMWPE binder.

We note one more advantage of the FP for the synthesis of superconducting nanocomposites [19-24].

With the use of superconducting yttrium and bismuth ceramics as additives in the polymerizing system in order to obtain superconducting polymer composites, we succeeded in synthesizing HTSC composites with the 95-97 K transition by the FP method. As it turned out, this possibility was associated with the intercalation of polymer molecules into nanoscale interlayer spaces of ceramics. As can be seen from Fig. 4 due to the shock wave, high-molecular chains are introduced into nano-sized ceramic layers (intercalation).

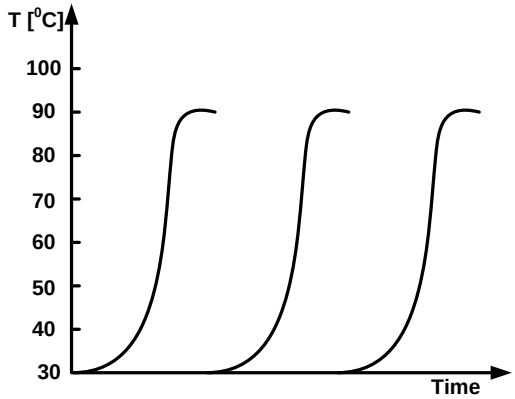

Fig. 5. Temperature profiles of stationary FP (AAm, Na acrylate, potassium persulfate).

As it is shown, the mode of FP is a process taking place in non-isothermal conditions of thermal propagation of the polymerization wave. It should be noted that along with significant advantages, there is a problem in the implementation of FP. Since every time with the change of the initial composition, the patterns on establishing stationarity change dramatically, in each particular case modeling, calculation of kinetic regularities are necessary, otherwise the technology cannot be implemented.

The propagation of the polymerization wave depending on the initial conditions, the kinetics and macro kinetics of the process must be stationary; as can be noted, in Fig. 5 the wave is stable and stationary; at any point the amplitude of the wave is stable. This is a linear, stable propagation of the polymerization wave. One of the most important conditions for stability is to ensure the flow of the process under conditions when there is no loss of heat to the environment.

Transition of the process from a linear stable state to an unstable (non-linear) state can lead to both a decrease in the non-uniform flow of the process and a decrease in the rate of proliferation, attenuation, and the formation of different spin regimes. Naturally, the properties of the resulting products will not meet the requirements, and the process may stop, or splash out of the reaction vessel.

Therefore, detailed study of kinetic and macro-kinetic models in the FP is necessary. Otherwise, all the advantages of the FP will be leveled by the instability of the process.

Having the appropriate data for the synthesis of various polymer and nanopolymer composites, we have the possibility of obtaining gradient polymeric samples. For example, if we have calculated methods for the synthesis of various composites including superconducting, electrically conductive composites, we can combine them in one sample and using the FP method obtain the corresponding gradient material with the required properties.

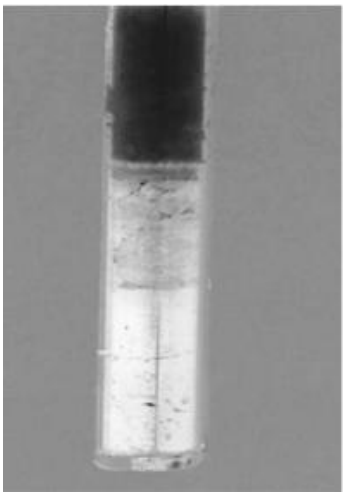

Fig. 6. A sample with gradient properties obtained by the FP method.

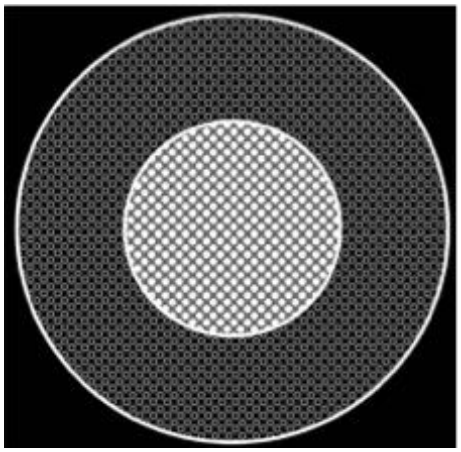

Fig.7. Schematic diagram of a film with (*1*) superconducting and (*2*) current-conducting properties obtained with the (*1*) UHMWPE and (*2*) AAM–MMA copolymer binder.

Fig. 6 exemplifies gradient polymeric material obtained by FP with sequentially arranged Co- and Ni-containing metal-complex monomers and AAM in which the chemical composition varies along the sample length. Here in the center we have a polymer composite with superconducting properties, obtained using the Cu complexes of acrylamide monomer with additives of superconducting ceramics, the next layer is complected with the Mn-acrylamide complexes with additives of nanosilver, due to which the resulting polymer composite acquires current-carrying properties.

When we interlace all these monomers, we require the desired gradient properties in advance. Such a sample cannot be obtained by traditional methods, since in the traditional process of polymerization the reagents are mixed in the volume of the reaction vessel and it is impossible to obtain material with different properties along the tube or radius.

Fig. 6 and 7 show the appropriate starting alternating initial reagents in the reaction ampoule, and the conditions for the polymerization process are set in advance for the implementation of the stationary reaction front. Then the FP will lead to the creation of a multifunctional gradient sample according to the form as required along the length or along the radius of sample.

It is well known that functionally gradient materials (FGMs) with gradual (polyfunctional) properties have a wide range of applications and are claimed in various areas of national economy and techniques. Polymer nanocomposites with gradient properties suggested by our research group possess a wide range of sensitivity due to the combination of different properties in one particular pattern. Such a gradient multifunctional sample is a microchip appropriate for all kinds of devices, which need gradient properties in a one general pattern: chips for superfast calorimeters, for medical and biological analyses and so on. In this way, we can perform FGMs along the length and along the radius of the obtained polymeric materials.

For obtaining gradient polymeric materials by a traditional technology (where properties along the length of a tube or radius of a tube vary according to requirements) it is necessary to obtain separately the materials with required different properties, then to combine them in one sample with alternation of properties either in a direction of a tube radius or in a direction of length of the tube. Auto wave process of frontal polymerization fixes set gradient properties in one sample according to in advance set distribution of an initial mix either along a tube or along a radius.

Conclusion

The article shows the frontal method, which is due to its specificity widely demanded in various fields of synthesis of polymers and polymer composites, as well as in high technologies, such as the synthesis of polymer nanocomposites, high-temperature superconducting interval composites, the gradient multifunctional composites in one polymerization stage. Thus, FP proved to be a unique method.

ՖՐՈՆՏԱԼ ՊՈԼԻՄԵՐԱՑՄԱՆ ՆՎԱՃՈՒՄՆԵՐԸ ԲԱՐՁՐ ՏԵԽՆՈԼՈԳԻԱՆԵՐՈՒՄ

Ա. Ն. ՏՈՆՈՅԱՆ և Ս. Պ. ԴԱՎԹՅԱՆ

Ֆրոնտալ պոլիմերացման մեթոդը, ի սկզբանե, գիտական հասարակության կողմից ընդունվում էր հիմնականում որպես պոլիմերների և պոլիմերային կոմպոզիտների սինթեզի բարձր արտադրողականությամբ և էկոլոգիապես անվտանգ մեթոդ: Սակայն վերջին տասնամյակներում պարզվեց, որ չնորհիվ ֆրոնտալ պոլիմերացման առանձնահատկությանը, մեթոդի կիրառումը բերում է զգալի նվաճումների բարձր տեխնոլոգիաների ասպարեզում՝ պոլիմերային նանոկոմպոզիտների, բարձրջերմաստիճանային ինտերկալացված պոլիմերային գերհաղորդիչների, բազմաֆունկցիոնալ գրադիենտային պոլիմերային նյութերի սինթեզի և այլ բնագավառներում:

Ներկայացված ակնարկային հոդվածում նկարագրված են հեղինակների կողմից ստացված արդյունքները և միջազգային տվյալները՝ վերը թվարկված խնդիրների վերաբերյալ:

ПРЕИМУЩЕСТВА МЕТОДА ФРОНТАЛЬНОЙ ПОЛИМЕРИЗАЦИИ В ВЫСОКИХ ТЕХНОЛОГИЯХ

А. А. ТОНОЯН и С. П. ДАВТЯН

Национальный политехнический университет Армении
Армения, 0009, Ереван, ул. Теряна, 105
E-mail: atonoyan@mail.ru

Изначально метод фронтальной полимеризации воспринимался научной общественностью в основном как высокопроизводительный и экологически безопасный метод синтеза полимеров и полимерных композитов. Однако за последние десятилетия выяснилось, что благодаря ее специфике использование метода фронтальной полимеризации приводит к существенным достижениям в области высоких технологий: синтез полимерных нанокомпозитов, синтез высокотемпературных интеркалированных полимерных сверхпроводников, синтез многофункциональных градиентных полимерных материалов и др.

В представленной обзорной статье авторами описываются собственные результаты и международные данные по вышеперечисленным проблемам.

REFERENCES

[1] *Davtyan S.P., Tonoyan A.O.* Teoriya i praktika adiabaticheskoi i frontal'noi polimerizatsii (Theory and Practice of Adiabatic and Frontal Polymerization), Palmarium, 2014

[2] *Тоноян А.О., Арутюнян Х.А., Давтян С.П., Розенберг Б.А., Ениколопян Н.С.* // Докл. АН СССР, 1973г., т.212., с.1128.

[3] *Begishev V.P., Volpert V.A., Davtyan S.P., Malkin A.Y.* // Dokl. Akad. Nauk SSSR, 1973, v. 208, p. 892.

[4] *Tonoyan A.O., Prikhozhenko A.I., Davtyan S.P., Milman V.D., Rozenberg B.A., Enikolopyan N.S.* // Dokl. Akad. Nauk SSSR, 1973, v. 211, №4, p. 673.

[5] *Tonoyan A.O., Lejkin A.D., Davtyan S.P., Rozenberg B.A., Enikolopyan N.S.* // Vysokomol. Soedin., Ser. A, 1974, v. 16, p. 1847.

[6] *Tonoyan A.O., Davtyan S.P., Rozenberg B.A., Enikolopyan N.S.* // Vysokomol. Soedin., Ser. A, 1974, v. 16, p. 624.

[7] *Kuvarina N.M., Tonoyan A.O., Davtyan,S.P., Aleksanyan G.G., Prut E.V., Zharov A.A., Enikolopyan N.S.* // Vysokomol. Soedin., Ser. A, 1974, v. 16, p. 1005.

[8] *Tonoyan A.O., Davtyan S.P., Rozenberg B.A., Enikolopyan, N.S.* // Vysokomol. Soed., Ser. A, 1974, v. 16, p. 799.

[9] *Masere J., Lewis L.L., Pojman J.A.* // J. Appl. Polym. Sci., 2001, v. 80, p. 686.

[10] *Daniele N., Alzari V., Pojman J.A., Sanna V., Ruiu A., Sanna D.M., Mariani A.* // ACS Appl. Mater. Interfaces, 2015, v. 7, p. 3600.

[11] *Alzari V., Ruiu A., Nuvoli D., Sanna R., Illescas J.M., Appelhans D., Voit B., Zschoche S., Mariani A.* // Polymer, 2014, v. 55, p. 5305.

[12] *Alzari V., Nuvoli D., Sanna R., Peponi L., Piccinini M., Bittolo B.S., Marceddu S., Valentini L., Kenny J.M., Mariani A.* // Colloid Polym. Sci., 2013, v. 291, №11, p. 2681.

[13] *Washington R.P., Steinbock O.J.* // Am. Chem. Soc., 2001, v. 123, p. 7933.

[14] *Lu G.D., Yan Q.Z., Ge C.C.* // Polym. Int., 2007, v. 56, p. 1016.
[15] *Davtyan S.P., Tonoyan A.O.* // The Frontal Polymerization Method in High Technology Applications ISSN 2079-9780, Review Journal of Chemistry, 2018, v. 8, №4, p. 432. © Pleiades Publishing, Ltd., 2018.
[16] *Davtyan S.P., Berlin A.A., Schick Ch., Tonoyan A.O., Rogovina S.Z.* // Nanotechnol. Russ., 2009, v. 4, 7–8, p. 489.
[17] *Davtyan S.P., Tonoyan A.O, Varderesyan A.Z., Muller S.C.* // Eur. Polym. J., 2014, v. 57, p. 182.
[18] *Tonoyan A.O., Davtyan S.P., Muller S.C.* // Influence of nanoparticles on the mechanism and properties of nanocomposites obtained in frontal regime, in Bottom-Up Self-Organization in Supramolecular Soft Matter. Principles and Prototypical Examples of Recent Advances, Muller, S.C. and Parisi, J., Eds., Springer, 2015, v. 217, p. 101.
[19] *Davtyan S.P., Tonoyan A.O.* Possibilites of current carrying superconducting polymer-ceramic nanocomposites obtainment, in Chemical Engineering of Polymers: Production of Functional and Flexible Materials, Apple Academic, 2017, part 3, ch. 30.
[20] *Tonoyan A.O., Tataryan A.A., Davtyan S.P., Schick Ch.* // Compos. Interfaces, 2006, v. 13, №4–6, p. 535.
[21] *Davtyan S.P., Tonoyan A.O., Sargsyan A.G., Schick Ch.* // J. Mater. Process. Technol., 2007, v. 163, №5, p. 734.
[22] *Davtyan S.P., Tonoyan A.O., Schick Ch., Tataryan A.A., Sargsyan A.G.* // J. Mater. Process. Technol., 2008, v. 200, №1–3, p. 319.
[23] *Tonoyan A., Davtyan S.* // Materials, 2009, v. 2, p. 2154.
[24] *Tonoyan, A.O., Davtyan, S.P.* High-temperature superconducting ceramic nanocomposites, in Ceramic Nanocomposites, New York: Woodhead, 2013, p. 284.

ՀԱՅԱՍՏԱՆԻ ՀԱՆՐԱՊԵՏՈՒԹՅԱՆ ԳԻՏՈՒԹՅՈՒՆՆԵՐԻ
ԱԶԳԱՅԻՆ ԱԿԱԴԵՄԻԱ
НАЦИОНАЛЬНАЯ АКАДЕМИЯ НАУК РЕСПУБЛИКИ АРМЕНИЯ
NATIONAL ACADEMY OF SCIENCES OF THE REPUBLIC OF ARMENIA

Հայաստանի քիմիական հանդես
Химический журнал Армении **71, №4, 2018** Chemical Journal of Armenia

UDC 547.81+547.83

SYNTHESIS AND BIOLOGICAL ACTIVITY OF NEW DERIVATIVES OF PYRANO[3-4-c][1,2,4]TRIAZOLO[4,3-a]PYRIDINES

E. G. PARONIKYAN, Sh. Sh. DASHYAN, N. S. MINASYAN, A. G. AKOPYAN and H. M. STEPANYAN

The Scientific and Technological Centre
of Organic and Pharmaceutical Chemistry NAS RA
26, Azatutyan Str., Yerevan, 0014, Armenia
E-mail: shdashyan@gmail.com

A new method for obtaining new heterocyclic systems – S-alkyl substituted pyrano[3-4-c]-[1,2,4]triazolo[4,3-a]pyridines on the basis of 8-hydrazino derivatives of pyrano[3,4-c]pyridines has been developed. Alkylation of 3-thioxopyrano[3,4-c][1,2,4]triazolo[4,3-a]pyridines with different alkylhalogenids resulted in the synthesis of S-alkylpyrano[3-4-c]-[1,2,4]triazolo[4,3-a]pyridine derivatives. The antimicrobial and neurotropic activities of the synthesized compounds have been investigated.

References 13.

Condensed pyridines have a broad spectrum of biological activity. In particular, derivatives of pyranopyridines have shown antimicrobial, anti-inflammatory, anticonvulsant activities [1-4].

At the same time, tricyclic triazolopyridines are little studied, there is only one report in the literature on the synthesis of 1,2,4-triazolo[4,3-a]pyrano[3,2-e]pyridines, which have antihypertensive action [5].

In continuation of studies on the synthesis of condensed pyridines [6,7] and with the purpose to study their biological activities we synthesized new S-alkyl substituted derivatives of pyrano[3,4-c][1,2,4]triazolo[4,3-a]pyridines **3a-n,** which are the derivatives of new heterocyclic systems.

As the starting material we used the 8-hydrazinopyrano[3,4-c]pyridines **1a,b**, which have been synthesized by us in the work [8].

In this work we developed a new method for obtaining 3-thioxopyrano[3,4-c][1,2,4]triazolo[4,3-a]pyridines **2a,b** by the interaction of compounds 1a,b with CS_2 in MeOH in the presence of KOH. A new method allowed to exclude pyridine from the reaction medium and increase the rate of cyclizations in contrast to work [8].

The obtained 3-thioxopyrano[3,4-c][1,2,4]triazolo[4,3-a]pyridines were transformed to the S-alkyl substituted derivatives **3a-n** under the action of different alkyl halogenids (Scheme).

Scheme

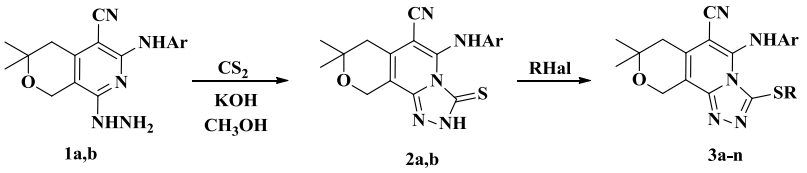

1a,b 2a,b 3a-n

Ar = C_6H_5 (1a, 2a, 3a-g); Ar = 4-$CH_3C_6H_4$ (1b, 2b, 3h-n);
3: R = $CH_2CON(C_2H_5)_2$ (a,k); CH_2-benzimidazol-2-yl (b); $CH_2CONHCH_2C_6H_5$ (c); $CH_2CONHCH_2$-4-$CH_3C_6H_4$ (d); CH_2CONH-3-ClC_6H_4 (e); CH_2CONH-2-$NO_2C_6H_4$ (f); CH_2CONH-1,3-thiazol-2-yl (g); $CH_2C_6H_5$ (h); $CH_2COC_6H_5$ (i); CH_2CONH-3-$CH_3C_6H_4$ (j); CH_2CONH-4-$COCH_3C_6H_4$ (l); CH_2CONH-2-naphthyl (m); CH_2CONH_2 (n)

The IR spectrum of compounds **3a–n** revealed the presence of absorption bands at 3306–3408 cm^{-1} assigned to NH group, and a strong absorption band at 2208–2226 cm^{-1} for C≡N group.

^{1}H NMR spectrum revealed the presence of signals at δ 3.92–4.88 ppm for SCH_2 protons. ^{13}C NMR spectra of compounds **3a,i,j,l** showed signals at δ 39.4-42.3 ppm corresponding to the SCH_2 group. The spectral data confirmed formation of *S*-alkyl derivatives [9]. The regioselectivity of this reaction was explained by the greater polarizability of the sulfur atom compared to the nitrogen atom [10].

The antimicrobial activity of compounds **3a–n** was studied by the agar diffusion assay [11]. Experiments were performed with Gram-positive staphylococci (*Staphylococcus aureus* 209P, JC-1) and Gram-negative rods (*Shigella dysenteriae flexneri* 6858, *Escherichia coli* 0-55). The studies showed that compounds **3a,b,f,g,j,k-n** had weak activity against all tested microbial strains: the diameters (d) of growth inhibition zones were 10–15 *mm*. The indicated compounds were significantly less active than the reference drug furazolidone (d 24–25 *mm*) [12].

Neurotropic activity of the newly synthesized triazolopyridine derivatives **3a-n** was studied by indicators characterizing the anticonvulsant activity and side effects. A study of 14 compounds **3a-n** and a reference drug diazepam was carried out on 120 white mice weighing 18–24 *g*. Anticonvulsant activity of the compounds was assessed by the prevention of the seizure clonic component induced by subcutaneous injection of corazole (90 *mg/kg*) to mice [13]. Unwanted side effects in these animals, namely the central myorelaxant effect and impaired motor coordination were examined by the rotating rod method [13].

The compounds under investigation were injected in a dose range of 50 *mg/kg* intraperitoneally 45 min before injection of corazole in the form of a suspension with Tween 80 and ethosuximide – at a dose of 150 *mg/kg*.

The study of anticonvulsant action revealed that not all synthesized derivatives had the same anticorazole activity. Thus, compounds **3a, c, i, j, l** at a dose of 50 *mg/kg* prevented convulsions only in 20–40% of animals, while ethosuximide

showed a 50% efficiency only at a dose of 150 *mg/kg*. Moreover, studies of these compounds and ethosuximide at the mentioned doses did not reveal the muscle relaxation phenomena.

Experimental Section

All chemicals, reagents, and solvents were of commercially high purity grade purchased from Sigma-Aldrich. Melting points (mp) were determined on a "Boetius" microtable. They are expressed in degree centigrade (ºC). ^{1}H NMR and ^{13}C NMR spectra were recorded on a Varian "Mercury 300VX" 300 (^{1}H) and 75.462 *MHz* (^{13}C) spectrometer. Chemical shifts were reported as δ (parts per million) relative to TMS (tetramethylsilane) as an internal standard. IR spectra were recorded on "Nicolet Avatar 330 FT-IR" spectrophotometer and the reported wave numbers are given in cm^{-1}. TLC analyses were performed on "Silufol UV-254" plates using pyridine–ethyl acetate, 2:1 (2), butanol–acetic acid–water, 4:2:5 (3) as eluent; spots were developed with iodine vapor.

General procedure for the synthesis of 3-thioxopyrano[3,4-c][1,2,4]-triazolo[4,3-a]- pyridines 2a,b. Compounds **1a,b** 4.5 *mmol* and 5*ml* of CS_2 were added to a solution of 0.3 *g* (5.4 *mmol*) of KOH in 50 *ml* of methanol. The mixture was refluxed for 5 *h*. After cooling, the obtained solution was acidified with 10% HCl, the formed crystals were filtered and recrystallized from 1:1 mixture of EtOH-$CHCl_3$. The spectral data of compounds **2a,b** corresponded to data in reference [8].

5-Anilino-8,8-dimethyl-3-thioxo-2,3,7,10-tetrahydro-8H-pyrano[3,4-c][1,2,4]triazolo[4,3-a]pyridine-6-carbonitrile (2a). Yield 1.42 g (90%), mp 259–260°C.

8,8-Dimethyl-5-(4-methylphenyl)amino-3-thioxo2,3,7,10-tetrahydro-8H-pyrano[3,4-c]- [1,2,4]triazolo[4,3-a]pyridine-6-carbonitrile (2b). Yield 1.50 g (91%), mp 238–239°C.

General procedure for alkylation of pyranotriazolothiones 3a–n. The appropriate 2 *mmol* of compounds **2a,b** was added to a solution of 112 *mg* (2 *mmol*) of KOH in a mixture of 2 *ml* of H_2O and 12 *ml* of EtOH. After complete dissolution, the appropriate 2 *mmol* of alkyl halide was added with cooling, and the reaction mixture was stirred for 6 h at room temperature. The obtained crystals were filtered off, washed with H_2O, dried, and recrystallized from a 2:1 mixture of EtOH–$CHCl_3$.

2-[(5-Anilino-6-cyano-8,8-dimethyl-7,10-dihydro-8*H*-pyrano[3,4-*c*][1,2,4]triazolo[4,3-*a*]- pyridin-3-yl)thio]-*N*,*N*-diethylacetamide (3a). Yield 0.75 *g* (81%), mp 228-229ºC, R_f 0.60. IR spectrum, *ν*, cm^{-1}: 1675 (C=O), 2226 (CN), 3306 (NH). ^{1}H NMR spectrum, δ, ppm, *MHz*: 1.08 t (3H, *J* = 7.1, CH_3); 1.19 t (3H, *J* = 7.1, CH_3); 1.35 s (6H, 2×CH_3); 2.63 s (2H, 7-CH_2); 3.34 q (2H, *J* = 7.1, NCH_2); 3.39 q (2H, *J* = 7.1, NCH_2); 4.24 s (2H, SCH_2); 4.86 s (2H, 10-CH_2); 6.97-7.03 m (3H, H_{Ar}); 7.26-7.32 m (2H, H_{Ar}); 10.05 s (1H, 5-NH). ^{13}C NMR spectrum, δ, ppm, *MHz*: 12.5 (CH_3), 13.7 (CH_3), 25.9 (2CH_3), 39.4 (CH_2), 39.8 (CH_2), 40.2 (CH_2), 41.6 (SCH_2), 57.8 (OCH_2), 69.8, 90.6 (C-6), 113.1 (CN), 115.4, 117.9 (2CH), 122.0

(CH), 128.6 (2CH), 132.0, 140.6, 141.5, 142.0, 148.3, 166.2 (CO). Found, %: C 62.13; H 6.03; N 18.23; S 6.78. $C_{24}H_{28}N_6O_2S$. Calculated, %: C 62.05; H 6.07; N 18.09; S 6.90.

5-Anilino-3-[(1*H*-benzimidazol-2-ylmethyl)thio]-8,8-dimethyl-7,10-dihydro-8*H*-pyrano- [3,4-*c*][1,2,4]triazolo[4,3-*a*]pyridine-6-carbonitrile (3b). Yield 0.76 *g* (79%), mp 204-206ºC, R_f 0.62. IR spectrum, *ν*, *cm*$^{-1}$: 2210 (CN), 3325, 3408 (NH). ^{1}H NMR spectrum, δ, ppm, *MHz*: 1.34 s (6H, 2×CH_3); 2.62 t (2H, *J* = 1.8, 7-CH_2); 4.65 s (2H, SCH_2); 4.84 t (2H, *J* = 1.8, 10-CH_2); 6.94-7.00 m (3H, H_{Ar}); 7.08-7.13 m (2H, H_{Ar}); 7.22-7.30 m (2H, H_{Ar}); 7.42-7.48 m (2H, H_{Ar}); 10.34 brs (1H, NH); 12.19 br.s (1H, 5-NH). Found, %: C 64.97; H 4.85; N 20.43; S 6.54. $C_{26}H_{23}N_7OS$. Calculated, %: C 64.85; H 4.81; N 20.36; S 6.66.

2-[(5-Anilino-6-cyano-8,8-dimethyl-7,10-dihydro-8*H*-pyrano[3,4-*c*][1,2,4]triazolo[4,3-*a*]- pyridin-3-yl)thio]-*N*-benzylacetamide (3c). Yield 0.76 *g* (76%), mp 209-210 ºC, R_f 0.62. IR spectrum, *ν*, *cm*$^{-1}$: 1670 (CO), 2212 (CN), 3325, 3367 (NH), ^{1}H NMR spectrum, δ, ppm, *MHz*: 1.36 s (6H, 2×CH_3); 2.65 s (2H, 7-CH_2); 3.99 s (2H, SCH_2); 4.29 d (2H, *J* = 5.8, NHC$\underline{H_2}$); 4.86 s (2H, 10-CH_2); 6.97-7.03 m (3H, H_{Ar}); 7.11-7.32 m (7H, H_{Ar}); 8.66 t (1H, *J* = 5.8, NH); 9.76 s (1H, 5-NH). Found, %: C 64.97; H 5.33; N 16.92; S 6.34. $C_{27}H_{26}N_6O_2S$. Calculated, %: C 65.04; H 5.26; N 16.86; S 6.43.

2-[(5-Anilino-6-cyano-8,8-dimethyl-7,10-dihydro-8*H*-pyrano[3,4-*c*][1,2,4]triazolo[4,3-*a*]- pyridin-3-yl)thio]-*N*-(4-methylphenyl)acetamide (3d). Yield 0.82 *g* (82%), mp 231-232ºC, R_f 0.58. IR spectrum, *ν*, *cm*$^{-1}$: 1666 (CO), 2208 (CN), 3327, 3372 (NH). ^{1}H NMR spectrum, δ, ppm: 1.34 s (6H, 2×CH_3); 2.29 s (3H, CH_3); 2.61 s (2H, 7-CH_2); 4.14 s (2H, SCH_2); 4.84 s (2H, 10-CH_2); 6.94-7.00 m (2H, H_{Ar}); 7.00-7.05 m (3H, H_{Ar}); 7.24-7.31 m (2H, H_{Ar}); 7.38-7.42 m (2H, H_{Ar}); 9.62 s (1H, NH); 10.07 s (1H, 5-NH). Found, %: C 64.97; H 5.33; N 16.92; S 6.34. $C_{27}H_{26}N_6O_2S$. Calculated, %: C 65.04; H 5.26; N 16.86; S 6.43.

2-[(5-Anilino-6-cyano-8,8-dimethyl-7,10-dihydro-8*H*-pyrano[3,4-*c*][1,2,4]triazolo[4,3-*a*]- pyridin-3-yl)thio]-*N*-(3-chlorophenyl)acetamide (3e). Yield 0.80 *g* (77%), mp 217-218ºC, R_f 0.61. IR spectrum, *ν*, *cm*$^{-1}$: 1668 (CO), 2208 (CN), 3325, 3372 (NH). ^{1}H NMR spectrum, δ, ppm, *MHz*: 1.35 s (6H, 2×CH_3); 2.63 t (2H, *J* = 1.9, 7-CH_2); 4.16 s (2H, SCH_2); 4.84 t (2H, *J* = 1.9, 10-CH_2); 6.91-7.00 m (4H, H_{Ar}); 7.21 t (1H, *J* = 8.2, H_{Ar}); 7.23-7.30 m (2H, H_{Ar}); 7.42 dd (1H, *J* = 8.2, 2.1, H_{Ar}); 7.69 t (1H, *J* = 2.1, H_{Ar}); 9.47 brs (1H, NH); 10.35 brs (1H, 5-NH). Found, %: C 60.28; H 4.54; N 16.23; S 6.09. $C_{26}H_{23}ClN_6O_2S$. Calculated, %: C 60.17; H 4.47; N 16.19; S 6.18.

2-[(5-Anilino-6-cyano-8,8-dimethyl-7,10-dihydro-8*H*-pyrano[3,4-*c*][1,2,4]triazolo[4,3-*a*]pyridin-3-yl)thio]-*N*-(2-nitrophenyl)acetamide (3f). Yield 0.81 *g* (76%), mp 245-247ºC, R_f 0.64. IR spectrum, *ν*, *cm*$^{-1}$: 1350, 1540 (NO_2), 1665 (CO), 2210 (CN), 3328, 3367 (NH). ^{1}H NMR spectrum, δ, ppm, *MHz*: 1.35 s (6H, 2×CH_3); 2.63 s (2H, 7-CH_2); 4.22 s (2H, SCH_2); 4.84 s (2H, 10-CH_2); 6.88-6.99 m (3H, H_{Ar}); 7.21-7.33 m (3H, H_{Ar}); 7.63 t.d (1H, *J* = 8.3, 1.4, H_{Ar}); 7.98 dd (1H, *J* = 8.3, 1.4, H_{Ar}); 8.05 dd (1H, *J* = 8.3, 1.1, H_{Ar}); 9.37 brs (1H, NH); 10.67 brs (1H, 5-

NH). Found, %: C 58.85; H 4.41; N 18.44; S 6.13. $C_{26}H_{23}N_7O_4S$. Calculated, %: C 58.97; H 4.38; N 18.51; S 6.06.

2-[(5-Anilino-6-cyano-8,8-dimethyl-7,10-dihydro-8*H*-pyrano[3,4-*c*][1,2,4]triazolo[4,3-*a*]- pyridin-3-yl)thio]-*N*-1,3-thiazol-2-ylacetamide (3g). Yield 0.78 *g* (79%), mp 262-263ºC, R_f 0.59. IR spectrum, *v*, cm^{-1}: 1672 (CO), 2210 (CN), 3329, 3377 (NH). ^{1}H NMR spectrum, δ, ppm, *MHz*: 1.35 s (6H, 2×CH_3); 2.63 t (2H, *J* = 1.8, 7-CH_2); 4.21 s (2H, SCH_2); 4.84 t (2H, *J* = 1.8, 10-CH_2); 6.90-6.97 m (3H, H_{Ar}); 6.99 d (1H, *J* = 3.5, SCH); 7.22-7.29 m (2H, H_{Ar}); 7.37 dd (1H, *J* = 3.5, NCH); 9.37 brs (1H, NH); 12.29 brs (1H, 5-NH). Found, %: C 56.30; H 4.28; N 19.99; S 12.91. $C_{23}H_{21}N_7O_2S_2$. Calculated, %: C 56.19; H 4.31; N 19.94; S 13.05.

3-(Benzylthio)-8,8-dimethyl-5-[(4-methylphenyl)amino]-7,10-dihydro-8*H*-pyrano[3,4-*c*][1,2,4]triazolo[4,3-*a*]pyridine-6-carbonitrile (3h). Yield 0.69 *g* (76%), mp 219-220ºC, R_f 0.61.IR spectrum, *v*, cm^{-1}: 2210 (CN), 3327 (NH). ^{1}H NMR spectrum, δ, ppm, *MHz*: 1.34 s (6H, 2×CH_3); 2.32 s (3H, CH_3); 2.60 t (2H, *J* = 1.7, 7-CH_2); 4.40 s (2H, SCH_2); 4.84 t (2H, *J* = 1.7, 10-CH_2); 6.70-6.75 m (2H, H_{Ar}); 7.01-7.06 m (2H, H_{Ar}); 7.18-7.27 m (5H, H_{Ar}); 8.98 brs (1H, 5-NH). Found, %: C 68.61; H 5.58; N 15.48; S 6.89. $C_{26}H_{25}N_5OS$. Calculated, %: C 68.55; H 5.53; N 15.37; S 7.04.

8,8-Dimethyl-5-[(4-methylphenyl)amino]-3-[(2-oxo-2-phenylethyl)thio]-7,10-dihydro-8*H*-pyrano[3,4-*c*][1,2,4]triazolo[4,3-*a*]pyridine-6-carbonitrile (3i). Yield 0.77 *g* (80%), mp 201-202ºC, R_f 0.66. IR spectrum, *v*, cm^{-1}: 1685 (CO), 2210 (CN), 3322 (NH). ^{1}H NMR spectrum, δ, ppm: 1.35 s (6H, 2×CH_3); 2.32 s (3H, CH_3); 2.62 s (2H, 7-CH_2); 4.83 s (2H, 10-CH_2); 4.88 s (2H, SCH_2); 6.83-6.88 m (2H, H_{Ar}); 7.04-7.09 m (2H, H_{Ar}); 7.46-7.52 m (2H, H_{Ar}); 7.57-7.64 m (1H, H_{Ar}); 7.98-8.03 m (2H, H_{Ar}); 9.30 s (1H, NH). ^{13}C NMR spectrum, δ, ppm: 20.3 (CH_3), 25.9 (2CH_3), 36.4 (CH_2), 42.3 (SCH_2), 57.8 (OCH_2), 69.8, 91.8 (C-6), 113.1(CN), 116.1, 117.9 (2CH), 128.0 (2CH), 128.1 (2CH), 129.3 (2CH), 131.0 (CH), 131.6, 133.0, 135.1, 138.9, 141.8, 142.2, 148.4, 192.6 (CO). Found, %: C 67.15; H 5.28; N 14.54; S 6.49. $C_{27}H_{25}N_5O_2S$. Calculated, %: C 67.06; H 5.21; N 14.48; S 6.63.

2-({6-Cyano-8,8-dimethyl-5-[(4-methylphenyl)amino]-7,10-dihydro-8*H*-pyrano[3,4-*c*]-[1,2,4]triazolo[4,3-*a*]pyridin-3-yl}thio)-*N*-(3-methylphenyl)acetamide (3j). Yield 0.83 *g* (81%), mp 220-222ºC, R_f 0.60. IR spectrum, *v*, cm^{-1}: 1666 (CO), 2209 (CN), 3325, 3371 (NH). ^{1}H NMR spectrum, δ, ppm: 1.34 s (6H, 2×CH_3); 2.32 s (3H, CH_3); 2.33 s (3H, CH_3); 2.61 s (2H, 7-CH_2); 4.14 s (2H, SCH_2); 4.83 s (2H, 10-CH_2); 6.78-6.83 m (1H, H_{Ar}); 6.88-6.93 m (2H, H_{Ar}); 7.06-7.13 m (3H, H_{Ar}); 7.28-7.35 m (2H, H_{Ar}); 9.52 brs (1H, NH); 10.06 brs (1H, 5-NH). ^{13}C NMR spectrum, δ, ppm: 20.3 (CH_3), 21.0 (CH_3), 25.9 (2CH_3), 36.4 (CH_2), 39.8 (SCH_2), 57.7 (OCH_2), 69.8, 90.4 (C-6), 113.0 (CN), 115.2, 116.2 (CH), 118.4 (2CH), 119.5 (CH), 123.7 (CH), 127.8 (CH), 129.2 (2CH), 131.3, 132.1, 137.3, 138.1, 138.2, 141.9, 142.0, 148.4, 165.3 (CO). Found, %: C 65.43; H 5.47; N 16.51; S 6.34. $C_{28}H_{28}N_6O_2S$. Calculated, %: C 65.60; H 5.51; N 16.39; S 6.26.

2-({6-Cyano-8,8-dimethyl-5-[(4-methylphenyl)amino]-7,10-dihydro-8*H*-pyrano[3,4-*c*]-[1,2,4]triazolo[4,3-*a*]pyridin-3-yl}thio)-*N*,*N*-diethylacetamide (3k).

Yield 0.75 *g* (78%), mp 208-209ºC, R_f 0.65. IR spectrum, *ν*, *cm*$^{-1}$: 1675 (C=O), 2225 (CN), 3308 (NH). ^{1}H NMR spectrum, δ, ppm, *MHz*: 1.08 t (3H, *J* = 7.1, $CH_2C\underline{H_3}$); 1.19 t (3H, *J* = 7.1, $CH_2C\underline{H_3}$); 1.34 s (6H, 2×CH_3); 2.35 s (3H, CH_3); 2.61 s (2H, 7-CH_2); 3.34 q (2H, *J* = 7.1, NCH_2); 3.38 q (2H, *J* = 7.1, NCH_2); 4.23 s (2H, SCH_2); 4.83 s (2H, 10-CH_2); 6.92-6.97 m (2H, H_{Ar}); 7.08-7.13 m (2H, H_{Ar}); 10.07 brs (1H, 5-NH). Found, %: C 62.83; H 6.25; N 17.71; S 6.59. $C_{25}H_{30}N_6O_2S$. Calculated, %: C 62.74; H 6.32; N 17.56; S 6.70.

***N*-(4-Acetylphenyl)-2-({6-cyano-8,8-dimethyl-5-[(4-methylphenyl)amino]-7,10-dihydro-8*H*-pyrano[3,4-*c*][1,2,4]triazolo[4,3-*a*]pyridin-3-yl}thio)acetamide (3l).** Yield 0.83 *g* (77%), mp 207-208ºC, R_f 0.62. IR spectrum, *ν*, *cm*$^{-1}$: 1665, 1710 (CO), 2208 (CN), 3325, 3373 (NH). ^{1}H NMR spectrum, δ, ppm: 1.34 s (6H, 2×CH_3); 2.33 s (3H, CH_3); 2.51 s (3H, $COCH_3$); 2.60 s (2H, 7-CH_2); 4.18 s (2H, SCH_2); 4.82 s (2H, 10-CH_2); 6.85-6.91 m (2H, H_{Ar}); 7.04-7.11 m (2H, H_{Ar}); 7.64-7.69 m (2H, H_{Ar}); 7.82-7.87 m (2H, H_{Ar}); 9.42 brs (1H, NH); 10.50 brs (1H, 5-NH). ^{13}C NMR spectrum, δ, ppm: 20.3 (CH_3), 25.7 (CH_3), 25.9 (2CH_3), 36.4 (CH_2), 39.4 (SCH_2), 57.7 (OCH_2), 69.8, 91.2 (C-6), 113.0 (CN), 115.6, 118.1 (2CH), 118.2 (2CH), 128.8 (2CH), 129.2 (2CH), 131.2, 131.8, 131.9, 138.5, 141.8, 142.1, 142.5, 148.4, 165.9, 194.6 (CO). Found, %: C 64.56; H 5.18; N 15.62; S 5.81. $C_{29}H_{28}N_6O_3S$. Calculated, %: C 64.43; H 5.22; N 15.54; S 5.93.

2-({6-Cyano-8,8-dimethyl-5-[(4-methylphenyl)amino]-7,10-dihydro-8*H*-pyrano[3,4-*c*][1,2,4]triazolo[4,3-*a*]pyridin-3-yl}thio)-*N*-2-naphthylacetamide (3m). Yield 0.82 *g* (75%), mp 249-250ºC, R_f 0.65. IR spectrum, *ν*, *cm*$^{-1}$: 1670 (CO), 2208 (CN), 3323, 3370 (NH). ^{1}H NMR spectrum, δ, ppm, *MHz*: 1.34 s (6H, 2×CH_3); 2.32 s (3H, CH_3); 2.60 brs (2H, 7-CH_2); 4.31 s (2H, SCH_2); 4.86 brs (2H, 10-CH_2); 6.84-6.89 m (2H, H_{Ar}); 7.03-7.08 m (2H, H_{Ar}); 7.40-7.50 m (3H, H_{Ar}); 7.66 brd (1H, *J* = 8.1, H_{Ar}); 7.76 brd (1H, *J* = 7.5, H_{Ar}); 7.79-7.85 m (1H, H_{Ar}); 8.00-8.06 m (1H, H_{Ar}); 9.48 brs (1H, NH); 10.20 brs (1H, 5-NH). Found, %: C 67.95; H 5.19; N 15.21; S 5.92. $C_{31}H_{28}N_6O_2S$. Calculated, %: C 67.86; H 5.14; N 15.32; S 5.84.

2-({6-Cyano-8,8-dimethyl-5-[(4-methylphenyl)amino]-7,10-dihydro-8*H*-pyrano[3,4-*c*]- [1,2,4]triazolo[4,3-*a*]pyridin-3-yl}thio)acetamide (3n). Yield 0.69 *g* (82%), mp 250-252ºC, R_f 0.67. IR-spectrum, *ν*, *cm*$^{-1}$: 1675 (CO), 2210 (CN), 3325 (NH), 3370, 3424 (NH_2). ^{1}H NMR spectrum, δ, ppm, *MHz*: 1.34 s (6H, 2×CH_3); 2.34 s (3H, CH_3); 2.60 t (2H, *J* = 1.8, 7-CH_2); 3.92 s (2H, SCH_2); 4.83 t (2H, *J* = 1.8, 10-CH_2); 6.91-6.96 m (2H, H_{Ar}); 7.07-7.12 m (2H, H_{Ar}); 7.15 brs (1H, NH_2); 7.61 brs (1H, NH_2); 9.87 brs (1H, 5-NH). Found, %: C 59.81; H 5.20; N 19.97; S 7.50. $C_{21}H_{22}N_6O_2S$. Calculated, %: C 59.70; H 5.25; N 19.89; S 7.59.

This work was supported by the RA MES State Commitee of Science in the frames of research project №18T-1D066

ՆՈՐ ՊԻՐԱՆՈ[3,4-c][1,2,4]ՏՐԻԱԶՈԼՈ[4,3-a]ՊԻՐԻԴԻՆՆԵՐԻ ԱԾԱՆՑՅԱԼՆԵՐԻ ՍԻՆԹԵԶԸ ԵՎ ԿԵՆՍԱԲԱՆԱԿԱՆ ԱԿՏԻՎՈՒԹՅՈՒՆԸ

Ե. Գ. ՊԱՐՈՆԻԿՅԱՆ, Շ. Շ. ԴԱՇՅԱՆ, Ն. Ս. ՄԻՆԱՍՅԱՆ, Ա. Գ. ՀԱԿՈԲՅԱՆ և Հ. Մ. ՍՏԵՓԱՆՅԱՆ

Մշակված է նոր հետերոցիկլիկ համակարգի – 3-թիօքսոպիրանո[3,4-c][1,2,4]–տրիազոլո-[4,3-a]–պիրիդինների ածանցյալների ստացման եղանակ՝ 8-հիդրազինոպիրանո[3,4-c]պիրիդինների փոխազդեցությամբ ածխածնահանձնի հետ, կալիումի հիդրօքսիդի մեթանոլային լուծույթի ներկայությամբ: Նոր եղանակը հնարավորություն է տալիս բացառել ռեակցիոն միջավայրում պիրիդինի առկայությունը և զգալիորեն մեծացնել ցիկլման ռեակցիայի արագությունը:

3-Թիօքսոպիրանո[3,4-c][1,2,4]տրիազոլո[4,3-a]պիրիդինների ալկիլացմամբ, տարբեր ալկիլ հալոգենիդներով, սինթեզված են S-ալկիլպիրանո[3,4-c][1,2,4]տրիազոլո[4,3-a]պիրիդինների ածանցյալներ: Ուսումնասիրված են սինթեզված միացությունների հակամանրէային և նեյրոտրոպ ակտիվությունները: Ուսումնասիրությունների արդյունքում պարզվել է, որ որոշ հետազոտվող միացություններ ցուցաբերում են հակամանրէային և նեյրոտրոպ ակտիվություններ:

СИНТЕЗ И БИОЛОГИЧЕСКАЯ АКТИВНОСТЬ НОВЫХ ПРОИЗВОДНЫХ ПИРАНО[3,4-c][1,2,4]ТРИАЗОЛО[4,3-a]ПИРИДИНОВ

Е. Г. ПАРОНИКЯН, Ш. Ш. ДАШЯН, Н. С. МИНАСЯН, А. Г. АКОПЯН и Г. М. СТЕПАНЯН

Научно-технологический центр органической и фармацевтической химии
НАН Республики Армения
Армения, 0014, Ереван, пр. Азатутян, 26
E-mail: shdashyan@gmail.com

Разработан новый метод получения производных 3-тиоксопирано[3,4-c][1,2,4]триазоло[4,3-a]пиридинов взаимодействием 8-гидразинопирано[3,4-c]пиридинов с сероуглеродом в присутствии метанольного раствора гидроксида калия. Новый метод позволил исключить из реакционной среды пиридин и увеличить скорость циклизации. Алкилированием 3-тиоксопирано[3,4-c][1,2,4]триазоло[4,3-a]пиридинов с различными алкилгалогенидами синтезированы производные *S*-алкилпирано[3,4-c][1,2,4]триазоло[4,3-a]пиридинов. Изучена антимикробная и нейротропная активность синтезированных соединений. Исследования показали, что некоторые производные новой гетероциклической системы оказывают антимикробное и нейротропное действие.

REFERENCES

[1] *Kumar R.R., Perumal S., Menéndez J.C., Yogeeswari P., Sriram D.* // Bioorg. Med. Chem., 2011, №19, p. 3444.

[2] *Kwak W.-J., Kim J.-H., Ryu K.-H., Cho Y.-B., Jeon S.-D., Moon C.-K.* // Biol. Pharm. Bull., 2005, v. 28, p. 750.

[3] *Nguyen S.T., Kwasny S.M., Ding X., Cardinale S.C., McCarthy C.T., Kim H.-S., Nikaido H., Peet N.P., Williams J.D., Bowlin T.L., Opperman T.J.* // Bioorg. Med. Chem., 2015, v. 23, p. 2024.

[4] *Paronikyan E.G., Sirakanyan S.N., Noravyan A.S., Melkonyan J.A.* // Arm. Chem. J., 1991, v. 44, № 4, p. 250.
[5] *Kumar N.V., Mashelkar U.C.* // Indian J. Chem., Sect. B: Org. Chem. Incl. Med. Chem., 2008, v. 47, p. 764.
[6] *Paronikyan E.G., Dashyan Sh.Sh., Noravyan A.S., Tamazyan R.A., Ayvazyan A.G., Panosyan H.A.* // Tetrahedron, 2015, v. 71, p. 2686.
[7] *Paronikyan E.G., Dashyan Sh.Sh., Dzhagatspanyan I. A., Paronikyan R.G., Nazaryan, I.M., Akopyan A.G., Minasyan N.S., Ayvazyan A.G., Tamazyan R.A., Babaev E.V.* // Russ. J. Bioorg. Chem., 2016, v. 42, p. 215.
[8] *Paronikyan E.G., Dashyan Sh.Sh., Minasyan N.S., Stepanyan G.M., Ayvazyan A.G., Tamazyan R.A.* // Chem. Heterocycl. Compd., 2016, v. 52, № 12, p. 2078.
[9] *Karataeva F.N., Klochkov V.V.* NMR Spectroscopy in Organic Chemistry. Kazan. fed. un-ta: Kazan, 2012, v., p. 49.
[10] *Pozharskii A.F.* Theoretical Foundations of Heterocyclic Chemistry. M., Chemistry, 1985, p. 159.
[11] *Mironov A.N.* Guidelines for Performing Clinical Studies of Pharmaceuticals. M., Meditsina, 2012, Part 1, p. 509.
[12] *Mashkovsky M.D.* Drugs. M., Novaya Volna, 2010, p. 851.
[13] *Vogel H.G., Vogel W.H.* Psychjtropic and neurotropic activity In Drug Discovery and Evaluation: Pharmacological Assays. Berlin & N-Y., Springer, 2008. p. 569.

ՀԱՅԱՍՏԱՆԻ ՀԱՆՐԱՊԵՏՈՒԹՅԱՆ ԳԻՏՈՒԹՅՈՒՆՆԵՐԻ
ԱԶԳԱՅԻՆ ԱԿԱԴԵՄԻԱ
НАЦИОНАЛЬНАЯ АКАДЕМИЯ НАУК РЕСПУБЛИКИ АРМЕНИЯ
NATIONAL ACADEMY OF SCIENCES OF THE REPUBLIC OF ARMENIA

Հայաստանի քիմիական հանդես
Химический журнал Армении **71, №4, 2018** Chemical Journal of Armenia

UDC 547.294.314.07

SYNTHESIS OF NEW ACHIRAL *BIS*-ALKYLATED GLYCINE ANALOGS

Z. Z. MARDIYAN[a,b], A. F. MKRTCHYAN[a,b] and A. S. SAGHYAN[a,b]

[a]Scientific and Production Center "Armbiotechnology" NAS RA
14, Gyurjyan Str., Yerevan, 0056, Armenia
Fax: (+37410) 654180, E-mail: zmardiyan89@gmail.com
[b]Yerevan State University
Institute of Pharmacy
1, A. Manoukyan Str., Yerevan, 0025, Armenia

A method for the synthesis of α-bis-alkyl substituted derivatives of glycine by means of C-alkylation of the amino acid moiety of Ni^{II}-complex of Schiff base of glycine with a chiral auxiliary reagent (S)-2-N-[N'-(benzylprolyl)amino]benzophenone (BPB) by propargyl-, allyl-, 2-bromobenzyl- and 4-fluorobenzyl bromides under conditions of base catalysis has been developed.

Tables 2, references 15.

α-Amino acids of non-protein origin, as irreversible inhibitors of enzymes with high specificity and duration of action, are widely used in medicine, pharmaceutical chemistry, microbiology and other fields of science and technology [1-4]. In a series of non-proteinogenic amino acids, α-alkyl substituted α-amino acids that have strong antihypertensive, antiseptic and antitumor activities [5-8] are of certain interest. Among them halogen-containing aromatic ring derivatives of phenylalanine and its α-alkylated analogs occupy a special place [9, 10]. Amino acids containing unsaturated groups (acetylene, allyl, etc.) in the side radical [11, 12] can have important pharmacological properties. There is a limited number of acetylenic amino acids, mainly isolated from fungal cells, which have an inhibitory effect on many enzymes [7]. For example, (*S*)-2-aminobut-3-ynic acid (propargylglycine) isolated from the fungi *Steroptpmyces catenula*, inhibits the action of *Saccharomyces cerevisiae* and *Esherichia coli* cells; it is an inhibitor of amylase synthesis, an activator of pyridoxalphosphate-dependent enzymes [8] and is a component of antibiotic FR 900130 [9].

Earlier, to obtain α-substituted α-amino acids, the unique properties of square-planar Ni^{II} complexes of Schiff base of amino acids and chiral auxiliary (*S*)-2-N-[N'-(benzylprolyl)amino] benzophenone (BPB) were used. Due to high CH-acidity of

the α-carbon atom of the amino acid moiety of these complexes, its C-alkylation by alkyl halides resulted in the asymmetric syntheses of a wide range of α-monosubstituted α-amino acids (glycine, alanine, etc.) containing different alkyl substituents in the side radical [13].

This paper reports on the synthesis of achiral α,α-disubsituted glycine analogs with the propargyl, allyl, 2-bromobenzyl, 2-fluorobenzyl and 3-fluorobenzyl groups in the α-position, by *bis*-alkylation of the glycine moiety of the Ni^{II} complex of its Schiff base with chiral auxiliary (*S*)-BPB (Scheme). To obtain achiral *bis*-alkylated glycine derivatives, the reactions of both stepwise monoalkylation of the amino acid moiety of complexes **1** and **2** (**a-e**) (**path A**), and direct *bis*-alkylation of the glycine moiety of complex **1** (**path B**) were studied.

Scheme

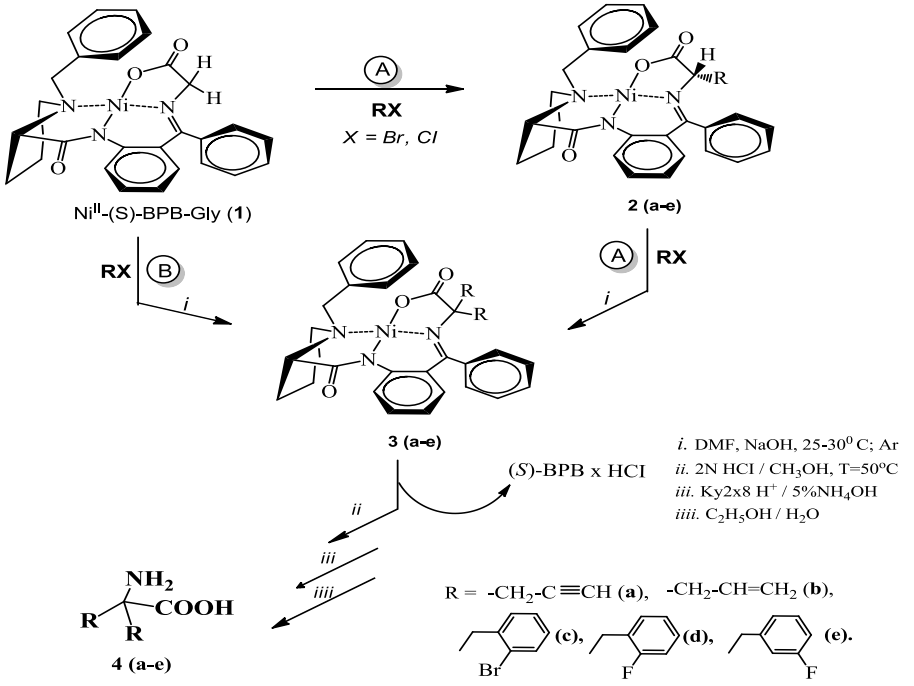

Complexes **2(a-e)** were obtained from complex **1** according to the previously developed procedure [12,14]. Propargyl bromide (***a***), allyl bromide (***b***), 2-bromobenzyl bromide (***c***), 2-fluorobenzyl chloride (***d***) and 3-fluorobenzyl bromide (***e***) were used as alkylating agents.

The alkylation reactions were tested in DMF/KOH, DMF/NaOH, CH_2Cl_2/NaOH, THF/NaOH and CH_3CN/NaOH at both room temperature and under heating to 55°C. To define the optimal conditions for alkylation on the example of propargyl bromide condensation (***a***) to complex **1**, different stoichiometric ratios of the substrate, alkylated reagent and base were studied. Investigations have shown that the optimal conditions for the alkylation reaction of complex **1** are: DMF as a

medium, NaOH – as a base, room temperature, the ratio of complex **1**/base/alkylating agent = 1/3/1.5 (see Table 1, exp. 9).

Table 1

Results of alkylating complex 1 by propargyl bromide (a) under different conditions*

No.	Quantity $Br\text{-}CH_2\text{-}C\equiv CH$(equiv.)	Medium	Base (equiv.)	Reaction time (min.)	T ^oC	Chemical yield (%) **
1	1.2	CH_3CN	NaOH (3)	120	60	<20
2	3	CH_3CN	NaOH (5)	120	20	<20
3	1.2	CH_3CN	KOH (3)	60	60	<20
4	1.2	CH_3CN	KOH (5)	60	20	<20
5	1.2	CH_2Cl_2	NaOH (5)	120	20	25
6	1.2	CH_2Cl_2	NaOH (3)	45	40	25
7	1.5	DMF	KOH (3)	70	20	42
8	1.2	DMF	NaOH (3)	30	60	55
9	**1.2**	**DMF**	**NaOH (3)**	**60**	**20**	**92**
10	1.2	DMF	NaOH (5)	60	20	62
11	**1.2**	**DMF**	**KOH (3)**	**60**	**20**	**74**
12	1.2	THF	NaOH (3)	100	20	<20
13	1.2	THF	NaOH (5)	60	60	<20
14	1.2	THF	KOH (5)	70	60	<20

**The reactions were carried out in the argon atmosphere, **chemical yield is based on the TLC data and the isolated quantity of the alkylated complex (after crystallization from methanol)*

The course of the alkylation reaction was monitored by TLC [SiO_2, $C_2H_5COOCH_3/CH_3COCH_3$(3/1)]. For quantitative assessment of the alkylation reaction, the TLC data were used, and for more successful TLC-based reactions, chemical yields were determined on the basis of the amount of isolated alkylated complexes after crystallization from methanol (Table 1, exp. 7-11).

A quantitative characteristic of the C-alkylation reaction of the amino acid moiety of complexes **1** and **2 (*a*-*e*)** is shown in Table 2.

Table 2

The results of alkylation of complexes by different alkyl halides in DMF in the presence of NaOH at room temperature*

No.	Alkyl halide	Chem. yield of *bis*-alkylated complexes (%)		
		Bis-alkylated complexes	Path A **	Path B
1	 (***a***)	**3*a***	83 (92)	45
2	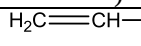 (***b***)	**3*b***	80 (89)	48
3	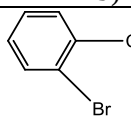 (***c***)	**3*c***	73 (82)	44
4	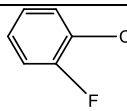 (***d***)	**3*d***	68 (76)	46
5	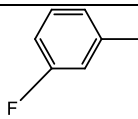 (***e***)	**3*e***	72 (84)	48

Chemical yield of bis-alkylated complexes based on the initial amount of the glycine complex (1**), ** in parenthesis is the chemical yield of bis-alkylated complexes **3(a-e)** after crystallization based on the amount of complexes **2(a-e)** (path A, stage 2).*

Both the stepwise alkylation of the amino acid moiety of complexes **1** and **2 (*a-e*)** (**path A**) and the direct *bis*-alkylation of complex **1** (**path B**) were conducted under specially selected optimal conditions for the alkylation reaction (See Table 1, exp. 9). However, in the case of direct *bis*-alkylation of the glycine complex, the alkylating agent and the base were taken in about double excess.

As follows from the data of Table 2, for almost all alkylating agents, *bis*-alkylation of glycine complex **1** proceeds most quantitatively with the method of two-step alkylation (**path A**) than in the case of the direct *bis*-alkylation of the glycine complex (**path B**). In the case of using the method of direct *bis*-alkylation of the glycine moiety of complex **1**, up to 30% of a side fraction, less mobile on the SiO_2, is formed with an unusual for these complexes dark color (oxidation products). Similar was also observed earlier in the study of the reaction of *bis*-alkylation of complex **1** by methyl iodide [14].

The main α,α-dialkyl-substituted **3(*a-e*)** complexes with a relatively large R_f value on the SiO_2 were isolated from the reaction mixture by crystallization from methanol and characterized by physicochemical analysis methods (see Experimental Part).

To isolate the target α,α–*bis*-alkylated glycine analogs, preparative experiments using the two-step stepwise alkylation method (**path A**) were carried out and the samples of **3**(***a-e***) complexes were obtained. Decomposition of **3**(***a-e***) complexes and isolation of the target α,α–dialkyl-substituted glycine derivatives **4*(a-e)*** were carried out according to a standard procedure [15]. The structures of the synthesized new achiral analogs of glycine were investigated and established by spectral analysis methods (see Experimental Part).

Thus, an efficient method for obtaining achiral α,α-*bis*-alkylated analogs of glycine by C-alkylation of glycine in the chiral Ni^{II} complex of its Schiff base with (*S*)-BPB by alkyl halides has been developed. For the first time the following complexes were synthesized - α,α-dipropargyl glycine (**4*a***), α,α-diallylglycine (**4*b***), α,α-di-(2-bromobenzyl)glycine (**4*c***),α,α-di-(2-fluorobenzyl)glycine (**4*d***) and α,α-di-(3-fluorobenzyl)glycine (**4*e***). The presence of acetylene, allyl and aromatic groups in the side radical of the synthesized amino acids allows makes it possible to use them as initial synthons in the reactions of Suzuki, Heck, Sonogashira to obtain more complex unsaturated amino acids.

The preliminary medicobiological screening of the obtained samples proves that the synthesized amino acids can serve as potential enzyme inhibitors of the amylase class.

Experimental Part

^{1}H NMR and ^{13}C NMR spectra were recorded on a "Mercury-300 Varian" (300 *MHz*), the melting point was measured on a "StuartSMP3" device. Amino acids and other chemical reagents produced by "Aldrich" and "Reachim" were used in the work.

Complex Ni^{II}-(S)-BPB-Gly (**1**) was obtained according to [15], and monoalkylated complexes **2(a-e)** were synthesized according to [13].

General procedure of monoalkylation of complexes 2(*a-e*) (Path A). To 10 *g* (0.018 *mol*) of complex **2*a*** in 50 *ml* of DMF were added at room temperature 2.2 *g* (0.055 *mol*) of NaOH and 1.9 *ml* (0.22 *mol*) of propargyl bromide (***a***). The reaction mixture was stirred for 1-1.5 *h* at room under argon atmosphere. The course of the reaction was monitored by TCL [SiO_2, CH_3COOEt/CH_3COCH_3(3/1)] following the disappearance of the traces of initial complex **2**. Upon completion of the reaction, the mixture was neutralized with CH_3COOH, 100 *ml* of water was added and the alkylated product was precipitated from water. The obtained complex **3*a*** was crystallized from methanol.

***Bis-alkylation of complex* 1 (*Path B*).** The direct *bis*-alkylation of the glycine moiety of complex **1** was carried out according to the afore-mentioned procedure for monoalkylation of complexes **2(*a-e*)** with the difference that the base and alkylating agents were taken in a 5-6-fold excess with respect to complex **1**, and the reaction mixture was stirred for 2-3 *h*. The results are given in Table 2.

Complex 3*a*. Yield 90%, mp 217-218 °C. ^{1}H NMR (300 *MHz*, $CDCl_3$): δ = 1.99-2.11 (m, 2 H, γ-Hα Pro); 2.12 (dd, 1 H, *J*=17.2, *J*=2.7, CH_2 C≡); 2.20 (dd, 1 H, *J*=17.2, *J*=2.5, CH_2 C≡); 2.38 (t,1 H, *J*=2.5, ≡CH); 2.46-2.65 (m, 2 H, β-CH_2Pro); 2.61 (t, 1 H, *J*=2.7, ≡CH); 2.67 (dd, 1 H, *J*=17.0, *J*=2.7 CH_2 C≡); 2.73 (dd, 1 H, *J*=17.2, *J*=2.5 CH_2 C≡); 3.40 (dd, 1 H, *J*=10.7, *J*=5.9 α-HPro); 3.50 (d, 1 H, *J*= 12.5, $\underline{CH_2}$Ph); 3.46-3.59 (m, 1 H, δ-H_bPro); 3.71-3.78 (m, δ-CH_2Pro); 4.47 (d, 1 H, *J*=12.5, $\underline{CH_2}$Ph); 6.57-6.65 (m, 2 H, H-3,4, C_6H_4), 7.09 (ddd, 1 H, *J*=8.6, *J*=4.8, *J*=3.7, H-5 C_6H_4); 7.17-7.26 (m, 2 H, H-Ar); 7.33-7.45 (m, 3 H, H-Ar); 7.48-7.55 (m, 2 H, H-Ar); 7.67-7.73 (m, 1 H, H-Ar); 7.90 (d, 1 H, *J*=8.6, H-Ar); 8.37-8.41 (m, 2 H, H-Ar); ^{13}C NMR (75 *MHz*, $CDCl_3$): δ = 23.2 (γ- CH_2Pro); 29.2 (CH_2); 30.9 (β-CH_2Pro); 31.9 (CH_2); 58.3 (δ-CH_2, Pro); 64.5 ($\underline{CH_2}$Ph); 70.8 (α-C$\underline{H}$Pro); 77.1 (Cq); 79.1 (≡CH), 79.7 (CH_2 $\underline{C}$≡); 120.7 (C-4 C_6H_4); 124.3 (CH-6 C_6H_4); 127.5, 127.7, 128.1, 128.3, 128.8 (CH-Ar); 128.9 (3,3'-CHPh); 129.0, 130.0, 131.7 (CH-Ar); 131.8 (2,2'-CHPh); 133.4, 134.4, 136.3, 142.1 (C); 172.8 (C=N-), 180.6, 180.8 (C=O).

Complex 3*b* Yield 87%, mp 203-204 °C. ^{1}H NMR (300 *MHz*, $CDCl_3$): δ = 1.96-2.12 (m, 2 H, γ-Hα Pro); 2.19 (ddt, 1 H, *J*=14.5, *J*=6.6, *J*=1.2, CH_2 CH=CH_2); 2.33-2.54 (m, 4 H, CH_2 CH=CH_2 и β-H_aPro); 2.62-2.73 (m, 1 H, β-H_bPro); 3.25-3.42 (m, 1 H, γ-H_bPro); 3.40 (dd, 1 H, *J*=10.7, *J*=5.9 α-HPro); 3.58 (d, 1 H, *J*= 12.5, $\underline{CH_2}$Ph); 3.65-3.72 (m, 1 H, δ-H_bPro); 4.38 (d, 1 H, *J*=12.5, $\underline{CH_2}$Ph); 5.24(ddt, 1 H, *J*=17.2, *J*=1.6, *J*=1.3, =CH_2); 5.31 (ddt, 1 H, *J*=10.5, *J*=1.6, *J*=1.3, =CH_2); 5.38 (ddt, 1 H, *J*=17.1, *J*=1.6, *J*=1.3, =CH_2); 5.49 (ddt, 1 H, *J*=10.3, *J*=1.6, *J*=1.2, =CH_2); 5.80 (ddt, 1 H, *J*=17.1, *J*=10.5, *J*=6.6, =CH); 6.62 (ddt, 1 H, *J*=17.2, *J*=10.3, *J*=6.6, =CH); 6.57-6.63 (m, 2 H, H-3.4, C_6H_4), 7.05-7.09 (m, 1 H, H-Ar); 7.11 (ddd, 1 H, *J*=8.7, *J*=5.5, *J*=3.0, C_6H_4); 7.22-7.28 (m, 1 H, H-Ar); 7.37-7.54 (m, 6 H, H-Ar); 7.95 (d, 1 H, *J*=8.7, H-Ar); 8.16-8.21 (m, 2 H, H-Ar); ^{13}C NMR (75 *MHz*, $CDCl_3$): δ = 23.3 (γ- CH_2Pro); 30.9 (β- CH_2Pro); 42.5, 44.2 (CH_2 CH=CH_2); 57.8 (δ-CH_2, Pro); 64.2 ($\underline{CH_2}$Ph); 70.9 (α-C$\underline{H}$Pro); 81.7 ($\underline{C}$-Alyl$_2$), 119.0, 119.7 (=CH_2); 120.7 (C-4 C_6H_4); 124.3 (CH-6 C_6H_4); 127.2, 127.9 128.0, 128.6, 128.7 (CH-Ar); 129.0 (3,3'-CHPh); 129.1, 129.8, 131.6(CH-Ar); 131.7 (2,2'-CHPh); 132.4, 132.7, 133.2 (CH-Ar); 134.3, 136.8, 141.9, (C); 172.8 (C=N-), 180.6, 180.8 (C=O).

Complex 3*c*. Yield 78%, mp 231-232 °C. ^{1}H NMR (300 *MHz*, $CDCl_3$): δ = 1.68-1.79 (m, 1 H, γ-Hα Pro); 2.01-2.13 (m, 1 H, δ-HPro); 2.25-2.46 (m, 3 H, γ-Hв и β-Hα, Pro); 2.44 (d, 1 H, *J*=18.0, CH_2 C_6H_4Br); 3.20 (d, 1 H, *J*=18.0, CH_2 C_6H_4Br); 3.22-3.28 (m, 1 H, δ-HPro); 3.39 (d, 1 H, *J*=14.4, CH_2 C_6H_4Br);3.41 (dd, 1 H, *J*=9.0, *J*=7.2, α-CHPro); 3.49 (d, 1 H, *J*=12.6, $\underline{CH_2}$Ph); 3.72 (d, 1 H, *J*=14.4, CH_2 C_6H_4Br); 4.39 (d, 1 H, *J*=12.6,$\underline{CH_2}$Ph); 6.33 (d, 1H, *J*=7.8, C_6H_5); 6.43-6.55 (m, 2 H, H-3.4, C_6H_4), 7.04-7.18 (m, 3H, H-Ar); 7.20-7.29 (m, 3H, H-Ar); 7.33-7.51 (m, 6 H, H-Ar); 7.56-7.64 (m, 2 H, H-Ar); 7.70-7.76 (m, 2 H, H-Ar); 8.04-8.16 (m, 3 H, H-Ar). ^{13}C NMR (75 *MHz*, $CDCl_3$): δ = 23.4 (γ- CH_2Pro); 30.9 (β- CH_2Pro); 46.5 (CH_2 C_6H_4Br); 47.2 (CH_2 C_6H_4Br); 58.1 (δ-CH_2, Pro); 64.1 ($\underline{CH_2}$Ph); 70.5 (α-CPro); 80.9 ($\underline{C}$-CH_2 C_6H_4Br), 120.5 (C-4 C_6H_4); 123.9 (CH-6 C_6H_4); 125.8, 126.5126.7, 127.3, 127.6 (CH-Ar); 127.8 (3,3'-CHPh); 127.9, 128.0, 128.2, 129.0, 129.6 (CH-

Ar);131.6 (2,2'-CHPh); 131.9, 133.2, 133.6, 133.7, 133.8 (CH-Ar); 133.9, 136.3, 136.4, 137.4, 142.5 (C); 172.6 (C=N-); 178.0, 180.3 (C=O).

Complex 3*d*. Yield 72%, mp 227-228 °C. ^{1}H NMR (300 *MHz*, $CDCl_3$): δ = 1.57-1.72 (m, 1 H, γ-Hα Pro); 2.01-2.32 (m, 4 H, δ-H, γ-Hв и β-Hα, Pro); 2.53 (d, 1 H, *J*=17.7, CH_2 C_6H_4F); 3.02 (d, 1 H, *J*=14.6, CH_2 C_6H_4F); 3.18 (d, 1 H, *J*=17.7, CH_2 C_6H_4F); 3.19-3.28 (m, 1 H, δ-HPro); 3.33 (dd, 1 H, *J*=9.3, *J*=7.4, α-CHPro); 3.40 (d, 1 H, *J*=14.6, CH_2 C_6H_4F); 3.43 (d, 1 H, *J*=12.6, $\underline{CH_2}$Ph);4.36 (d, 1 H, *J*=12.6,$\underline{CH_2}$Ph); 6.50 (dd, 1 H, *J*=8.5,*J*=2.1 C_6H_4); 6.53 (ddd, 1 H, *J*=8.5,*J*=6.4,*J*=1.1 C_6H_4); 6.64 (dt, 1 H, *J*=7.8,*J*=1.4 C_6H_4); 7.03-7.11 (m, 2 H, H-3.4, H-Ar); 7.16-7.25 (m, 4 H, H-Ar); 7.28-7.53 (m, 8 H, H-Ar); 7.72-7.79 (m, 1 H, H-Ar); 7.83 (td, 1 H, *J*=7.6, *J*=1.6 H-Ar); 7.99-8.06 (m, 3 H, H-Ar). ^{13}C NMR (75 *MHz*, $CDCl_3$): δ = 23.1 (γ- CH_2Pro); 30.8 (β- CH_2Pro); 39.5 (CH_2 C_6H_4F); 40.6 (CH_2 C_6H_4F); 58.0 (δ-CH_2, Pro); 63.9 ($\underline{CH_2}$Ph); 700 (α-CHPro); 79.8 (C-CH_2 C_6H_4F), 115.2 (d, *J*=22.1C_6H_4F); 115.9 (d, *J*=23.0C_6H_4F); 120.4 (CHC_6H_4); 123.6 (CHC_6H_4); 124.0 (d, ^{3}*J*=15.8C_6H_4F); 124.1 (d, *J*=3.8C_6H_4F); 124.8 (d, *J*=3.2C_6H_4F); 125.1 (d, ^{2}*J*=14.7C_6H_4F); 127.1 (d, *J*=6.3C_6H_4F); 127.4, 127.9 128.0, 128.2, 128.3 (CH-Ar); 129.0 (3,3'-CHPh); 129.3 (d, *J*=8.2C_6H_4F); 129.6 (CH-Ar); 129.9 (d, *J*=4.0C_6H_4F); 131.6 (2,2'-CHPh); 131.8, 133.2 (d, ^{4}*J*=4.5C_6H_4F); 133.6, 133.9 (CH-Ar); 136.7, 142.4 (C); 161.0 (d, ^{1}*J*=246.0C_6H_4F); 162.3 (d, *J*=246.4CF); 173.6 (C=N-), 179.3, 180.3 (C=O).

Complex 3*e*. Yield 81%, mp 205-206 °C. ^{1}H NMR (300 *MHz*, $CDCl_3$): δ = 1.62-1.74 (m, 1H, γ-HaPro); 1.96-2.36 (m, 4H, β-Ha,b, γ-Hb, δ–HaPro); 2.74 (d, 1H, *J*=16.9, CH_2-Ar); 3.01 (d, 1H, *J*=14.4, CH_2-Ar); 3.12 (d, 1H, *J*=14.4, CH_2-Ar); 3.21 (dd, 1H, *J*=10.5,*J*=5.8,α-HPro); 3.25-3.33 (m, 1H, δ–HbPro); 3.29 (d, 1H, *J*=16.9, CH_2-Ar); 3.29 (d, 1H, *J*=12.5, CH_2-Ph); 4.34 (d, 1H, *J*=12.5, CH_2-Ph); 6.51 (dd, 1H, *J*=8.4, 1.7, H-C_6H_4); 6.56 (dd, 1H, *J*=8.4, *J*=6.8, *J*=1.1, H-C_6H_4); 6.96-7.21 (m, 8H, Ar.); 7.29-7.55 (m, 9H, Ar.); 7.84 (dd, 1H, *J*=8.7, *J*=1.1, H-C_6H_4); 8.04-8.08 (m, 2H, H-Ph). ^{13}C NMR (75 *MHz*, $CDCl_3$): δ = 23.0 (γ-$\underline{C}H_2$Pro); 30.7 (β-$\underline{C}H_2$Pro); 45.1 ($\underline{C}H_2$-Ar); 46.0 ($\underline{C}H_2$-Ar); 58.5 (δ-$\underline{C}H_2$Pro); 64.3 ($\underline{C}H_2$-Ph); 70.1 (α-$\underline{C}$HPro); 80.5 ($\underline{C}$-CH_2-Ar.); 113.6 (d, $J_{C,F}$=21.0, C_6H_4F); 114.5 (d, $J_{C,F}$=20.9, C_6H_4F); 116.2 (d, $J_{C,F}$=21.6, C_6H_4F); 118.2 (d, $J_{C,F}$=21.1, C_6H_4F); 120.6 (CH-C_6H_4); 124.2 (CH-C_6H_4); 125.2 (d, $J_{C,F}$=2.6, C_6H_4F); 126.7 (d, $J_{C,F}$=2.8, C_6H_4F); 127.4 (CH); 127.6 (CH); 127.9; 128.2 (CH); 128.9 (CH); 129.0 (3,3'-CHPh); 130.0 (d, $J_{C,F}$=8.4, C_6H_4F); 130.3 (d, $J_{C,F}$=8.4, C_6H_4F); 131.6 (2,2'-CHPh); h); 131.7 (CH); 131.9 (CH-C_6H_4); 133.5 (CH-C_6H_4); 133.7; 136.8; 139.1 (d, $J_{C,F}$=7.3, C_6H_4F); 139.5 (d, $J_{C,F}$=7.3, C_6H_4F); 142.5; 163.1 (d, $J_{C,F}$=246.4, C_6H_4F); 163.3 (d, $J_{C,F}$=246.4, C_6H_4F); 172.7 (C=N-); 179.3; 180.5(C=O).

Isolation of the target amino acids 4(*a-e*). Decomposition of complexes **3(*a-e*)** and isolation of α,α-dialkylated analogs of glycine **4**(***a-e***) were carried out according to the standard procedure [15]. For this, the dry moiety of the complexes was dissolved in 50 *ml* of CH_3OH and the solution was slowly added to 50 *ml* of 2N HCl solution heated to 60°C. After the disappearance of red color, typical for these complexes, the solution was concentrated under vacuum, 50 *ml* of water was added

and the initial chiral auxiliary reagent (*S*)-BPB was filtered off as hydrochloride. From the aqueous filtrate, the amino acid was isolated by passing the solution through an ion exchange column with 100 *ml* of Ku-2x8 resin in H^+-form, and the resin was washed with 5% NH_4OH solution. The ammonia eluate was concentrated in vacuum and the amino acid was crystallized from a water-alcohol (1/1) solution. The structure of the obtained α,α-dialkyl-substituted glycine derivatives **4(*a-e*)** was studied by spectral analysis methods.

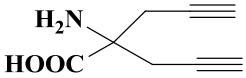

2-Amino-2-(prop-2-yn-1-yl)pent-4-ynoic acid. 4*a*. Yield 81%, mp 227-228 °C. ^{1}H NMR (300 *MHz*, DOD): δ = 2.53 (t, 2 H, *J*=2.44, CH_2-C≡CH); 2.82 (dd, 4H, *J*=17.7, *J*=2.5 CH_2-C≡CH): ^{13}C NMR (75 *MHz*, DOD): δ = 25.5 (CH_2-C≡CH); 62.2 (C-CH_2-C≡CH); 74.3 (CH_2-C≡CH); 76.8 (CH_2-C≡CH); 173.0 (C=O).

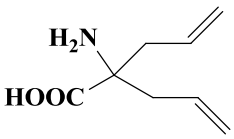

2-Allyl-2-aminopent-4-enoic acid. 4*b*.Yield 75%, mp 234-235°C. ^{1}H NMR (300 *MHz*, DOD): δ = 2.46 (dd, 2 H, *J*=14.5, *J*=8.5 CH_2-CH=CH_2); 2.67 (dd, 2 H, *J*=14.5, *J*=6.4 CH_2-CH=CH_2); 5.26 (d, 4 H, *J*=14.5, CH_2-CH=CH_2); 5.66-5.78 (m, 2 H, CH_2-CH=CH_2). ^{13}C NMR (75 *MHz*, DOD): δ = 40.1 (CH_2-CH=CH_2); 63.9 (C-CH_2-CH=CH_2); 121.5 (CH_2-CH=CH_2); 130.3 (CH_2-CH=CH_2); 174.8 (C=O).

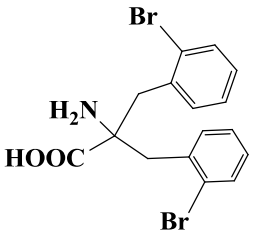

2-Amino-2-(2-bromobenzyl)-3-(2-bromophenyl) propanoic acid. 4*c*. Yield 78%, mp 181-182°C. ^{1}H NMR (300 *MHz*, DMSO/CCl_4): δ = 3.50 (d, 2 H, *J*=14.6, CH_2 C_6H_4Br); 3.68 (d, 2 H, *J*=14.6, CH_2 C_6H_4Br); 7.16 (ddd, 2 H, *J*=8.0, *J*=7.4, *J*=1.6, C_6H_4); 7.30 (ddd, 2 H, *J*=7.7, *J*=7.4, *J*=1.3, C_6H_4); 7.54 (dd, 2 H, *J*=8.0, *J*=1.3, C_6H_4); 7.65 (dd, 2 H, *J*=7.7, *J*=1.6, C_6H_4); 8.92 (m, 3H, NH_2 and COOH). ^{13}C NMR (75 *MHz*, DMSO/CCl_4): δ = 39.47 (CH_2 C_6H_4Br); 62.6(C- CH_2 C_6H_4Br), 125.7 (C-Ar); 127.2, 128.5, 132.4, 132.5 (CH-Ar); 133.5 (C-Ar); 170.2 (C=O).

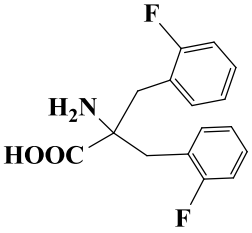

2-Amino-2-(2-fluorobenzyl)-3-(2-fluorophenyl) propanoic acid. 4*d*. Yield 70%, mp 228-229°C. ^{1}H NMR (300 MHz, DOD): δ = 3.31 (d, 2 H, *J*=14.7, CH_2 C_6H_4F); 3.39 (d, 2 H, *J*=14.7, CH_2 C_6H_4F); 7.04-7.14 (m, 4 H, C_6H_4F); 7.22-7.35 (m, 4 H, C_6H_4F).

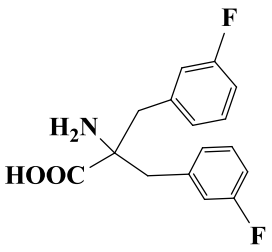

2-Amino-2-(3-fluorobenzyl)-3-(3-fluorophenyl) propanoic acid. 4*e*. Yield 62%, mp 231-232 °C. ^{1}H NMR (300 *MHz*, DOD): δ = 3.18 (d, 2 H, *J*=14.6, CH_2 C_6H_4F); 3.29 (d, 2 H, *J*=14.6, CH_2 C_6H_4F); 7.01-7.09 (m, 4 H, C_6H_4F); 7.12-7.24 (m, 4 H, C_6H_4F).

ԳԼԻՑԻՆԻ α,α-ԲԻՍ-ՏԵՂԱԿԱԼՎԱԾ ԱՔԻՐԱԼ ՆՄԱՆԱԿՆԵՐԻ ՍԻՆԹԵԶ

Զ. Զ. ՄԱՐԴԻՅԱՆ, Ա. Ս. ՍԱՂՅԱՆ և Ա. Ֆ. ՄԿՐՏՉՅԱՆ

Աշխատանքում հետազոտվել է գլիցինի α,α-երկտեղակալված աքիրալ նմանակների սինթեզի հնարավորությունը միևնույն ալկիլող ագենտով՝ գլիցինի էլեկտրոֆիլ բիս-տեղակալման ճանապարհով: Դրա համար որպես ելային ամինոթթվային սինտոն օգտագործվել է գլիցինի NiII-(S)-BPB-Gly (1) կոմպլեքսը: Ուսումնասիրվել է այդ կոմպլեքսի ամինոթթվային մնացորդի էլեկտրոֆիլ տեղակալումը պրոպարգիլբրոմիդով (a), ալիլբրոմիդով (b), 2-բրոմբենզիլբրոմիդով (c), 2-ֆտորբենզիլբրոմիդով (R) և 3-ֆտորբենզիլբրոմիդով (e), ինչպես հաջորդաբար մոնոտեղակալմամբ արդեն իսկ հայտնի մեթոդներով (A), այնպես էլ անմիջական (միանգամից) երկտեղակալման ճանապարհով (B):

Էլեկտրոֆիլ տեղակալման ռեակցիաներն իրականացվել են DMF/NaOH համակարգում, արգոնի մթնոլորտում, սենյակային ջերմաստիճանի պայմաններում: Տեղակալման ռեակցիաների ընթացքին հարմար է հետևել ՆՇՔ մեթոդով՝ սիլիկագելի թիթեղների վրա, $CH_3COOC_2H_5/(CH_3)_2CO$ (3/1) լուծիչների համակարգում:

Ինչպես երևում է արձանագրված արդյունքներից, նպատակահարմար է սինթեզն իրականացնել երկփուլանի (A) ալկիլման եղանակով, քանզի միաժամանակյա (B) երկտեղակալման ժամանակ ելքը չի գերազանցում 50%-ը: Իսկ հաջորդաբար՝ մոնոտեղակալմամբ երկտեղակալման դեպքում արգասիք կոմպլեքսների ելքը գերազանցում է 70%-ը հաշվարկված (1) կոմպլեքսի ելային քանակությամբ:

Նպատակային ոչ սպիտակուցային աքիրալ α,α-երկտեղակալված ամինոթթուների (4a-e) անջատումը արգասիք կոմպլեքսներից (3a-e) իրականացվել է նախկինում մշակված ստանդարտ մեթոդով:

Այսպիսով, սինթեզվել են գրականությյան մեջ չնկարագրված գլիցինի α,α-բիս-տեղակալված աքիրալ նմանակներ 2,2-դի(պրոպարգիլ)գլիցին, 2,2-դի(ալիլ)գլիցին, 2-ամինո-2-(պրոպ-2-ին-1-իլ)պենտ-4-յինաթթու (4a), 2-ալիլ-2-ամինոպենտ-4-էնաթթու (4b), 2-ամինո-2-(2-բրոմբենզիլ)-3-(2-բրոմֆենիլ)պրոպա-նաթթու (4c), 2-ամինո-2-(2-ֆտորբենզիլ)-3-(2-ֆտորֆենիլ)պրոպանաթթու (4d) 2-ամինո-2-(3-ֆտորբենզիլ)-3-(3-ֆտորֆենիլ)պրոպանաթթու (4e).

СИНТЕЗ НОВЫХ АХИРАЛЬНЫХ *БИС*-АЛКИЛИРОВАННЫХ АНАЛОГОВ ГЛИЦИНА

З. З. МАРДИЯН [а,б], А. Ф. МКРТЧЯН [а,б] и А. С. САГИЯН

[а]Научно-производственный центр “Армбиотехнология” НАН РА
Ереван 0056, ул. Гюрджяна, 14
Факс: (+37410) 654180, E-mail: zmardiyan89@gmail.com
[б]Ереванский государственный университет, институт Фармации
Ереван 0025, ул. А. Манукяна, 1

Разработан метод синтеза α-*бис*-алкилзамещенных производных глицина путем С-алкилирования аминокислотного остатка Ni^{II}-комплекса основания Шиффа глицина и хирального вспомогательного реагента (S)-2-N-[N’-(бензилпролил)амино]бензофенона (BPB) пропаргил-, аллил-, 2-бромбензил- и 4-фторбензилбромидами в условиях основного катализа.

REFERENCES

[1] *Yoshioka H., Aoki T., Goko H., Nakatsu K., Noda T.,Sakakibara H., Take T., Nagata A., Abe J.,Wakamiya T., Shiba T., Kaneko T.* // Tetrahedron Letters, 1971, p. 2043.

[2] *Takita T., Muraoka Y., Yoshioka T., Fuji A., Naeda K., Umezawa H.* // J. Antibiot., 1972, v. 25, p. 755.

[3] *Jakubke H6D., Jeschkeit H.* Aminosauren, Peptide, Proteine, Akademie6Veriag, Berlin, 1982.

[4] *Radahhisman A.N.* // J. Biochem., 1970, p.117.

[5] *Lambertine J.B., Coulier A.W., Talalay P.* // Mol. Pharmacol., 1970, v. 6, p. 481.

[6] *Mori Y., Truboi M., Fukushima K., Aroi T.* // Jour. Soc. Chem. Comm., 1982, p. 94.

[7] *Barret G.C.* Chemistry and Biochemistry of Amino acids, Chapman and Hall, Oxford, 1984, p.132.

[8] *Burnett G., Marcotte P., Walsh C.* // J. Biol. Chem., 1980, v.255, p. 3487

[9] *Kuroda Y., Okuhara M., Goto T., Iguchi R., Kohsaka M., Aoki H., Imanaka H.* // Antibiot. (Tokyo), 1980, v. 33, p. 125.

[10] *Janecka A., Janecki T., Bowers C., Janecka K. Reduced-Aize* // A. J. Med Chem., 1995, v. 38, p. 2922.

[11] *Dong L., Markovits J., Hou X., Guo Ch., Gteasley S.* // Biootg . Med. Chem., 2010 Lett. 20, p. 2210.

[12] *Collet S., Bauchat P., Danion-Bougot R., Danion D.* // Tetrahedron: Asymmetry, 1998, v. 9, p. 2121.

[13] *Belokon' Yu.N., Chernoglazava N.I., Kachetkov K.A.* // J.Chem. Soc. Commun., 1985. p. 171.

[14] *Сагиян А.С.* Энантиомерно чистые небелковые аминокислоты. Способы получения. М., Наука, 2010, с. 88.

[15] *Belokon' Yu.N., Tararov V.I., Maleev V.I.* // Tetrahedron: Asymmetry, 1998 v. 9, p. 4249.

ՀԱՅԱՍՏԱՆԻ ՀԱՆՐԱՊԵՏՈՒԹՅԱՆ ԳԻՏՈՒԹՅՈՒՆՆԵՐԻ
ԱԶԳԱՅԻՆ ԱԿԱԴԵՄԻԱ
НАЦИОНАЛЬНАЯ АКАДЕМИЯ НАУК РЕСПУБЛИКИ АРМЕНИЯ
NATIONAL ACADEMY OF SCIENCES OF THE REPUBLIC OF ARMENIA

Հայաստանի քիմիական հանդես
Химический журнал Армении 71, №4, 2018 Chemical Journal of Armenia

UDC 547.787

EVALUATION OF THE DEHYDRATING PROPERTIES OF SOME SILILATING AGENTS IN THE SYNTHESIS OF IMIDAZOLE-5-ONE

V. O. TOPUZYAN, V. M. GHAZOYAN, G. Sh. HOVHANNISYAN and A. A. HOVHANNISYAN

The Scientific and Technological Centre
of Organic and Pharmaceutical Chemistry NAS RA
26, Azatutyan Str., Yerevan, 0014, Armenia
E-mail: vtop@web.am

The effect of solvent, some additives and temperature on the dehydrating properties of dimethyldichlorosilane (DMDCS), trimethylchlorosilane (TMCS) and 1,1,1,3,3-hexamethyldi- silazane (HMDS) in the synthesis of 1-benzyl-2-phenyl-4-benzylidene-5-imidazolone from benzylamide N-benzoyl-α,β-dehydrophenylalanine was investigated. It was found that in the case of using DMDCS or TMHS as a reagent, the formation of a by-product - 2-phenyl-4-benzylidene-5-oxazolone was observed. Formation of the latter was not detected in the presence of triethylamine when TMCS was used as a silylating agent. The best results for the synthesis of imidazol-5-one (84%) were obtained with boiling the reaction mixture of benzylamide and HMDS in DMF for 15 *min*. Replacing DMF with dimethylacetamide, acetamide, formamide or pyridine, and lowering temperature of the reaction mixture reduces the yield of the target product. On the basis of the data obtained, it has been concluded that HMDS is an effective reagent for the synthesis of 1,2,4-tri-substituted imidazol-5-ones by dehydrating the amides of N-acyl-α,β-dehydroamino acids.

Table 1, references 13.

In the organic synthesis, silylating agents have found wide application. It is known that trimethylchlorosilane (TMCS) is used in the synthesis of ethers [1] and esters [2], and also promotes the reaction of Bedginelli [3]. 1,1,1,3,3,3-Hexamethyldisilazane (HMDS) has found application in the synthesis of imides of dicarboxylic acids [4] and phthalocyanines [5]. In recent years, TMCS [6], HMDS [7-10] and N, O-bistrimethylsilylacetamide (BTMSA) [11,12] have been used in the synthesis of 1,2-di- and 1,2,4-trisubstituted imidazol-5-ones.

The present work is devoted to the evaluation of dehydrating properties of some silylating agents in the synthesis of imidazol-5-ones. As the silylating agents (SA) TMCS, HMDS and dimethyldichlorosilane (DMDCS) were used. To assess the

dehydrating properties of some SA as a model, they were reacted with benzylamide of N-benzoyl-α,β-dehydrophenylalanine (**1**), dehydration of which resulted in the formation of 1-benzyl-2-phenyl-4-benzylidenimidazole-5-one (**2**).

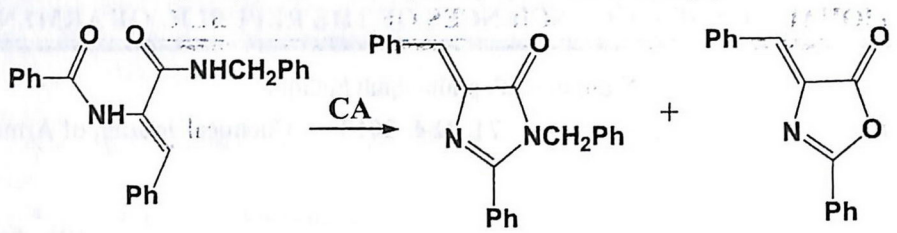

1 **2** **3**

The influence of both the reaction conditions (reaction time, solvent, temperature, reagent ratio) and some additives (pyridine, triethylamine, N-methylmorpholine, imidazole) on the target product **2** was studied. The yield of product **2** was determined spectrophotometrically at 370-375 *nm* (maximum absorption of compound **2** in the UV spectrum). Amide **1** in this region did not show absorption. As the standard, we chose the absorption intensity at 275 nm of pure imidazolone **2** (Io). After the synthesis, the product, without purification, was studied for both the UV and IR spectra. To estimate the yield of compound **2**, the intensity (Ie) of the absorption spectrum of the reaction mixture at 370-375 *nm* was used. Calculations were carried out for compound **2** according to equation (1).

$$\% = \frac{\text{Iex } 100}{\text{Io}} \quad (1)$$

The IR spectrum was used to determine the presence in the reaction mixture of the parent substance **1** (3177-3271 cm^{-1}, NH-amide), the desired imidazole-4-one 2 (1710-1716 cm^{-1}, CO imidazolone) and the by-product 2-phenyl-4-benzylidene-5(4H)-oxazolone (3) (1791-1796 cm^{-1}, CO of oxazolone). The obtained results are given in the Table.

The results in the Table show that the use of DMDCS in DMF leads to the formation of a mixture, IR spectrum of which contains the characteristic absorption of both the starting material 1, the desired product 2 and the by-product 3 (table entries1-3). A similar picture is also observed in the case of using TMCS both separately (entries 4.5), and in the presence of pyridine (entries 8-10) or imidazole (entry 6) as additives. However, when triethylamine (entries11-12) or N-methyl-morpholine (entry 13) is used as an additive, by-product 3 is absent, but desired product 2 is obtained in low yields (11.8-25.5%). The reaction involving TMCS in DMF (entry 5), acetamide (entry 14) and dimethylacetamide (entry 15) proceeds with the formation of by-product 3. In formamide (entries 17,18), we do not register the formation of a by-product, however, desired product 2 is obtained in low yields (6.69-8.85%). When compound 1 is reacted with TMCS in dioxane or acetonitrile, the starting material is obtained unchanged back (entries 16,19).

Table

Influence of sililating agents (SA) - dimethyldichlorosilane (DMDCS), trimethylchlorosilane (TMCS), 1,1,1,3,3,3-hexamethyldisilazane (HMDS), some additives (A) and the reaction conditions on the yield of imidazole-5-one 2, and IR spectrum of the obtained compounds

Entry №	SA	Relation **1**:SA	Solvent*	(A)**	Relation SA:A	Conditions	Time, *min*	Reaction product	Yield of prod.**2**, %	IR spectrum, ν, cm^{-1}
1	DMDCS	1:3	DMF	–		boiling	60	mixture **1,2,3**	–	1716 (C=O **2**) 1792 (C=O **3**) 3233 (NH **1**)
2	DMDCS	1:3	DMF	Py	1:1	boiling	60	mixture **1,2,3**	–	1714 (C=O **2**) 1794 (C=O **3**) 3245 (NH **1**)
3	DMDCS	1:3	DMF	NEt_3	1:1	boiling	60	mixture **1,2,3**	–	1715 (C=O **2**) 1794 (C=O **3**) 3232 (NH **1**)
4	TMCS	1:3	DMF	–	–	boiling	30	mixture **1,2,3**	–	1713 (C=O **2**) 1794 (C=O **3** 3221 (NH **1**)
5	TMCS	1:3	DMF	–	–	boiling	60	mixture **1,2,3**	–	1715 (C=O **2**) 1791 (C=O **3** 3225 (NH **1**)
6	TMCS	1:3	DMF	Im	1:1	boiling	60	mixture **1,2,3**	–	1710 (C=O **2**) 1796 (C=O **3**) 3235 (NH **1**)
7	TMCS	1:3	DMF	Py	3:1	boiling	60	mixture **1,2**	10.21	1716 (C=O **2**) 3255 (NH **1**)
8	TMCS	1:3	DMF	Py	1:1	boiling	60	mixture **1,2,3**	–	1712 (C=O **2**) 1794 (C=O **3**)

										3238 (NH **1**)
9	TMCS	1:3	DMF	Py	3:10	boiling	60	mixture **1,2,3**	–	1712 (C=O **2**) 1794 (C=O **3**) 3234 (NH **1**)
10	TMCS	1:3	DMF	Py	3:20	boiling	90	mixture **1,2,3**	–	1710 (C=O **2**) 1794 (C=O **2**) 3262 (NH **1**)
11	TMCS	1:3	DMF	NEt_3	1:1	boiling	60	mixture **1,2**	24.41	1716 (C=O **2**) 3215 (NH **1**)
12	TMCS	1:3	DMF	NEt_3	3:10	boiling	60	mixture **1,2**	25.49	1716 (C=O **2**) 3242 (NH **1**)
13	TMCS	1:3	DMF	NMM	1:1	boiling	60	mixture **1,2**	11.76	1715 (C=O2) 3231 (NH **1**)
14	TMCS	1:3	AA	–	–	120°C	60	mixture **1,2,3**	–	1715 (C=O2) 1796 (C=O **3**) 3258 (NH **1**)
15	TMCS	1:3	DMAA	–	–	150°C	60	mixture **1,2,3**	–	1716(C=O2) 1792 (C=O **3**) 3271 (NH **1**)
16	TMCS	1:3	AN	–	–	boiling	60	**1**	0	3177 (NH **1**)
17	TMCS	1:3	FA	–	–	150°C	30	mixture **1,2**	6.69	1714 (C=O **2**) 3242 (NH **1**)
18	TMCS	1:3	FA	–	–	150°C	60	mixture **1,2**	8.85	1714 (C=O **2**) 3237 (NH **1**)
19	TMCS	1:3	DO	–	–	boiling	60	**1**	0	3226 (NH **1**)
20	TMCS/HMDS 1:1	1:3	DMF	–	–	boiling	60	**1**	0	3222 (NH **1**)
21	HMDS	1:2	DMF	–	–	boiling	60	mixture	52.13	1711 (C=O **2**)

								1,2		3243 (NH **1**)
22	HMDS	1:3	DMF	–	–	boiling	10	mixture **1,2**	39.42	1711 (C=O **2**) 3223 (NH **1**)
23	HMDS	1:3	DMF	–	–	boiling	15	**2**	84.05	1716 (C=O **2**)
24	HMDS	1:3	DMF	–	–	boiling	20	**2**	75.25	1710 (C=O **2**)
25	HMDS	1:3	DMF	–	–	boiling	30	**2**	70.99	1716 (C=O **2**)
26	HMDS	1:3	DMF	–	–	boiling	60	**2**	67.88	1716 (C=O **2**)
27	HMDS	1:3	DMF	–	–	100°C	60	mixture **1,2**	9.26	1711 (C=O **2**) 3208 (NH **1**)
28	HMDS	1:3	DMF	–	–	120°C	60	mixture **1,2**	26.16	1713 (C=O-**2**) 3247 (NH **1**)
29	HMDS	1:7	–	–	–	100°C	60	**1**	0	3213 и 3285 (NH **1**)
30	HMDS	1:3	AN	–	–	boiling	60	**1**	0	3243 (NH **1**)
31	HMDS/ DMFA 1:2	1:3	AN	–	–	boiling	60	**1**	0	3211 (NH **1**)
32	HMDS	1:3	Py	–	–	boiling	60	mixture **1,2**	13.32	1716 (C=O **2**) 3218 (NH **1**)
33	HMDS	1:3	DO	–	–	boiling	60	**1**	0	3227 (NH **1**)
34	HMDS	1:3	FA	–	–	150°C	30	mixture **1,2**	10.07	1713 (C=O **2**) 3242 (NH **1**)
35	HMDS	1:3	FA	–	–	150°C	60	mixture **1,2**	12.78	1710 (C=O**2**) 3247 (NH **1**)
36	HMDS	1:3	DMAA	–	–	150°C	60	**1**	0	3266 (NH **1**)

*DMF – dimethylformamid, AA –acetamid, DMAA – dimethylacetamid, FA – formamide, AN – acetamide; DO – dioxin; ** Im – imidazole, Py – pyridine, NMM – N-methylmorpholine.

The results in the Table also show that dioxane or acetonitrile do not allow the reaction to proceed with HMDS (entries 30, 33), however, the reaction in dimethylformamide has good results after 15 *min* (entry 23). Moreover, in the IR spectrum of the obtained reaction product, in addition to absorption at 1716 cm-1, no other absorption characteristic of compounds 1 and 3 is observed. It should be noted that prolongation of the interaction time leads to a decrease in the yield of desired product 2 (entries 24-26). In this case tar formation occurs. When the reaction is carried out at relatively low temperatures (100 or 120°C, entries 27 and 28) no satisfactory results are observed. A similar result is also obtained when compound 1 is reacted with HMDS in the solvent-free conditions or in pyridine, acetonitrile, dioxane, acetamide, formamide or dimethylacetamide (entries 29-36). The use of a mixture of TMCS-HMDS in DMF does not result in the formation of desired product 2 (entry20).

Thus, from the investigated silylating agents for the synthesis of imidazol-5-one, HMDS is the best one, which in DMF comparatively quickly (15 *min*) leads to the formation of the desired product in high yield (84%). Also note that the proposed [11] BDSA cyclization of amides of N-formyl-α,β-dehydroamino acids in imidazol-5-ones is carried out in pyridine at 100°C for 12 *h* with a yield of 52-98%. Based on this, it can be concluded that HMDS exhibits high efficiency as a cyclocondensing agent for the synthesis of imidazol-5-ones from the corresponding amides of N-substituted α,β-dehydroamino acids.

Experimental Section

The IR spectra were recorded on a spectrometer in vaseline oil, the ^{1}H NMR spectra were measured on a Varian "Mercury-300" spectrometer in DMSO-d_6 using TMS as internal standard. The UV spectra were recorded on Thermo Electron Corporation "Helios Y" spectrometer. TLC was carried out on "Silica Gel" 60 F_{254} plates in the system benzene:methanol= 5:2, developer – iodine vapor. 4-Benzylidene-5(4H)-oxazolone was synthesized according to [13].

N-benzoyl-α,β-dehydrophenylalaninebenzylamide (1). To a solution of 2.5 *g* (10 mmol) of 2-phenyl-4-benzylidene-5(4H)-oxazolone in 25 *ml* of ethylacetate was added 1.18 *g* (1.2 *ml*, 11 *mmol*) of amine and allowed to stand at room temperature for 24 *h*. The formed precipitate was filtered off, washed with 25 *ml* of diethyl ether and air-dried. Recrystallized from 50% ethanol. Yield 85.71%, mp 178-180°C, R_f 0.48. IR spectrum, γ, cm^{-1}: 1639 (C=O-amide), 3265 (NH). NMR spectrum, ^{1}H NMR, δ, ppm, *Hg*: 4.45 (2H, d, J 6,1, CH_2), 7,16-7,38 (9H, m, Ar), 7.43-7,59 (5H, m, Ar), 8.02-8.08 (2H, m, Ar), 8.45 (1H, t, J 6.1 NHCH_2), 9.76 (1H, s, NH). UV spectrum, λ, nm (lg ε): 276 (1.098).

1-Benzyl-2-phenyl-4-benzylidene-5-imidazolone (2). To a solution of 0.5 *g* (1.4 *mmol*) of compound 1 in 5 *ml* of DMF was added 0.68 *g* (0.89 *ml*, 4.2 *mmol*) of 1,1,1,3,3,3-hexamethyl- disilazane and the reaction mixture was refluxed for 30 *min*. 45 *ml* of water was added, acidified to pH 6. The formed precipitate was filtered off,

washed with water and air-dried. The product was dissolved in 30 *ml* of benzene, 1.0 *g* of activated carbon was added, the mixture was refluxed for 30 *min*, cooled to room temperature and filtered. After removal of benzene on a rotary evaporator, the residue was 0.31 *g* (65.96%). Yield 65.96 %, mp 147-149, R_f 0.79. IR spectrum, γ, cm^{-1}: 1715 (C=O-cycle). ^{1}H NMR spectrum, δ, ppm: 4.95 (2H, s, CH_2), 7.09-7.14 (2H, m, Ar), 7.19 (1H, s, =CH), 7.21-7.31 (3H, m, Ar), 7.35-7.56 (6H, m, Ar), 7.67-7.72 (2H, m, Ar), 8.23-8.28 (2H, m, Ar). UV spectrum, λ, *nm* (lg ε): 248 (0.949), 295 (0.620), 371 (1.479).

Preparation of samples for UV research. To a solution of 0.5 *g* (1.4 *mmol*) of compound **1** in 5 *ml* of a solvent, 2.8-4.2 *mmol* of silylating reagent was added, and, if necessary, an appropriate additive (Table), and the mixture was boiled for 10 to 90 *min*. 45 *ml* of water was added and left at room temperature for 3 *h*. The precipitate formed was filtered off and thoroughly air dried to obtain a homogeneous mass. To 10 *mg* of the latter, 10 *ml* of ethanol was added, the resulting solution was diluted with ethanol 100 times, and the UV spectrum of the resulting solution was recorded.

ԻՄԻԴԱԶՈԼ-5-ՈՆՆԵՐԻ ՍԻՆԹԵԶՈՒՄ ՈՐՈՇ ՍԻԼԻԼԱՑՆՈՂ ԱԳԵՆՏՆԵՐԻ ԴԵՀԻԴՐԱՏԱՑՆՈՂ ՀԱՏԿՈՒԹՅՈՒՆՆԵՐԻ ԳՆԱՀԱՏՈՒՄԸ

Վ. Օ. ԹՈՓՈՒԶՅԱՆ, Վ. Մ. ՂԱԶՈՅԱՆ,
Գ. Շ. ՀՈՎՀԱՆՆԻՍՅԱՆ և Ա. Ա. ՀՈՎՀԱՆՆԻՍՅԱՆ

Ուսումնասիրված է լուծիչի, ջերմաստիճանի և մի քանի հավելանյութերի ազդեցությունը դիմեթիլդիքլորսիլանի (ԴՄԴՔՍ), տրիմեթիլքլորսիլանի (ՏՄՔՍ) և 1,1,1,3,3,3-հեքսամեթիլդիսիլազանի դեհիդրատացնող հատկությունների վրա N-բենզոիլ-α,β-դեհիդրոֆենիլալանինից 1-բենզիլ-2-ֆենիլ-4-բենզիլիդեն-5-իմիդազոլոնի ստացման ռեակցիայում: Պարզված է, որ ԴՄԴՔՍ և ՏՄՔՍ օգտագործման դեպքում, բացի նպատակային իմիդազոլոնից, գոյանում է նաև կողմնակի արգասիք՝ 2-ֆենիլ-4-բենզիլիդեն-5-օքսազոլոն: Վերջինիս առաջացումը չի նկատվում տրիէթիլամինի ներկայությամբ ՏՄՔՍ որպես դեհիդրատացնող ագենտ կիրառման դեպքում: Իմիդազոլ-5-ոնի ստացման լավագույն արդյունքները (84%) ստացվում են ՀՄԴՍ և բենզիլամիդի խառնուրդը ԴՄՖԱ 15 րոպե եռացնելու դեպքում: ԴՄՖԱ-ի փոխարինումը դիմեթիլացետամիդով, ացետամիդով, ֆորմամիդով կամ պիրիդինով հանգեցնում է նպատակային միացության ելքի նվազմանը: Ստացված արդյունքների հիման վրա արված է եզրակացություն, որ ՀՄԴՍ հանդիսանում է արդյունավետ ռեագենտ N-ացիլ-α,β-դեհիդրոամինաթթուների ամիդներից 1,2,4-եռատեղակալված իմիդազոլ-5-ոների սինթեզի համար:

ОЦЕНКА ДЕГИДРАТИРУЮЩИХ СВОЙСТВ НЕКОТОРЫХ СИЛИЛИРУЮЩИХ АГЕНТОВ ПРИ СИНТЕЗЕ ИМИДАЗОЛ-5-ОНА

В. О. ТОПУЗЯН, В. М. КАЗОЯН, Г. Ш. ОГАННИСЯН и А. А. ОГАНЕСЯН

Исследовано влияние растворителя, некоторых добавок и температуры на дегидратирующие свойства диметилдихлорсилана (ДМДХС), триметилхлорсилана (ТМХС) и 1,1,1,3,3,3-гекса-метилдисилазана (ГМДС) при синтезе 1-бензил-2-фенил-4-бензилиден-5-имидазолона из бензиламида N-бензоил-α,β-дегидрофенилаланина. Установлено, что в случае применения в качестве реагента ДМДХС или ТМХС наблюдается образование побочного продукта – 2-фенил-4-бензилиден-5-оксазолона. Образование последнего не обнаружено в присутствии триэтиламина

при применении в качестве силилирующего агента ТМХС. Наилучшие результаты синтеза имидазол-5-она (84%) получены при кипячении реакционной смеси бензиламида, ГМДС в ДМФА в течение 15 *мин*. Замена ДМФАна диметилацетамид, ацетамид, формамид или пиридин, а также снижениетемпературы реакционной смеси приводит к уменьшению выхода целевого продукта. На основании полученных данных сделано заключение, что ГМДС является эффективным реагентом для синтеза 1,2,4-тризамещенных имидазол-5-онов дегидратацией амидов N-ацил-α,β-дегидроаминокислот.

REFERENCES

[1] *Izumi M., Fukase K., Kusumoto Sh.* // Biosci.Biotechnol.Biochem., 2002, v.66, №1, p.211.

[2] *Jordi E.J., Francisca V.T., Ramon C.G.* // RevistaTumbagu, 2007, v.2, p.85.

[3] *Ryabukhin S.V., Plaskon A.S., Ostapchuk E.M., Volochnyuk D.M.* // Synthesis, 2007, №3, p.417.

[4] *Reddy P.Y., Kondo S., Toru T., Ueno Y.* // J. Org. Chem., 1997, v.62, p. 2652.

[5] *Uchida H., Yoshiyama H., Reddy P.Y., Nakamura Sh., Toru T.* // Bull.Chem.Soc.Jpn., 2004, v.77, p.1401.

[6] *Топузян В.О., Оганесян А.А., Паносян Г.А.* // ЖОрХ, 2004, т.40, №11, с.1692.

[7] *Топузян В.О., Арутюнян Л.Г., Оганесян А.А.* // ЖОрХ, 2007, т.43, №6, с.870.

[8] *Топузян В.О., Арутюнян Л.Г., Оганесян А.А., Паносян Г.А.* // ЖОрХ, 2007, т.43, №6, с.936

[9] *Топузян В.О., Арутюнян Л.Г., Оганесян А.А., Паносян Г.А.* // ЖОрХ, 2008, т.44, №3, с.474.

[10] *Тосунян С.Р.* Хим.ж.Армении, 2013, т.66, №2, с.316.

[11] *Muselli M., Colombeau L., Hedouin J., Hoarau C., Bishoff L.* // Synlett, 2016, v.27, p. 2819.

[12] *Muselli M., Beudequin C, Perrio C., Hoarau C., Bishoff L.* // Chem. Eur. J., 2016, v.22, p.5520.

[13] *Wang Y., Shi D., Lu Z., Dai G.* // Synthet.commun., 2000, v.30, №4, p.707.

ՀԱՅԱՍՏԱՆԻ ՀԱՆՐԱՊԵՏՈՒԹՅԱՆ ԳԻՏՈՒԹՅՈՒՆՆԵՐԻ
ԱԶԳԱՅԻՆ ԱԿԱԴԵՄԻԱ
НАЦИОНАЛЬНАЯ АКАДЕМИЯ НАУК РЕСПУБЛИКИ АРМЕНИЯ
NATIONAL ACADEMY OF SCIENCES OF THE REPUBLIC OF ARMENIA

Հայաստանի քիմիական հանդես
Химический журнал Армении **71, №4, 2018** Chemical Journal of Armenia

SYNTHESIS OF FURFURYL DERIVATIVES OF 4-ALLYL-1-(4-HYDROXY-3-NITROBENZYL)-3-[2-(4-ALKOXYPHENYL)QUINOLIN-4-YL]-4,5-DIHYDRO-1*H*-1,2,4-TRIAZOL-5-THIONS AND THEIR CYTOTOXIC ACTION ON HUMAN CANCER CELLS

M. A. IRADYAN[1], N. S. IRADYAN[1], A. A. HAMBARDZUMYAN[2], H. A. PANOSYAN[1], C. ROUSSAKIS[3] and V. A. SAKANYAN[3,4]

[1]The Scientific Technological Centre
of Organic and Pharmaceutical Chemistry NAS RA
26, Azatutyan Str., Yerevan, 0014, Armenia
[2]Scientific and Production Center "Armbiotehnology" NAS RA
14, Gyurjyan Str., Yerevan, 0056, Armenia
[3]Université de Nantes IICiMed EA-1155, Nantes, France
[4]ProtNeteomix, Nantes, France
E-mail: melkon.iradyan@mail.ru

Furfuryl derivatives of 4-allyl-1-(4-hydroxy-3-nitrobenzyl)-3-[2-(4-alkoxyphenyl)quinolin-4- yl]-4,5-dihydro-1H-1,2,4-triazol-5-thiones were synthesized in this study. The docking analysis revealed the affinity of compounds for Epidermal Growth Factor Receptor (EGFR). New compounds exhibit low cytotoxicity in non-small cell lung cancer and breast cancer cell lines.

In the series of furancarboxylic acids, it has been revealed that the cytotoxic effect is enhanced with an increase of the alkoxy radical, while in the series of esters, an increase in the alkoxy radical leads to a loss of activity. The data suggest that chemical invasion of compounds leads to protein degradation in cancer cells.

Fig. 1, tables 2, references 16.

Targeting cancer with small chemical molecules is of great importance giving new possibilities of modulating not only the catalytic activity of proteins, but also functions leading to protein degradation. We have recently shown that furfuryl derivatives of 4-allyl-5-[2-(4-alkoxyphenyl)- quinolin-4-yl]-4H-1,2,4-triazole-3-thiols (compounds **1**, **2**) have a high affinity for the receptor tyro-sine kinase EGFR, and appear to induce degradation of the receptor in cancer cells [1]. It has been established that the pentyloxy derivative in the series of furancarboxylic acids (compound **2**, $R^1 = C_5H_{11}$) is the most potent modulator of EGFR activity and downstream signaling pathways in cancer cell lines. In addition, an antitumor activity detected in murine 180 sarcoma treated with compounds **1** and **2** seems to

correlate with the decrease in the level of DNA methylation in tumor tissue [2]. Structure of active anti-cancer compounds is given below.

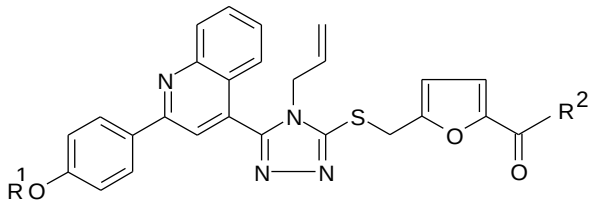

1,2

$R^1 = CH_3 – C_5H_{11}$(**1**, **2**); $R^2 = OCH_3$ (**1**), R^2= OH (**2**).

Continuing structure-designed strategy in this direction, new furfuryl derivatives of 4-allyl-1-(4-hydroxy-3-nitrobenzyl)-3-[2-(4-alkoxyphenyl)quinolin-4-yl]-4,5-dihydro-1H-1,2,4-triazol-5-thiones have been synthesized and their toxicity studied in four cancer cell lines: non-small cell lung cancer (strains A549, NSCLC-L6), breast cancer (MDA MB468) and tumor cells of the NCTC 2544 line, representing human transformed keratinocytes.

Docking of compounds **9-16** was first carried out with the catalytic domain of EGFR using the high-resolution structure of 3W32 [5]. The analysis showed that the binding energy for compounds **9-16** was rather high and comparable to known antitumor drugs cabozantinib [6], linsitinib [7] and zarnestra [8] (Table 1). These drugs are blockers of tyrosine kinase receptors, contain quinoline in their structure and have a high energy of interaction with the EGFR receptor. The results of the docking analyses suggest that the catalytic domain of EGFR is a putative target for compounds **9-16**.

Furfuryl derivatives **9-13** were obtained by reaction of potassium salts **3-7** [3] with 5-chloro-methylfuran-2-carboxylic acid methyl ether (**8**)[4] in DMFA at 95-100°C. Ethers **9-13** were then hydrolyzed by potassium hydroxide in an aqueous methanol medium to acids **14-16**.

In ^{1}H NMR spectra of compounds **9-16**, the signal from NCH_2-aryl is manifested in the region of 5.55 ppm, which is characteristic of N-substituted 1,2,4-triazol-5-thione derivatives. In IR spectra **9-16**, the signal from the C=S group is fixed at 1203 cm^{-1}, the signal from the C=O groups – in the range of 1720-1727 cm^{-1} for ethers and 1691-1705 cm^{-1} for acids. The synthetic root of compounds **9-16** is shown in Scheme 1.

Scheme 1

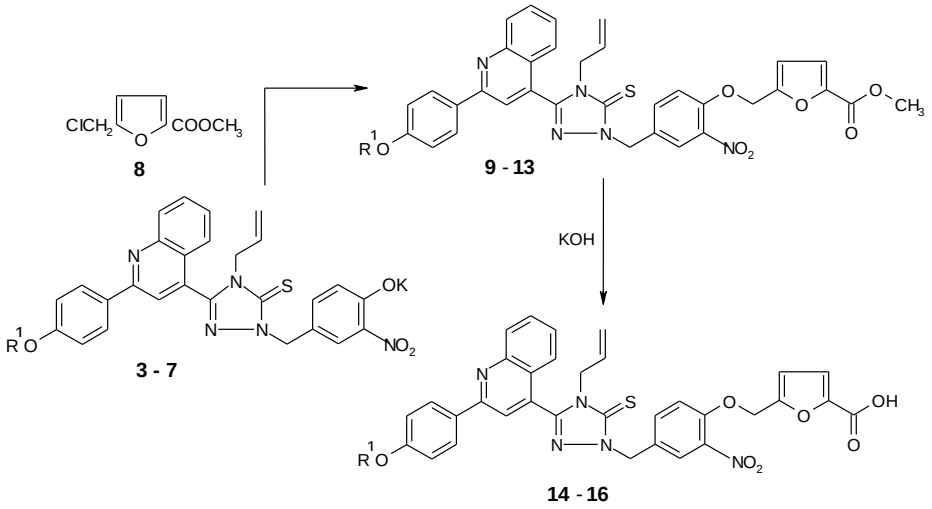

R^1 = CH_3 (**3**,**9**,**14**), C_2H_5 (**4**,**10**,**15**), C_3H_7 (**5**,**11**,**16**), C_4H_9 (**6**,**12**), C_5H_{11} (**7**,**13**).

Discussion of the results of Doking analyses

Models of newly synthesized compounds and antitumor drugs Cabozantinib, Linsitinib and Zarnestra were created in the PDB format using the ChemBioDraw Ultra 12.0 software package (http://software.informer.com/getfree-chembio3d-ultra-12.0/). The MM2 program of the ChemBio-Draw Ultra 12.0 software package was used to perform the minimization of the free energy of chemical compounds. Modeling of the interaction of these compounds with a high-resolution 3D structure 3W32 of the cytoplasmic region of EGFR [5] was carried out using the AutoDock Vina software package (http://vina.scripps.edu/index.html) [9]. The interaction profiles were characterized by AutoDock Tools 1.5.6rc3. For each interaction, the 9 conformations with the highest free energies were calculated using the scoring function of Vina.

To determine the mode of interaction with the receptor, the interaction energies of compounds **9-16** with the catalytic domain of EGFR 3W32 were calculated using the docking analysis. The same calculations were carried out for control antitumor drugs. The results of the docking analysis are shown in Table 1.

Table 1

Binding parameters of compounds 9-16 with the catalytic domain of EGFR (human 3W32) cabozantinib, linsitinib, and zarnestra were used as reference molecules for comparison.

Ligand	ΔG_o, *kcal/mol*	K_D, μM
Cabozantinib (XL-184)	-10.1	0.0395
Linsitinib (OSI-906)	-11.1	0.0073
Zarnestra (R-115777)	-11.1	0.0073
9	-10.3	0.0282
10	-10.8	0.0121
11	-10.6	0.0170
12	-9.6	0.0919
13	-10.4	0.0238
14	-10.1	0.0395
15	-10.5	0.0201
16	-10.7	0.0143

The spatial form of representative interactions of cabozantinib and compounds **11** and **16** is shown in Figure.

From presented data it can be seen that all compounds interact nearly in the same site of studied receptor (left side pictures). However, from precise mode of interactions (right side pictures) it can be seen that compounds **11** and **16** interact with receptor in a somewhat different place when compared to cabozantinib.

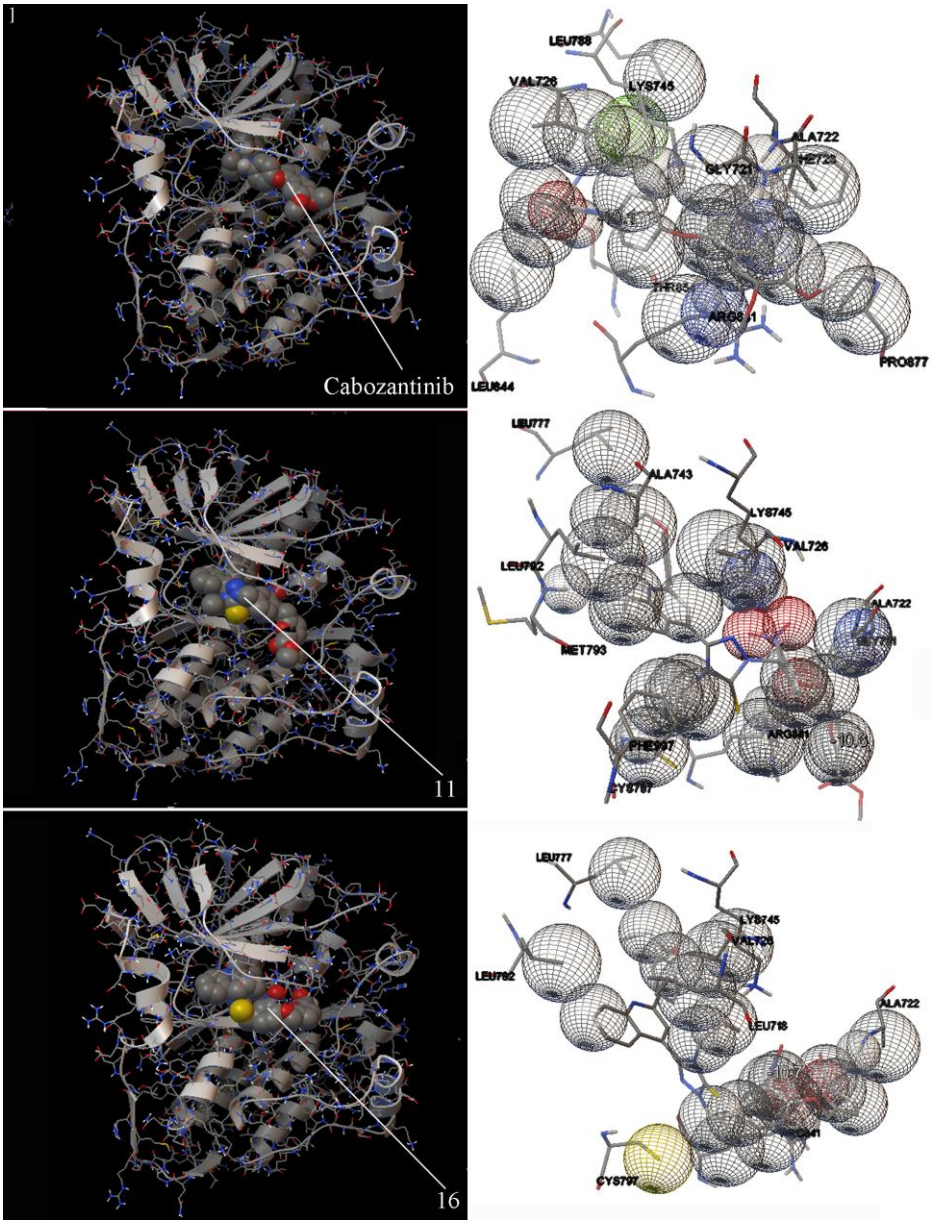

Figure. The binding of compounds **11** and **16** and cabozantinib (for comparison) to the catalytic site of EGFR (3W32).

Discussion of the biological experiments and results

Cell lines. Non-Small-Cell-Lung-Cancer (NSCLC) A549 and NSCLC-L6 cell lines originate from an adenocarcinoma and an epidermoid lung cancer, respectively. NSCLC-L6 is a cell line derived from a NSCLC of a previously untreated patient (moderately differentiated classified as T2N0M0) [10]. A triple negative breast cancer MDA MB468 is characterized by overproduction of epidermal growth factor receptor [11]. The cell line NCTC 2544 represents

transformed human keratinocytes, and A549, NSCLC-L6 and NCTC cell lines were grown in RPMI-1640 supplemented with 2 *mM* glutamine and 5% fetal bovine serum in a humidified atmosphere of 5% CO_2 at 37°C. MDA MB468 cell line was grown in Dulbecco modified eagle medium supplemented with 10% serum.

Cell viability test. Cell lines were seeded at 2×10^4 cells per well in 96-well microtitre plates and the viability of each cell line was assessed by incubation with novel compounds in parallel assays. Each compound was serially diluted and added in cell cultures followed by incubation for 72 h at 37°C. The detection of viable cells was performed with a colorimetric method based on the conversion of tetrazolium dye to blue formazan by live mitochondria [12]. The IC_{50} value of compounds was determined by measuring colour intensity at 570 *nm*. Eight repeats were carried out for each concentration of the compound to be tested.

Next, the evaluation of cell viability revealed that compounds of series **14-16** were more toxic in cell lines than compounds of series **9-13** (Table 2). The level of cytotoxicity of compounds **14-16** was similar in four cell lines tested, with the highest toxicity for compound **16** (IC_{50} 9,9 μM in MDA MB468). Among lower toxic compounds, the most toxic compound **9** had IC_{50} values in the range from 41 μM to 46 μM in cell lines A549, MDA MB468 and NCTC whereas compounds **12** and **13** were inactive at the concentration of 60 μM in all cell lines in the conditions used.

Noteworthy, the range of compound toxicity follows the increasing order of **16** > **15** > **14** in all cell lines whereas the toxicity of less toxic compounds **9-13** appears to have the increasing order of **9** > **10** > **11** > **12** > **13** (see Table 2). Comparison of structures of compounds **1** and **2** suggests that the chemical composition of the side chains R^1 and R^2 can affect the activity of compounds in cancer cells. Indeed, the cytotoxicity of new compounds, which share the same core structure, clearly depends on the length of a hydrophobic chain R^1. The longer hydrophobic R^1 chain gradually increases the cytotoxicity in acids **14-16**. On the contrary, a longer hydrophobic R^1 reduces the cytotoxicity in the series of the ethers **9-13**.

Table 2

Cytotoxicity of novel compounds (IC_{50} in μM) in four cell lines. The viability of cells was determined in parallel assays after incubation with chemical compounds for 72 hours.

Compound	A549	NSCLC-L6	MDA MB468	NCTC
9	41.4 ± 3.3	17.6 ± 0.3	46.9 ± 3.3	42.6 ± 4.3
10	52.4 ± 9.3	> 60	51.4 ± 4.8	44.6 ± 2.9
11	> 60	> 60	45.3 ± 4.7	> 60
12	> 60	Inactive	Inactive	> 60
13	Inactive	Inactive	Inactive	Inactive
14	19.4 ± 0.8	24.8 ± 1.9	22.3 ± 2.5	21.1 ± 0.6
15	16.3 ± 0.3	17.0 ± 0.2	12.9 ± 0.3	14.8 ± 0.3
16	12.3 ± 0.2	12.0 ± 0.6	9.9 ± 0.1	14.3 ± 0.2

Since recently, the apoptotic death of cancer cells caused by chemical agents that enhance protein degradation has attracted great attention in fighting cancer drug resistance. In particular, EGFR inhibitors can induce degradation of the receptor [13] caused by autophagy and explained as a result of cytoprotective response in cells [14]. Low toxicity of the new compounds described in our study suggests that the binding to EGFR could enhance endocytosis of the receptor leading to autophagic protein degradation. Moreover, the presence of a nitro group in the structure of new compounds suggests the possibility of generating reactive oxygen species that could have an additional impact on the cytotoxicity, as shown by dissection of compounds containing nitrobenzoxydiazole [15,16]. Further studies are required to elucidate the anti-cancer effect of new compounds.

Experimental part

IR spectra were recorded on the spectrophotometer "Nexus" (USA) in vaseline oil. ^{1}H NMR spectra and ^{13}C registered on the device Varian "Mercury-300 VX" in DMSO-d_6 / CCL_4, 1/3, internal standard – TMS. Melting point was defined on the microheating table "Boetius" in ^{o}C. TLC was carried out on "Silufol UV-254" plates for compounds **9-13** in the solvent system benzene-ethyl acetate, 5:1; **14-16** – benzene-ethyl acetate, 1: 1. Revelation of plates was carried out with UV light.

General procedure for the synthesis of methyl 5-{4-allyl-3-[2-(4'-alkoxyphenyl)quinolin-4-yl]-5-thioxo-4,5-dihydro-1H-1,2,4-triazol-1-ylmethyl-2-nitrophenoxymethyl}-2-furoates (**9-13**). 0.005 *mol* of the corresponding potassium salt **3-7** [3] is dissolved in 10 *ml* of DMF, 0.87 *g* (0.005 *mol*) of methyl ester of 5-chloromethylfuran-2-carboxylic acid (**8**) [4] is added to the solution and heated at 95-100°C for 4-5 *hours*. Then, the greater part of the DMFA is distilled off in vacuo and water is added to the residue. The precipitate formed is filtered off and recrystallized from dimethyl sulfoxide (**9**,**10**,**12**,**13**), from methanol (**11**).

Methyl 5-{4-allyl-3-[2-(4'-methoxyphenyl)quinolin-4-yl]-5-thioxo-4,5-dihydro-1H-1,2,4-triazol-1-ylmethyl-2-nitrophenoxymethyl}-2-furoate (9). Yield 69%, mp 154-155^{o}C. R_f 0.43. IR spectrum, ν, cm^{-1}: 1723(C=O), 1623, 981, 933(CH=CH_2), 1603, 1499, 833, 768 (CH=CH, aromatic), 1530 (NO_2), 1203 (C=S). ^{1}H NMR, δ, ppm, *Hz*: 3.84 (s, 3H, OCH_3), 3.89 (s, 3H, OCH_3), 4.65 (brd, 2H, J=5,6, $\underline{CH_2}CH=CH_2$), 4.83 (brd, 1H, J=17.3, $CH_2CH=\underline{CH_2}$), 5.02 (brd, 1H, J=10.4, $CH_2CH=\underline{CH_2}$), 5.33 (s, 2H, OCH_2), 5.55 (s, 2H, NCH_2-aryl), 5.77 (ddt,1H, J_1=17.3, J_2=10.4, J_3=5.6, $CH_2\underline{CH}=CH_2$), 6.72 (d, 1H, J=3.5, =CH, fur.), 6.99–7.05 (m, 2H, C_6H_4), 7.16 (d, 1H, J=3.5, =CH, fur.), 7.48 (d,1H, J=8.7, C_6H_3), 7.51–7.58 (m, 1H, C_6H_4), 7.73–7.81 (m, 2H, C_6H_4), 7.80 (dd, 1H, J_1=8.7, J_2=2.2, C_6H_3), 8.02 (d, 1H, J=2.2, C_6H_3), 8.10–8.14 (m, 1H, C_6H_4), 8.21–8.26 (m, 2H, C_6H_4), 8.27 (s, 1H, =CH, pyr.). Found, %: N, 10.48; S, 4.62. $C_{35}H_{29}N_5O_7S$. Calculated, %: N, 10.55; S, 4.83.

Methyl 5-{4-allyl-3-[2-(4'-ethoxyphenyl)quinolin-4-yl]-5-thioxo-4,5-dihydro-1H-1,2,4-triazol-1-ylmethyl-2-nitrophenoxymethyl}-2-furoate (10). Yield 70%, mp 134-135°C. R_f 0.47. IR spectrum, ν, cm^{-1}: 1727(C=O), 1620, 982, 936 (CH=CH_2), 1602, 1499, 824, 768 (CH=CH, aromatic), 1530, 1330 (NO_2), 1203 (C=S). ^{1}H NMR, δ, ppm, *Hz*: 1.45 (t, 3H, J=7.0, $CH_2\underline{CH_3}$), 3.84 (s, 3H, OCH_3), 4.13 (q, 2H, J=7.0, $\underline{CH_2}CH_3$), 4.65 (brd, 2H, J=5.5, $\underline{CH_2}CH=CH_2$), 4.82 (brd, 1H, J=17.1, $CH_2CH=\underline{CH_2}$), 5.02 (brd, 1H, J=10.3, $CH_2CH=\underline{CH_2}$), 5.32 (s, 2H, OCH_2), 5.55 (s, 2H, NCH_2-aryl), 5.77 (ddt, 1H, J_1=17.1, J_2=10.3, J_3=5.5, =CH), 6.72 (d, 1H, J=3.5, =CH, fur.), 6.97–7.02 (m, 2H, C_6H_4), 7.15 (d, 1H, J=3.5, =CH, fur.), 7.48 (d, 1H, J=8.7, C_6H_3), 7.51–7.57 (m, 1H, C_6H_4), 7.74–7.82 (m, 3H, C_6H_4), 8.02 (d, 1H, J=2.2, C_6H_3), 8.09–8.14 (m, 1H, C_6H_4), 8.19–8.25 (m, 2H, C_6H_4), 8.25 (s, 1H, =CH, pyr.). Found, %: N, 10.21; S, 4.59. $C_{36}H_{31}N_5O_7S$. Calculated, %: N 10.33; S 4.73.

Methyl 5-{4-allyl-3-[2-(4'-propoxyphenyl)quinolin-4-yl]-5-thioxo-4,5-dihydro-1H-1,2,4-triazol-1-ylmethyl-2-nitrophenoxymethyl}-2-furoate (11). Yield 58%, mp 108-110°C. R_f 0.54. IR spectrum, ν, cm^{-1}: 1722 (C=O), 1623, 990, 920 (CH=CH_2), 1603, 1502, 837, 769 (CH=CH, aromatic), 1530, 1340 (NO_2), 1203 (C=S). ^{1}H NMR, δ, ppm, *Hz*: 1.09 (t, 3H, J=7.4, CH_3), 1.78–1.90 (m, 2H, $\underline{CH_2}CH_3$), 3.84 (s, 3H, OCH_3), 4.02 (t, 2H, J=6.6, OCH_2), 4.65 (brd, 2H, J=5.6, $\underline{CH_2}CH=CH_2$), 4.82 (brd, 1H, J=17.2, $CH_2CH=\underline{CH_2}$), 5.02 (brd, 1H, J=10.3, $CH_2CH=\underline{CH_2}$), 5.33 (s, 2H, OCH_2), 5.55 (brs, 2H, NCH_2-aryl), 5.76 (ddt, 1H, J_1=17.2, J_2=10.3, J_3=5.6, $CH_2\underline{CH}=CH_2$), 6.72 (d, 1H, J=3.5, =CH, fyr.), 6.97–7.03 (m, 2H, C_6H_4), 7.16 (d, 1H, J=3.5, =CH, fur.), 7.49 (d, 1H, J=8.7, C_6H_3), 7.54 (ddd, 1H, J_1=8.3, J_2=6.8, J_3=1.1, C_6H_4), 7.74–7.82 (m, 3H, C_6H_4), 8.02 (d, 1H, J=2.2, C_6H_3), 8.11 (dd, 1H, J_1=8.7, J_2=1.1, C_6H_4), 8.20–8.25 (m, 2H, C_6H_4), 8.26 (s, 1H, =CH, pyr.). ^{13}C: 10.1(CH_3), 21.9 (CH_3), 47.4(NCH_2), 50.2(NCH_2), 51.1(OCH_3), 63.1(OCH_2), 68.7(OCH_3), 111.9(=CH_2), 114.1(2C, C_6H_4), 115.5(CH), 118.0(CH), 118.1(CH), 119.3(CH), 123.7(C), 124.2 (CH), 124.8(CH), 126.5(CH), 128.3(2C, C_6H_4), 128.4(C), 129.4(CH), 129.7(CH), 129.8(C), 130.6 (C), 131.3(C), 133.9(CH), 139.5(C), 144.0(C), 147.0(C), 147.9(C), 150.2(C), 152.8 (C), 155.2(C), 157.5(C), 160.2(C), 167.1(C). Found, %: N, 10.39; S, 4.49. $C_{37}H_{33}N_5O_7S$. Calculated, %: N, 10.12; S, 4.63.

Methyl 5-{4-allyl-3-[2-(4'-butoxyphenyl)quinolin-4-yl]-5-thioxo-4,5-dihydro-1H-1,2,4-triazol-1-ylmethyl-2-nitrophenoxymethyl}-2-furoate (12). Yield 64%, mp 138-139°C. R_f 0.58. IR spectrum, ν, cm^{-1}: 1720 (C=O), 1623, 990, 920 (CH=CH_2), 1603, 1501, 835, 772 (CH=CH, aromatic), 1531, 1340 (NO_2), 1205 (C=S). ^{1}H NMR, δ, ppm, *Hz*: 1.02 (t, 3H, J=7.3, $CH_2\underline{CH_3}$), 1.48–1.61 (m, 2H, $\underline{CH_2}CH_3$), 1.75–1.85 (m, 2H, $\underline{CH_2}CH_2CH_3$), 3.84 (s, 3H, OCH_3), 4.05 (t, 2H, J=6.4, OCH_2), 4.65 (dt, 2H, J_1=5.6, J_2=1.4, $\underline{CH_2}CH=CH_2$), 4.83 (dq, 1H, J_1=17.1, J_2=1.4, $CH_2CH=\underline{CH_2}$), 5.02 (dq, 1H, J_1=10.3, J_2=1.4, $CH_2CH=\underline{CH_2}$), 5.33 (s, 2H, OCH_2), 5.55 (s, 2H, NCH_2-aryl), 5.77 (ddt, 1H, J_1=17.1, J_2=10.3, J_3=5.6, $CH_2\underline{CH}=CH_2$), 6.72 (d, 1H, J=3.5, =CH, fur.), 6.97–7.02 (m, 2H, C_6H_4), 7.16 (d, 1H, J=3.5, =CH, fur.), 7.48 (d, 1H, J=8.7, C_6H_3), 7.51–7.57 (m, 1H, C_6H_4), 7.74–7.80 (m, 2H, C_6H_4), 7.80 (dd, 1H, J_1=8.7, J_2=2.2, C_6H_3), 8.02 (d, 1H, J=2.2, C_6H_3), 8.09–8.14 (m, 1H,

C_6H_4), 8.19–8.25 (m, 2H, C_6H_4), 8.26 (s, 1H, =CH, pyr.). ^{13}C: 13.3 (CH_3), 18.6(CH_2), 30.6(CH_2), 47.4 (NCH_2), 50.3(OCH_3), 51.0(NCH_2), 63.1(OCH_2), 66.9(OCH_2), 111.7(CH_2), 111.8(CH), 114.1(2C, C_6H_4), 115.5 (CH), 118.0(2CH), 119.3(C), 123.7(C), 124.2 (CH), 124.9(CH), 126.5(CH), 128.3(2C, C_6H_4), 128.3(C), 129.4(CH), 129.6(CH), 129.8(C), 130.6 (CH), 131.2(C), 133.9(CH), 139.5(C), 144.0(C), 147.0(C), 147.9(C), 150.1(C), 152.8(C), 154.9 (C), 160.7(C), 167.1(C). Found, %: N, 9.83; S, 4.39. $C_{38}H_{35}N_5O_7S$. Calculated, %: N, 9.92; S, 4.54.

Methyl 5-{4-allyl-3-[2-(4'-pentyloxyphenyl)quinolin-4-yl]-5-thioxo-4,5-dihydro-1H-1,2,4-triazol-1-ylmethyl-2-nitrophenoxymethyl}-2-furoate (13). Yield 61%, mp 129-130°C. R_f 0.64. IR spectrum, ν, *cm*$^{-1}$: 1726 (C=O), 1622, 985, 936 (CH=CH_2), 1602, 1499, 830, 768 (CH=CH, aromatic), 1530, 1340 (NO_2), 1203 (C=S). ^{1}H NMR, δ, ppm, *Hz*: 0.97 (t, 3H, J=7.0, CH_3), 1.36–1.55 (m, 4H, $\underline{CH_2}CH_2CH_3$), 1.76–1.87 (m, 2H, CH_2),3.84 (s, 3H, OCH_3), 4.04 (t, 2H, J=6.4, OCH_2), 4.66 (brd, 2H, J=5.4, $\underline{CH_2}CH=CH_2$), 4.83 (brd, 1H, J=17.1, $CH_2CH=\underline{CH_2}$), 5.02 (brd, 1H, J=10.3, $CH_2CH=\underline{CH_2}$), 5.33 (s, 2H, OCH_2), 5.55 (s, 2H, NCH_2-aryl), 5.77 (ddt, 1H, J_1=17.1, J_2=10.3, J_3=5.4, $CH_2\underline{CH}=CH_2$), 6.72 (d, 1H, J=3.5, =CH, fur.), 6.96–7.02 (m, 2H, C_6H_4O), 7.16 (d, 1H, J=3.5, =CH, fur), 7.48 (d, 1H, J=8.7, C_6H_3), 7.51–7.57 (m, 1H, C_6H_4), 7.74–7.82 (m, 3H, C_6H_4 and C_6H_3), 8.02 (d, 1H, J=2.1, C_6H_3), 8.09–8.14 (m, 1H, C_6H_4), 8.18–8.25 (m, 2H, C_6H_4O), 8.26 (s, 1H, =CH, pyr). Found, %: N, 9.70; S, 4.61. $C_{39}H_{37}N_5O_7S$. Calculated, %: N, 9.73; S, 4.45.

General procedure for the synthesis of 5-{4-allyl-3-[2-(4'-alkoxyphenyl) quinolin-4-yl]-5-thioxo-4,5-dihydro-1H-1,2,4-triazol-1-ylmethyl-2-nitrophenoxy}-2-furoate (**14-16**). A mixture of 0.001 *mol* of the corresponding ester **9-11**, 0.11 *g* (0.002 *mol*) of potassium hydroxide and 16 *ml* of 50% methanol is boiled for 3-4 *h*, the solution is acidified with acetic acid, the precipitate is filtered off and recrystallized from ethanol.

5-{4-Allyl-3-[2-(4'-methoxyphenyl)quinolin-4-yl]-5-thioxo-4,5-dihydro-1H-1,2,4-triazol-1- ylmethyl-2-nitrophenoxymethyl}-2-furoate (14). Yield 62%, mp 128-130°C. R_f 0.44. IR spectrum, ν, *cm*$^{-1}$: 3100-2500 (OH), 1691 (C=O), 1620, (CH=CH_2), 1603, 1500, 834, 765 (CH=CH, aromatic), 1529 (NO_2), 1203 (C=S). ^{1}H NMR, δ, ppm, *Hz*: 3.89 (s, 3H, OCH_3), 4.65 (dt, 2H, J_1=5.6, J_2=1.7, $\underline{CH_2}CH=CH_2$), 4.82 (dq, 1H, J_1=17.2, J_2=1.7, $CH_2CH=\underline{CH_2}$), 5.02 (dq, 1H, J_1= 10.3, J_2=1.7, $CH_2CH=\underline{CH_2}$), 5.31 (s, 2H, OCH_2), 5.55 (s, 2H, NCH_2-aryl), 5.76 (ddt, 1H, J_1=17.2, J_2=10.3, J_3=5.6, $CH_2\underline{CH}=CH_2$), 6.68 (d, 1H, J=3.4, =CH, fur.), 7.00–7.05 (m, 2H, C_6H_4O), 7.06 (d, 1H, J=3.4, =CH, fur.), 7.50 (d, 1H, J=8.7, C_6H_3), 7.54 (ddd, 1H, J_1=8.3, J_2=6.8, J_3=1.2, C_6H_4), 7.74–7.82 (m, 3H, C_6H_4 and C_6H_3), 8.01 (d, 1H, J=2.2, C_6H_3), 8.10–8.14 (m, 1H, C_6H_4), 8.21–8.26 (m, 2H, C_6H_4O), 8.28 (s, 1H, =CH, pyr.). Found, %: N, 10.62; S, 4.80. $C_{34}H_{27}N_5O_7S$. Calculated, %: N, 10.78; S, 4.93.

5-{4-Allyl-3-[2-(4'-ethoxyphenyl)quinolin-4-yl]-5-thioxo-4,5-dihydro-1H-1,2,4-triazol-1-ylmethyl-2-nitrophenoxymethyl}-2-furoate (15). Yield 64%, mp 134-136°C. R_f 0.46. IR spectrum, ν, *cm*$^{-1}$: 3100-2500 (OH), 1705 (C=O), 1625

($CH=CH_2$), 1604, 1503, 762 (CH=CH, aromatic), 1529 (NO_2), 1203 (C=S). ^{1}H NMR, δ, ppm, *Hz*: 1.45 (t, 3H, J=6.9, CH_3), 4.13 (q, 2H, J=6.9, $\underline{CH_2}CH_3$), 4.65 (brd, 2H, J=5.1, $\underline{CH_2}CH=CH_2$), 4.83 (d, 1H, J=17.3, $CH_2CH=\underline{CH_2}$), 5.02 (d, 1H, J=10.3, $CH_2CH=\underline{CH_2}$), 5.31 (s, 2H, CH_2), 5.55 (s, 2H, NCH_2-aryl), 5.77 (ddt, 1H, J_1=17.3, J_2=10.3, J_3=5.1, $CH_2=\underline{CH}CH_2$), 6.68 (d, 1H, J=3.4, =CH, fur.), 6.96–7.03 (m, 2H, C_6H_4O), 7.08 (d, 1H, J=3.4, =CH, fur.), 7,49 (d, 1H, J=8.7, C_6H_3), 7.50–7.57 (m, 1H, C_6H_4), 7.71–7.82 (m, 3H, C_6H_4), 8.02 (d, 1H, J=2.1, C_6H_3), 8.12 (brd, 1H, J=8.5, C_6H_4), 8.19–8.25 (m, 2H, C_6H_4O), 8.26 (s, 1H, =CH, pyr.), 12.06 (br, 1H, COOH). Found, %: N, 10.47; S, 4.76. $C_{35}H_{29}N_5O_7S$. Calculated, %: N, 10.55; S, 4.83.

5-{4-Allyl-3-[2-(4'-propoxyphenyl)quinolin-4-yl]-5-thioxo-4,5-dihydro-1H-1,2,4-triazol-1-ylmethyl-2-nitrophenoxymethyl}-2-furoate (16). Yield 71%, mp 144-145°C. R_f 0.47. IR spectrum, ν, cm^{-1}: 3100-2500 (OH), 1717 (C=O), 1620 ($CH=CH_2$), 1602, 1500, 835, 768 (CH=CH, aromatic), 1529 (NO_2), 1203 (C=S). ^{1}H NMR, δ, ppm, *Hz*: 1.09 (t, 3H, J=7.4, CH_3), 1.78–1.91 (m, 2H, $\underline{CH_2}CH_3$), 4.02 (t, 2H, J=6.4, OCH_2), 4.65 (brd, 2H, J=5.3, $\underline{CH_2}CH=CH_2$), 4.82 (brd, 1H, J=17.2, $CH_2CH=\underline{CH_2}$), 5.02 (brd, 1H, J=10.3, $CH_2CH=\underline{CH_2}$), 5.32 (s, 2H, OCH_2), 5.55 (s, 2H, NCH_2-aryl), 5.76 (ddt, 1H, J_1=17.2, J_2=10.3, J_3=5.3, $CH_2\underline{CH}=CH_2$), 6.68 (d, 1H, J=3.4, =CH, fur.), 6.97–7.03 (m, 2H, C_6H_3), 7.08 (d, 1H, J=3.4, =CH, fur.), 7.50 (d, 1H, J=8.8, C_6H_3), 7.52–7.58 (m, 1H, C_6H_4), 7.74–7.82 (m, 3H, C_6H_4 and C_6H_3), 8.02 (d, 1H, J=2.1, C_6H_3), 8.09–8.14 (m, 1H, C_6H_4), 8.19–8.25 (m, 2H, C_6H_4O), 8.27 (s, 1H, =CH, pyr.), 12.80 (br, 1H, COOH). Found, %: N, 10.48; S, 4.59. $C_{36}H_{31}N_5O_7S$. Calculated, %: N, 10.33; S, 4.73.

4-ԱԼԻԼ-1-(4-ՀԻԴՐՕՔՍԻ-3-ՆԻՏՐՈԲԵՆԶԻԼ)-3-[2-(4-ԱԼԿՕՔՍԻՖԵՆԻԼ)ԽԻՆՈԼԻՆ-4-ԻԼ]-4,5-ԴԻՀԻԴՐՈ-1Հ-1,2,4-ՏՐԻԱԶՈԼ-5-ԹԻՈՆՆԵՐԻ ՖՈՒՐՖՈՒՐԻԼ ԱԾԱՆՑՅԱԼՆԵՐԻ ՍԻՆԹԵԶԸ ԵՎ ՄԱՐԴՈՒ ՔԱՂՑԿԵՂԱՅԻՆ ԲՋԻՋՆԵՐԻ ՎՐԱ ԴՐԱՆՑ ՑԻՏՈՏՈՔՍԻԿ ԱԶԴԵՑՈՒԹՅՈՒՆԸ

Մ.Ա. ԽՌԱԴՅԱՆ, Ն.Մ. ԽՌԱԴՅԱՆ, Ա.Ա. ՀԱՄԲԱՐՁՈՒՄՅԱՆ, Ն.Մ. ՄԻՆԱՍՅԱՆ, Ս. ՌՈՒՍՍԱԿԻՍ և Վ.Ա. ՍԱՔԱՆՅԱՆ

Ներկայացված աշխատանքում բերված է 4-ալիլ-1-(4-հիդրօքսի-3-նիտրոբենզիլ)-3-[2-(4-ալկօքսիֆենիլ)խինոլին-4-իլ]-4,5-դիհիդրո-1Հ-1,2,4-տրիազոլ-5-թիոնների ֆուրֆուրիլ ածանցյալների սինթեզը և կառուցվածքային անալիզը: Դոքինգ անալիզի միջոցով հնարավոր սպիտակուցային թիրախների հետ մոլեկուլային փոխազդեցության ուսումնասիրությունը ցույց տվեց, որ EGFR-ի կատալիտիկ դոմենի հետ նոր նյութերի կապման էներգիան բարձր է և մակարդակով մոտ է համեմատության համար օգտագործված հակաքաղցկեղային պրեպարատների (կաբոզանտինիբ, լինսիտինիբ և զոնեստրա) փոխազդեցության էներգիաներին: Ուսումնասիրվել է նյութերի ցիտոտոքսիկ ազդեցությունը հետևյալ բջջային գծերի վրա. կրծքագեղձի քաղցկեղ՝ MDA MB468, թոքերի ոչ մանր բջջային քաղցկեղ՝ NSCLC A549 և NSCLC-L16, մարդու տրանսֆորմացված կերատինոցիտներ՝ NCTC 2544: Ցույց է տրվել, որ ֆուրանկարբո-նաֆթիունների շարքում ցիտոտոքսիկ ակտիվությունը մեծանում է ալկօքսի ռադիկալի մեծացման հետ, իսկ էսթերների դեպքում ալկօքսի ռադիկալի մեծացումը բերում է ակտիվության անկման:

Նյութերի ցածր տոքսիկությունը ենթադրում է, որ քիմիական ինվազիան բերում է EGFR-ի էնդոցիտոզի և ռեցեպտորի և քաղցկեղային բջջում դրա հետ ասոցված սպիտակուցների հետագա դեգրադացման:

СИНТЕЗ ФУРФУРИЛЬНЫХ ПРОИЗВОДНЫХ 4-АЛЛИЛ-1-(4-ГИДРОКСИ-3-НИТРОБЕНЗИЛ)-3-[2-(4-АЛКОКСИФЕНИЛ)ХИНОЛИН-4-ИЛ]-4,5-ДИГИДРО-1*H*-1,2,4-ТРИАЗОЛ-5-ТИОНОВ И ИХ ЦИТОТОКСИЧЕСКОЕ ДЕЙСТВИЕ НА РАКОВЫЕ КЛЕТКИ ЧЕЛОВЕКА

М. А. ИРАДЯН[1], Н. С. ИРАДЯН[1], А. А. АМБАРЦУМЯН[2], Г. А. ПАНОСЯН[1], С. РУССАКИС[3] и В. А. САКАНЯН[4]

[1] Научно-технологический центр органической и фармацевтической химии
НАН Республики Армения
Армения, 0014, Ереван, пр. Азатутян, 26
[2] Научно-производственный центр "Армбиотехнология"
НАН Республики Армения
Армения, 0056, Ереван, ул. Гюрджяна, 14
[3] Университет Нанта, IICiMed EA-1155, Нант, Франция
[4] ПротНетеомикс, Нант, Франция
E-mail: melkon.iradyan@mail.ru

В представленной работе проведен синтез и структурный анализ фурфурильных произ- водных 4-аллил-1-(4-гидрокси-3-нитробензил)]-3-[2-(4-алкоксифенил)хинолин-4-ил]-4,5-дигидро-1*H*-1,2,4-триазол-5-тионов. Изучение молекулярных взаимодействий с возможными белковыми мишенями методом докинга показал, что энергия связывания новых соединений с каталитическим доменом EGFR высокая и находится на уровне, близком для противоопухолевых препаратов кабозантиниба, линситиниба и зарнестры, использованных для сравнения. Исследовано цитотоксическое действие соединений на клеточной линии рака молочной железы MDA MB468, линиях немелкоклеточного рака легких NSCLC A549 и NSCLC-L16, а также на линии трансформированных кератиноцитов человека NCTC 2544. Выявлено, что в ряду фуранкарбоновых кислот цитотоксическое действие усиливается с повышением алкоксильного радикала, а в ряду эфиров повышение алкоксильного радикала приводит к потере активности. Низкая токсичность соединений предполагает, что химическая инвазия приводит к повышенному эндоцитозу EGFR и последующей деградации рецептора и ассоциированных с ним белков в раковых клетках.

REFERENCES

[1] *Sakanyan V.A., Alves de Susa R., Bollot G., Boves K., Hambardzumyan A.A., Gulhandanyan A., Stepanyan G.A., Iradyan M.A., Iradyan N.S. //* Scientific Conference of the Armenian Chemical Society “Actual problems of fundamental and applied chemistry ”, Yerevan, 2017, p.41.

[2] *Iradyan M.A., Iradyan N.S., Hambardzumyan A.A., Nersesyan L.E., Agaronyan A.C., Danielyan I.S., Muradyan R.E., Paronikyan R.V., Stepanyan G.M. //* Biolog. Journ. Of Armenia, 2018, v.70, № 2, p.100.

[3] *Iradyan M.A., Iradyan N.S., Hambardzumyan A.A., Panosyan H.A., Tamazyan R.A., Ayvazyan A.G., Hovhannisyan G.Sh., Alves de Susa R., Sakanyan V.A.* // Chem. Journ. of Armenia, 2018, v. 71, №3, p. 389.

[4] *Mnjoyan A.L., Grigoryan M.T.* // Collection "Synthesis of heterocyclic compounds", Yerevan, 1956, v. 1, p. 36.

[5] *Kawakita Y., Seto M., Ohashi T., Tamura T., Yusa T., Miki H., Iwata H., Kamiguchi H., Tanaka T., Sogabe S., Ohta Y., Ishikawa T.* // Bioorg. Med. Chem., 2013, v. 21, p. 2250.

[6] *Choueiri T.K., Escudier B., Powles T., Mainwaring P.N., Rini B.I., Donskov F., Hammers H., Hutson T.E., Lee J.L., Peltola K., Roth B.J., Bjarnason G.A., Géczi L., Keam B., Maroto P., Heng D.Y., Schmidinger M., Kantoff P.W., Borgman-Hagey A., Hessel C., Scheffold C., Schwab G.M., Tannir N.M., Motzer R.J.* // The New England Journal of Medicine, 2015, v. 373, №19, p. 1814.

[7] *Mulvihill M.J., Cooke A., Rosenfeld-Franklin M., Buck E., Foreman K., Landfair D., O'Connor M., Pirritt C.* // Future medicinal chemistry. 2009, v. 1, №6, p, 1153.

[8] *Witzig T.E., Tang H., Micallef I.N.M., Ansell S.M., Link B.K., Inwards D.J., Porrata L.F., Johnston P.B., Colgan J.P., Markovic S.N., Nowakowski G.S., Thompson C.A., Allmer C., Maurer M.J., Gupta M., Weiner G., Hohl R., Kurtin P.J., Ding H., Loegering D., Schneider P., Peterson K., Habermann T.M., Kaufmann S.H.* // Blood, 2011, v. 118, №18, p. 4882.

[9] *Trott O., Olson A.J.* // J. Comput. Chem., 2010, v. 31, p. 455.

[10] *Rousseau B., Jacquot J., Le Palabe J., Malleter M., Tomasoni C., Boutard T., Sakanyan V, Roussakis C.* // Sci. Rep., 2015, v.5, p. 10356.

[11] *Filmus J., Pollak M.N., Cailleau R., Buick R.N.* // Biochem. Biophys. Res. Commun., 1985, v. 128, p. 898.

[12] *Vindelov L.L.* Virchows Arch. B Cell Pathol., 1977, v. 24, p. 227.

[13] *Han W., Pan H., Chen Y., Sun J., Wang Y., Li J., Ge W., Feng L., Lin X., Wang X., Wang X., Jin H.* // PLoS One, 2011, 6, e18691.

[14] *Yin Z., Pascual C., Klionsky D.* // J. Microb. Cell., 2016, v. 3, p. 588.

[15] *Sakanyan V., Hulin P., Alves de Sousa R., Silva V., Hambardzumyan A., Nedellec S., Tomasoni C., Logé C., Pineau C., Roussakis C., Fleury F., Artaud I.* // Sci. Rep., 2016, v.6, p. 21088.

[16] *Sakanyan V.* Reactive chemicals and electrophilic stress in cancer: a minireview. High-Throughput, 2018, v.7, p. 12.

ՀԱՅԱՍՏԱՆԻ ՀԱՆՐԱՊԵՏՈՒԹՅԱՆ ԳԻՏՈՒԹՅՈՒՆՆԵՐԻ
ԱԶԳԱՅԻՆ ԱԿԱԴԵՄԻԱ
НАЦИОНАЛЬНАЯ АКАДЕМИЯ НАУК РЕСПУБЛИКИ АРМЕНИЯ
NATIONAL ACADEMY OF SCIENCES OF THE REPUBLIC OF ARMENIA

Հայաստանի քիմիական հանդես
Химический журнал Армении **71, №4, 2018** Chemical Journal of Armenia

TARGETED SYNTHESIS OF 9-FLUORENYLMETHYLOXYCARBONYLGLYCYL-(*S*)-β-[4-ALLYL-3-PROPYL-5-THIOXO-1,2,4-TRIAZOL-1-YL]-α-ALANINE AND STUDY OF ITS EFFECT ON COLLAGENASE ACTIVITY

Yu. M. DANGHYAN[b] , T. H. SARGSYAN[a, b] S. M. JAMGARYAN[b], A. S. SARGSYAN[b], E. A. GYULUMYAN[b], N. A. HOVHANNISYAN[a,b], A. M. HOVHANNISYAN[a,b], A. H. TSATURYAN[a, b] , H. A. PANOSYAN[c] and A. S. SAGHYAN[a, b]

[a]Yerevan State University
1, A. Manoukyan Str., Yerevan, 0025, Armenia
[b]Scientific and Production Center "Armbiotechnology" NAS RA
14, Gyurjyan Str., Yerevan, 0056, Armenia
[c]The Scientific Technological Center of Organic and Pharmaceutical Chemistry
26, Azatutyan Str., Yerevan, 0014, Armenia

More than 15 new peptides have been constructed on the basis of (S)-β-[4-allyl-3-propyl-5-thioxo-1,2,4-triazol-1-yl]-α-alanine non-protein amino acid by ChemOffice software. The study of their possible interaction with collagenase enzyme was implemented by molecular docking program – AutoDockVina software. Analyzing the obtained results, 9-fluorenylmethyloxycarbonylglycyl-(S)-β-[4-allyl-3-propyl-5-thioxo-1,2,4-triazol-1-yl]-α-alanine dipeptide was identified by maximum values of Gibbs free energy (ΔG=8.6 *kcal/mol*) and minimum values of dissociation constant ($K_{D=}$0.497 *μmol*) of ligand-macromolecular interaction.

The synthesis of a new undescribed in the literature 9-fluorenylmethyloxycarbonylglycyl-(S)-β-[4-allyl-3-propyl-5-thioxo-1,2,4-triazol-1-yl]-α-alanine dipeptide has been carried out by the activated ester method.

In vitro study of the synthesized dipeptide effect on the activity of collagenase enzyme by various peptide concentrations has been carried out. The value of IC_{50} was calculated. It was 0.892 *μmol/l*:

Figs. 2, table 1, references 15.

For more than 70 years the research in the field of synthesis and study of peptides as well as the possibility of their introduction to the medical practice has been carried out [1].

Currently, there are around 60-70 approved peptide drugs in the global market, with 100-200 more in clinical trials, 400-600 more in pre-clinical studies and possibly hundreds to thousands more on the laboratory bench [2]. It should be

mentioned that most of them contain non-proteinogenic amino acid moieties [3]. There are well-known medicinal preparations created on the basis of synthetic peptides that are used in the following diseases: hypertension, type 2 diabetes, postmenopausal osteoporosis, Paget's disease, hypercalcaemia, advanced prostate cancer, acromegaly, carcinoidsyndrome, central diabetes insipidus.

It is established that the moiety of non-protein amino acid extends the process of enzyme-substrate recognition that in turn leads to retardation of the peptide bond destruction. These and other properties of peptides, containing a fragment of non-protein amino acid, enable to create on their basis physiologically and pharmacologically active drugs [4].

Matrix metalloproteases (MMPs) is a major group of enzymes that regulates cell-matrix composition. Matrix metalloproteases (MMPs) play an important role in degradation of extracellular matrix in both norm and various pathologies [5]. Metalloproteases are targets for a wide range of medications, including antitumor and anti-inflammatory drugs [6,7]. Matrix metalloproteases are responsible for many proteolytic processes that lead to tumor development. Involvement of gelatinizes (MMP-9 and MMP-2) in the process of metastases and angiogenesis formation stimulated creation of synthetic gelatinize inhibitors able to stop the development of tumors [6,7]. MMP-1 is also validated as a cancer target [8].

Unfortunately, clinical trials of gelatinize inhibitors on oncological patients so far have not revealed therapeutic effect; moreover undesirable side effects were registered. The majority of inhibitors are zinc-chelating compounds of a wide spectrum of action that did not have a specific effect. For example, calprotectin inhibits MMP by blocking zinc binding [9]. The search for new highly specific compounds able to inhibit metalloproteases is one of the directions in creation of drugs preventing spread of metastases [10]. It has been shown that some low-molecular-weight compounds are able to inhibit MMPs [11].

Taking into account the above mentioned, we aimed at constructing a new undescribed in the literature dipeptide on the basis of (*S*)-β-[4-allyl-3-propyl-5-thioxo-1,2,4-triazol-1-yl]-α-alanine non-protein amino acid, implementing software research of the mentioned peptides, selecting possible active peptides to carry out their target synthesis and study the biological effect of the synthesized peptides.

In the first stage the structure-based drug design approach was used to identify potential inhibitors of enzyme. For this aim docking analysis was done for identification of substances capable of interacting with collagenase.

Amino acids and peptides structures were built by ChemBioOffice 2010 (ChemBio3D Ultra12.0). Ligand free energy was minimized using MM2 force field and truncated Newton–Raphson method. Crystallographic structure of collagenase was taken from http://www.rcsb.org website (PDB-ID: 1NQJ). Docking of ligand to enzyme was done by AutoGrid 4, AutoDock Vina software [12]. AutoDock used the Lamarckian genetic algorithm by alternating local search with selection and crossover [13]. The ligands were ranked using an energy-based scoring function and

a grid-based protein–ligand interaction was used to speed up the score calculation. Dissociation constant was calculated by using the following formula:

$K_D = \exp((\Delta G \times 1000)/(Rcal \times TK))$

Rcal=1.98719 cal/(*mol* × K) (gas constant)

TK = 298.15 *K* (room temperature by Kelvin)

The data of enzyme-peptide interaction are presented in Table.

Table

Data of molecular modeling

Experimental dipeptides	Gibbs free energy (ΔG) *kcal/mol*	Dissociation constant (K_D) *μmol*
N-formyl-(*S*)-methionyl-(*S*)-β-[4-allyl-3-propyl-5-thioxo-1,2,4-triazol-1-yl]-α-alanine	-5.8	56.05
(*S*)-methionyl-(*S*)-β-[4-allyl-3-propyl-5-thioxo-1,2,4-triazol-1-yl]-α-alanine	-6.1	33.78
9-Fluorenylmethyloxycarbonyl-(*S*)-alanyl-(*S*)-β-[4-allyl-3-propyl-5-thioxo-1,2,4-triazol-1-yl]-α- alanine	-7.7	2.27
(*S*)-alanyl-(*S*)-β-[4-allyl-3-propyl-5-thioxo-1,2,4-triazol-1-yl]-α-alanine	-6.2	28.53
N-tretbutoxycarbonyl-(*S*)-alanyl-(*S*)-β-[4-allyl-3-propyl-5-thioxo-1,2,4-triazol-1-yl]-α- alanine	-6.7	12.27
N-tretbutoxycarbonylalanylglycyl-(*S*)-β-[4-allyl-3-propyl-5-thioxo-1,2,4-triazol-1-yl]-α-alanine	-6.6	14.53
N-tretbutoxycarbonyl-(*S*)-β-phenyl-alanyl-(*S*)-β-[4-allyl-3-propyl-5-thioxo-1,2,4-triazol-1-yl]-α-alanine	-6.9	8.75
(*S*)-β-phenyl-alanyl-(*S*)-β-[4-allyl-3-propyl-5-thioxo-1,2,4-triazol-1-yl]-α-alanine	-7.2	5.28
9-Fluorenylmethyloxycarbonylglycyl-(*S*)-β-[4-allyl-3-propyl-5-thioxo-1,2,4-triazol-1-yl]-α- alanine	-8.6	0.497
Glycyl-(*S*)-β-[4-allyl-3-propyl-5-thioxo-1,2,4-triazol-1-yl]-α-alanine	-6.1	33.78

The negative value of ΔG proves that the complex has been generated. According to Table, the value of ΔG is negative for all compounds, which proves that all dipeptides are interacting with the enzyme. Based on the results obtained, we aimed to perform further research on a compound with a maximum value of the Gibbs free energy, which turned out to be 9-fluorenylmethyloxycarbonylglycyl-(*S*)-β-[4-allyl-3-propyl-5-thioxo-1,2,4-triazol-1-yl]-α-alanine.

The docking data are presented in the Figure, where the fragments of ligand-collagenase interaction are shown.

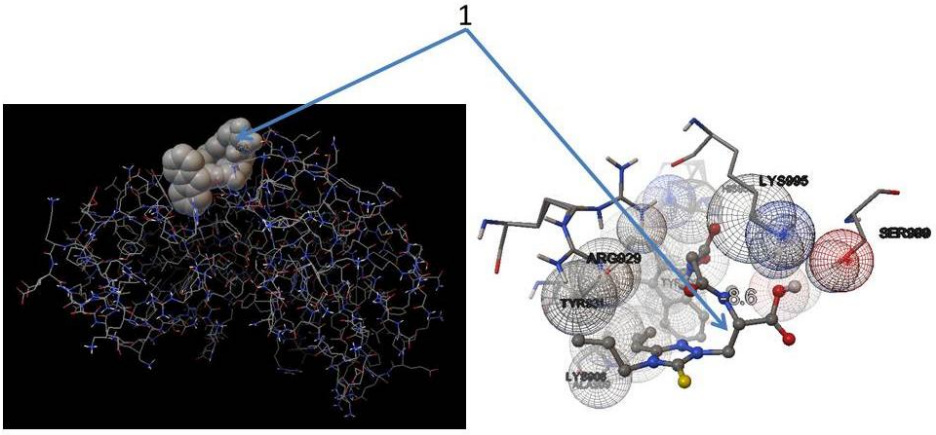

Fig. 1. The bond of Fmoc-glycyl-(*S*)-β-[4-allyl-3-propyl-5-thioxo-1,2,4-triazol-1-yl]-α-alanine with collagenase enzyme by software.

Taking into account the data of software modeling, Fmoc-glycyl-(*S*)-β-[4-allyl-3-propyl-5-thioxo-1,2,4-triazol-1-yl]-α-alanine dipeptide was selected from the mentioned range for further research, that is for carrying out the peptide synthesis followed by studying the synthesized peptide effect on the activity of collagenase enzyme.

The synthesis of peptide was carried out by the method of activated esters in a solution. The method is distinguished by its simplicity and makes it possible to obtain final products in good yields and high purity [14].

At the first stage with the help of dicyclohexylcarbodiimide from 9-fluorenylmethyloxycarbonyl-glycyl (1) was obtained its succinimide ether **(2)**, transformed by condensation with (*S*)-β-[4-allyl-3-propyl-5-thioxo-1,2,4-triazol-1-yl]-α-alanine non-protein amino acid in alkaline aqueous-organic medium in the corresponding dipeptide Fmoc-glycyl-(*S*)-β-[4-allyl-3-propyl-5-thioxo-1,2,4-triazol-1-yl]-α-alanine (4) (Scheme).

Scheme

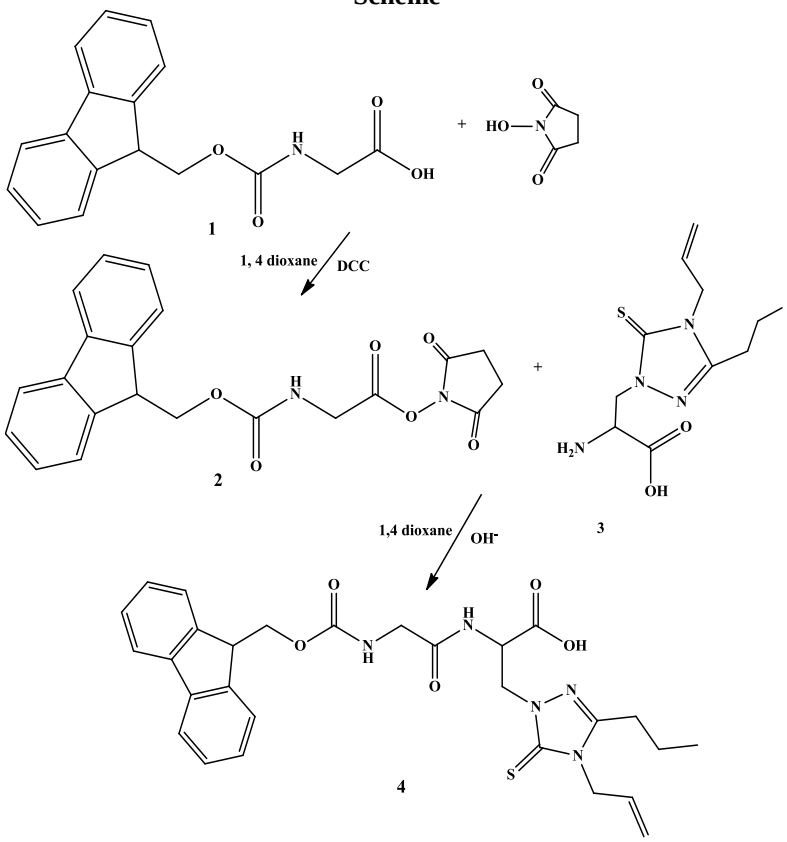

Experimental Part

^{1}H NMR spectra were recorded on a "Varian Mercury 300VX" device with an operating frequency of 300.08 *MHz* in a solution of DMSO-D6/CCl4 1/3 using the method of double resonance. TLC was conducted on "Silufol UV-254" plates in a mixture of chloroform-ethyl acetate-methanol (4:4:1), developer – chlorotoluidine. Elemental analysis was performed on elemental analyzer CNS-O "Euro EA3000".

Synthesis of N-9-fluorenylmethyloxycarbonylglycine succinimide ester (2). 0.218 *g* (1.06 *mmol*) of dicyclohexylcarbodiimide, preliminary dissolved in 3 *ml* of dioxane was added at 0^{o}C to 0.29 *g* (1.0 *mmol*) of N-9-fluorenylmethyloxycarbonyl-glycine **(2)** and 0.127 *g* (1.1 *mmol*) of N-hydroxysuccinimide in a mixture of 6 *ml* of dioxane and 3 *ml* of methylene chloride. The reaction mixture was stirred for ~ 2 h at 0^{o}C and left overnight in a refrigerator.

The analysis was performed by TLC [SiO_2, $CHCl_3$/ethyl acetate/CH_3OH (4:2:1), developer - chlorotoluidine]. The precipitate formed was filtered off, the solvent distilled off on a rotary evaporator, and the precipitate crystallized from a mixture of ethyl acetate hexane (1:2).

Yield 0.25 g (67.5%). Mp = 175 °C [14].

Synthesis of N-9-fluorenylmethyloxycarbonylglycyl-(S)-β-(3-propyl-4-allyl-5-thioxo-1,2,4-triazol-1-yl)-α-alanine (4). The resulting succinimide ether **2** was used in the next stage of dipeptide synthesis. In a flat-bottomed flask with a magnetic stirrer, 0.18 *g* (0.66 *mmol*) of (*S*)-β-(3-propyl-4-allyl-5-thioxo-1,2,4-triazol-1-yl)-α-alanine, 1.25 *ml* (0.63 *mmol*) of 0.5*M* sodium hydroxide solution and 0.016 (0.19 *mmol*) of baking soda were placed. At room temperature, 0.24 *g* (0.6 *mmol*) of N-9-fluorenylmethyloxycarbonylglycine succinimide ester (**2**) was added to 2 *ml* of dioxane, and the reaction mixture was stirred for 3 *h*. The next day, 5 *ml* of ethyl acetate and 1.45 *ml* of 10% citric acid were added to the flask contents. After vigorous stirring, the organic layer was separated, and the aqueous layer was extracted twice with ethyl acetate (5 *ml* each). The organic layer was dried with anhydrous sodium sulfate, then the solvent was evaporated to dryness.

The product was isolated by column chromatography using SiO_2 L-40/100 silica gel. Analysis by TLC [SiO_2, $CHCl_3$/ethyl acetate/CH_3OH (4: 2: 1), the developer – chloro-toluidine]. The product yield per succinimide ester 72.8%, Mp 99-100^oC. Found, %: C, 61.25; H, 5.61; N, 12.71. $C_{28}H_{31}N_5O_5S$ Calc., %: C, 61.19; H, 5.68; N, 12.74. ^1H NMR (DMSO, δ, ppm) 0.9 (m, 3H, CH_3-$\underline{CH_2}$); 1.44 (m, 2H, CH_3-$\underline{CH_2}$); 1.5 (m, 2H, CH_3-CH_2-$\underline{CH_2}$); 3.65 (m, 2H, $NHCH_2$), 3.8 (dd, 1H, J_1=13.6,J_2=8.2, NH-CH-$\underline{CH_2}$); 4.06 (dd, 1H, J_1=13.6,J_2=5.1, NH-CH-$\underline{CH_2}$); 4.46 (m, 1H, OCH_2-CH); 4.7 (ddd, 1H, J_1=8.2,J_2=8.1, J_3=5.1, NH-$\underline{CH}$-CH_2); 4.7 (m, 2H, O-CH_2-$\underline{CH}$);5.19 (dq, 1H, J_1=17.2, J_2~J_3=1.5, CH_2-CH=$\underline{CH_2}$); 5.22 (dq, 1H, J_1=10.4, J_2~J_3=1.5, CH_2-CH=$\underline{CH_2}$); 5.87 (ddt, 1H, J_1=17.2, J_3=10.4, J_3=4.9, CH_2-$\underline{CH}$=CH_2);7.28-7.87 (m, 8H, fluorenyl); 8.03 (t, 1H, ^3J=8.1, $\underline{NH}$-CH-CH_2); 8.03 (m, 1H, $\underline{NH}$-CH_2);11 (br, 1H, COOH):

Collagenase activity. Collagenase activity was determined by measuring free amino groups according to o-phthalaldehyde (OPA) method [15].

The reaction mixture contained 0.05 M HEPES buffer, pH 7.2, 10 *mg*/*ml* gelatin and 0.025 *mg*/*ml* collagenase (activated by 0.36 M $CaCl_2$). The concentration of investigated compounds in the reaction mixture was 5*mM*. The aliquot (50 *ul*) was taken and the remaining mixture was incubated at 37^oC. Every 30 *min* the aliquot was picked up and the reaction was stopped by adding 10 ul of 30% trichloroacetic acid. The concentration of free amino groups in the reaction mixture was determined by OPA reagent containing 0.2 *M* borate buffer, pH 9.7, 0.1667 *mg*/*ml* OPA and 1.25 *mM* mercaptoethanol. The reaction mixture (50 *ul*) was added to OPA reagent (1.5 *ml*) and H_2O (1.5 *ml*). A340 was recorded after 5 *min* incubation at RT.

Peptides have been tested in different concentrations in order to link the concentration and effect. The dependence curve of the inhibition percentage dependent on concentration is presented in Fig. 2.

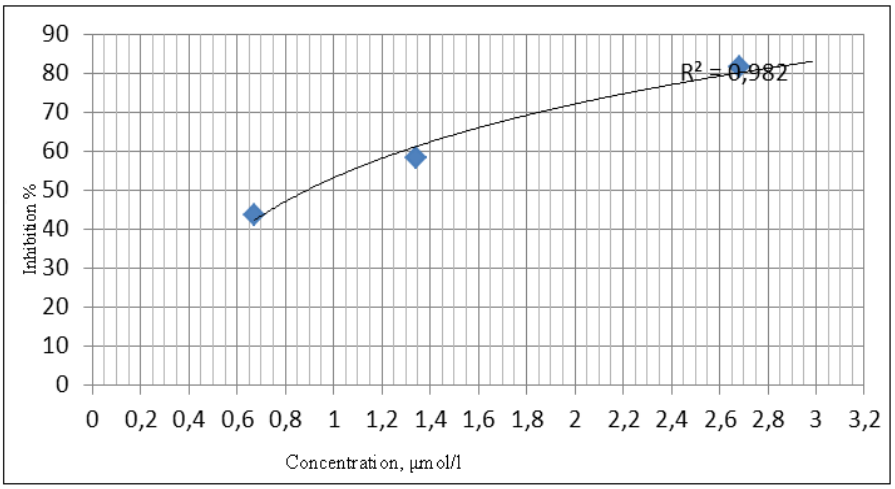

Fig. 2. The effect of various concentrations of Fmoc-glycyl-(S)-β-[4-allyl-3-propyl-5-thioxo-1,2,4-triazol-1-yl]-α-alanine on the activity of collagenase enzyme.

According to the data obtained, in case of Fmoc-glycyl-(*S*)-β-[4-allyl-3-propyl-5-thioxo-1,2,4-triazol-1-yl]-α-alanine IC_{50} is 0.892 *μmol/l*:

9-ՖԼՈՒՈՐԵՆԻԼՄԵԹԻԼՕՔՍԻԿԱՐԲՈՆԻԼԳԼԻՑԻԼ-(S)-β-[4-ԱԼԻԼ-3-ՊՐՈՊԻԼ-5-ԹԻՕՔՍՈ-1,2,4-ՏՐԻԱԶՈԼ-1-ԻԼ]-α-ԱԼԱՆԻՆ ԴԻՊԵՊՏԻԴԻ ՆՊԱՏԱԿԱՅԻՆ ՍԻՆԹԵԶԸ ԵՎ ԿՈԼԱԳԵՆԱԶ ՖԵՐՄԵՆՏԻ ԱԿՏԻՎՈՒԹՅԱՆ ՎՐԱ ԱԶԴԵՑՈՒԹՅԱՆ ՀԵՏԱԶՈՏՈՒՄԸ

Յու. Մ. ԴԱՆՂՅԱՆ, Տ.Հ. ՍԱՐԳՍՅԱՆ, Ս. Մ. ՋԱՄԳԱՐՅԱՆ, Ա. Ս. ՍԱՐԳՍՅԱՆ, Է. Ա. ԳՅՈՒԼՈՒՄՅԱՆ, Հ. Ա. ՓԱՆՈՍՅԱՆ, Ն. Ա. ՀՈՎՀԱՆՆԻՍՅԱՆ, Ա. Մ. ՀՈՎՀԱՆՆԻՍՅԱՆ, Ա. Հ. ԾԱՏՈՒՐՅԱՆ և Ա. Ս. ՍԱՂՅԱՆ

(S)-β-[4-Ալիլ-3-պրոպիլ-5-թիօքսո-1,2,4-տրիազոլ-1-իլ]-α-ալանին ոչ սպիտակուցային ամինաթթվի հենքի վրա ChemOffice software ծրագրի կիրառմամբ կառուցվել են ավելի քան 15 նոր գրականության մեջ չնկարագրված դիպեպտիդներ:

Իրականացվել է կառուցված պեպտիդների և կոլագենազ ֆերմենտի հնարավոր փոխազդեցության մոդելավորում AutoDockVina software համակարգչային ծրագրի կիրառմամբ:

Ստացված տվյալների վերլուծության արդյունքում՝ ընտրվել է 9-ֆլուորենիլմեթիլ-օքսիկարբոնիլգլիցիլ-(S)-β-[4-ալիլ-3-պրոպիլ-5-թիօքսո-1,2,4-տրիազոլ-1-իլ]-α-ալանին դիպեպտիդը, որը ունեցել է Գիբսի ազատ էներգիայի (ΔG=8.6 կկալ/մոլ) առավելագույն և դիսոցման հաստատունի (KD=0.497 մկմոլ) նվազագույն արժեքներ:

Նոր գրականության մեջ չնկարագրված 9-ֆլուորենիլմեթիլօքսիկարբոնիլգլիցիլ-(S)-β-[4-ալիլ-3-պրոպիլ-5-թիօքսո-1,2,4-տրիազոլ-1-իլ]-α-ալանին դիպեպտիդի սինթեզը իրականացվել է՝ ակտիվացված էսթերների մեթոդի կիրառմամբ:

Կատարվել է սինթեզված դիպեպտիդի ազդեցության in vitro հետազոտում կոլագենազ ֆերմենտի ակտիվության վրա՝ պեպտիդի տարբեր կոնցենտրացիաների կիրառմամբ: Հաշվարկվել է IC50-ի արժեքը, որը ստացվել է 0.892 մկմոլ/լ:

ЦЕЛЕНАПРАВЛЕННЫЙ СИНТЕЗ 9-ФЛУОРЕНИЛМЕТИЛОКСИКАРБОНИЛГЛИЦИЛ-(*S*)-β-[4-АЛЛИЛ-3-ПРОПИЛ-5-ТИОКСО-1,2,4-ТРИАЗОЛ-1-ИЛ]-α-АЛАНИН ДИПЕПТИДА И ИССЛЕДОВАНИЕ ЕГО ДЕЙСТВИЯ НА АКТИВНОСТЬ КОЛЛАГЕНАЗЫ

Ю. М. ДАНГЯН, Т. О. САРГСЯН, С. М. ДЖАМГАРЯН, А. С. САРГСЯН, Э. А. ГЮЛУМЯН, Г. А. ПАНОСЯН, Н. А. ОГАННИСЯН, А. М. ОГАННИСЯН и А. С. САГЯН

С помощью программы ChemOffice software были построены структуры 15 новых не описанных в литературе дипептидов, содержащих небелковую аминокислоту (*S*)-β-[4-аллил-3-пропил-5-тиоксо-1,2,4-триазол-1-ил]-α-аланин.

С использованием программы AutoDockVina software было проведено моделирование вероятного взаимодействия дипептидов с ферментом колагеназ. На основании полученных данных был выбран 9-флуоренилметилоксикарбонилглицил-(*S*)-β-[4-аллил-3-пропил-5-тиоксо-1,2,4-триазол-1-ил]-α-аланин, который имеет наибольшую свободного энергию (*ΔG=8.6 ккал/мол*) и минимальное значение константы диссоциации ($K_{D=}$0.497 *мкмол*).

Синтез 9-флуоренилметилоксикарбонилглицил-(*S*)-β-[4-аллил-3-пропил-5-тиоксо-1,2,4-триазол-1-ил]-α-аланина осуществлен методом активированных эфиров.

Проведено *in vitro* исследование влияния синтезированого дипептида на активность фермента колагеназ при различных концентрациях пептида. Рассчитано значение IC_{50} -0.892 *мкмол/л*.

REFERENCES

[1] *Gregory A.* Grant Synthetic peptides Oxford University press, second edition, 2002.
[2] *Sun L.* // Mod. Chem. Appl. 2013; 1: e103. doi: 10.4172/2329-6798.1000E103.
[3] *Vlieghe P., Lisowski V., Martinez J., Khrestchatisky M.* // Drug Discov Today, 2010 Jan. 15(1-2), p. 40.
[4] *Hughes A.* // WILEY-VCH Verlag GmbH & Co. KGaA, Weinheim. v. 4 Protection Reactions, Medicinal Chemistry & Combinatoral Synthesys, 2011, v. 4, p. 538.
[5] *Baker A.B.* // A. Baker, D. Edwards, G. Murphy // J. Cell Science, 2002, v. 115, p. 3719.
[6] *Hsieh M.J., Chen J.C., Yang W.E., Chien S.Y., Chen M.K., Lo Y.S., His Y.T., Chuang Y.C., Lin C.C., Yang S.F.* // Biochem Pharmacol., 2017, 2952(17), p. 30041-2,
[7] *Krüger A., Arlt M.J., Gerg M., Kopitz C., Bernardo M.M., Chang M., Mobashery S., Fridman R.* // Cancer Res., 2005, 65(9), p. 3523.
[8] *Overall CM, Kleifeld O.* // 2006, Nat. Rev. Cancer, 6(3), p. 227.
[9] *Isaksen B., Fagerhol M.K.* // J.Clin pathol: Mol pathol., 2001, v. 54, p. 289.
[10] *Hsieh M.J., Chen J.C., Yang W.E., Chien S.Y., Chen M.K., Lo Y.S., His Y.T., Chuang Y.C., Lin C.C., Yang S.F.* // Biochem Pharmacol., 2017, 2952(17), p. 30041.
[11] *Bannikov G.A., Lakritz J., Premanandan C., Mattoon J.S., Abrahamsen E.J.* // Am J Vet Res. 2009; 70(5):633-9.
[12] *Trott O., Olson A.J.* // J. Comput. Chem., 2010, v. 31, p. 455.
[13] *Morris, G.M., Goodsell, D.S., Halliday, R.S., Huey, R., Hart, W.E., Belew, R.K., Olson, A.J.* Automated Docking. // J.Comput.Chem., 1998, v. 19, p. 1639.
[14] *Anderson G., Zimmerman J., Callahan F.* // J. Am. Chem. Soc., 1964, v. 86, issue. 9, p. 1839.
[15] *Gade W., Brown J.* // Biochemica and Biophysica Acta 1981, v. 13, p. 86.

ՀԱՅԱՍՏԱՆԻ ՀԱՆՐԱՊԵՏՈՒԹՅԱՆ ԳԻՏՈՒԹՅՈՒՆՆԵՐԻ
ԱԶԳԱՅԻՆ ԱԿԱԴԵՄԻԱ
НАЦИОНАЛЬНАЯ АКАДЕМИЯ НАУК РЕСПУБЛИКИ АРМЕНИЯ
NATIONAL ACADEMY OF SCIENCES OF THE REPUBLIC OF ARMENIA

Հայաստանի քիմիական հանդես
Химический журнал Армении **71, №4, 2018** Chemical Journal of Armenia

UDC 547.854

SYNTHESES AND BIOLOGICAL PROPERTIES OF BENZO[4',5']IMIDAZO[2',1': 6,1]PYRIDO[2,3-d]PYRIMIDINES: MINI-REVIEW

A. A. HARUTYUNYAN[1,2]

[1]Russian-Armenian (Slavonic) University, Yerevan
[2] The Scientific Technological Centre
of Organic and Pharmaceutical Chemistry of NAS RA
26, Azatutyan Ave., Yerevan, 0014, Armenia
E-mail: harutyunyan.arthur@yahoo.com

The known methods for the synthesis of benzo[4',5']imidazo[2',1': 6,1]pyrido[2,3-d]pyrimidine heterocyclic derivatives based on heterocyclic reactions of substituted benzimidazoles and alternative approaches using substituted pyrimidinyl-5-propanoic acids have been considered. It was shown that the developed synthetic strategy based on the heterocyclization of substituted pyrimidinyl-5-propanoic acids is a successful addition to the previously described methods, since it allows to bypass the significant limitations associated with the use of substituted benzimidazoles and introduce various types of functional substituents in the target heterocyclic system and at different positions of the ring. The available data on the biological properties of synthesized compounds are summarized.

Figs. 2, references 18.

1. Introduction

Polycyclic heteroaromatic compounds based on annelated azaheterocycles, the most important structural feature of which is the planar structure, exhibit high biological activity, including antitumor, antibacterial, antiviral and others [1,2]. The biological activity of this class of compounds is due to their ability to interact with DNA, being associated with small and large grooves or intercalation between adjacent bases in a double helix, the interaction mechanism of the latter being considered as the main one. In both cases, the secondary structure of DNA is distorted and its functioning is disrupted, and therefore the connections with this mechanism of action are considered as the most promising in developing new-generation drugs for the treatment of tumor diseases and viral and bacterial infections [3]. It should be noted that bi-and tricyclic compounds are best known as

intercalating heterocycles, while tetra- and higher-annealed compounds are less well studied, although the possibility of intercalation and the associated pharmacological activity are shown for them [4].

Among the tetracyclic heteroaromatic compounds, we have drawn attention to the syntheses and biological properties of the derivatives of the benzo[4′,5′]imidazo[2',1': 6,1]pyrido[2,3-d]pyrimidine (1) condensed on the basis of three nitrogen-containing heterocycles, and of which there are a limited number of publications in the literature. Therefore, in view of the growing interest in the synthesis and biological properties of polycyclic azaheterocycles and limited information on benzo[4′,5′]imidazo-[2',1': 6,1]pyrido[2,3-d]pyrimidines, this review summarizes all available works in this area, including own research, especially since the latter constitute an essential part of the available data.

2. Synthesis of benzo[4′,5′] imidazo[2',1': 6,1]pyrido[2,3-d]pyrimidine derivatives

Before proceeding to the discussion of works in this area, it is appropriate to dwell briefly on the name of the heterocyclic system 1, which can be compiled in accordance with the nomenclature rules and recommendations of the IUPAC and CAS rules using computer programs based on the above nomenclature rules. Thus, compound 1 can be named pyrimido[5',4': 5,6]pyrido[1,2-a]benzimidazole (ACD / ChemSketch package, version ACD / Labs 6.0) and benzo[4,5]imidazo[2 ',1': 6,1]pyrido[2,3-d]pyrimidin (package ACD / Name, version 1.0), therefore, in the further presentation of the work the names of the derivatives are given in author's versions and are treated as synonyms.

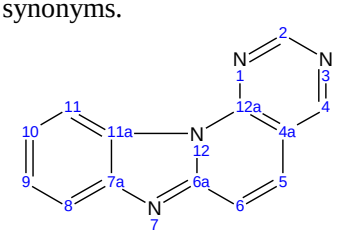

1

In order to systematize the presentation, the known syntheses of the derivatives of the heterocyclic system under discussion are conventionally divided into two groups according to two alternative synthetic strategies that are based on the annealating of functionalized benzimidazoles or on the heterocyclization of substituted pyrimidinyl-5-propanoic acids.

2.1. Synthesis based on substituted benzimidazoles

For the first time, the pyrimido[5',4': 5,6]pyrido[1,2-a]benzimidazole derivatives 2 were obtained in good yields by heating 5-carbaldehydebarbituric acid or 2,4,6-trichloropyrimidinyl-5-carbaldehyde with 2-substituted benzimidazoles in

N-methylpyrrolidone according to Scheme 1 and patented as photographic materials and fluorescent dyes [5-7].

Scheme 1

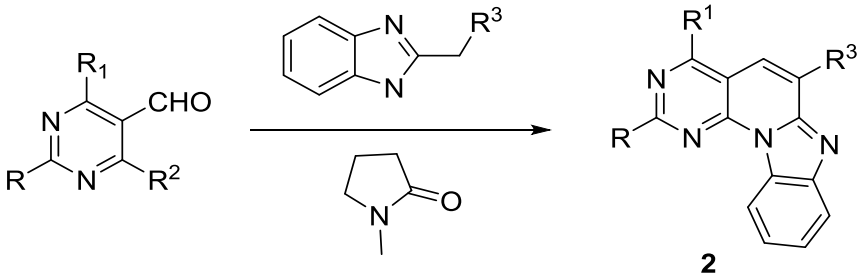

2. R, R^1, R^2 = Hal, OH, $N(Et)_2$, NHPh; R^3 = benzimidazol-2-yl, benzoxazol-2-yl, benzothiazol-2-yl, 4-$NO_2C_6H_4$, CN, COOH.

According to the method proposed by the Polish authors, 1H-benzimidazole-2-acetonitrile (3) is condensed with arylidene malononitriles under the Michael reaction conditions, after which the adduct formed is boiled in MeCN in the presence of piperidine in a six-membered cycle with simultaneous aromatization. The thus formed 1-amino-3-arylpyrido[1,2-a]benzimidazole-2,4-dicarbonitriles 4 are converted by boiling with formamide to the desired 5-aryl-4-methylpyrimido[5',4': 5,6]pyrido[1,2-a]- benzimidazole-6-carbonitrile 5, according to Scheme 2 [8]:

Scheme 2

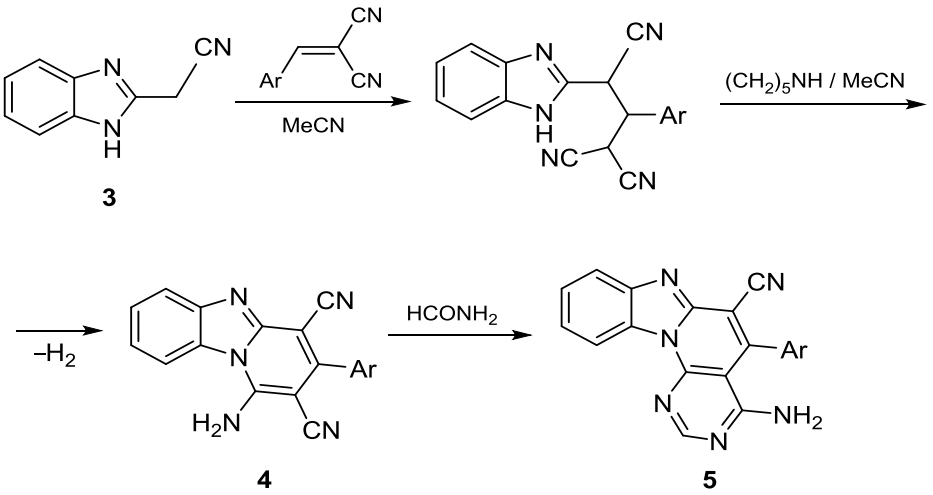

4.5: Ar = Ph, 4-MeC_6H_4, 4-$MeOC_6H_4$, 4-ClC_6H_4, 3-$NO_2C_6H_4$, 4-$NMe_2C_6H_4$.

Dicarbonitriles 4 were the starting compounds also in the synthesis of the 3-amino-4-imino derivatives of the heterocyclic system under discussion according to scheme 3 [9]:

Scheme 3

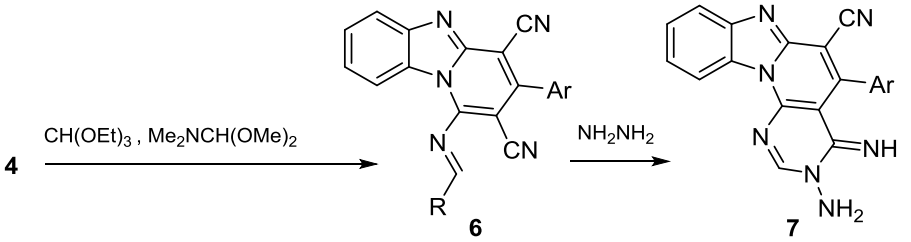

6.7: R = OEt, NMe_2; Ar = Ph, 4-MeC_6H_4, 4-$MeOC_6H_4$, 4-ClC_6H_4.

The interaction of 1-amino-3-arylpyrido[1,2-a]benzimidazole-2,4-dicarbonitriles 4 with triethyl orthoformate or dimethylformamidedimethylacetal gives imines 6 which with hydrazine hydrate form 3-amino-5-aryl-4-iminopyrimido[5',4': 5,6]pyrido[1,2-a]benzimidazole-6-carbonitrile.

In the synthesis of spirocondensed pyrimido[5',4': 5,6]pyrido[1,2-a]benzimidazole derivatives, by reacting 2-methylbenzimidazole with 3-dicyanomethylidene-1-ethyl-2-oxoindoline, cyano-3,4-dihydro-1'-ethylspiro {benzimidazo[1,2-a]pyridine-3,3'-indolin}-2'-one (8) were synthesized, which are cyclized by the action of formamide or formic acid thus forming 4-amino-5,6-dihydro-1'-ethylspiro-{benzimidazo[1',2': 1,6]pyrido[2,3-d]pyrimidine-5,3'-indoline}-2'-one (9a) and 3,5,6-trihydro-1'-ethylspiro{benzimidazo[1',2': 1,6]pyrido [2,3-d]pyrimidine-5,3'-indoline}-2',4-dione (9b). The latter was subsequently converted to 4-chloro- and 4-hydrazino derivatives 10a, b by the subsequent chlorination with $POCl_3$ and hydrazinolysis according to Scheme 4 [10]:

Scheme 4

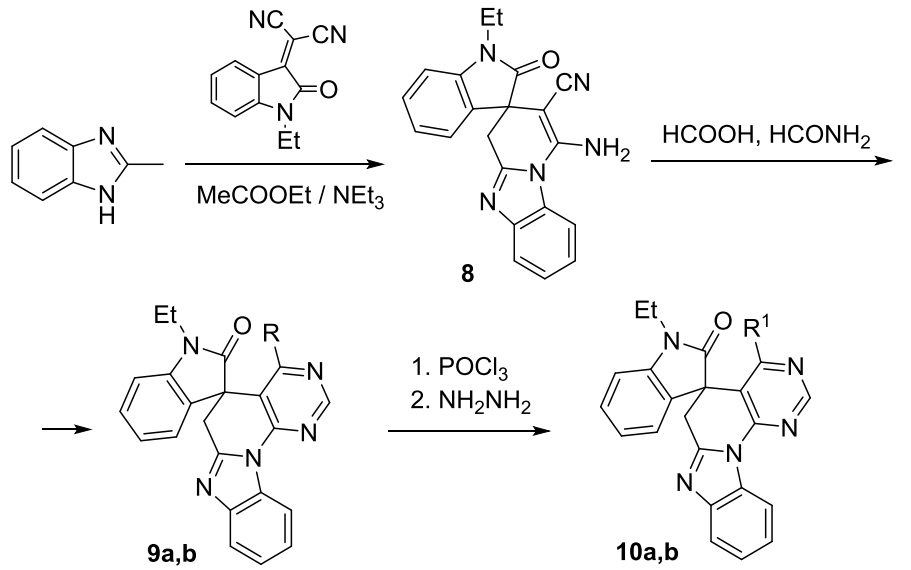

9a, b: R = MH_2 (a), OH (b); 10a, b: R^1 = Cl (a), $NHNH_2$ (b).

2.2. Syntheses based on substituted pyrimidinyl-5-propanoic acids

As follows from the above syntheses, in all the developed approaches as one of the initial synthons, 2-substituted benzimidazole necessarily appears and the substituents in the resulting compounds are limited to benzazoles, nitrile- and amino groups and aryl groups.

Interestingly, the number of synthesized pyrimido[5',4':5,6]pyrido[1,2-a]benzimidazole derivatives according to the indexes of Subject Index CAS and RZhChimia was only 28 compounds and their biological activity data was absent. The limitations of the described approaches are related to the fundamental impossibility to introduce into the molecules, in particular, methylene and methyl groups at different positions of the ring, aryl and sulfanyl groups into the pyrimidine fragment. Meanwhile, the presence of methylene and methyl groups in π-deficient heterocyclic systems can substantially increase the possibilities of obtaining new types of derivatives by condensation of these groups with aromatic aldehydes to produce heteroaromatic compounds with extended π-conjugation chains, as well as a sulfanyl group possessing wide functionality.

In this regard, in recent years, a fundamentally new method for constructing the heterocyclic system under discussion has been developed based on readily available synthons – 2-substituted pyrimidinyl-5-propanoic acids, allowing methylene, methyl and sulfanyl groups to be introduced into the molecule according to Scheme 5:

Scheme 5

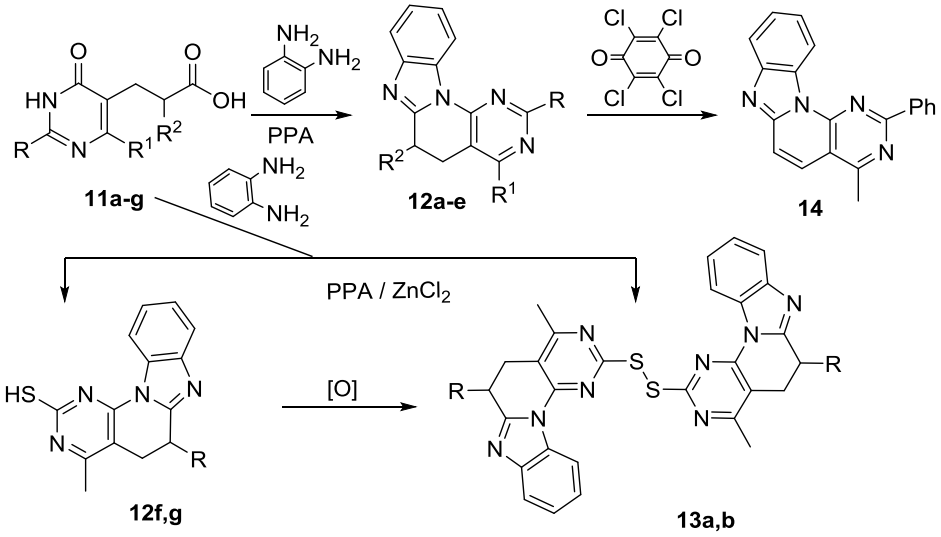

11a-g: R, R^1, R^2 = Ph, Me, H (a), 4-MeC_6H_4, Me, H (b), Ph, Me, Me (c), Ph, OH, H (d), Ph, OH, Me (e), SH, Me, H (f), SH, Me, Me (g); 12a-e: R, R^1, R^2 = Ph, Me, H (a), 4-MeC_6H_4, Me, H (b), Ph, Me, Me (c), Ph, OH, H (d), Ph, OH, Me (e); 12f,g: R = H (f), Me (g).

It was found that the reaction of the corresponding 2-aryl-6-methyl(hydroxy)-3,4-dihydro-4-oxopyrimidine-5-ylpropanoic and 2-methylpropanoic acids 11a-e with 1,2-diaminobenzene in polyphosphoric acid (PPA), of acids 11f, g ‾ in a mixture of PPA-$ZnCl_2$ proceeded by a cascade mechanism and led in a single step to a 4-methyl-, 4,6-dimethyl-4-hydroxy-6-methyl derivative of 2-aryl-5,6-dihydro-benzo[4',5']imidazo[2',1': 6,1]pyrido[2,3-d]pyrimidines 12a-e and the corresponding thiols 12f,g, and two disulfides 13a,b. Disulfides are formed in the form of an impurity with a yield of about 15% directly as a result of condensation, and also in the oxidation of 2-thioxoderivatives 12f,g with air oxygen. Oxidative aromatization of 5,6-dihydropyrrolidene 12a with chloranyl was carried out to form a substituted benzo[4',5']imidazo[2',1': 6,1]pyrido[2,3d]pyrimidine 14 with a 16π electron circuit [11-15].

The presence of the thiol group in the molecule substantially increased the possibilities of chemical transformation of the starting compounds 12f,g into new derivatives, as shown in Scheme 6:

Scheme 6

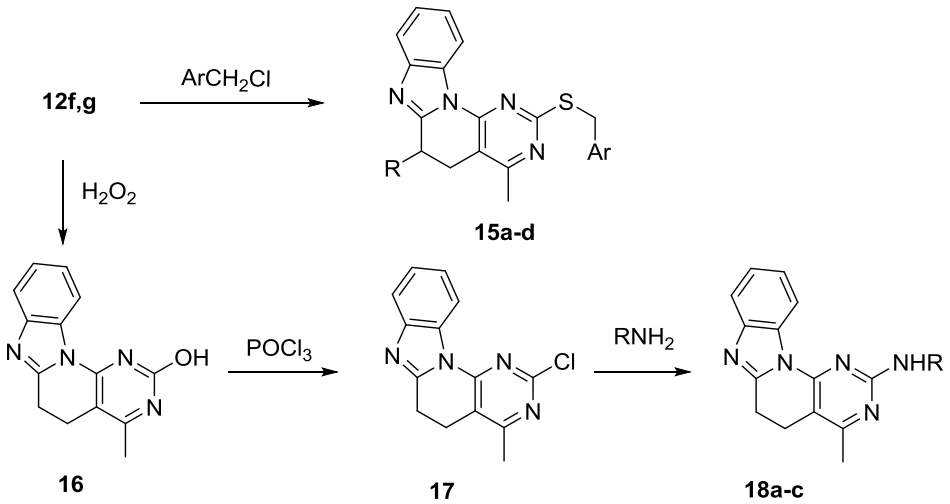

15a-d: R, Ar = H, 3-NO_2-4-$MeOC_6H_3$ (a); H, 2-ClC_6H_4 (b); Me, 2-ClC_6H_4 (c); Me, 4-FC_6H_4 (d); 18a-c: R = H (a), Me (b), Ph (c).

Alkylation of thiols 12f,g with substituted benzyl chlorides produced S-benzyl derivatives 15a-d, by oxidation of H_2O_2 in an alkaline medium ‾ 2-hydroxy derivative 16. Chlorination of the latter yielded 2-chloro derivative 17, aminolysis of which synthesized 2-amino derivatives 18a-c.

The spatial structure of the 2-chloro-4-methyl-5,6 dihydrobenzo[4',5']imidazo [2',1': 6,1]pyrido[2,3-d]pyrimidine (17) and that of its tetramer are shown in Fig. 1 and 2 (the numbering of atoms is arbitrary).

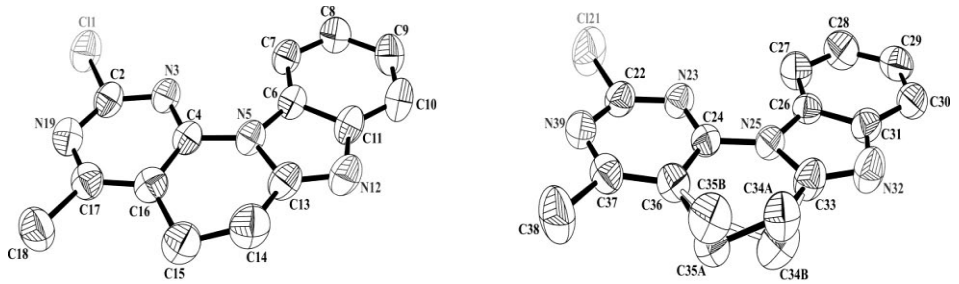

a b

Fig. 1. Structures of symmetrically nonequivalent molecules of compound 17 with ordered structure (a) and with disordered structure (b). Ellipsoids are depicted with 50% probability.

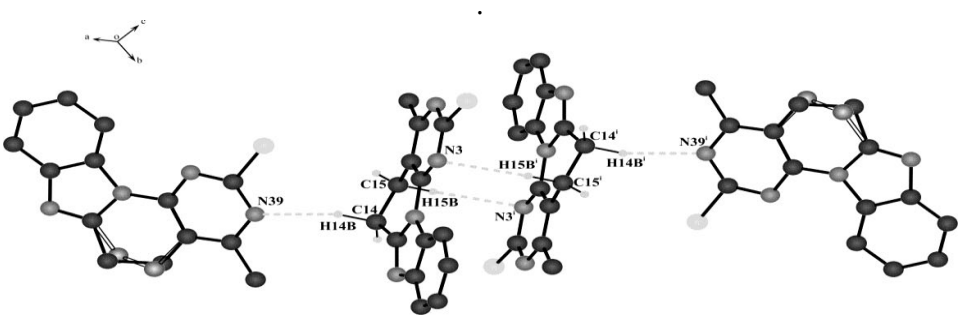

Fig. 2. A tetramer of the molecules of compound 17, formed by non-classical hydrogen bonds.

X-ray diffraction analysis of the tetracycle 17 crystal showed that the phenyl, imidazole and pyrimidine rings had an almost flat conformation, the molecules forming a tetramer (Fig. 2) by binding non-classical hydrogen bonds (C14-H14B ... ..N39 and C15H15B ... ..N3i).

Based on the new method for the synthesis of benzo[4',5']imidazo[2',1': 6,1] pyrido[2,3-d]pyrimidine derivatives, an additional possibility of functionalization of the starting compounds by condensation of 4-methyl-, (RS)-4,6-dimethyl-2-phenyl-5,6-dihydrobenzo[4',5']imidazo[2',1': 6,1]pyrido[2,3-d]pyrimi-dines 12a,c and 4-methyl-5,6-dihydrobenzo[4',5']imidazo[2',1': 6,1]pyrido[2,3-d]pyrimidin-2-ol (16) with aromatic and heterocyclic aldehydes under various experimental conditions was realized, according to the following Scheme 7 [16]:

Scheme 7

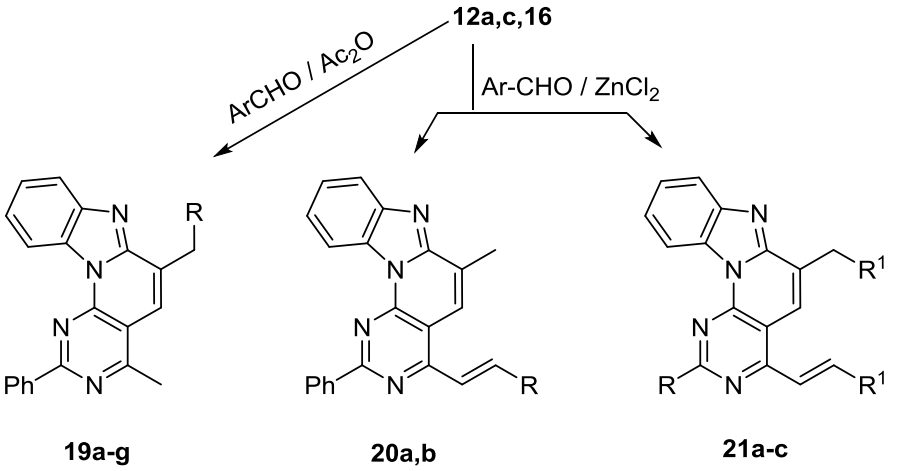

19a-g: R = Ph (a), 2-AcO-naphthalen-1-yl (b), 2,4-$Cl_2C_6H_3$ (c), 4-$MeOC_6H_4$ (d), CH = CHC_6H_4 (e), thiophene-2-yl (f), 4-$C_6H_5CH_2OC_6H_4$ (g); 20a, b: R = 4-NO_2 (a), Cl (b). 21a-c: R, R^1 = Ph, 4-$NO_2C_6H_4$ (a), OH, 4-$NO_2C_6H_4$ (b), OH, 4-ClC_6H_4 (d).

It was shown that the reactive 4-methyl- and 6-methylene groups in the substituted 5,6-dihydro-benzo[4',5']imidazo[2',1':6,1]pyrido[2,3-d]pyrimidines reacted with aromatic aldehydes under various conditions: boiling in acetic anhydride to form 6-aryl (heteryl)methyl-4-methyl derivatives 19a-g, and by co-heating in the presence of $ZnCl_2$ – 4-substituted derivatives 20a,b and bis-derivatives 21a-c.

Thus, the available methods for the synthesis of substituted benzo[4',5'] imidazo[2',1',6,1]pyrido-[2,3-d]pyrimidines provide efficient preparation of a variety of heterocycle derivatives for subsequent biological and technical studies.

3. Biological properties of benzo[4,5] imidazo[2',1':6,1]pyrido[2,3-d]pyrimidines derivatives

In the literature, only the antibacterial and antimonoaminoxidase properties of benzo[4′,5′]imidazo[2',1':6,1]pyrido[2,3-d]pyrimidine derivatives are described, exclusively in the works of domestic authors.

Antibacterial properties of some derivatives of benzo[4′,5′]imidazo[2',1': 6,1]pyrido[2,3-d]pyrimidi-nes have been studied for strains of gram-positive bacteria (*Staphylococcus aureus* 209p and *S. aureus* 1) and gram-negative rods (*Shigella flexneri* 6858, *Escherichia coli* 0-55) by the methods of "diffusion in agar" and "two-fold serial dilutions", the control drug is furazolidone. It has been shown that benzo[4′,5′]imidazo[2',1': 6,1]pyrido[2,3-d]pyrimidines 12b,i, 13a, 15a, 16 show weak antibacterial activity on all four strains, and the compounds 12a, 13b, 15b-d, 19a-f, 20a,b, 21a,c are completely devoid of activity.

At the same time, as a result of the modification of completely inactive heterocycle 12a, the derivatives 12d, 14 were obtained, exhibiting moderate antimicrobial properties, somewhat higher for gram-positive bacteria [17].

The antimonoaminoxidase properties of compounds were studied by their effect on the deamination of serotonin (5-OT) by the brain monoamine oxidase (MAO) *in vitro*, the control ‑ drug indopan. It has been found that tetracycles 19d, 20b, 21a show pronounced anti-MAO activity, inhibiting enzyme activity by 60-63%, while derivatives 12a, c, e, 19b are much weaker [18].

ԲԵՆԶՕ[4',5']ԻՄԻԴԱԶՕ[2',1':6,1]ՊԻՐԻԴՕ[2,3-d]ՊԻՐԻՄԻԴԻՆՆԵՐԻ ՍԻՆԹԵԶՆԵՐԸ ԵՎ ԿԵՆՍԱԲԱՆԱԿԱՆ ՀԱՏԿՈՒԹՅՈՒՆՆԵՐԸ: ՀԱԿԻՐՃ ԱՄՓՈՓԱԳԻՐ

Ա. Ա. ՀԱՐՈՒԹՅՈՒՆՅԱՆ

Դիտարկվել են հետերոցիկլիկ համակարգի՝ բենզո[4',5']իմիդազո[2',1':6,1]պիրիդո-[2,3-d]պիրիմիդինի սինթեզի հայտնի մեթոդներ, հիմնված տեղակալված բենզիմիդազոլի հետերոցիկլման և այլընտրանքային մոտեցումներ տեղակալված պիրիմիդինիլ-5-պրոպա-նաթթվի կիրառման վրա: Ցույց է տրվել, որ մշակված սինթետիկ ռազմավարությունը՝ հիմնված տեղակալված պիրիմիդինիլ-5-պրոպանաթթվի հետերոցիկլման վրա, համար-վում է հաջողված լրացում նախկինում նկարագրված մեթոդներին, քանի որ թույլ է տա-լիս շրջանցել էական սահմանափակումները՝ կապված տեղակալված բենզիմիդազոլի կի-րառման հետ, և ներմուծել ամբողջական հետերոցիկլիկ համակարգ տարբեր տիպի ֆունկցիոնալ տեղակալիչներ՝ տարբեր դիրքերում: Ընդհանրացվել են սինթեզված միա-ցությունների կենսաբանական հատկությունների վերաբերյալ առկա տվյալները:

СИНТЕЗЫ И БИОЛОГИЧЕСКИЕ СВОЙСТВА БЕНЗО[4′,5′]ИМИДАЗО[2′,1′: 6,1]ПИРИДО[2,3-d]ПИРИМИДИНОВ: МИНИ-ОБЗОР

А. А. АРУТЮНЯН[1,2]

[1]Российско-Армянский (Славянский) университет, Ереван
[2]Научно-технологический центр органической и фармацевтической химии
НАН Республики Армения
Армения, Ереван, 0014, пр. Азатутян, 26
E-mail: harutyunyan.arthur@yahoo.com

Рассмотрены известные методы синтеза производных гетероциклической системы бензо[4′,5′]имидазо[2′,1′:6,1]пиридо[2,3-d]пиримидина, основанные на реакциях гетероциклизации замещенных бензимидазолов и альтернативные подхо-ды с использованием замещенных пиримидинил-5-пропановых кислот. Показано, что разработанная синтетическая стратегия, основанная на гетероциклизациях за-мещенных пиримидинил-5-пропановых кислот, является удачным дополнением ранее описанных методов, поскольку позволяет обходить существенные ограниче-ния, связанные с использованием замещенных бензимидазолов и вводить в целе-вую гетероциклическую систему различные типы функциональных заместителей и по различным положениям кольца. Обобщены имеющиеся данные по биологиче-ским свойствам синтезированных соединений.

REFERENCES

[1] *Lyakhova Ye.A., Guseva Yu.A., Lyakhov S.A., Andronati S.A.* // J. Org. Pharm. Chem., 2010, v. 8, №2(30), p. 3.

[2] *Aicher B., Günther E., Holzer W., Leepasert T., Müller G., Nagel T., Shahabi M., Spreitzer H.* // 3rd Meeting of the Paul Ehrlich MedChem Euro-PhD Network. Abstracts, Santa Margherita di Pula, Cagliari, Sardinia, Italy, 2013, O-12.

[3] *Palchaudhuri R., Hergenrother P.* // J. Current Opinion in Biotechnology, 2007, v. 18, p. 497.

[4] *Leepasert T., Shahabi M., Shanab K., Schrimer E., Holzer W., Spreitzer H., Aicher B., Muller G., Gunter E.* // Bioorg. Med. Chem. Lett., 2013, v. 23, p. 5264.

[5] Pyrimido[5',4':5,6]pyrido[1,2-a]benzimidazoles. Ger. Offen. 2.929. 414. // Chem. Abstr., 1981, v. 95, P44732. РЖХимия, 1981, 22Н232.

[6] Electrophotographic recording material. Ger. Offen. DE 3.502.689. // Chem. Abstr., 1987, v. 106, 41561 j.

[7] Electrophotographic recording material. Ger. Offen. DE 3.502.681. // Chem. Abstr., 1988, v. 108, 122003x.

[8] *Bogdanowicz-Szwed K., Czarny A.* // J. prakt. Chem., 1993, v. 335, p. 279.

[9] *Elwan N.M.* // J. Heterocyclic Chem., 2004, v. 41, p. 281.

[10] *El-Zohry M.F., Mohamed T.A., Hussein E.M.* // Monatsh. Chem., 2009, v. 140, p. 265.

[11] *Harutyunyan A.A.* // Chemical Journal of Armenia, 2012, v. 65, №2, p. 257.

[12] *Harutyunyan A.A.* // Russian Journal of Organic Chemistry, 2014, v. 50, №1, p. 94.

[13] *Harutyunyan A.A.* // Russian Journal of Organic Chemistry, 2016, v. 52, №2, p. 235.

[14] *Harutyunyan A.A., Panosyan H.A., Tamazyan R.A., Ayvazyan A.G.* // Chemical Journal of Armenia, 2016, v. 69, №3, p. 266.

[15] *Harutyunyan A.A.* Studies in the field of the pyrimidines and polycyclic azaheterocycles synthesis. The dissertation abstract of the doctor of chemical sciences. Republic of Armenia, Yerevan, 2017.

[16] *Harutyunyan A.A., Ghukasyan G.T., Danagulyan G.G.* // International Conference «100 Years of Development of Chemistry: From Synthesis of Polyethylene to Stereodivergence» Dedicated to the 100th anniversary of the Department of Organic Chemistry of Perm State University. Perm, May 16-18, 2018, p. 69.

[17] *Harutyunyan A.A., Avakimyan J.A., Stepanyan H.M.* // Biological Journal of Armenia, 2016, v. 68, №2, p. 88.

[18] *Harutyunyan A.A., Sukasyan R.S., Grigoryan A.S.* // Biological Journal of Armenia, 2016, v. 68, №1, p. 60.

ՀԱՅԱՍՏԱՆԻ ՀԱՆՐԱՊԵՏՈՒԹՅԱՆ ԳԻՏՈՒԹՅՈՒՆՆԵՐԻ
ԱԶԳԱՅԻՆ ԱԿԱԴԵՄԻԱ
НАЦИОНАЛЬНАЯ АКАДЕМИЯ НАУК РЕСПУБЛИКИ АРМЕНИЯ
NATIONAL ACADEMY OF SCIENCES OF THE REPUBLIC OF ARMENIA

Հայաստանի քիմիական հանդես
Химический журнал Армении **71, №4, 2018** Chemical Journal of Armenia

UDC 548.737+541.124+547.314

THE PECULIARITIES OF THE INTERACTION OF A SERIES OF β,γ-UNSATURATED PHOSPHONIUM SALTS AND DEHYDROBROMINATION OF THE OBTAINED DIBROMO DERIVATIVES

M. Zh. OVAKIMYAN, G. Ts. GASPARYAN, A. S. BICHAKHCHYAN, A. S. POGHOSYAN and L. V. DERDZYAN

The Scientific Technological Centre
of Organic and Pharmaceutical Chemistry of NAS RA
26, Azatutyan Ave., Yerevan, 0014, Armenia
E-mail: arpenikb@mail.ru

By bromination of but-, 3-phenylprop-, hex- and cyclohex-2-enyltriphenylphosphonium bromides with molecular bromine in chloroform the corresponding 2,3-dibromo derivatives have been obtained. It is established that 2,3-dibromo-butyl- and 3-phenylpropyl-triphenylphosphonium bromides under the action of sodium carbonate are dehydrobrominated with participation of the hydrogen atom in α-position of the side chain forming the corresponding α,β-unsaturated phosphonium salts. As a result of the interaction of 2,3-dibromobutyltriphenylphosphonium bromide with triethylamine, 3-bromobut-2-enyltriphenylphosphonium bromide was unexpectedly obtained The formation of the latter apparently takes place due to the “reverse prototropic isomerization” of the initially formed 3-bromobut-1-enyltriphenylphosphonium bromide.

References 8.

Recently, we have found that prop-2-enyltributyl- and triphenylphosphonium bromides are easily brominated by the β,γ-double bond with molecular bromine in the cold (-3÷-5^{o}C) in a chloroform solution with formation of the corresponding adducts with almost quantitative yields. It should also be noted that, according to X-ray structural analysis, the triphenylphosphonium analogue is a mixture of R- and S-conformers with a synclinic arrangement of bromine atoms [1].

In continuation of these studies we have synthesized but-2-enyl- (**1)** [2], 3-phenylprop-2-enyl- (**2)** [3] and hex-2-enyltriphenylphosphonium (**3**) bromides, as well as a cyclic analog of allylphosphonium salt – cyclohex-2-enyltriphenylphosphonium bromide (4) [4] in high yields by interaction of triphenylphosphine with the appropriate allyl halogenides. It should be noted that

phosphonium salt **1**, according to the ^{1}H and ^{13}C NMR spectral data, is the mixture of two geometric isomers in the 67:33 ratio.

Our investigations have shown that all of the above β,γ-unsaturated phosphonium salts **1-4** are easily brominated with the molecular bromine in the cold to form the corresponding 2,3-dibromo derivatives of phosphonium salts **5-8**, respectively, in high yields.

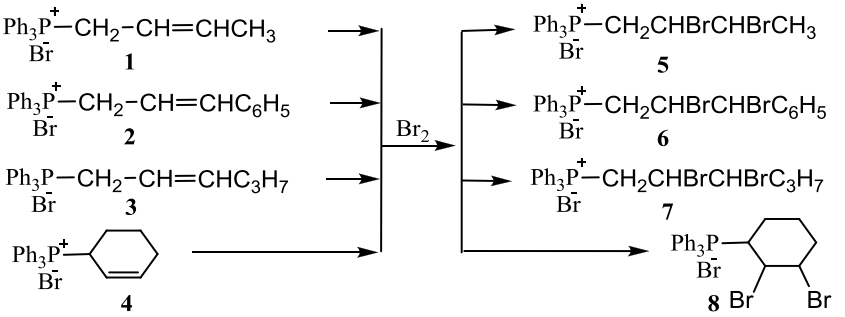

It should be noted that phosphonium salts **1** and **2** are also easily brominated under the action of hν-irradiation in chloroform. In both cases, there is the formation of a mixture of diastereomers with signals in ^{31}P NMR spectra at 23.70, 24.25 (**5**) and 23.69, 23.73 (**6**) ppm, respectively. From the obtained diastereomers mixture of phosphonium salt **6** by adding acetonitrile, we have succeeded in isolating one diastereomer in a pure form with a signal in ^{31}P spectrum at 23.69 ppm.

In our previous report [1], it was found that triphenyl-2,3-dibromopropylphosphonium bromide under the action of sodium carbonate in chloroform undergoes dehydrobromination to form 3-bromoprop-1-enyltriphenylphosphonium bromide in ~75% yield. The data obtained indicate that dehydrobromination proceeds with the participation of the most mobile α-hydrogen atom of the side radical.

In this paper, it is shown that in a similar way, phosphonium salt **5** under the action of the fourfold amount of sodium carbonate in chloroform at room temperature is dehydrobrominated to form 3-bromobut-1-enyltriphenylphosphonium bromide (**9**) in 71% yield.

When carrying out the same reaction using triethylamine as a dehydrobrominating agent, 3-bromobut-2-enyltriphenylphosphonium bromide (**10**) was unexpectedly isolated in 80% yield and identified.

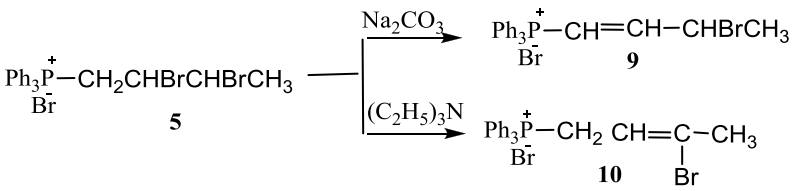

In continuation of the studies, phosphonium salt **5** was involved in reactions with ethylene glycol and ethylenediamine in the presence of a fourfold excess of soda in order to realize the cyclization reaction in the side radical by means of double nucleophilic substitution of vicinal bromine atoms. However, as a result of the conducted reactions, only dehydrobromination products **9** and **10** were obtained.

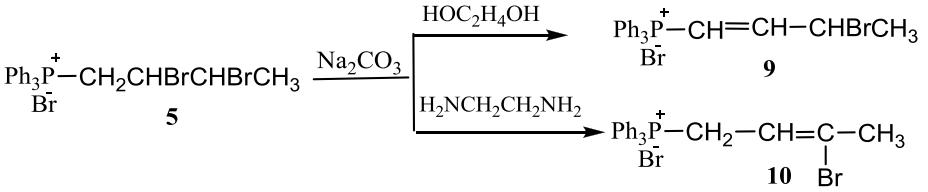

Comparing the obtained results on the behavior of phosphonium salt **5** in relation to the used dehydrobrominating agents, it can be assumed that in all cases at the first stage dehydrobromination of salt **5** with participation of the most mobile α-hydrogen atom takes place. Then the formed α,β-unsaturated phosphonium salt under the action of nitrogenous bases - triethylamine and ethylenediamine is subjected to the reverse prototropic isomerization according to the following Scheme:

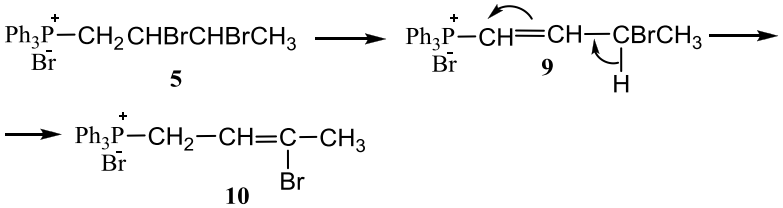

By a specially set experiment it was actually established that 3-bromobut-1-enyltriphenyl-phosphonium bromide (**9**) under the action of triethylamine underwent the reverse prototropic isomerization to form phosphonium salt **10**.

In the literature, there are examples of prototropic isomerization of β,γ-unsaturated phosphonium salts to the α,β-unsaturated analogs [5-7], however, examples of the reverse isomerization are not known to us.

Proceeding from the above-mentioned, it should be assumed that the action of different bases, in our case, soda or triethylamine on phosphonium salt **6** would make it possible to obtain phenyl analogues of salts **9** or **10**, respectively.

However, if, in the case of using soda as a dehydrobrominating agent, an analogue of salt **9** -3-bromo-3-phenylprop-1-enyltriphenylphosphonium bromide (**11**) was actually obtained, then in the case of triethylamine the reaction product was exclusively triphenylphosphine oxide, formed, most likely, according to the Scheme below:

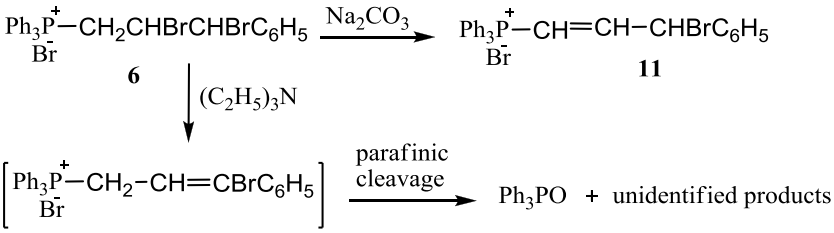

In continuation of the research, we found that phosphonium salt **8** under the action of the excess of triethylamine in chloroform at room temperature was dehydrobrominated to form 3-bromocyclohex-1-enyltriphenylphosphonium bromide, which, according to ^{31}P NMR, was a mixture of two geometric isomers in the 95:5 ratio.

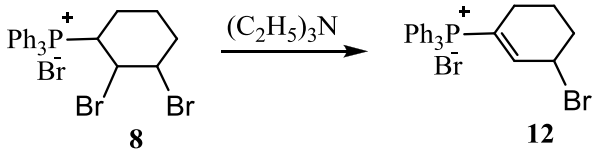

8 **12**

Experimental Section

^{1}H, ^{13}C and ^{31}P spectra were recorded on a Varian Mercury in DMSO-d_6:CCl_4 (1:3) at 300 *MHz* and 121 *MHz*, using TMS and 85% H_3PO_4 as an internal standard, respectively.

2,3-Dibromobutyltriphenylphosphonium bromide (5).

1. Bromination of but-2-enyltriphenylphosphonium bromide (**1**). To a solution of 2 *g* (5 *mmol*) of phosphonium salt (**1**) in 20 *ml* of chloroform 0.8 *g* (5 *mmol*) of bromine was added at -3÷-5°C. Then the solvent was evaporated and the residue was washed with benzene, abs. ether and dried in vacuo, affording 2.8 *g* (100%) of phosphonium salt **5** with mp 195-196°C. Found, %: Br^- 14.65. $C_{22}H_{23}Br_3P$. Calcd.,%: Br^- 14.37. ^{1}H NMR, δ, ppm, *Hz*: 1.73 (d, CH_3, J =7.0, 47%); 1.85 (d, CH_3, J =7.0, 53%); 4.2-4.96 (m, 4H, CH_2CHBr-CHBr); 7.7-8.05 (m, 15H, Ph_3P^+). ^{31}P NMR, δ, ppm: 23.70 (47%) (s) and 24.25 (53%) (s).

2. Bromination of but-2-enyltriphenylphosphonium bromide (**1**) **under hν-irradiation**. To a vigorously stirred solution of 1 *g* (2.5 *mmol*) of phosphonium salt **1** in 15 *ml* of chloroform 0.4 *g* (2.5 *mmol*) of bromine was added during hν-irradiation. The reaction mixture was refluxed for 5 *h*, then the solvent was evaporated and the residue was washed with benzene, abs. ether and dried in vacuo, affording 1.4 *g* (100%) of phosphonium salt **5**.

2,3-Dibromo-3-phenylpropyltriphenylphosphonium bromide (6).

1. The experiment was carried out similarly to the described above. 3 *g* (6.5 *mmol*) of 3-phenylprop-2-enyltriphenylphosphonium bromide (**2**) and 1 *g* (6.5 *mmol*) of bromine yielded 3.2 *g* (80%) of phosphonium salt **6** with mp 108-109°C. Found, %: Br^- 13.04. $C_{27}H_{24}Br_3P$. Calcd., %: Br^- 12.92. ^{1}H NMR, δ, ppm, *Hz*: 4.2-5.39 (m, 3H, CH_2CHBr); 5.95 (d, 1H, CHBrPh, J =7.5, 38%), 6.35 (d, 1H,

CHBrPh, J =2.2, 62%); 7.19-7.39 (m, 5H, Ph, 62%); 7. 5-7.63 (m, 5H, Ph, 38%); 7.69-8.02 (m, 15H, Ph_3P^+). ^{31}P NMR, δ, ppm: 23.69 (38%) (s) and 23.73 (62%) (s).

2. The experiment was carried out similarly to the described above. 0.8 *g* (1.7 *mmol*) of 3-phenyl-prop-2-enyltriphenylphosphonium bromide (**2**) and 0.28 *g* (1.7 *mmol*) of bromine under hν-irradiation afforded 0.96 *g* (91.4%) of phosphonium salt **6.**

2,3-Dibromohexyl triphenylphosphonium bromide (7). The experiment was carried out similarly to the described above. 0.14 *g* (0.33 *mmol*) of hex-2-enyltriphenylphosphonium bromide (**3**) and 0.053 *g* (0.33 *mmol*) of bromine yielded 0.2 *g* (100%) of phosphonium salt **7** with mp 108-109°C. Found, %: Br^- 13.35. $C_{24}H_{26}Br_3P$. Calcd., %: Br^- 13.68. ^1H NMR, δ, ppm, *Hz*: 0.93 (t, 3H, J =6.9); 1.28-1.99 (m, 4H, CH_2CH_2); 4.28-4.8 (m 4H, CH_2CHBr-CHBr); 7.67-8.03 (m, 15H, Ph_3P^+). ^{31}P NMR, δ, ppm: 23.80 (s).

2,3-Dibromocyclohexyltriphenylphosphonium bromide (8). The experiment was carried out similarly to the described above. 3 *g* (7.1 *mmol*) of cyclohex-2-enyltriphenylphosphonium bromide (**4**) and 1.1 *g* (7.1 *mmol*) of bromine yielded 3.3 *g* (80.5%) of phosphonium salt **8** with mp 154-155°C. Found, %: Br^- 13.35. $C_{24}H_{26}Br_3P$. Calcd., %: Br^- 13.68. ^1H NMR, δ, ppm, *Hz*: 1.88-2.48 (m, 6H, cyclohexyl); 4.45-4.56 (m, 1H, CHBr-cyclohexyl.); 4.84-4.94 (m, 2H, Ph_3P^+-CH-CHBr-cyclohexyl); 7.74-7.99 (m, 15H, Ph_3P^+). ^{13}C NMR, δ, p.p.m, *Hz*: 20.17 (d, J_{pc} =13.2); 22.79 (d, J_{pc} =2.5); 34.85 (d, J_{pc} =54.2); 49.43 (d, J_{pc} =3.1); 52.64 (d, J_{pc} =10.5); 115.78 (d, J_{pc} =84.7); 130.19 (d, J_{pc} =12.5); 134.05 (d, J_{pc} =9.7); 135.01 (d, J_{pc} =3.0). ^{31}P NMR, δ, ppm: 26.17 (s).

3-Bromobut-1- enyltriphenylphosphonium bromide (9). To a solution of 0.5 *g* (1 *mmol*) of phosphonium salt **5** in 10 *ml* of chloroform 0.38 *g* (3.6 *mmol*) of sodium carbonate was added at room temperature, and the reaction mixture was stirred for 12 *h*. The solvent was filtered and evaporated, then the residue was washed with benzene, abs. ether and dried in vacuo to afford 0.43 *g* (92.3%) of phosphonium salt **9** with mp 117-119°C. Found, %: Br^-17.05. $C_{22}H_{21}Br_2P$. Calcd., %: Br^- 16.81. ^1H NMR, δ, ppm, *Hz*: 1.91 (d, 3H, J =7.0); 5.28-5.4 (m, 1H, -CHBr); 6.7 (ddd, 1H, CH=C<u>H</u>, J_1=20.2, J_2=16.4, J_3=8.4); 7.71-7.79 (16H, C<u>H</u>=CH, Ph_3P^+). ^{13}C NMR, δ, ppm, *Hz*: 23.41 (s); 45.66 (d, J_{pc} =21.7); 109.53 (d, J_{pc} =83.4); 117.45 (d, J_{pc} =90.4); 129.98 (d, J_{pc} =13.0); 133.64 (d, J_{pc} =10.8); 134.83 (d, J_{pc} =3.0); 159.27 (d, J_{pc} =3.6). ^{31}P NMR, δ, ppm: 19.34 (s).

3-Bromobut-2-enyltriphenylphosphonium bromide (10). To a solution of 0.5 *g* (0.89 *mmol*) of phosphonium salt **5** in 10 *ml* of acetonitrile 0.18 *g* (1.78 *mmol*) of triethylamine was added at room temperature, and the reaction mixture was stirred for 18 *h*. The reaction mixture was then washed with water and dried over anhydrous magnesium sulfate. The solvent was evaporated, and the residue was washed with benzene, abs. ether and dried in a vacuum, affording 0.4 *g* (95.2%) of phosphonium salt **10** with mp 163-165°C. Found, %: Br^-17.13. $C_{22}H_{21}Br_2P$. Calc., %: 16.81. ^1H NMR, δ, ppm, *Hz*: 2.31 (dq, 3H, CH_3, J_1=6.4, J_2=1.2); 4.65 (dd, 2H, C<u>H</u>$_2$CH=, J_1=15.9, J_2=7.5); 5.89-5.98 (m, 1H, CH_2C<u>H</u>=); 7.62-7.97 (m, 15 H, Ph_3P^+). ^{31}P NMR, δ, ppm: 22.07 (s).

Interaction of phosphopnium salt 5 with ethylene glycol. To a solution of 0.1 *g* (1.4 *mmol*) of ethylene glycol in 10 *ml* of chloroform 0.6 *g* (5.6 *mmol*) of sodium carbonate was added at room temperature and stirred for 30 *min*. Then to the resulting solution 0.8 *g* (1.4 *mmol*) of phosphonium salt **5** was added dropwise, and the reaction mixture was stirred for 12 *h* at the same temperature. The solution was filtered, evaporated and the residue washed with benzene, abs. ether and dried in a vacuum to yield 0.55 *g* (82.1%) of phosphonium salt **9**.

Interaction of phosphopnium salt 5 with ethylenediamine. To a solution of 1 *g* (1.8 *mmol*) of phosphonium salt **5** in 20 *ml* of chloroform 0.11 *g* (1.8 *mmol*) of ethylenediamine was added at room temperature and the reaction mixture was stirred for 3 *h*. Then to the reaction mixture 0.76 *g* (7.2 *mmol*) of sodium carbonate was added and stirred for 3 *h* at the same temperature. The solvent was filtered and evaporated and the residue washed with benzene, abs. ether and dried in vacuo to afford 0.66 *g* (76.7%) of phosphonium salt **10**.

Interaction of phosphopnium salt 9 with triethylamine. To a solution of 1 *g* (1.8 *mmol*) of phosphonium salt **9** in 15 *ml* of acetonitrile, 0.36 *g* (3.6 *mmol*) of triehtylamine was added at room temperature, and the reaction mixture was stirred for 6 *h*. The solvent was evaporated and the residue washed with abs. ether and dried in vacuo to afford 0.95 *g* (95%) of phosphonium salt **10**.

3-Bromo-3-phenylprop-1-enyltriphenylphosphonium bromide (11). To a solution of 2 *g* (3.2 *mmol*) of phosphonium salt **6** in 25 *ml* of chloroform, 1.02 *g* (9.7 *mmol*) of sodium carbonate was added at room temperature and the reaction mixture was stirred for 18 *h*. The solution was filtered, evaporated and the residue washed with benzene, abs. ether and dried in vacuo. By fractional recrystallization of the residue, 0.88*g* (52%) of phosphonium salt **11** was obtained. Found, %: Br^-14.49 $C_{27}H_{23}Br_2P$. Br^- 14.87. ^{1}H NMR, δ, ppm, *Hz*: 6.55 (d, 1H, J=8.6, CHBr); 7.02 (ddd, 1H, J_1=20.3, J_2=16.3, J_3=8.5, CH=C<u>H</u>,); 7.44-7.62 (m, 6H, CH=C<u>H</u>C$_6$<u>H</u>$_5$); 7.7-8.0 (m, 15H, Ph_3P^+). ^{31}P NMR, δ, ppm: 19.0 (s).

Interaction of phosphopnium salt 6 with triethylamine. To a solution of 1 *g* (1.6 *mmol*) of phosphonium salt **6** in 15 *ml* of chloroform 0.4 *g* (4 *mmol*) of triehtylamine was added at room temperature and the reaction mixture was stirred for 3.5 *h*. The latter was then washed with water and dried over anhydrous magnesium sulfate. The solvent was evaporated and the residue washed with abs. ether and dried in vacuo to afford 0.38 *g* (86.4%) of triphenylphosphinoxide with mp 155-156^{o}C.

3-Bromocyclohex-1-enyltriphenylphosphonium bromide (12). The experiment was carried out similarly to the described above. 0.5 *g* (0.86 *mmol*) of 2,3-dibromocyclohexylptriphenylphosphonium bromide (**8**) and 0.13 *g* (1.3 *mmol*) of triethylamine in 15 *ml* of chloroform yielded 0.4 *g* (93%) of phosphonium salt **12** with mp 146-148^{o}C. Found, %: Br^-14.02. $C_{24}H_{24}Br_2P$. Calcd.,%: 13.72. ^{1}H NMR, δ, ppm, *Hz*: 1.91-2.53 (m, 6H, CH_2-cyclohexyl); 5.08-5.14 (m, 1H, -CHBr-cyclohexyl); 6.59-6.72 (m, 1H, =CH-cyclohexyl); 7.7-7.99 (m, 15H, Ph_3P^+). ^{31}P NMR, δ, ppm: 23.85 (95%) (s) and 23.19 (5%) (s).

ՄԻ ՇԱՐՔ β,γ-ՉՀԱԳԵՑԱԾ ՖՈՍՖՈՆԻՈՒՄԱՅԻՆ ԱՂԵՐԻ ՄՈԼԵԿՈՒԼՅԱՐ ԲՐՈՄՈՎ ԲՐՈՄԱՑՄԱՆ ԵՎ ՍՏԱՑՎԱԾ ԴԻԲՐՈՄԱԾԱՆՑՅԱԼՆԵՐԻ ԴԵՀԻԴՐՈԲՐՈՄԱՑՄԱՆ ՌԵԱԿՑԻԱՆԵՐԻ ԱՌԱՆՁՆԱՀԱՏԿՈՒԹՅՈՒՆՆԵՐԸ

Մ. Ժ. ՀՈՎԱԿԻՄՅԱՆ, Գ. Ց. ԳԱՍՊԱՐՅԱՆ, Ա. Ս. ԲԻՉԱԽՉՅԱՆ և Լ. Վ. ԴԵՐՁՅԱՆ

Բուտ-, 3-ֆենիլպրոպ-, հեքս- և ցիկլոհեքս-2-ենիլֆոսֆոնիումային բրոմիդների բրոմացմամբ մոլեկուլյար բրոմով, քլորոֆորմի մեջ ստացվել են համապատասխան 2,3-դիբրոմածանցյալներ: Ցույց է տրվել, որ 2,3-դիբրոմբուտիլ- և -3-ֆենիլպրոպիլ-տրիֆենիլֆոսֆոնիումային բրոմիդները α-ջրածնի ատոմի հաշվին նատրիումի կարբոնատի ազդեցությամբ դեհիդրոբրոմանում են, առաջացնելով համապատասխան α,β-չհագեցած ֆոսֆոնիումային աղեր: 2,3-դիբրոմբուտիլտրիֆենիլֆոսֆոնիումային բրոմիդի և տրիէթիլամինի փոխազդեցության արդյունքում անսպասելիորեն ստացվել է 3-բրոմբուտ-2-ենիլտրիֆենիլֆոսֆոնիումային բրոմիդ: Վերջինիս առաջացումը, ամենայն հավանականությամբ, տեղի է ունենում սկզբնական փուլում ստացված 3-բրոմբուտ-1-ենիլտրիֆենիլֆոսֆոնիումային բրոմիդի, հետադարձ պրոտոտրոպ իզոմերիզացիայի արդյունքում:

ОСОБЕННОСТИ РЕАГИРОВАНИЯ РЯДА β,γ-НЕПРЕДЕЛЬНЫХ ФОСФОНИЕВЫХ СОЛЕЙ С МОЛЕКУЛЯРНЫМ БРОМОМ И ДЕГИДРОБРОМИРОВАНИЕ ПОЛУЧЕННЫХ ДИБРОМПРОИЗВОДНЫХ

М. Ж. ОВАКИМЯН, Г. Ц. ГАСПАРЯН, А. С. БИЧАХЧЯН, А. С.ПОГОСЯН и Л. В. ДЕРДЗЯН

Бромированием бут-, 3-фенилпроп-, гекс- и циклогекс-2-енилтрифенилфосфоний бромидов молекулярным бромом в хлороформе получены соответствующие 2,3-дибромпроизводные. Установлено, что 2,3-дибромбутил- и -3-фенилпропилтрифенилфосфоний бромиды под действием карбоната натрия дегидробромируются с участием α-водородного атома боковой цепи, образуя соответствующие α,β-ненасыщенные фосфониевые соли. В результате же взаимодействия 2,3-дибромбутилтрифенилфосфоний бромида с триэтиламином неожиданным образом получен 3-бромбут-2-енилтрифенилфосфоний бромид. Образование последнего, по-видимому, имеет место в результате “обратной прототропной изомеризации” первоначально образовавшегося 3-бромбут-1-енилтрифенилфосфоний бромида.

REFERENCES

[1] *Ovakimyan M.Zh., Gasparyan G.Ts., Bichakhchyan A.S., Bagratyan R.R., Derdzyan L.V, Tamazyan R.A., Aivazyan A.G.* // Rus.J.Gen.Chem.,2017, v. 87, №8, p. 1727.

[2] *Schweizer E.E, Light K.K.* // J.Org.Chem., 1966, v.31, №9, p. 2912.

[3] *Fridrich K., Henning H.* // Chem.Ber., 1959, v. 92, №11, p. 2756.

[4] *Ovakimyan M.Zh., Gasparyan G.Ts., Bichakhchyan A.S., Derdzyan L.V.* // Chem. J. of Armenia, 2014, v 71, №3, p. 428.

[5] *Keough P.T., Grayson M.* // J. Org. Chem., 1964, v. 29, №3, p. 631.

[6] *Saaman S.* // Tetrahedron Lett., 1974, №45, p. 3927.

[7] *Nesmeyanov N.A., Mikulshina V.V., Kharitonov V.G., Petrovsky P.V., Reutov O.A.* // Izv. AN SSSR, Ser.Khim., 1989, №5, p. 1182.

[8] *Baghdasaryan G.B, Pogosyan P.S, Panosyan G.A, Inzhikyan M.G.* // Rus.J.Gen.Chem., 2008, v. 78, №6, p. 950.

ՀԱՅԱՍՏԱՆԻ ՀԱՆՐԱՊԵՏՈՒԹՅԱՆ ԳԻՏՈՒԹՅՈՒՆՆԵՐԻ
ԱԶԳԱՅԻՆ ԱԿԱԴԵՄԻԱ
НАЦИОНАЛЬНАЯ АКАДЕМИЯ НАУК РЕСПУБЛИКИ АРМЕНИЯ
NATIONAL ACADEMY OF SCIENCES OF THE REPUBLIC OF ARMENIA

Հայաստանի քիմիական հանդես
Химический журнал Армении **71, №4, 2018** Chemical Journal of Armenia

SYNTHESIS AND ANTITUMOR PROPERTIES OF 3-(2,2-DIMETHYLTETRAHYDRO-2H-PYRAN-4-YL)SPIRO[BENZO[h]QUINAZOLINE-5,1'-CYCLOHEPTAN]-4(6H)-ONES

A. I. MARKOSYAN, Kh. S. HAKOPYAN, A. S. AYVAZYAN, S. S. MAMYAN, A. G. AYVAZYAN, R. A. TAMAZYAN, F. H. ARSENYAN and J. A. AVAKIMYAN

The Scientific and Technological Center
of Organic and Pharmaceutical Chemistry of NAS RA
26, Azatutyan Ave., Yerevan, 0014, Armenia
E-mail: ashot@markosyan.am

Regioselective addition of benzylmagnesium chloride to ethyl 2-cyano-2-cycloheptylidene-acetate yielded 2-(1-benzylcycloheptyl)-2-cyanoacetate, cyclization of which was used to synthesize ethyl-4'-amino-1'H-spiro[cycloheptane-1,2'-naphthalene]-3'-carboxylate (aminoester). By reacting the amino ester with 4-isothiocyanato-2,2-dimethyltetrahydro-2H-pyran the corresponding thioreido derivative was obtained, which without isolation from the reaction medium, was subjected to cyclization, leading to the synthesis of 3-(2,2-dimethyltetrahydro-2H-pyran-4-yl)-2-thioxo-2,3-dihydro-1H-spiro[benzo[h]-quinazoline-5,1'-cycloheptan]-4(6H)-one. In the presence of bases, thioxoderivative reacted with halides, leading to the formation of 2-sulfanyl-substituted 3-(2,2-dimethyl-tetrahydro-2H-pyran-4-yl)-3H-spiro[benzo[h]quinazoline-5,1'-cycloheptan]-4(6H)-ones. The antitumor and antibacterial activity of synthesized compounds was studed.

Figs. 2, tables 2, references 18.

Benzo[h]quinazoline compounds have antimicrobial [1-3], antitumor [4,5], antidepressant [6], serotonin antagonist [7], antiphlogistic [8], antiviral [9], antitubercular [10] properties. Our previous work on the synthesis of spirocondensed benzo[h]quinazolines, containing cyclopentane cyclohexane or cycloheptan rings at C5 position, has shown that they possess antimonoaminoxidaze, antitumor, anticonvulsant properties [11-15]. There is a report on the synthesis of benzo[h]quinazolines containing tetrahydropyranic substituents in the 3rd position that act directly on muscarinic M1 receptors and can be used in the treatment of schizophrenia, sleep disorders and Alzheimer's disease [16]. of schizophrenia and sleep disorders

We set ourselves the goal of developing methods for the synthesis of 3-(2,2-dimethyltetrahydro-2H-pyran-4-yl)-2-thioxo-2,3-dihydro-1H-spiro[benzo[h]quinazoline-5,1'-cycloheptan]-4(6H)-one, which will make it possible

to obtain the corresponding 2-sulfanyl-substituted derivatives and to study some of the biological properties of the synthesized compounds. To carry out the planned work, it was necessary to develop a method for the synthesis of the corresponding β-aminoester of the dihydronaphthalene series and a method for the synthesis of the isothiocyanate of the tetrahydropyran series.

Ethyl 2-cyano-2-cycloheptylideneacetate (**1**) was put into reaction with benzylmagnesium chloride and, as a result of regioselective addition, ethyl 2-(1-benzylcycloheptyl)-2-cyanoacetate (**2**) was obtained. The latter was cyclized in the presence of sulfuric acid leading to ethyl 4'-amino-1'H-spiro[cycloheptane-1,2'-naphthalene]-3'-carboxylate (**3**) (aminoester **3**).

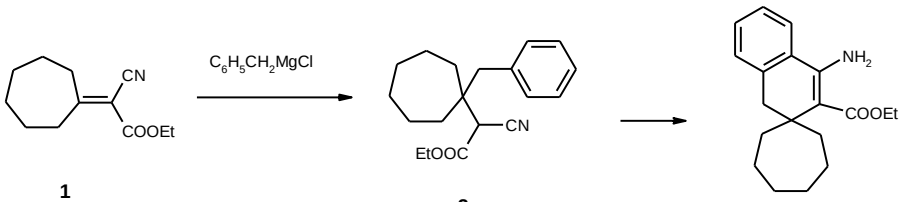

1 **2** **3**

In the IR spectrum of compound **3** there is characteristic absorption of the aromatic ring, C=C double bond and aminogroup in the regions of 1600, 1632 and 3305 cm^{-1}. However, there is no absorption in the spectrum, characteristic of the ester group at 1700-1750 cm^{-1}. An explanation of this phenomenon is given by the X-ray structural analysis, according to which the molecules of compound 3 contain both intramolecular and intermolecular hydrogen bonds. All diffraction measurements were carried out at room temperature on an Enraf-Nonius Cad-4 automated diffractometer (graphite monochromator, Mo-Kα radiation, θ/2θ-scan). The monoclinic unit cell parameters were measured and refined using the diffraction angles of 24 reflections ($14<\theta<16$). The structure was determined by direct method and refined using the software package SHELXTL [17]. All non-hydrogen atoms were refined anisotropically by full-matrix least squares method. The coordinates of all hydrogen atoms were determined from difference Fourier map and refined freely. Crystallographic and experimental data are listed in Table 1. The full crystallographic data in CIF format available free of charge via internet at: http://www.ccdc.cam.ac.uk/products/csd/request/, deposition number: CCDC 1860664.

Table 1

Crystallographic and experimental data

Crystal Data	
Formula	$C_{19}H_{25}NO_2$
Formula Weight	299.40
Crystal System	monoclinic
Space group	$P2_1/n$
a, b, c [Å]	15.060(3), 7.3505(15), 16.331(3)
α, β, γ [deg.]	90, 114.79(3), 90
V [$Å^3$]	1641.2(7)
Z	4
D(calc) [g/cm^3]	1.212
μ(MoKα) [mm^{-1}], T_{min}, T_{max}	0.078
F(000)	648
Crystal Size [mm]	0.42×0.36×0.30
Data Collection	
Temperature (K)	293
Radiation [Å]	MoKα 0.71073
θ_{min}, θ_{max} [Deg]	1.5, 30.0
Dataset	$0 \leq h \leq 21$; $0 \leq k \leq 10$; $-22 \leq l \leq 22$
Tot., Uniq. Data, R(int)	4937, 4772, 0.058
Observed data [I > 2.0 σ(I)]	2819
Refinement	
Nref, Npar	4772, 299
R, wR2, S	0.0656, 0.2271, 1.03

The atomic structure of the molecule is shown in Fig. 1. The conformational analysis of cyclic fragments has shown that the atoms of phenyl ring are in the plane (maximum deviation does not exceed 0.0070 (2) Å), the cyclohexene ring has a half-chair conformation, the C7, C9, C15 and C17 atoms are in the plane while C6 and the C16 atoms are deviated from the plane accordingly -0.4743 (2) Å and -0.9142 (2) Å, the cycloheptanone ring has twist-boat conformation C17, C18, C20 and C21 atoms are in the plane, and C16, C19 and C22 atoms are shifted from the plane on 1.0679(2)Å Å, -0.6535 (2) Å and 1.1495 (2) Å, respectively. There is an intramolecular hydrogen bond between the N8-H8A ..... O5 atoms, the donor-acceptor distance is 2.572 (4) Å (Fig.1). Considering the 3D packing of molecules in the crystal structure, it has been found that there is also an intermolecular hydrogen bond between the N8-H8B ..... $O5^i$ atoms, the donor-acceptor distance is 2.959 (3) Å (Fig. 2). By contacting the molecules, this hydrogen bond generates an infinite chain parallel to the [0 1 0] crystallographic direction (Fig. 2), and the interaction between the chains may be mainly described by the Van der Waals forces.

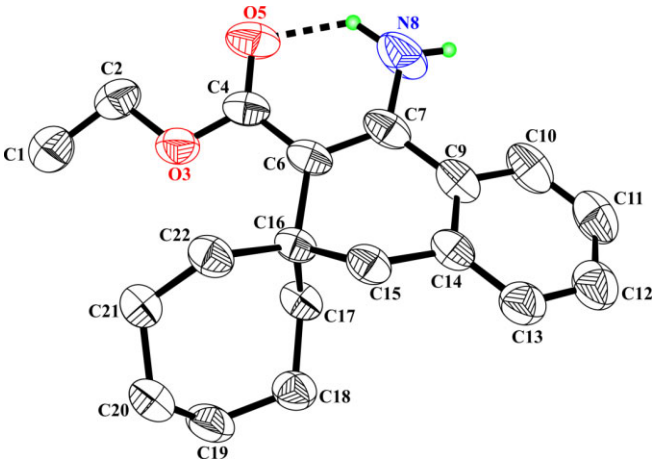

Fig 1. Atomic structure of the molecule $C_{19}H_{25}NO_2$, the ellipsoids of thermal vibrations are drawn on 50% probability level. The intramolecular hydrogen bond is shown by dashed line, for the simplicity of the Figure, the hydrogen atoms not involved in bonding are not drawn.

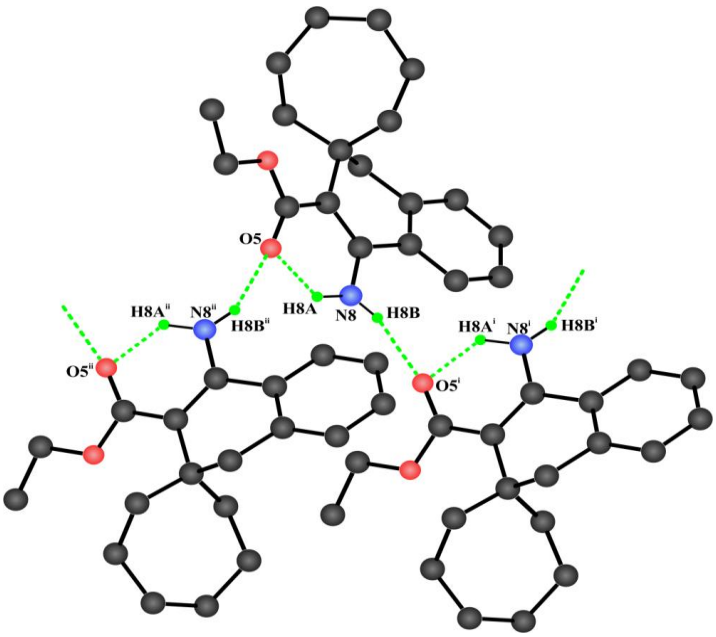

Fig. 2. The infinite chain formed by molecules $C_{19}H_{25}NO_2$ via hydrogen bonds, shown by dashed lines.

Based on 2,2-dimethyltetrahydro-2H-pyran-4-amine (**4**), a method for the synthesis of 4-isothiocyanato-2,2-dimethyltetrahydro-2H-pyran (**5**) has been developed. By reacting the aminoester **3** with isothiocyanate **5** corresponding thioreido derivative **6** was obtained, which, without isolation from the reaction medium, was subjected to cyclization, leading to the synthesis of 3-(2,2-dimethyltetrahydro-2H-pyran-4-yl)-2-thioxo-2,3-dihydro-1H-spiro[benzo[h]quinazoline-5,1'-cyclo-heptan]-4(6H)-one (**7**). The latter in the presence of potassium hydroxide reacted with halides of various structures resulting in 2-sulfanyl-

substituted 3-(2,2-dimethyltetrahydro-2H-pyran-4-yl)-3H-spiro[benzo[h]quinazoline-5,1'-cycloheptan]-4(6H)-ones (**8-16**).

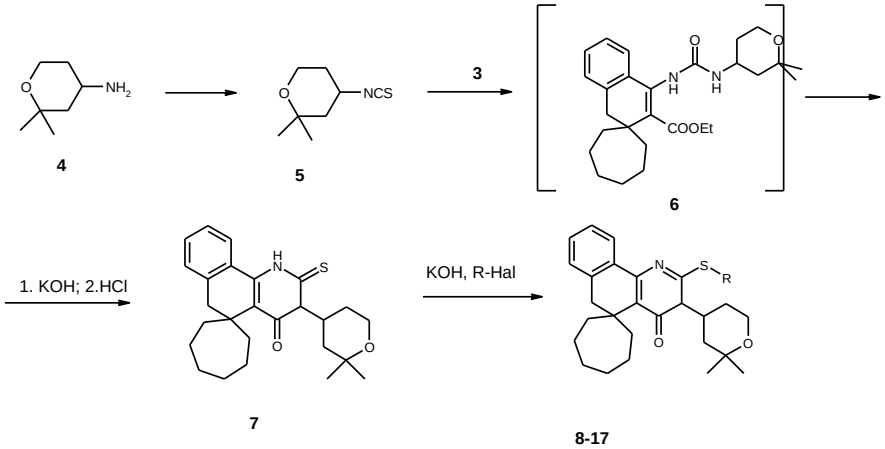

4 **5** **6** **7** **8-17**

R=CH_3 (**8**), C_2H_5 (**9**), C_3H_7 (**10**), i-C_3H_7 (**11**), $CH_2CH_2CH(CH_3)_2$ (**12**), $CH_2CH{=}CH_2$ (**13**), $CH_2C(CH)_3{=}CH_2$ (**14**),$CH_2C_6H_5$ (**15**), 2-$CH_3C_6H_4CH_2$ (**16**)

The antitumor properties of compounds on sarcoma 180 model were studied [6]. In chemotherapeutic experiments compounds **7, 9, 11** showed average therapeutic action against sarcoma 180 (inhibition of tumor growth by 40-56%). Weak activity showed compounds **8, 12, 15, 16,** which in a dose of 155-170 *mg*/*kg* inhibited the growth of sarcoma 180 in the range of 32-38%. Compounds **13** and **14** did not exhibit extreme antitumor activity.

The antibacterial activity of synthesized compounds was studied according to the method of diffusion in agar at microbial loading of 20 million Microbial cells per 1 *mL* of media. Gram-positive cocci (Staph. aureus 209P, and 1 and gram-negative bacteria (Sh. dysenteriae 6858, and E. coli O55) were used as the test-objects and Furazolidone was used as a control (Table 2).

Table 2

The antibacterial activity of synthesized compounds

Comp. №	Zone of microbial absence (d, *mm*)			
	Staphylococcus aureus		Sh. Flexneri 6858	E.coli 0-55
	209p	1		
8	0	0	10	0
9	10	10	10	10
10	11	10	10	10
11	10	10	10	10
12	10	10	11	15
13	10	10	13	11
Furazolidone	25	24	24	24,5

Experimental Section

The IR spectra were recorded on a Thermo Nicolet Nexus FT-IR spectrometer from samples dispersed in mineral oil. The ^{1}H and ^{13}C NMR spectra were recorded on a Varian Mercury-300 instrument from solutions in DMSO-*d*6–CCl_4 (1 : 3); the chemical shifts were measured relative to tetramethylsilane or hexamethyldisiloxane as internal standard. Silufol plates were used for analytical TLC; spots were visualized by treatment with iodine vapor.

Ethyl 2-(1-benzylcycloheptyl)-2-cyanoacetate (2). The solution of 41.4 *g* (0.2 *mol)* of ethyl-2-cyano-2-cycloheptylideneacetate **(1)** in 100 *ml* of absolute ether was added dropwise to the ethereal solution of the Grignard reagent, which had been obtained from 7.6 *g* (0.3 *mol*) of magnesium shavings and 38 *g* (0.3 *mo*l) of benzylchloride in 500 *ml* of absolute diethyl ether. The reaction mixture was mixed at room temperature for 5 *h*, then 125 *ml* of 18% HCl was added while maintaining the temperature at 18-22°C and mixed at room temperature until the complex was decomposed completely. The organic layer was separated, washed with water and dried with sodium sulfate. After distilling off the solvent, the residue was distilled in vacuo. Yield 50.2 *g* (83%) of **2**, bp 205–206°C/5 *mm*, R_f 0.44 (benzene–hexane, 5:2). IR spectrum, ν, cm^{-1}: 1580, 1602 (C=C arom); 1731 (C=O); 2241 (CN). ^{1}H NMR spectrum, δ, ppm: 1.32 (t, 3H, J=7.12, O-CH_2-$\underline{CH_3}$), 1.35-1.56 (m, 8H, cycloheptane), 1.60-1.75 (m, 3H, cycloheptane), 1.85-1.96 (m, 1H, cycloheptane), 2.75 (d, 1H, J=13.57, CH_a-Ph), 2.87 (d, 1H, J=13.57, CH_b-Ph), 3.42 (s, 1H, CH-C≡N), 4.21 (q, 2H, J=7.12, O-$\underline{CH_2}$-CH_3), 7.18-7.31 (m, 5H, Ph). ^{13}C NMR spectrum, δ_C, ppm: 13.49 (O-CH_2-$\underline{CH_3}$), 22.38 (CH_2 cycloheptane), 22.43 (CH_2 cycloheptane), 29.94 (CH_2 cycloheptane), 29.96 (CH_2 cycloheptane), 35.04 (CH_2 cycloheptane), 35.28 (CH_2 cycloheptane), 43.81 (C cycloheptane), 43.88 ($\underline{CH_2}$-Ph), 45.84 ($\underline{CH}$-C≡N), 61.44 (O-$\underline{CH_2}$-CH_3), 115.54 (C≡N), 126.18 (CH Ar), 127.57 (2×CH Ar), 130.08 (2×CH Ar), 135.88 (C Ar), 164.79 (C=O). Found, %: C 76.11; H 8.59; N 4.53.$C_{19}H_{25}NO_2$. Calculated, %: C 76.22; H 8.42; N 4.68.

Ethyl 4'-amino-1'H-spiro[cycloheptane-1,2'-naphthalene]-3'-carboxylate (3). 30.2 *g* (0.1 *mol*) of ethyl 2-(1-benzylcycloheptyl)-2-cyanoacetate **(2)** was inserted into the reaction flask and 60 *ml* of concentrated sulfuric acid was added by mixing at 5-10 °C. The mixing at this temperature lasted for 7 *h*, then it was neutralized by NH_4OH and extracted by ether. The extract was washed with water and dried with $MgSO_4$. Then the solvent was removed and the residue was recrystallized from 80% ethanol. Yield 19.3 *g* (64 %) of **3**, mp 57-58°C. R_f 0.67 (ethylacetate–benzene, 1□1). IR spectrum, ν, cm^{-1}: 1600 (C=C arom); 1632 (C=C); 3305.8 (NH_2). ^{1}H NMR spectrum, δ, ppm. 1.25-1.68 (m, 10H, cycloheptane), 1.33 (t, 3H, J=7.14, O-CH_2-$\underline{CH_3}$), 2.03-2.16 (m, 2H, cycloheptane), 2.74 (s, 2H, C1'H_2), 4.18 (q, 2H, J=7.14, O-$\underline{CH_2}$-CH_3), 6.94 (br.s, 2H, NH_2), 7.08-7.16 (m, 1H, CH Ar), 7.18-7.27 (m, 2H, 2×CH Ar), 7.52-7.60 (m, 1H, CH Ar). ^{13}C NMR spectrum, δ_C, ppm: 14.15 (O-CH_2-$\underline{CH_3}$), 24.20 (2×CH_2, cycloheptane), 29.26 (2×CH_2, cycloheptane), 37.20 (2×CH_2, cycloheptane), 39.00 (C, cycloheptane), 41.40

(C1'H_2), 57.77 (O-$\underline{CH_2}$-CH_3), 104.14 (C3'), 122.49 (CH Ar), 125.69 (CH Ar), 127.07 (CH Ar), 128.46 (CH Ar),130.72 (C Ar), 136.39 (C Ar), 149.74 (C4'), 169.50 (C=O). Found, %: C 76.11; H 8.59; N 4.53. $C_{19}H_{25}NO_2$. Calculated, %: C 76.22; H 8.42; N 4.68.

4-Isothiocyanato-2,2-dimethyltetrahydro-2H-pyran (5). A mixture of 12.9 g (0.1 *mol*) of 2,2-dimethyltetrahydro-2H-pyran-4-amine, 10.1 g (0.1 *mol*) of Rt_3N and 100 *ml* of $CHCl_3$ was placed into the reaction flask. At 10-15 °C, were added 7.6 g (0.1 *mol*) of CS_2, then successively 10.1 g (0.1 *mol*) of Rt_3N and 7.85 g (0.1 *mol*) of acetyl chloride. The reaction mixture was stirred at room temperature for 5 *h*, washed with water and dried with Na_2SO_4. After distilling off the solvent, the residue was distilled in vacuo.Yield 10.0 *g* (58%) of **5**, bp 105–106 °C/5mm. IR spectrum, ν, cm^{-1}: 1194 (C-O-C); 2094 (N=C=S). ^{1}H NMR spectrum, δ, ppm: 1.17 (s, 3H, C2-$(CH_3)_a$), 1.21 (s, 3H, C2-$(CH_3)_b$), 1.50-1.72 (m, 2H, C3H_a, C5H_a), 1.91-2.04 (m, 2H, C3H_b, C5H_b), 3.56 (ddd, 1H, J=2.61, 11.27, 12.37, C6H_a), 3.70 (ddd, 1H, J=2.87, 5.01, 12.37, C6H_b), 4.05 (tt, 1H, J=4.22, 10.83, C4H). ^{13}C NMR spectrum, δ_C, ppm: 22.37 (C2-$(CH_3)_a$), 29.89 (C2-$(CH_3)_b$), 32.94 (C5H_2), 42.88 (C3H_2), 50.42 (C4H), 58.34 (C6H_2), 70.87 (C2), 130.86 (N=C=S). Found, %: 56.23; H 7.45; N 8.08; S 18.57. $C_8H_{13}NOS$. Calculated, %: C 56.11; H 7.65; N 8.18; S 18.72.

3-(2,2-Dimethyltetrahydro-2H-pyran-4-yl)-2-thioxo-2,3-dihydro-1H-spiro[benzo[h]- quinazoline-5,1'-cycloheptan]-4(6H)-one (7). A mixture of 15.0 g (0.05 *mol*) of ethyl 4'-amino-1'H-spiro[cycloheptane-1,2'-naphthalene]-3' carboxylate (**3**), 100 *ml* of ethanol, 8.51g (0.05 *mol*) of 4-isothiocyanato-2,2-dimethyltetrahydro-2H-pyran was placed into a 250 *ml* round-bottomed flask. The reaction mixture was refluxed for 20 *h*, a solution of 5.6 *g* (0.1 *mol*) of KOH in 50 ml of H_2O was added and the mixture was boiled for an additional 3 h. After cooling, the mixture was acidified with a solution of 10% hydrochloric acid. The precipitated crystals were filtered, washed with water, hexane, and recrystallized from ethanol. Yield 13.0 *g* (61%) of **7,** mp 238-239°C, R_f 0.60 (ethylacetate-benzene–hexane, 1□5□5). IR spectrum, ν, cm^{-1}: 1615 (C=C arom); 1673 (C=O); 3169 (NH). ^{1}H NMR spectrum, δ, ppm: 1.23 (s, 3H, C2'-$(CH_3)_a$), 1.23-1.32 (m, 2H, CH_2, cycloheptane), 1.32 (c, 3H, C2'-$(CH_3)_b$), 1.40-1.86 (m, 10H, 5×CH_2, cycloheptane), 2.14-2.32 (m, 2H, C3'H_a, C5'H_a), 2.51-2.60 (m, 1H, C3'H_b), 2.67-2.84 (m, 1H, C5'H_b), 2.84 (s, 2H, C_6H_2), 3.63-3.81 (m, 2H, C6'H_2), 6.05-6.18 (m, 1H, C4'H), 7.17-7.40 (m, 3H, 3×CH Ar), 7.90-7.96 (m, 1H, CH Ar), 11.88 (br, 1H, NH). ^{13}C NMR spectrum, δ_C, ppm: 21.51 (C2'-$\underline{(CH_3)_a}$), 23.71 (CH_2, cycloheptane), 23.77 (CH_2, cycloheptane), 27.29 (C5'H_2), 29.20 (CH_2, cycloheptane), 29.30 (CH_2, cycloheptane), 31.26 (C2'-$\underline{(CH_3)_b}$), 34.95 (CH_2, cycloheptane), 35.45 (CH_2, cycloheptane), 37.16 (C3'H_2), 39.56 (C5), 40.11 (C_6H_2), 55.58 (C4'H), 60.55 (C6'H_2), 72.05 (C2'), 120.61 ($C4_a$), 124.46 (CH Ar), 125.17 (C Ar), 126.04 (CH Ar), 127.63 (CH Ar), 130.35 (CH Ar), 136.38 (C Ar), 141.77 ($C10_b$), 159.75 (C=O), 176.26 (C=S). Found, %: C 70.88; H 7.75; N 6.78; S 7.44. $C_{25}H_{32}N_2O_2S$. Calculated, %: C 70.72; H 7.60; N 6.60; S 7.55.

2-Alkylthio-3-(2,2-dimethyltetrahydro-2H-pyran-4-yl)-3H-spiro[benzo[h]quinazoline-5,1'-cycloheptan]-4(6H)-ones (8-16) (General method). A mixture of 2.12 *g* (0.005 *mol*) of **7**, 0.4 g (0.007 *mol*) of KOH and 30 *ml* of absolute ethanol was placed into a single-necked round-bottomed flask and boiled for 30 *min*. Then 0.07 *mol* of halogenide was added and boiling was continued for 12 *h*. The reaction mixture was cooled and 20 *ml* of water was added. The precipitate was filtered off and recrystallized from ethanol.

3-(2,2-Dimethyltetrahydro-2H-pyran-4-yl)-2-(methylthio)-3H-spiro[benzo[h]quinazoline-5,1'-cycloheptan]-4(6H)-one (8), (R=CH_3): Yield 1.85 g (84%), mp 197-198^{o}C, R_f 0.62 (ethylacetate-benzene–hexane, 1:5:7): IR spectrum, ν, cm^{-1}. 1600 (C=C arom); 1666 (C=O). ^{1}H NMR spectrum, δ, ppm. 1.26 (s, 3H, C2'-$(CH_3)_a$), 1.30 (c, 3H, C2'-$(CH_3)_b$), 1.31-1.41 (m, 2H, CH_2, cycloheptane), 1.45-1.87 (m, 10H, 5×CH_2, cycloheptane), 2.18-2.40 (m, 2H, C3'H_a, C5'H_a), 2.67 (s, 3H, S-CH_3), 2.68-2.79 (m, 1H, C3'H_b), 2.86 (s, 2H, C6H_2), 2.87-3.02 (m, 1H, C5'H_b), 3.60-3.73 (m, 1H, C6'H_a), 3.76-3.85 (m, 1H, C6'H_b), 4.44-4.66 (m, 1H, C4'H), 7.12-7.17 (m, 1H, CH Ar), 7.20-7.32 (m, 2H, 2×CH Ar), 7.98-8.04 (m, 1H, CH Ar). ^{13}C NMR spectrum, δ_C, ppm:14.82 (S-CH_3), 21.23 (C2'-$\underline{(CH_3)_a}$), 23.78 (CH_2, cycloheptane), 23.86 (CH_2, cycloheptane), 27.57 (C5'H_2), 29.38 (CH_2, cycloheptane), 29.49 (CH_2, cycloheptane), 31.06 (C2'-$\underline{(CH_3)_b}$), 35.24 (CH_2, cycloheptane), 35.75 (CH_2, cycloheptane), 37.56 (C3'H_2), 39.79 (C5), 40.03 (C6H_2), 54.82 (C4'H), 60.26 (C6'H_2), 71.73 (C2'), 124.08 (C Ar), 124.59 (CH Ar), 125.89 (CH Ar), 127.19 (CH Ar), 129.46 (CH Ar), 131.88 ($C4_a$), 136.22 (C Ar), 149.77 ($C10_b$), 157.92 (C2), 161.07 (C=O). Found, %: C 71.33; H 7.96; N 6.23; S 7.15. $C_{26}H_{34}N_2O_2S$. Calculated, %: C 71.19; H 7.81; N 6.39; S 7.31.

3-(2,2-Dimethyltetrahydro-2H-pyran-4-yl)-2-(ethylthio)-3H-spiro[benzo[h]quinazoline-5,1'-cycloheptan]-4(6H)-one (9), (R=C_2H_5):Yield 1.8 g (79%), mp 164–165^{o}C, R_f=0.63 (ethylacetate-benzene–hexane, 1:5:7):IR spectrum, ν, cm^{-1}. 1603 (C=C arom); 1661 (C=O). ^{1}H NMR spectrum, δ, ppm: 1.26 (s, 3H, C2'-$(CH_3)_a$), 1.30 (s, 3H, C2'-$(CH_3)_b$), 1.31-1.42 (m, 2H, CH_2, cycloheptane), 1.45-1.88 (m, 10H, 5×CH_2, cycloheptane), 1.49 (t, 3H, J=7.34, S-CH_2-$\underline{CH_3}$), 2.18-2.40 (m, 2H, C3'H_a, C5'H_a), 2.68-2.80 (m, 1H, C3'H_b), 2.86 (s, 2H, C6H_2), 2.87-3.02 (m, 1H, C5'H_b), 3.29 (q, 2H, J=7.34, S-$\underline{CH_2}$-CH_3), 3.61-3.74 (m, 1H, C6'H_a), 3.76-3.85 (m, 1H, C6'H_b), 4.45-4.65 (m, 1H, C4'H), 7.12-7.17 (m, 1H, CH Ar), 7.20-7.32 (m, 2H, 2×CH Ar), 7.93-7.98 (m, 1H, CH Ar). ^{13}C NMR spectrum, δ_C, ppm: 13.56 (S-CH_2-$\underline{CH_3}$), 21.25 (C2'-$\underline{(CH_3)_a}$), 23.77 (CH_2, cycloheptane), 23.86 (CH_2, cycloheptane), 26.25 (S-$\underline{CH_2}$-CH_3), 27.53 (C5'H_2), 29.38 (CH_2, cycloheptane), 29.49 (CH_2, cycloheptane), 31.06 (C2'-$\underline{(CH_3)_b}$), 35.26 (CH_2, cycloheptane), 35.76 (CH_2, cycloheptane), 37.53 (C3'H_2), 39.81 (C5), 40.06 (C_6H_2), 54.70 (C4'H), 60.24 (C6'H_2), 71.73 (C2'), 124.16 (C Ar), 124.39 (CH Ar), 125.93 (CH Ar), 127.24 (CH Ar), 129.45 (CH Ar), 131.91 ($C4_a$), 136.25 (C Ar), 149.82 ($C10_b$), 157.47 (C2), 161.13 (C=O). Found, %: C 71.79; H 8.19; N 6.03; S 7.23. $C_{27}H_{36}N_2O_2S$. Calculated, %: C 71.64; H 8.02; N 6.19; S 7.08.

3-(2,2-Dimethyltetrahydro-2H-pyran-4-yl)-2-(propylthio)-3H-spiro[benzo[h]quinazoline-5,1'-cycloheptan]-4(6H)-one (10), (R=C_3H_7): Yield 1.9 g (81%), mp 144–145°C, R_f 0.66 (ethylacetate-benzene–hexane, 1:5:7): IR spectrum, ν, cm^{-1}. 1603 (C=C arom); 1659 (C=O). ^{1}H NMR spectrum, δ, ppm. 1.12 (t, 3H, J=7.36, S-CH_2-CH_2-$\underline{CH_3}$), 1.26 (s, 3H, C2'-$(CH_3)_a$), 1.30 (s, 3H, C2'-$(CH_3)_b$), 1.31-1.41 (m, 2H, CH_2, cycloheptane), 1.45-1.87 (m, 10H, 5×CH_2, cycloheptane), 1.79-1.93 (m, 2H, S-CH_2-$\underline{CH_2}$-CH_3), 2.18-2.40 (m, 2H, C3'H_a, C5'H_a), 2.68-2.80 (m, 1H, C3'H_b), 2.86 (s, 2H, C6H_2), 2.87-3.02 (m, 1H, C5'H_b), 3.17-3.34 (m, 2H, S-$\underline{CH_2}$-CH_2-CH_3), 3.61-3.74 (m, 1H, C6'H_a), 3.76-3.85 (m, 1H, C6'H_b), 4.45-4.65 (m, 1H, C4'H), 7.12-7.17 (m, 1H, CH Ar), 7.20-7.32 (m, 2H, 2×CH Ar), 7.91-7.97 (m, 1H, CH Ar). ^{13}C NMR spectrum, δ_C, ppm: 13.07 (S-CH_2-CH_2-$\underline{CH_3}$),21.26 (C2'-$\underline{(CH_3)_a}$), 21.61 (S-CH_2-$\underline{CH_2}$-CH_3), 23.77 (CH_2, cycloheptane), 23.85(CH_2, cycloheptane), 27.53 (C5'H_2), 29.37 (CH_2, cycloheptane), 29.49 (CH_2, cycloheptane), 31.06 (C2'-$\underline{(CH_3)_b}$), 33.76 (S-$\underline{CH_2}$-CH_2-CH_3), 35.24 (CH_2, cycloheptane), 35.75 (CH_2, cycloheptane), 37.53 (C3'H_2), 39.80 (C5), 40.06 (C_6H_2), 54.69 (C4'H), 60.25 (C6'H_2), 71.73 (C2'), 124.13 (C Ar), 124.33 (CH Ar), 125.91 (CH Ar), 127.25 (CH Ar), 129.43 (CH Ar), 131.91 ($C4_a$), 136.26 (C Ar), 149.78 (C*10*$_b$), 157.56 (C*2*), 161.15 (C=O). Found, %: C 71.88; H 8.37; N 6.18; S 6.72. $C_{28}H_{38}N_2O_2S$. Calculated, %: C 72.06; H 8.21; N 6.00; S 6.87.

3-(2,2-Dimethyltetrahydro-2H-pyran-4-yl)-2-(isopropylthio)-3H-spiro[benzo[h]quinazoline -5,1'-cycloheptan]-4(6H)-one (11), (R=i–C_3H_7):Yield 1.7 g (73%), mp 181–182°C, R_f=0.65 (ethylacetate-benzene–hexane,1:7:7): IR spectrum, ν, cm^{-1}. 1600.7 (C=C arom); 1662 (C=O). ^{1}H NMR spectrum, δ, ppm. 1.25 (s, 3H, C2'-$(CH_3)_a$), 1.30 (s, 3H, C2'-$(CH_3)_b$), 1.31-1.42 (m, 2H, CH_2, cycloheptane), 1.45-1.87 (m, 10H, 5×CH_2, cycloheptane), 1.52 (d, 6H, J=6.94, S-CH-$\underline{(CH_3)_2}$), 2.18-2.40 (m, 2H, C3'H_a, C5'H_a), 2.68-2.80 (m, 1H, C3'H_b), 2.86 (s, 2H, C_6H_2), 2.87-3.02 (m, 1H, C5'H_b), 3.61-3.74 (m, 1H, C6'H_a), 3.76-3.85 (m, 1H, C6'H_b), 4.12 (sp, 1H, J=6.94, S-$\underline{CH}$-$(CH_3)_2$), 4.40-4.63 (m, 1H, C4'H), 7.12-7.17 (m, 1H, CH Ar), 7.20-7.32 (m, 2H, 2×CH Ar), 7.90-7.96 (m, 1H, CH Ar). ^{13}C NMR spectrum, δ_C, ppm: 21.30 (C2'-$\underline{(CH_3)_a}$), 22.21 (S-CH-$\underline{(CH_3)_2}$), 23.76 (CH_2, cycloheptane), 23.85(CH_2, cycloheptane), 27.48 (C5'H_2), 29.37 (CH_2, cycloheptane), 29.49 (CH_2, cycloheptane), 31.06 (C2'-$\underline{(CH_3)_b}$), 35.28 (CH_2, cycloheptane), 35.75 (CH_2, cycloheptane), 37.47 (S-$\underline{CH}$-$(CH_3)_2$), 37.53 (C3'H_2), 39.81 (C5), 40.07 (C6H_2), 54.69 (C4'H), 60.21 (C6'H_2), 71.73 (C2'), 124.15 (C Ar), 124.32 (CH Ar), 125.95 (CH Ar), 127.26 (CH Ar), 129.43 (CH Ar), 131.92 ($C4_a$), 136.26 (C Ar), 149.88 ($C10_b$), 157.51 (C2), 161.11 (C=O). Found, %: C 71.88; H 8.37; N 6.18; S 6.72. $C_{28}H_{38}N_2O_2S$. Calculated, %: C 72.06; H 8.21; N 6.00; S 6.87.

3-(2,2-Dimethyltetrahydro-2H-pyran-4-yl)-2-(isopentylthio)-3H-spiro[benzo[h]quinazoline-5,1'-cycloheptan]-4(6H)-one (12), (R=i-C_5H_{11}): Yield 2.0 g (81%), mp 137–138°C, R_f 0.61 (ethylacetate-benzene–hexane, 1:5:7):IR spectrum, ν, cm^{-1}. 1602.7 (C=C arom); 1665 (C=O). ^{1}H NMR spectrum, δ, ppm. 1.01 (d, 6H, J=6.40, S-CH_2-CH_2-CH-$\underline{(CH_3)_2}$), 1.25 (s, 3H, C2'-$(CH_3)_a$), 1.30 (s, 3H, C2'-$(CH_3)_b$), 1.30-1.42 (m, 2H, CH_2, cycloheptane), 1.45-1.88 (m, 13H, 5×CH_2,

cycloheptane), S-CH_2-CH_2-CH-$(CH_3)_2$, S-CH_2-CH_2-CH-$(CH_3)_2$), 2.18-2.40 (m, 2H, C3'H_a, C5'H_a), 2.67-2.80 (m, 1H, C3'H_b), 2.86 (s, 2H, C_6H_2), 2.87-3.02 (m, 1H, C5'H_b), 3.22-3.33 (m, 2H, S-CH_2-CH_2-CH-$(CH_3)_2$), 3.58-3.72 (m, 1H, C6'H_a), 3.75-3.85 (m, 1H, C6'H_b), 4.45-4.65 (m, 1H, C4'H), 7.11-7.17 (m, 1H, CH Ar), 7.19-7.32 (m, 2H, 2×CH Ar), 7.92-7.99 (m, 1H, CH Ar). ^{13}C NMR spectrum, δ_C, ppm: 21.24 (C2'-$(CH_3)_a$), 21.86 (S-CH_2-CH_2-CH-$(CH_3)_2$), 23.76 (CH_2, cycloheptane), 23.84 (CH_2, cycloheptane), 27.20 (S-CH_2-CH_2-CH-$(CH_3)_2$), 27.51 (C5'H_2), 29.36 (CH_2, cycloheptane), 29.48 (CH_2, cycloheptane), 29.99 (S-CH_2-CH_2-CH-$(CH_3)_2$), 31.05 (C2'-$(CH_3)_b$), 35.24 (CH_2, cycloheptane), 35.75 (CH_2, cycloheptane), 37.19 (S-CH_2-CH_2-CH-$(CH_3)_2$), 37.52 (C3'H_2), 39.81 (C5), 40.03 (C_6H_2), 54.76 (C4'H), 60.24 (C6'H_2), 71.73 (C2'), 124.12 (C Ar), 124.37 (CH Ar), 125.80 (CH Ar), 127.25 (CH Ar), 129.44 (CH Ar), 131.87 ($C4_a$), 136.25 (C Ar), 149.80 ($C10_b$), 157.54 (C2), 161.13 (C=O). Found, %: C 72.98; H 8.38; N 5.82; S 6.31. $C_{30}H_{42}N_2O_2S$. Calculated, %: C 72.83; H 8.56; N 5.66; S 6.48.

2-(Allylthio)-3-(2,2-dimethyltetrahydro-2H-pyran-4-yl)-3H-spiro[benzo[h]quinazoline-5,1'-cycloheptan]-4(6H)-one (13), (R=$CH_2CH=CH_2$): Yield 1.95 g (84%), mp 149–150°C, R_f 0.67 (ethylacetate-benzene–hexane, 1:7:7). IR spectrum, ν, cm^{-1}. 1605 (C=C arom); 1664 (C=O). ^{1}H NMR spectrum, δ, ppm. 1.25 (s, 3H, C2'-$(CH_3)_a$), 1.30 (s, 3H, C2'-$(CH_3)_b$), 1.31-1.42 (m, 2H, CH_2, cycloheptane), 1.45-1.87 (m, 10H, 5×CH_2, cycloheptane), 2.18-2.40 (m, 2H, C3'H_a, C5'H_a), 2.67-2.79 (m, 1H, C3'H_b), 2.85-3.02 (m, 1H, C5'H_b), 2.87 (s, 2H, C_6H_2), 3.60-3.73 (m, 1H, C6'H_a), 3.75-3.85 (m, 1H, C6'H_b), 3.96 (d, 2H, J=7.09, S-CH_2-CH=CH_2), 4.43-4.65 (m, 1H, C4'H), 5.17-5.23 (m, 1H, S-CH_2-CH=CH_a), 5.33-5.43 (m, 1H, S-CH_2-CH=CH_b), 5.94-6.10 (m, 1H, S-CH_2-CH=CH_2), 7.12-7.18 (m, 1H, CH Ar), 7.21-7.33 (m, 2H, 2×CH Ar), 7.94-8.00 (m, 1H, CH Ar). ^{13}C NMR spectrum, δ_C, ppm: 21.23 (C2'-$(CH_3)_a$), 23.76 (CH_2, cycloheptane), 23.85(CH_2, cycloheptane), 27.55 (C5'H_2), 29.36 (CH_2, cycloheptane), 29.48 (CH_2, cycloheptane), 31.05 (C2'-$(CH_3)_b$), 34.62 (S-CH_2-CH=CH_2), 35.22 (CH_2, cycloheptane), 35.72 (CH_2, cycloheptane), 37.57 (C3'H_2), 39.82 (C5), 40.02 ($C6H_2$), 55.03 (C4'H), 60.21 (C6'H_2), 71.73 (C2'), 118.40 (S-CH_2-CH=CH_2), 124.26 (C Ar), 124.46 (CH Ar), 125.97 (CH Ar), 127.25 (CH Ar), 129.50 (CH Ar), 131.79 ($C4_a$), 132.10 (S-CH_2-CH=CH_2), 136.24 (C Ar), 149.81 ($C10_b$), 156.97 (C2), 161.07 (C=O). Found, %: C 72.21; H 7.65; N 6.22; S 6.72. $C_{28}H_{36}N_2O_2S$. Calculated, %: C 72.38; H 7.81; N 6.03; S 6.90.

3-(2,2-Dimethyltetrahydro-2H-pyran-4-yl)-2-((2-methylallyl)thio)-3H-spiro [benzo[h]-quinazoline-5,1'-cycloheptan]-4(6H)-one (14), (R=$CH_2C(CH_3)=CH_2$): Yield 2.0 g (83%), mp 164–165°C, R_f 0.65 (ethylacetate-benzene–hexane, 1:7:7): IR spectrum, ν, cm^{-1}. 1605 (C=C arom); 1654 (C=O). ^{1}H NMR spectrum, δ, ppm. 1.26 (s, 3H, C2'-$(CH_3)_a$), 1.31 (s, 3H, C2'-$(CH_3)_b$), 1.31-1.42 (m, 2H, CH_2, cycloheptane), 1.45-1.87 (m, 10H, 5×CH_2, cycloheptane), 1.90 (s, 3H, S-CH_2-C(CH_3)=CH_2), 2.18-2.40 (m, 2H, C3'H_a, C5'H_a), 2.68-2.81 (m, 1H, C3'H_b), 2.85-3.03 (m, 1H, C5'H_b), 2.87 (s, 2H, C_6H_2), 3.61-3.74 (m, 1H, C6'H_a), 3.76-3.86 (m, 1H, C6'H_b), 3.98 (d, 1H, J=13.19, S-CH_a-$C(CH_3)=CH_2$), 4.03 (d, 1H, J=13.19, S-CH_b-$C(CH_3)=CH_2$), 4.48-

4.68 (m, 1H, C4'H), 4.92-4.96 (m, 1H, S-CH_2-C(CH_3)=$\underline{CH_a}$), 5.08-5.12 (m, 1H, S-CH_2-C(CH_3)=$\underline{CH_b}$), 7.12-7.18 (m, 1H, CH Ar), 7.21-7.33 (m, 2H, 2×CH Ar), 7.94-8.00 (m, 1H, CH Ar). ^{13}C NMR spectrum, δ_C, ppm: 21.06 (S-CH_2-C($\underline{CH_3}$)=CH_2), 21.27 (C2'-$(\underline{CH_3})_a$), 23.75 (CH_2, cycloheptane), 23.83(CH_2, cycloheptane), 27.54 (C5'H_2), 29.35 (CH_2, cycloheptane), 29.47 (CH_2, cycloheptane), 31.04 (C2'-$(\underline{CH_3})_b$), 35.19 (CH_2, cycloheptane), 35.70 (CH_2, cycloheptane), 37.57 (C3'H_2), 38.78 (S-$\underline{CH_2}$-C(CH_3)=CH_2), 39.81 (C5), 39.99 (C_6H_2), 55.11 (C4'H), 60.21 (C6'H_2), 71.73 (C2'), 114.87 (S-CH_2-C(CH_3)=$\underline{CH_2}$), 124.25 (C Ar), 124.46 (CH Ar), 125.91 (CH Ar), 127.25 (CH Ar), 129.47 (CH Ar), 131.76 ($C4_a$), 136.23 (C Ar), 138.89 (S-CH_2-$\underline{C}$(CH_3)=CH_2), 149.70 ($C10_b$), 157.17 (C2), 161.08 (C=O). Found, %: C 72.57; H 8.18; N 5.68; S 6.88. $C_{29}H_{38}N_2O_2S$. Calculated, %: C 72.76; H 8.00; N 5.85; S 6.70.

2-(Benzylthio)-3-(2,2-dimethyltetrahydro-2H-pyran-4-yl)-3H-spiro [benzo[h]quinazoline-5,1'-cycloheptan]-4(6H)-one (15), (R=$CH_2C_6H_5$):Yield 2.2 g (85%), mp 173–174°C, R_f 0.68 (ethylacetate-benzene–hexane, 1:7:7): IR spectrum, ν, cm^{-1}. 1605 (C=C arom); 1662 (C=O). ^{1}H NMR spectrum, δ, ppm. 1.24 (s, 3H, C2'-$(CH_3)_a$), 1.27 (s, 3H, C2'-$(CH_3)_b$), 1.32-1.44 (m, 2H, CH_2, cycloheptane), 1.45-1.88 (m, 10H, 5×CH_2, cycloheptane), 2.20-2.39 (m, 2H, C3'H_a, C5'H_a), 2.66-2.79 (m, 1H, C3'H_b), 2.85-3.00 (m, 1H, C5'H_b), 2.87 (s, 2H, C_6H_2), 3.58-3.70 (m, 1H, C6'H_a), 3.74-3.83 (m, 1H, C6'H_b), 4.43-4.62 (m, 1H, C4'H), 4.52 (d, 1H, J=13.02, S-CH_a), 4.59 (d, 1H, J=13.02, S-CH_b), 7.13-7.18 (m, 1H, CH Ar), 7.20-7.35 (m, 5H, 5×CH Ar), 7.39-7.45 (m, 2H, 2×CH Ar), 7.98-8.03 (m, 1H, CH Ar). ^{13}C NMR spectrum, δ_C, ppm: 21.28 (C2'-$(\underline{CH_3})_a$), 23.76 (CH_2, cycloheptane), 23.84(CH_2, cycloheptane), 27.53 (C5'H_2), 29.35 (CH_2 cycloheptane), 29.46 (CH_2 cycloheptane), 31.03 (C2'-$(\underline{CH_3})_b$), 35.22 (CH_2, cycloheptane), 35.69 (CH_2, cycloheptane), 36.51 (S-CH_2), 37.53 (C3'H_2), 39.84 (C5), 40.00 (C_6H_2), 54.93 (C4'H), 60.16 (C6'H_2), 71.70 (C2'), 124.41 (C Ar), 124.59 (CH Ar), 125.95 (CH Ar), 127.04 (CH Ar), 127.25 (CH Ar), 128.06 (2×CH Ar), 128.67 (2×CH Ar), 129.51 (CH Ar), 131.76 ($C4_a$), 135.21 (C Ar), 136.22 (C Ar), 149.81 ($C10_b$), 157.34 (C2), 161.03 (C=O). Found, %: C 74.50; H 7.62; N 5.27; S 6.39. $C_{32}H_{38}N_2O_2S$. Calculated, %: C 74.67; H 7.44; N 5.44; S 6.23.

3-(2,2-Dimethyltetrahydro-2H-pyran-4-yl)-2-((2-methylbenzyl)thio)-3H-spiro[benzo[h]-quinazoline-5,1'-cycloheptan]-4(6H)-one (16), (R=2–$CH_3C_6H_4CH_2$): Yield 2.1 g (79%), mp 182–183°C, R_f 0.64 (ethylacetate-benzene–hexane 1:7:7): IR spectrum, ν, cm^{-1}. 1603 (C=C arom); 1661.7 (C=O). ^{1}H NMR spectrum, δ, ppm. 24 (s, 3H, C2'-$(CH_3)_a$), 1.25 (s, 3H, C2'-$(CH_3)_b$), 1.32-1.44 (m, 2H, CH_2, cycloheptane), 1.46-1.89 (m, 10H, 5×CH_2, cycloheptane), 2.22-2.40 (m, 2H, C3'H_a, C5'H_a), 2.45 (s, 3H, $\underline{CH_3}$-Ph), 2.68-2.80 (m, 1H, C3'H_b), 2.85-3.00 (m, 1H, C5'H_b), 2.88 (s, 2H, C_6H_2), 3.57-3.69 (m, 1H, C6'H_a), 3.73-3.83 (m, 1H, C6'H_b), 4.40-4.61 (m, 1H, C4'H), 4.52 (d, 1H, J=12.87, S-CH_a), 4.57 (d, 1H, J=12.87, S-CH_b), 7.08-7.38 (m, 7H, 7×CH Ar), 7.99-8.05 (m, 1H, CH Ar). ^{13}C NMR spectrum, δ_C, ppm: 18.72 ($\underline{CH_3}$-Ph), 21.31 (C2'-$(\underline{CH_3})_a$), 23.77 (CH_2, cycloheptane), 23.86 (CH_2, cycloheptane), 27.53 (C5'H_2), 29.36 (CH_2, cycloheptane), 29.47 (CH_2, cycloheptane), 31.03 (C2'-$(\underline{CH_3})_b$), 35.22 (CH_2, cycloheptane), 35.25 (S-CH_2), 35.69

(CH_2, cycloheptane), 37.52 (C3'H_2), 39.86 (C5), 40.02 (C_6H_2), 54.70 (C4'H), 60.15 (C6'H_2), 71.69 (C2'), 124.38 (C Ar), 124.58 (CH Ar), 125.79 (CH Ar), 125.96 (CH Ar), 127.26 (CH Ar), 127.55 (CH Ar), 129.53 (CH Ar), 129.84 (CH Ar), 129.97 (CH Ar), 131.82 ($C4_a$), 132.25 (C Ar), 136.25 (C Ar), 136.39 (C Ar), 149.84 ($C10_b$), 157.50 (C2), 161.03 (C=O). Found, %: C 74.81; H 7.82; N 5.48; S 6.24. $C_{33}H_{40}N_2O_2S$. Calculated, %: C 74.96; H 7.63; N 5.30; S 6.06.

3-(2,2-ԴԻՄԵԹԻԼՏԵՏՐԱՀԻԴՐՕ-2H-ՊԻՐԱՆ-4-ԻԼ)ՍՊԻՐՕ [ԲԵՆԶՕ[h]ԽԻՆԱԶՕԼԻՆ-5,1'-ՑԻԿԼՕՀԵՊՏԱՆ]-4 (6H)-ՕՆՆԵՐԻ ՍԻՆԹԵԶԸ ԵՎ ՀԱԿԱՕՒՌՈՒՑՔԱՅԻՆ ՀԱՏԿՈՒԹՅՈՒՆՆԵՐԸ

Ա. Ի. ՄԱՐԿՈՍՅԱՆ, Խ. Ս. ՀԱԿՈԲՅԱՆ, Ա. Ս. ԱՅՎԱԶՅԱՆ, Ս.Ս.ՄԱՄՅԱՆ, Ա. Գ. ԱՅՎԱԶՅԱՆ, Ռ. Ա. ԹԱՄԱԶՅԱՆ, Ֆ. Ղ. ԱՐՍԵՆՅԱՆ և Ջ. Ա. ԱՎԱԿԻՄՅԱՆ

Էթիլ 2-ցիանո-2-ցիկլոհեպտիլիդենացետատին բենզիլմագնեզիում քլորիդի ռեգիոսելեկտիվ միացումը հանգեցրել է 2-(1-բենզիլցիկլհեպտիլ)-2-ցիանոացետատի, որի ցիկլումն օգտագործվել է էթիլ 4'-ամինո-'H-սպիրո[ցիկլոհեպտան-1,2'-նավթալին]-3'-կարբոքսիլատի (ամինոէսթեր) սինթեզի համար: Ամինոէսթերի և 4-իզոթիոցիանատո-2,2-դիմեթիլտետրահիդրո-2H-պիրանի փոխազդեցությունից ստացված թիոուրեիդոածանցյալն, առանց ռեակցիոն միջավայրից անջատելու, ենթարկվել է ցիկլման, ինչը բերել է 3-(2,2-դիմեթիլտետրահիդրո-2H-պիրան-4-իլ)-2-թիօքսո-2,3-դիհիդրո-1H-սպիրո[բենզո[h]խինազոլին-5,1'-ցիկլոհեպտան]-4(6H)-ոնի սինթեզին: Թիօքսոածանցյալը հիմքի ներկայությամբ փոխազդում է հալոգենիդների հետ, որի արդյունքում ստացվում են 2-սուլֆանիլ-տեղակալված 3-(2,2-դիմեթիլտետրահիդրո-2H-պիրան-4-իլ)-3H-սպիրո[բենզո[h]խինազոլին-5,1'-ցիկլոհեպտան]-4(6H)-ոններ: Ուսումնասիրվել է սինթեզված միացությունների հակաուռուցքային և հակաբակտերիալ ակտիվությունը:

СИНТЕЗ И ПРОТИВООПУХОЛЕВЫЕ СВОЙСТВА 3-(2,2-ДИМЕТИЛТЕТРАГИДРО-2H-ПИРАН-4-ИЛ)СПИРО[БЕНЗО[h]ХИНАЗОЛИН-5,1'-ЦИКЛОГЕПТАН]-4 (6H)-ОНОВ

А. И. МАРКОСЯН, Х. С. АКОПЯН, А. С. АЙВАЗЯН, С. С. МАМЯН, А. Г. АЙВАЗЯН, Р. А. ТАМАЗЯН, Ф. Г. АРСЕНЯН и Дж. А. АВАКИМЯН

Научно-технологический центр органической и фармацевтической химии
НАН Республики Армения
Армения, 0014, Ереван, пр. Азатутяна 26
Телефон: +374 10 288 443
E-mail: ashot@markosyan.am

Региоселективное присоединение бензилмагнийхлорида к этил-2-циано-2-циклогептилиденацетату привело к 2-1-бензилциклогептил)-2-цианоацетату, циклизация которого использовали для синтеза этил-4'-амино-1'H-спиро[циклогептан-1,2'-нафталин]-3'-карбоксилата (аминоэфир). Реакцией аминоэфира с 4-изотиоцианато-2,2-диметилтетрагидро-2H-пираном было получено соответствующее тиореидопроизводное, которое без выделения из реакционной среды подвергалось циклизации, что привело к синтезу 3-(2,2-диметилтетрагидро-2H-пиран-4-ил)-2-тиоксо-2,3-дигидро-1H-спиро[бензо[h]хиназолин-5,1'-циклогептан]-4(6H)-она. В присутствии оснований тиоксопроизводное реагирует с галогенидами, что приво-

дит к образованию 2-сульфанилзамещенных 3-(2,2-диметилтетрагидро-2H-пиран-4-ил)-3H-спиро[бензо[h]хиназолин-5,1'- циклогептан]-4(6H)-онов. Изучены противоопухолевая и антибактериальная активности синтезированных соединений.

REFERENCES

[1] *Shafi S.S., Kumar S.S. //* International Journal of ChemTech Research (USA), 2015, v. 8 (1), p. 164.

[2] *Gupta R., Chaudhary R.P.* // Phosphorus, sulfur and silicon, 2012, v. 187 (6), p. 735.

[3] *Chidananda N., Poojary B., Sumangala V., Kumari Suchetha N.* // Indian J heterocyclic Chem., 2011, 20(4), p. 337.

[4] *Keshari A.K., Singh A.K., Raj V., Rai A., Trivedi P., Ghosh B., Kumar U., Rawat A., Kumar D., Saha S. // Drug Des Devel Ther.*, 2017, v. 11, p. 1623.

[5] *Liang J.L., Park S.E., Kwon Y., Jahng Y.* // Bioorg. Med. Chem., 2012, v. 20(16), p. 4962.

[6] *Ohtomo H., Tagata T., Sasaki K., Hirota T., Okuda K.* // Tetrahedron, 2007, v. 63 (51), p. 12541.

[7] *Sati N., Kumar S., Rawat M.S.M.* // Indian Journal of Pharmaceutical Sciences, 2009, v. 71 (5), p. 572.

[8] *Brullo C., Rocca M., Fossa P., Cichero E., Barocelli E., Ballabeni V., Flammini L., Giorgio C., Saccani F., Domenichini G., Brono O.* // Bioorg. Med. Chem. Lett., 2012, 22 (2), p. 1125.

[9] *Sahoo M.,, Jena L., Daf S., Kumar S.* // Genomics Inform., 2016 14(3), p. 104.

[10] *Maurya H. K., Vema R., Alam S., Pandey Sh., Pathak V., Shama S., Srivastava K. K. Negi A.S., Gupta A.* // Bioorg. Med. Chem. Lett., 2013, v. 23 (21), p. 5844.

[11] *Markosyan A.I., Gabrielyan S.H., Arsenyan F.H., Sukasyan R.S.* // Chem.-pharm. J. (Moscow), 2010, v.44, №8, p. 3.

[12] *Markosyan A.I., Gabrielyan S.H., Arsenyan F.H., Sukasyan R.S., Sarkisyan I.S.* // Chem.-pharm. J. (Moscow), 2010, v. 44 (8), p. 7.

[13] *Markosyan A.I., Dilanyan S.V., Arsenyan F.H., Sukasyan R.S., Gharibjanyan B T.* // Chem.-pharm. J. (Moscow), 2010, v. 44, №3, p. 3.

[14] *Grigoryan N.P., Markosyan A.I., Grigoryan A.S., Stepanyan H.A., Sukasyan R.S., Paronikyan R.G.* // Chem.-pharm. J. (Moscow), 2017, v. 51 (12), p. 11.

[15] *Markosyan A., Gabrielyan S., Arsenyan F.* / 3-nd International congress on technology - engineering & science (ICONTES) – 09-10 Feb. 2017, Kuala Lumpur, Malaysia. Abstract book, p. 244.

[16] *Kuduk S.D., Beshore D.C., Dimarco Ch.Ng., Greshock T.J.* / Aminobenzoquinazolinone M1 receptor positive allosteric modulators . US patent 8383638 B2, 2013.

[17] *Sheldrick G.M.* // Acta Cryst., 2015, C71, p. 3.

ՀԱՅԱՍՏԱՆԻ ՀԱՆՐԱՊԵՏՈՒԹՅԱՆ ԳԻՏՈՒԹՅՈՒՆՆԵՐԻ
ԱԶԳԱՅԻՆ ԱԿԱԴԵՄԻԱ
НАЦИОНАЛЬНАЯ АКАДЕМИЯ НАУК РЕСПУБЛИКИ АРМЕНИЯ
NATIONAL ACADEMY OF SCIENCES OF THE REPUBLIC OF ARMENIA

Հայաստանի քիմիական հանդես
Химический журнал Армении **71, №4, 2018** Chemical Journal of Armenia

UDC 546.492 + 547.31/547.37 + 547.442.3

ON THE INTERACTION OF PROPARGYL MALONATE WITH NUCLEOPHILES IN THE PRESENCE OF MERCURY(II) ACETATE

N. G. HOBOSYAN*[a,b], K. V. BALYAN[a], H. S. NERSISYAN[a], L. M. GHALECHYAN[a,b], S. A. HOVAKIMYAN[b], H. B. SARGSYAN[a] and Zh. A. CHOBANYAN[a]

[a]The Scientific and Technological Centre
of Organic and Pharmaceutical Chemistry of NAS RA
26, Azatutyan Ave., Yerevan, 0014, Armenia
E-mail: ninahobosyan@mail.ru
[b]Armenian State Pedagogical University after Khachatur Abovian
17, Tigran Mets Ave., Yerevan, 0010, Armenia
E-mail: svetachem@gmail.com

The regiochemistry of the reaction of diethyl 2-(prop-2-yn-1-yl)malonate with various nucleophiles in the presence of mercury(II) acetate has been investigated. The derivative of cyclopentadiene and unsaturated ketoesters were isolated depending on the nature of the dicarbonyl compound and the conditions for the reduction of the organomercury intermediates.

References 6

Earlier, based on the reaction of solvomercuration-demercuration of the terminal triple bond, methods for one-step functionalization were developed and the reasons for obtaining both furan derivatives and the linear products of vinylation were identified [1-4].

Extending the research in this area, diethyl 2-(prop-2-yn-1-yl)malonate **2** synthesized from malonic ester **1** with various CH- and NH-nucleophiles was involved as the substrate in the mercuration-demerculation reaction. The substrate optimally combined model terminal acetylene and dicarbonyl fragments that can influence regiochemistry of the studied reaction.

It turned out that the interaction of diethyl 2-(prop-2-yn-1-yl)malonate **2** with sodium acetylacetonate in the presence of mercury(II) acetate in dioxane, followed by demerculation of intermediates **3** and **4** with sodium borohydride, in contrast to alkyl acetylenes, propargyl ethers and proparyl acetate, affords a mixture of diethyl-3-acetyl-2,4-dimethylcyclopenta-2,4-diene-1,1-dicarboxylate **6** and diethyl 2-(3-acetyl-4-hydroxy-2-methylenepent-3-enyl)malonate **5**.

It should be noted that the formation of cyclopentadienyl derivative **6** is a consequence of the prototropic migration of the exomethylene double bond, further dehydration and cyclization according to the following Scheme:

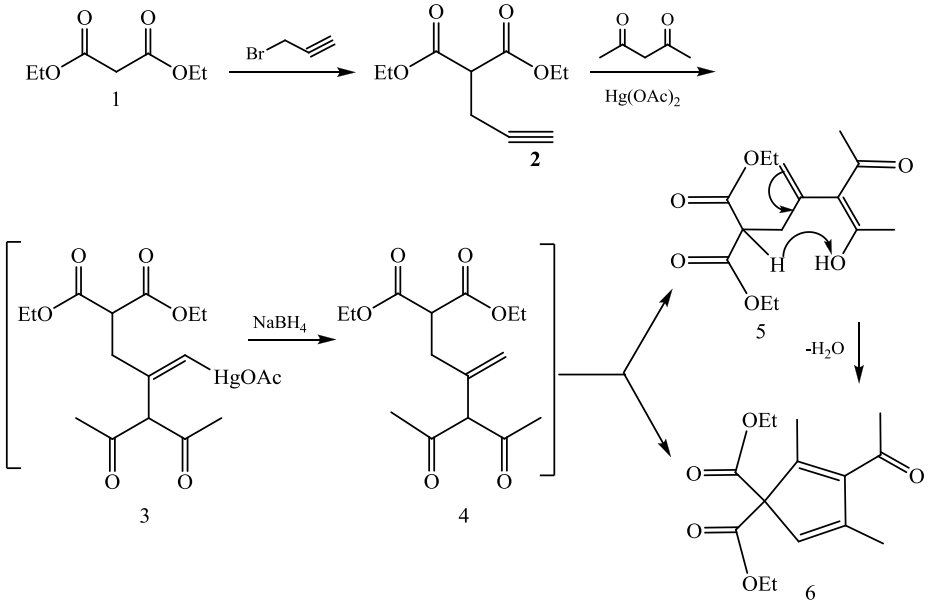

The mixture of linear **5** and cyclopentadienyl **6** derivatives was separated into the individual components by column chromatography.

In this work, we attempted to alkylate diethyl 2-(prop-2-yn-1-yl)malonate **2** with an equilibrium system obtained by condensation of acetylacetone and aniline [5] containing Schiff base **8** and its tautomeric form **9** in a 50: 50 ratio, as per ^{1}H NMR. A characteristic test for the presence of the imine-enamine mixture of **8** and **9** was the ratio of hydrogen atoms of enol **8** (12.4 ppm) and aniline **9** (5.1 ppm).

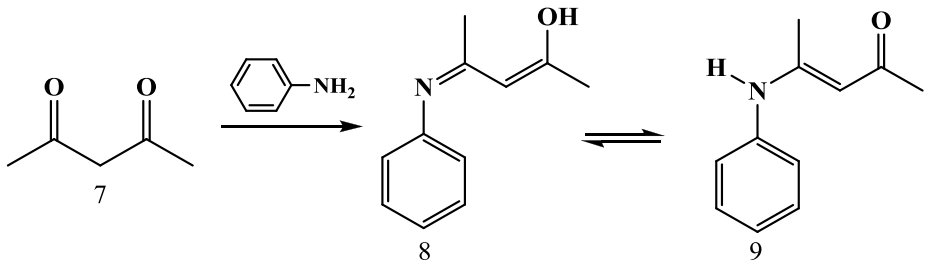

Similar to the data obtained earlier in [3], after solvolysis with sodium borohydride, products of N-alkylation of the terminal triple bond of diethyl 2-(prop-2- yn-1-yl)malonate were not isolated. It is likely that the reaction proceeded through the intermediate formation of unsaturated amines **10** and **11**, which under demercuration conditions were hydrolyzed to enol **12,** stabilized to diethyl 2-(2-oxopropyl)malonate **13**.

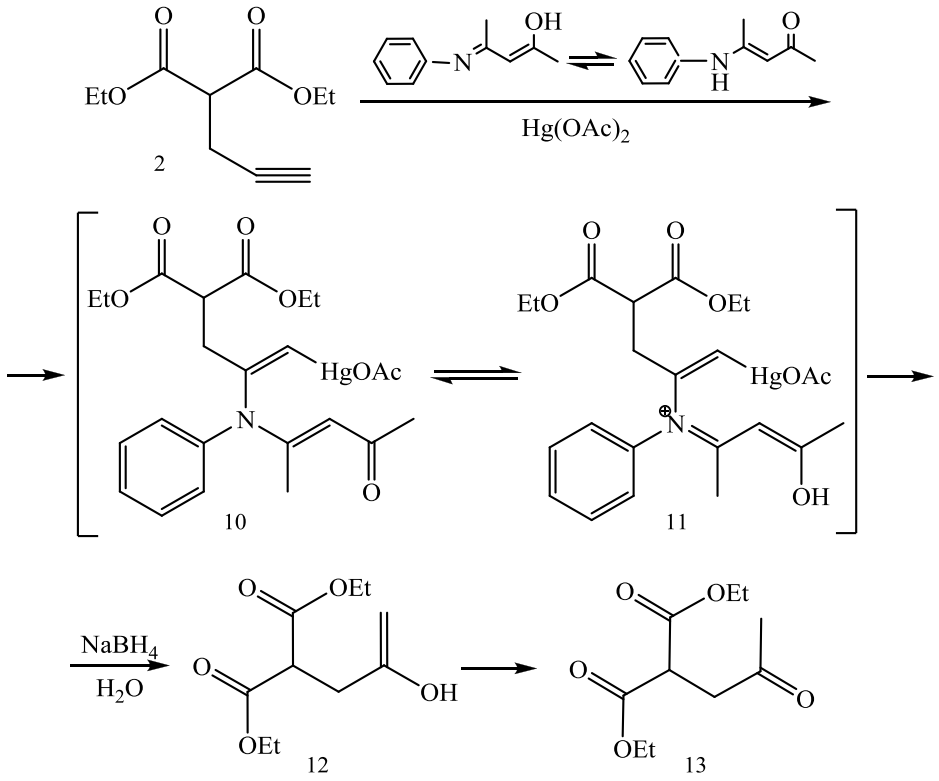

We failed to perform direct hydration (without the participation of amine) in the presence of mercury(II) acetate: only the initial substrate was present in the reaction mixture.

In conclusion, the reactions of diethyl 2-(prop-2-yn-1-yl)malonate with acetylacetone and its derivatives in the presence of mercury(II) acetate have been studied and derivatives of cyclopentadiene and ketoesters were formed.

Experimental Part

^{1}H and ^{13}C NMR spectra (300.07 and 75.46 *MHz* respectively) of the solutions in DMSO-*d6*–CCl4 (1:3) were recorded on a Varian "Mercury-300 VX" spectrometer at 303 K relative to internal TMS. The reaction progress was monitored by TLC using Silufol UV-254 plates, developing with $KMnO_4$ and iodine vapor. GLC analysis was performed using a LHM-80MD instrument (model 3) (1.5 *m* column, AW-NMDC sorbent soaked with 10% Carbovax-20M, rate of carrier gas 40 *mL*/*min*, detector temperature 200°C, evaporator temperature 250°C). Diethyl-2-(prop-2-ynyl)malonate was obtained by reacting sodium malonic ester with propargyl bromide as described in [6]**.**

Diethyl 2-(3-acetyl-4-hydroxy-2-methylenepent-3-enyl)malonate 5, diethyl 3-acetyl-2,4-dimethylcyclopenta-2,4-diene-1,1-dicarboxylate 6. 3.2 *g* of mercury(II) acetate (0.01 *mol*) was dissolved in 50 *ml* of THF, 1.98 *g* (0,01 *mol*) of diethyl 2-(prop-2-yn-1-yl)malonate **2** was added and the mixture was stirred for 1h

at 25 °C. Separately, from 0.23 *g* (0.01 *mol*) of sodium and 1 ml of acetylacetone in 10 *ml* of THF, sodium salt of acetylacetone was obtained, the complex was added and stirred for 12 *h*. Demercuration was carried out by adding 0.2 *g* (0.026 *mol*) of powdered sodium borohydride, the mixture was stirred for another 2 *h*, then the water-ether mixture was added in a 2: 1 ratio, the extracts were dried over magnesium sulfate.

After removal of the solvent, 2.0 *g* of residue was obtained, which was purified by chromatography on a column containing 70 *g* of silica gel (40-100 *μm*). Elution with CCl_4/ether in a 3:1 ratio yielded 0.95 *g* of diethyl 2-(3-acetyl-4-hydroxy-2-methylenepent-3-enyl)malonate **5** with R_f 0.65 (hexane/ether 1:1) and 0.86 *g* of diethyl 3-acetyl-2,4-dimethylcyclopenta-2,4-diene-1,1-dicarboxylate **6** with R_f 0.51 (hexane/ether 1:2).

^{1}H NMR for **5**, (300.07 MHz, DMSO-d6) δ, Hz: 1.77 (t, 3H, CH_3, *J*=7.1), 2.04 (s, 3H, $COCH_3$), 2.71 (ddd, 2H, CH_2, *J*=7.4, 1.5, 1.2Hz), 3.51 (t, 1H, CH, *J*=7,4), 4,15 (q, 2H, OCH_2, *J*=7.1), 5.00 (dt, 2H, =CH_2, *J*=1.5, 1.2), 5.3 (q, 2H, =CH_2, *J*=1.5). Found, %: C 60.79; H 7.39; Calc. for $C_{15}H_{22}O_6$, %: C 60.39; H 7.43.

^{1}H NMR for **6**, (300.07 MHz, DMSO-d6) δ: 1.23 (t, 6H, CH_3), 1.52 (s, 3H, CH_3), 1.95 (s, 3H, CH_3), 2.28 (s, 3H, CH_3), 4.13 (q, 4H, -CH_2CH_3), 5.05 (s, 1H, -C=CH-). Found, %: C 64.71; H 7.2; Calc. for $C_{15}H_{20}O_5$, %: C 64.27; H 7.19.

Reaction of acetylacetone with aniline. 19 *g* (0.2 *mol*) of aniline was dissolved in 160 *ml* of ethanol and 22 *ml* of acetylacetone was added. The reaction mixture was boiled with stirring for 15 *h* [5]. The ethanol was distilled in vacuo, cooled, crystals were separated and washed with ice water, dried under vacuum, heated in a water bath at 45^{o}C. Distillation of the residue in vacuo gave 4 *g* of a mixture of compounds **8** and **9** (the ratio by ^{1}H NMR 50:50).

^{1}H NMR of mixtures **8** and **9**, (400 MHz, DMSO-d6) δ: 1.23 (t, 6H, CH_3), 1.52 (s, 3H, CH_3), 1.95 (s, 3H, CH_3), 2.28 (s, 3H, CH_3), 4.13 (q, 4H, -CH_2CH_3), 5.05 (s, 1H, -C=CH-).

Diethyl 2-(2-oxopropyl)malonate 13. 4.8 g (0.015 *mol*) of mercury(II) acetate was dissolved in 50 *ml* of THF, 3 g (0.015 *mol*) of diethyl 2-(prop-2-yn-1-yl)malonate **2** was added and the mixture was stirred for 1 h at 25 °C. Separately, from 0.345 *g* (0.015 *mol*) of sodium and 2.6 *g* (0.015 *mol*) of imine-enamine mixture the corresponding salt was obtained, the complex was added and stirred for 15 *h* at 25°C. Demercuration was carried out by adding 0.3 *g* of powdered sodium borohydride with stirring for another 2 *h* and the water/ether mixture in a 2:1 ratio was added, the extracts were dried over magnesium sulfate. After removal of the solvent, 2.5 *g* of the residue was obtained. 1 *g* of this residue was purified by chromatography on a column containing 40 *g* of silica gel (40-100 *μm*). Elution with hexane/ether in a 5:1 ratio yielded 0.8 *g* of diethyl 2-(2-oxopropyl)malonate **13.** ^{1}H NMR (300.07 *MHz*, DMSO-d6) δ, *Hz*: 1.26 (t, 6H, CH_3, *J*=7.1), 2.16 (s, 3H, CH_3), 2.98 (d, 2H, CH_2, *J*=7.2), 3.68 (t, 1H, CH, *J*=7,2), 4.14 (q, 4H, OCH_2, *J*=7.1). ^{13}C NMR **13** (75.46 *MHz*, DMSO-d6) δ: 13.5 (CH_3), 28.9(CH_3), 41.1(CH_2), 46.1(CH), 60.5 (OCH_2), 167.6 (O-CO), 203.2 (CO).

ՊՐՈՊԱՐԳԻԼՄԱԼՈՆԱՏԻ ԵՎ ՆՈՒԿԼԵՈՖԻԼՆԵՐԻ ՓՈԽԱԶԴԵՑՈՒԹՅՈՒՆԸ ՄՆԴԻԿԻ(II) ԱՑԵՏԱՏԻ ՆԵՐԿԱՅՈՒԹՅԱՄԲ

Ն. Գ.ՀՈԲՈՍՅԱՆ, Ք. Վ.ԲԱԼՅԱՆ, Ռ. Ս.ՆԵՐՍԻՍՅԱՆ, Լ. Մ.ՂԱԼԵՉՅԱՆ, Ս. Ա.ՀՈՎԱԿԻՄՅԱՆ, Ռ.Բ.ՍԱՐԳՍՅԱՆ և Ժ. Ա. ՉՈԲԱՆՅԱՆ

Հետազոտվել է դիէթիլ-2-(պրոպ-2-ինիլ)մալոնատի փոխազդեցությունը տարաբնույթ նուկլեոֆիլների հետ մնդիկի (II) ացետատի ներկայությամբ: Դիկարբոնիլային միացության և միջանկյալ միացությունների վերականգնման բնույթից կախված ստացվել են չհագեցած կետոններ և ցիկլոպենտադիենի ածանցյալներ:

О РЕАГИРОВАНИИ ПРОПАРГИЛМАЛОНАТА С НУКЛЕОФИЛАМИ В ПРИСУТСТВИИ АЦЕТАТА РТУТИ (II)

Н. Г.ОБОСЯН, К. В. БАЛЯН, Р. С. НЕРСИСЯН, Л. М. ГАЛЕЧЯН, С. А. ОВАКИМЯН, А. Б. САРГСЯН и Ж. А. ЧОБАНЯН

Исследована региохимия взаимодействия диэтил-2-(проп-2-инил)малоната с различными нуклеофилами в присутствии ацетата (II) ртути. В зависимости от природы дикарбонильного соединения и условий восстановления промежуточных ртутьорганических соединений выделены непредельные кетоны и производное циклопентадиена.

REFERENCES

[1] *Боев В.И., Москаленко А.И., Боев А.М.* // Успехи химии, 1997, т. 66, с. 874 [Russ. Chem. Rev., 1997, 66, 789].

[2] *Баданян Ш.О., Чобанян Ж.А., Тиракян М.Р., Даниелян А.О.* // ХГС, 1998, т. 34, с. 904 [Chem. Heterocycl. Compd., 1998, 34, 781].

[3] *Обосян Н.Г., Балян К.В., Нерсисян Р.С., Саргсян А.Б., Чобанян Ж.А.* // ЖОХ, 2016, т. 86, с 746 [Russ. J. Gen. Chem., 2016, 86, 1011].

[4] *Балян К.В., Генджоян Л.М., Акопян В.В., Обосян Н.Г., Чобанян Ж.А*. // ЖОХ, 2014, т. 84, с. 1800 [Russ. J. Gen. Chem, 2014, 84, 2098].

[5] Adnan dib. // Int. J. Chem. Tech. Res., 2013, v. 5, p. 204.

[6] *Weygand-Hilgetag* Organisch-Chemische Experimentierkunst 3. Neubearbeitete Auflage, Johann Ambrosius Barth /Verlag/Leipzig, 1964, p. 944.

ՀԱՅԱՍՏԱՆԻ ՀԱՆՐԱՊԵՏՈՒԹՅԱՆ ԳԻՏՈՒԹՅՈՒՆՆԵՐԻ
ԱԶԳԱՅԻՆ ԱԿԱԴԵՄԻԱ
НАЦИОНАЛЬНАЯ АКАДЕМИЯ НАУК РЕСПУБЛИКИ АРМЕНИЯ
NATIONAL ACADEMY OF SCIENCES OF THE REPUBLIC OF ARMENIA

Հայաստանի քիմիական հանդես
Химический журнал Армении **71, №4, 2018** Chemical Journal of Armenia

UDC 548.737+541.124+547.314

SYNTHESIS OF NEW AMINO DERIVATIVES OF 9-(METHYLTHIO)THIENO[3,2-*d*]PYRIMIDINE AND AZIDE-TETRAZOLE EQUILIBRIUM

E. K. HAKOBYAN

The Scientific and Technological Centre
of Organic and Pharmaceutical Chemistry of NAS RA
26, Azatutyan Ave., Yerevan, 0014, Armenia
E-mail: hakobyan.elmira@mail.ru

Starting from the 7-chloro derivative of thieno[3,2-d]pyrimidine **1** a series of new amino derivatives of cyclopenta[4',5']pyrido[3',2':4,5]thieno[3,2-d]pyrimidine **2** were synthesized. By treatment of compound **3** with nitrous acid fused thieno[2,3-e]tetrazolo[1,5-c]pyrimidine **4** was synthesized. The azide/tetrazole equilibrium in this system **4A/4T** was observed and investigated.

References 15.

Fused thieno[3,2-*d*]pyrimidines are one of the ‘privileged medicinal scaffolds’, which are used for the development of pharmaceutical agents, showing a wide range of pharmacological activities [1]. In particular, the amino derivatives of pyrido[3',2':4,5]- thieno[3,2-*d*]pyrimidine have been shown to interact with a number of molecular targets including phosphodiesterase IV with potential use in the treatment of asthma and chronic obstructive pulmonary disease [2] and release control of tumor necrosis factor-α (TNFα) [3]. They also showed beta2 adrenoreceptor agonist activity [4] and distinguished by the pronounced antimicrobial activity [5].

On the other hand, the study of an azide-tetrazole equilibrium has attracted large attention and new condensed systems containing the tetrazole ring have always been investigated by both physico-chemical and computational methods [6–8].

In view of the above observations, the aim of this work is the synthesis and study of the properties of compounds containing amino groups in the pyrimidine ring, as well as compounds with a condensed tetrazolo[1,5-*c*]pyrimidine moiety.

The starting compound was 7-chloro-4-isobutyl-9-(methylthio)-2,3-dihydro-1*H*-cyclopenta[4',5']pyrido[3',2':4,5]thieno[3,2-*d*]pyrimidine (**1**) [9], which contains an ‘activated’ chlorine atom that could easily be displaced by nucleophiles. Thus, 7-

chlorothieno[3,2-*d*]- pyrimidine **1** was reacted with various amines to give a series of 7-amino-4-isobutyl-9-(methylthio)-2,3-dihydro-1*H*-cyclopenta[4',5']pyrido [3',2':4,5]thieno[3,2-*d*]pyrimidines **2a**–**w** in high yields (Scheme 1).

Scheme 1

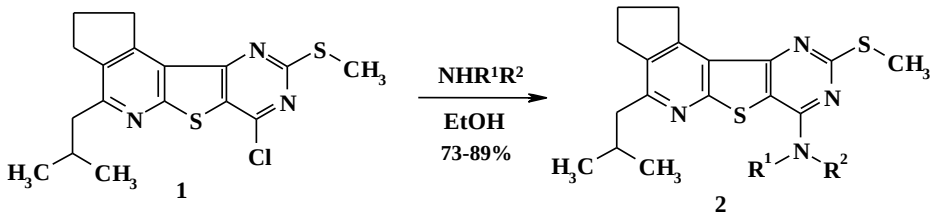

1 **2**

R^1 + R^2 = -$(CH_2)_5$- (**a**); R^1 + R^2 = -$(CH_2)_2O(CH_2)_2$- (**b**); R^1+ R^2 = -$(CH_2)_2NMe(CH_2)_2$- (**c**); R^1+ R^2 = -$(CH_2)_2NEt(CH_2)_2$- (**d**); R^1 + R^2 = -$(CH_2)_2N(CH_2)_2OH(CH_2)_2$- (**e**); R^1 = H, R^2 = CH_2CH_2OH (**f**); R^1 = H, R^2 = CH_2CH_2OMe (**g**); R^1 = H, R^2 = $CH_2CH(OMe)_2$ (**h**); R^1 = H, R^2 = $CH_2CH(Me)OH$ (**i**); R^1 = H, R^2 = $CH_2CH_2N(Me)_2$ (**j**); R^1 = H, R^2 = $CH_2CH_2N(Et)_2$ (**k**); R^1 = H, R^2 = 2-morpholinoethyl (**l**); R^1 = H, R^2 = $(CH_2)_3N(Me)_2$ (**m**); R^1 = H, R^2 = $(CH_2)_3OH$ (**n**); R^1 = H, R^2 = $(CH_2)_3OCH_3$ (**o**); R^1 = H, R^2 = 2-furylmethyl (**p**); R^1 = H, R^2 = Bn (**q**); R^1 = H, R^2 = 2-pyridylmethyl (**r**); R^1 = H, R^2 = 3-pyridylmethyl (**s**); R^1 = H, R^2 = CH_2CH_2Ph (**t**); R^1 = R^2 = C_2H_5 (**u**); R^1 = CH_3, R^2 = CH_2CH_2OH(**v**); R^1 = C_2H_5, R^2 = CH_2CH_2OH (**w**).

7-Chlorothieno[3,2-*d*]pyrimidine **1** was reacted with an excess of hydrazine hydrate in ethanol at reflux affording the 7-hydrazino-4-isobutyl-9-(methylthio)-2,3-dihydro-1*H*-cyclopenta[4',5']pyrido[3',2':4,5]thieno[3,2-*d*]pyrimidine (**3**) [9] (Scheme 2). Next, the 7-hydrazino derivative **3** was treated with sodium nitrite in acetic acid at 0−5°C, giving the targeted 7-azidothieno[3,2-*d*]pyrimidine/thieno[2,3-*e*]tetrazolo[1,5-*c*]pyrimidine **4A/T** in excellent yield (Scheme 2).

It was observed that the azide/tetrazole equilibrium was present in newly synthesized compound **4**. In fact, its ^{1}H NMR spectrum in DMSO-d_6/CCl_4 1/3 showed the expected double set of signals. The ratio of the tautomers **4A**:**4T** in the solution of DMSO-d_6/CCl_4 1/3 was found to be 3:2. In the solution of $CDCl_3$ the **4A**:**4T** ratio was not essentially changed, while in the solution of DMSO-d_6 the **4A**:**4T** ratio was 1:4.56. Moreover, all of the chemical shifts of the tetrazolo form, as a rule, appeared in a weaker field than the corresponding ones of the azido form [6–8, 10, 11].

The IR spectrum of compound **4** in the solution of $CHCl_3$ showed the characteristic bonds of azido group at ν 2155 and 2138 cm^{-1}. Thus, based on spectroscopic results it can be concluded that compound **4** in the solid state is present exclusively in the tetrazolo tautomeric form, while in the solution it exists as a mixture of two isomeric forms.

Scheme 2

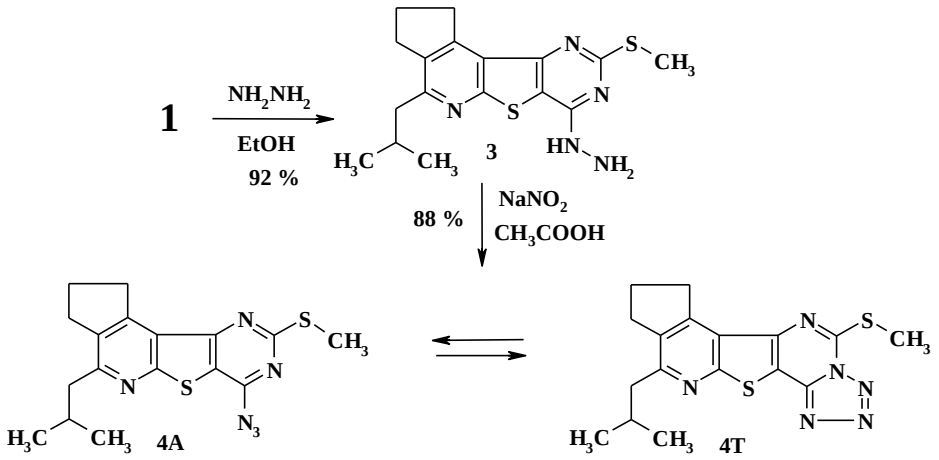

It was also interesting to examine nucleophilic reactivity in compound **4**. For this purpose compound **4** was reacted with some amines (2-aminoethanol, morpholine and pyrrolidine) under harsher experimental conditions: i.e., by refluxing (5 h) in the absence of any solvent and using an excess of amine (substrate:amine ratio = 1:5). Under these experimental conditions, the substitution of an azide group took place only in the case of pyrrolidine. Moreover, the nucleophilic substitution not only of an azide group, but also of the SCH_3 group occurred with formation of the relevant 4-isobutyl-7,9-dipyrrolidin-1-yl-2,3-dihydro-1*H*-cyclopenta[4',5']pyrido[3',2':4,5]thieno[3,2-*d*]pyrimidine (**5**) (Scheme 3). The ^{1}H NMR spectra of compound **5** did not show the singlet signal of the SCH_3 group at 2.65/2.94 ppm characteristic of initial compound **4**, but showed the protons of the pyrrolidino group twice. The structure of compound **5** was also supported by the IR and ^{13}C NMR data.

In the case of 2-aminoethanol and morpholine under such experimental conditions the decomposition of the azido group [12–15] with formation of 4-isobutyl-9-(methylthio)-2,3-dihydro-1*H*-cyclopenta[4',5']pyrido[3',2':4,5]thieno[3,2-*d*]pyrimidin-7-amine (**6**) [9] took place (Scheme 3).

Further, with the aim to avoid decomposition of azido group and by lengthening the reaction time (15 h) compound **4** was reacted with morpholine in ethanol. As a result the desired 7-azido-4-isobutyl-9-morpholin-4-yl-2,3-dihydro-1*H*-cyclopenta[4',5']pyrido[3',2':4,5] -thieno[3,2-*d*]pyrimidine (**7**) was obtained (Scheme 3). Interestingly, the azide-tetrazole equilibrium in this compound **7** was not observed. Thus, in the ^{1}H NMR spectra of compound **7** in the solution of DMSO-d_6/CCl_4 1/3 the expected double set of signals was absent. Moreover, the signal of the SCH_3 group at 2.65/2.94 ppm was also absent, while the presence of the morpholino fragment was observed. The IR spectra of compound **7** in the cyristalline state showed the characteristic bond of azido group at ν 2131 cm^{-1}.

Scheme 3

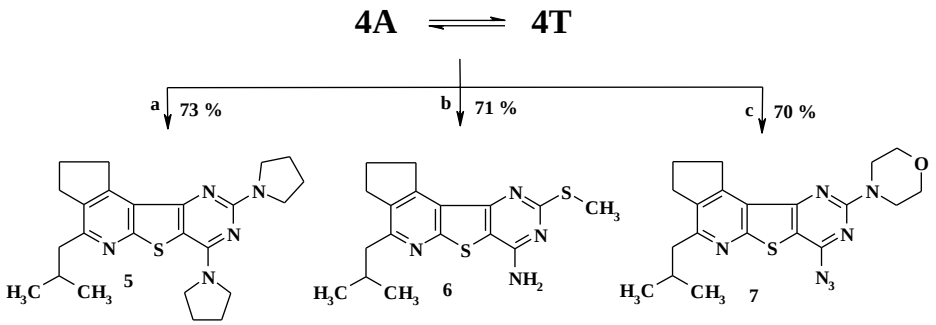

(a) pyrrolidine, reflux 5 h; (b) morpholine or 2-aminoethanol, reflux 5 h; (c) morpholine, EtOH, reflux 15 h

In summary, the synthesis of new amino derivatives of cyclopenta[4',5']pyrido-[3',2':4,5]thieno[3,2-*d*]pyrimidine **2** as well as of 7-azidothieno[3,2-*d*]pyrimidine/thieno[2,3-*e*] -tetrazolo[1,5-*c*]pyrimidine **4A/T** has been described starting from the corresponding 7-chlorothieno[3,2-*d*]pyrimidine **1**. The studies of azide/tetrazole equilibrium revealed that the insertion of the SCH_3 group in the pyrimidine ring in compound **4** shifted the azide-tetrazole equilibrium to the azido side [8]. In addition, the replacement of SCH_3 as well as azido groups with amines was carried out. It was interesting that the insertion of the amino fragment in the pyrimidine ring (compound **7**) significantly affected the azide/tetrazole equilibrium and completely shifted the azide-tetrazole equilibrium to the azido form.

Experimental Section

^1H and ^{13}C NMR spectra were recorded in DMSO-d_6, DMSO/CCl_4, 1/3 and $CDCl_3$ solutions (300 *MHz* for ^1H and 75 *MHz* for ^{13}C, respectively) on a Varian "Mercury 300VX" spectrometer. Chemical shifts were reported as δ (parts per million) relative to TMS as an internal standard. IR spectra were recorded on "Nicolet Avatar 330 FT-IR" spectrophotometer and the reported wave numbers were given in cm^{-1}. The elemental analyses were obtained by the Korshun–Klimova (C, H) and Dumas–Pregl methods (N). The melting points were determined with a Boetius micro hot stage. Compounds **1**, **6** and **3** [9] were already described.

General procedure for the synthesis of compounds 2a–w. A mixture of compound **1** (1.82 *g*, 5 *mmol*) and of corresponding amine (11 *mmol*) in absolute ethanol (50 *mL*) was refluxed for 5 *h*. The ethanol was distilled off to dryness, water (25 *mL*) was added to the residue. The separated crystals were filtered off, washed with water, dried, and recrystallized from ethanol.

4-Isobutyl-9-(methylthio)-7-piperidin-1-yl-2,3-dihydro-1*H*-cyclopenta[4',5'] pyrido-[3',2':4,5]thieno[3,2-*d*]pyrimidine (2a). Yield 85%; mp 122-124°C. Anal. Calcd for $C_{22}H_{28}N_4S_2$: C 64.04; H 6.84; N 13.58 %. Found: C 64.34; H 7.02; N 13.82 %. ^1H NMR δ, ppm, *Hz*: 0.98 (d, 6H, *J* = 6.7, $CH(C\underline{H}_3)_2$); 1.67–1.82 (m, 6H, $(CH_2)_3$, $C_5H_{10}N$); 2.15-2.33 (m, 3H, $C\underline{H}(CH_3)_2$, 2-CH_2); 2.55 (s, 3H, SCH_3); 2.71 (d,

2H, *J* = 7.2 *Hz*, CHC$\underline{H}_2$); 2.99 (t, 2H, *J* = 7.5, 3-CH_2); 3.56 (t, 2H, *J* = 7.6, 1-CH_2); 3.87-3.99 (m, 4H, N(CH_2)$_2$).

4-Isobutyl-9-(methylthio)-7-morpholin-4-yl-2,3-dihydro-1*H*-cyclopenta [4',5']pyri-do[3',2':4,5]thieno[3,2-*d*]pyrimidine (2b). Yield 89%; mp 159-161^{o}C. Anal. Calcd for $C_{21}H_{26}N_4OS_2$: C 60.84; H 6.32; N 13.51 %. Found: C 61.17; H 6.54; N 13.76%. ^{1}H NMR δ, ppm, *Hz*: 0.98 (d, 6H, *J* = 6.7, CH(C$\underline{H}_3$)$_2$); 2.15-2.33 (m, 3H, C$\underline{H}$(CH_3)$_2$, 2-CH_2); 2.56 (s, 3H, SCH_3); 2.72 (d, 2H, *J* = 7.2, CHC$\underline{H}_2$); 3.00 (t, 2H, *J* = 7.5, 3-CH_2); 3.58 (t, 2H, *J* = 7.6, 1-CH_2); 3.76-3.85 (m, 4H, N(CH_2)$_2$); 3.90–3.98 (m, 4H, O(CH_2)$_2$).

4-Isobutyl-7-(4-methylpiperazin-1-yl)-9-(methylthio)-2,3-dihydro-1*H*-cyclopenta-[4',5']-pyrido[3',2':4,5]thieno[3,2-*d*]pyrimidine (2c). Yield 74%; mp 132-134^{o}C. Anal. Calcd for $C_{22}H_{29}N_5S_2$: C 61.79; H 6.84; N 16.38%. Found: C 62.14; H 7.04; N 16.63 %. ^{1}H NMR δ, ppm, *Hz*: 0.98 (d, 6H, *J* = 6.7, CH(C$\underline{H}_3$)$_2$); 2.15-2.33 (m, 3H, C$\underline{H}$(CH_3)$_2$, 2-CH_2); 2.29 (s, 3H, NCH_3); 2.48-2.53 (m, 4H, CH_3N(C$\underline{H}_2$)$_2$); 2.54 (s, 3H, SCH_3); 2.70 (d, 2H, *J* = 7.2 *Hz*, CHC$\underline{H}_2$), 2.98 (t, 2H, *J* = 7.5, 3-CH_2); 3.54 (t, 2H, *J* = 7.6, 1-CH_2); 3.86–3.99 (m, 4H, N(CH_2)$_2$).

7-(4-Ethylpiperazin-1-yl)-4-isobutyl-9-(methylthio)-2,3-dihydro-1*H*-cyclopenta-[4',5']-pyrido[3',2':4,5]thieno[3,2-*d*]pyrimidine (2d). Yield 77%; mp 157-159^{o}C. Anal. Calcd for $C_{23}H_{31}N_5S_2$: C 62.55; H 7.07; N 15.86%. Found: C 62.87; H 7.25; N 16.10 %.^{1}H NMR δ, ppm, *Hz*: 0.98 (d, 6H, *J* = 6.7, CH(C$\underline{H}_3$)$_2$); 1.15 (t, *J* = 7.2 *Hz*, 3H, $NCH_2C\underline{H}_3$), 2.16-2.33 (m, 3H, C$\underline{H}$(CH_3)$_2$, 2-CH_2); 2.45 (q, *J* = 7.2 *Hz*, 2H, $NC\underline{H}_2CH_3$); 2.54–2.60 (m, 4H, C_2H_5N(C$\underline{H}_2$)$_2$); 2.55 (s, 3H, SCH_3); 2.70 (d, 2H, *J* = 7.2 *Hz*, CHC$\underline{H}_2$); 3.00 (t, 2H, *J* = 7.5, 3-CH_2); 3.58 (t, 2H, *J* = 7.6, 1-CH_2); 3.96–4.07 (m, 4H, N(CH_2)$_2$).

2-{4-[4-Isobutyl-9-(methylthio)-2,3-dihydro-1*H*-cyclopenta[4',5']pyrido [3',2':4,5]-thieno[3,2-*d*]pyrimidin-7-yl]piperazin-1-yl}ethanol (2e). Yield 81%; mp 166-168^{o}C. Anal. Calcd for $C_{23}H_{31}N_5OS_2$: C 60.36; H 6.83; N 15.30%. Found: C 60.67; H 7.04; N 15.52 %. ^{1}H NMR δ, ppm, *Hz*: 0.98 (d, 6H, *J* = 6.7, CH(C$\underline{H}_3$)$_2$); 2.16-2.33 (m, 3H, C$\underline{H}$(CH_3)$_2$, 2-CH_2), 2.56 (s, 3H, SCH_3); 2.48–2.54 (m, 2H, OHC$\underline{H}_2$); 2.71 (d, 2H, *J* = 7.2 *Hz*, CHC$\underline{H}_2$); 2.62-2.73 (m, 4H, CH_2N(C$\underline{H}_2$)$_2$); 3.00 (t, 2H, *J* = 7.5, 3-CH_2); 3.57 (t, 2H, *J* = 7.6, 1-CH_2); 3.53–3.61 (m, 2H, OHCH_2C$\underline{H}_2$); 3.82–3.96 (br, 1H, O$\underline{H}$CH_2CH_2); 3.92–4.02 (m, 4H, N(CH_2)$_2$).

2-{[4-Isobutyl-9-(methylthio)-2,3-dihydro-1*H*-cyclopenta[4',5']pyrido [3',2':4,5]-thieno-[3,2-*d*]pyrimidin-7-yl]amino}ethanol (2f). Yield 87%; mp 134-136^{o}C. Anal. Calcd for $C_{19}H_{24}N_4OS_2$: C 62.14; H 6.78; N 14.49 %. Found: C 62.50; H 6.97; N 14.73%. ^{1}H NMR δ, ppm, *Hz*: 0.99 (d, 6H, *J* = 6.7, CH(C$\underline{H}_3$)$_2$); 2.15–2.33 (m, 3H, C$\underline{H}$(CH_3)$_2$, 2-CH_2); 2.55 (s, 3H, SCH_3); 2.71 (d, 2H, *J* = 7.2 *Hz*, CHC$\underline{H}_2$); 3.00 (t, 2H, *J* = 7.5, 3-CH_2); 3.57 (t, 2H, *J* = 7.6, 1-CH_2); 3.61–3.72 (m, 4H, NHC$\underline{H}_2$C$\underline{H}_2$OH); 3.66 (br, 1H, OH); 7.32 (br. t, 1H, *J* = 4.8, NH).

4-Isobutyl-N-(2-methoxyethyl)-9-(methylthio)-2,3-dihydro-1*H*-cyclopenta[4',5']pyri-do[3',2':4,5]-thieno[3,2-*d*]pyrimidin-7-amine (2g). Yield 77%; mp 148-150^{o}C. Anal. Calcd for $C_{20}H_{26}N_4OS_2$: C 59.67; H 6.51; N 13.92%. Found: C 60.02; H 6.71; N 14.18 %.^{1}H NMR δ, ppm, *Hz*: 0.98 (d, 6H, *J* = 6.7,

CH(C<u>H</u>$_3$)$_2$); 2.15–2.33 (m, 3H, C<u>H</u>(CH$_3$)$_2$, 2-CH$_2$); 2.55 (s, 3H, SCH$_3$); 2.70 (d, 2H, *J* = 7.2 *Hz*, CHC<u>H</u>$_2$); 3.00 (t, 2H, *J* = 7.5, 3-CH$_2$); 3.35 (s, 3H, OCH$_3$); 3.56 (t, 2H, *J* = 7.6, 1-CH$_2$); 3.51–3.62 (m, 2H, NHCH$_2$C<u>H</u>$_2$OCH$_3$); 3.66–3.76 (m, 2H, HNC<u>H</u>$_2$CH$_2$); 7.51 (br. t, 1H, *J* = 5.5, NH).

***N*-(2,2-Dimethoxyethyl)-4-isobytyl-9-(methylthio)-2,3-dihydro-1*H*-cyclopenta-[4',5']pyrido[3',2':4,5]thieno[3,2-*d*]pyrimidin-7-amine (2h).** Yield 84%; mp 138-140°C. Anal. Calcd for $C_{21}H_{28}N_4O_2S_2$: C 58.30; H 6.52; N 12.95%. Found: C 58.64; H 6.73; N 13.18%.^{1}H NMR δ, ppm, *Hz*: 0.98 (d, 6H, *J* = 6.7, CH(C<u>H</u>$_3$)$_2$); 2.15–2.33 (m, 3H, C<u>H</u>(CH$_3$)$_2$, 2-CH$_2$); 2.56 (s, 3H, SCH$_3$); 2.70 (d, 2H, *J* = 7.2 *Hz*, CHC<u>H</u>$_2$); 3.00 (t, 2H, *J* = 7.5, 3-CH$_2$); 3.36 (s, 6H, CH(OC<u>H</u>$_3$)$_2$); 3.56 (t, 2H, *J* = 7.6, 1-CH$_2$); 3.58–3.65 (m, 2H, HNC<u>H</u>$_2$); 4.64 (t, *J* = 5.7 *Hz*, 1H, HNCH$_2$C<u>H</u>); 7.57 (br. t, 1H, *J* = 5.7, NH).

1-{[4-Isobutyl-9-(methylthio)-2,3-dihydro-1*H*-cyclopenta[4',5']pyrido [3',2':4,5]-thieno[3,2-*d*]pyrimidin-7-yl]amino}propan-2-ol (2i). Yield 82%; mp 153-155°C. Anal. Calcd for $C_{20}H_{26}N_4OS_2$: C 59.67; H 6.51; N 13.92%. Found: C 59.97; H 6.69; N 14.17%. ^{1}H NMR δ, ppm, *Hz*: 0.98 (d, 6H, *J* = 6.7, CH(C<u>H</u>$_3$)$_2$); 1.17 (d, *J* = 6.3 *Hz*, 3H, CHC<u>H</u>$_3$); 2.15–2.33 (m, 3H, C<u>H</u>(CH$_3$)$_2$, 2-CH$_2$); 2.56 (s, 3H, SCH$_3$); 2.70 (d, 2H, *J* = 7.2, CHC<u>H</u>$_2$); 3.00 (t, 2H, *J* = 7.5, 3-CH$_2$); 3.35 (ddd, 1H, *J* = 13.4, 7.4, 5.0, NHC<u>H</u>$_2$); 3.55 (t, 2H, *J* = 7.6, 1-CH$_2$); 3.60 (br, 1H, OH); 3.63 (ddd, 1H, *J* = 13.4, 6.4, 4.4, NHC<u>H</u>$_2$); 3.88–3.99 (m, 1H, C<u>H</u>CH$_3$); 7.21 (t, 1H, *J* = 5.7, NH).

***N'*-[4-Isobutyl-9-(methylthio)-2,3-dihydro-1*H*-cyclopenta[4',5']pyrido [3',2':4,5]-thieno[3,2-*d*]pyrimidin-7-yl]-*N*,*N*-dimethylethane-1,2-diamine (2j).** Yield 89%; mp 112-114°C. Anal. Calcd for $C_{21}H_{29}N_5S_2$: C 60.69; H 7.03; N 16.85 %. Found: C 61.01; H 7.25; N 17.09 %. ^{1}H NMR δ, ppm, *Hz*: 0.98 (d, 6H, *J* = 6.7, CH(C<u>H</u>$_3$)$_2$); 2.15–2.31 (m, 3H, C<u>H</u>(CH$_3$)$_2$, 2-CH$_2$); 2.33 (s, 6H, N(CH$_3$)$_2$), 2-CH$_2$); 2.56 (s, 3H, SCH$_3$); 2.63 (t, *J* = 6.7, 2H, C<u>H</u>$_2$N(CH$_3$)$_2$); 2.70 (d, 2H, *J* = 7.2, CHC<u>H</u>$_2$); 3.00 (t, 2H, *J* = 7.5, 3-CH$_2$); 3.57 (t, 2H, *J* = 7.6, 1-CH$_2$); 3.67 (td, 2H, *J* = 6.5, 5.9, NHC<u>H</u>$_2$); 7.20 (t, 1H, *J* = 5.5, NH).

***N*,*N*-diethyl-*N'*-[4-isobutyl-9-(methylthio)-2,3-dihydro-1*H*-cyclopenta[4',5'] pyrido[3',2':4,5]thieno[3,2-*d*]pyrimidin-7-yl]ethane-1,2-diamine (2k).** Yield 78%; mp 99-101°C. Anal. Calcd for $C_{23}H_{33}N_5S_2$: C 62.26; H 7.50; N 15.78 %. Found: C 61.95; H 7.71; N 16.00 %. ^{1}H NMR δ, ppm, *Hz*: 0.98 (d, 6H, *J* = 6.7, CH(C<u>H</u>$_3$)$_2$); 1.06 (t, 6H, *J* = 7.0, (CH$_2$C<u>H</u>$_3$)$_2$); 2.15–2.31 (m, 3H, C<u>H</u>(CH$_3$)$_2$, 2-CH$_2$), 2.57 (s, 3H, SCH$_3$); 2.54–2.64 (m, 4H, (CH$_2$C<u>H</u>$_3$)$_2$); 2.60 (t, *J* = 7.0, 2H, C<u>H</u>$_2$N(C$_2$H$_5$)$_2$); 2.70 (d, 2H, *J* = 7.2, CHC<u>H</u>$_2$); 2.98 (t, 2H, *J* = 7.5, 3-CH$_2$); 3.50–3.63 (m, 2H, NHC<u>H</u>$_2$); 3.56 (t, 2H, *J* = 7.6, 1-CH$_2$); 7.12 (br. t, 1H, *J* = 4.8, NH).

4-Isobutyl-9-(methylthio)-*N*-(2-morpholin-4-ylethyl)-2,3-dihydro-1*H*-cyclopenta-[4',5']pyrido[3',2':4,5]thieno[3,2-*d*]pyrimidin-7-amine (2l). Yield 84%; mp 125-127°C. Anal. Calcd for $C_{23}H_{31}N_5OS_2$: C 60.36; H 6.83; N 15.30 %. Found: C 59.99; H 6.63; N 15.06 %. ^{1}H NMR δ, ppm, *Hz*: 0.98 (d, 6H, *J* = 6.7, CH(C<u>H</u>$_3$)$_2$); 2.15–2.31 (m, 3H, C<u>H</u>(CH$_3$)$_2$, 2-CH$_2$); 2.56 (s, 3H, SCH$_3$); 2.48–2.58 (m, 4H, N(CH$_2$)$_2$); 2.59 (t, *J* = 6.7, 2H, C<u>H</u>$_2$N(CH$_2$)$_2$); 2.71 (d, 2H, *J* = 7.2, CHC<u>H</u>$_2$);

3.00 (t, 2H, *J* = 7.5, 3-CH_2); 3.57 (t, 2H, *J* = 7.6, 1-CH_2); 3.56–3.62 (m, 4H, O(CH_2)$_2$); 3.70 (td, 2H, *J* = 6.5, 5.9, NHC$\underline{H}_2$); 7.29 (t, 1H, *J* = 5.6, NH).

***N'*-[4-Isobutyl-9-(methylthio)-2,3-dihydro-1*H*-cyclopenta[4',5']pyrido [3',2':4,5]-thieno[3,2-*d*]pyrimidin-7-yl]-*N*,*N*-dimethylpropane-1,3-diamine (2m).** Yield 84%; mp 129-131°C. Anal. Calcd for $C_{22}H_{31}N_5S_2$: C 61.50; H 7.27; N 16.30 %. Found: C 61.85; H 7.46; N 16.55 %. ^{1}H NMR δ, ppm, *Hz*: 0.98 (d, 6H, *J* = 6.7, CH(C$\underline{H}_3$)$_2$); 1.78–1.90 (m, 2H, NHCH$_2$C$\underline{H}_2$); 2.15–2.31 (m, 3H, C$\underline{H}$(CH$_3$)$_2$, 2-CH_2); 2.30 (s, 6H, N(CH_3)$_2$); 2.45 (br, 2H, C$\underline{H}_2$N(CH_3)$_2$); 2.55 (s, 3H, SCH_3); 2.71 (d, 2H, *J* = 7.2, CHC$\underline{H}_2$); 3.00 (t, 2H, *J* = 7.5, 3-CH_2); 3.56 (t, 2H, *J* = 7.6, 1-CH_2); 3.61 (td, 2H, *J* = 6.8, 5.5, NHC$\underline{H}_2$); 7.73 (t, 1H, *J* = 5.5, NH).

3-{[4-Isobutyl-9-(methylthio)-2,3-dihydro-1*H*-cyclopenta[4',5']pyrido [3',2':4,5]-thieno[3,2-*d*]pyrimidin-7-yl]amino}propan-1-ol (2n). Yield 89%; mp 177-179°C. Anal. Calcd for $C_{20}H_{26}N_4OS_2$: C 59.67; H 6.51; N 13.92 %. Found: C 59.98.; H 6.68; N 14.15 %.^{1}H NMR δ, ppm, *Hz*: 0.98 (d, 6H, *J* = 6.7, CH(C$\underline{H}_3$)$_2$); 1.77–1.87 (m, 2H, NHCH$_2$C$\underline{H}_2$); 2.15–2.31 (m, 3H, C$\underline{H}$(CH$_3$)$_2$, 2-CH_2); 2.56 (s, 3H, SCH_3); 2.70 (d, 2H, *J* = 7.2 *Hz*, CHC$\underline{H}_2$); 2.99 (t, 2H, *J* = 7.5, 3-CH_2); 3.55 (t, 2H, *J* = 7.6, 1-CH_2); 3.57–3.68 (m, 4H, OHC$\underline{H}_2$, NHC$\underline{H}_2$); 4.17 (br, 1H, OH); 7.42 (br t, 1H, *J* = 5.5, NH).

4-Isobutyl-*N*-(3-methoxypropyl)-9-(methylthio)-2,3-dihydro-1*H*-cyclopenta [4',5']-pyrido[3',2':4,5]thieno[3,2-*d*]pyrimidin-7-amine (2o). Yield 83%; mp 142-144°C. Anal. Calcd for $C_{21}H_{28}N_4OS_2$: C 60.54; H 6.77; N 13.45 %. Found: C 60.88; H 6.98; N 13.70 %. ^{1}H NMR δ, ppm, *Hz*: 0.98 (d, 6H, *J* = 6.7, CH(C$\underline{H}_3$)$_2$); 1.85–1.97 (m, 2H, NHCH$_2$C$\underline{H}_2$); 2.15–2.33 (m, 3H, C$\underline{H}$(CH$_3$)$_2$, 2-CH_2); 2.55 (s, 3H, SCH_3); 2.71 (d, 2H, *J* = 7.2, CHC$\underline{H}_2$); 3.00 (t, 2H, *J* = 7.5, 3-CH_2); 3.31 (c, 3H, OCH_3); 3.45 (t, 2H, *J* = 7.6, 1-CH_2); 3.51–3.64 (m, 4H, NHC$\underline{H}_2$C$\underline{H}_2$); 7.44 (br t, 1H, *J* = 5.5, NH).

***N*-(2-Furylmethyl)-4-isobutyl-9-(methylthio)-2,3-dihydro-1*H*-cyclopenta [4',5']pyrido[3',2':4,5]thieno[3,2-*d*]pyrimidin-7-amine (2p).** Yield 80%; mp 80-82 °C. Anal. Calcd for $C_{22}H_{24}N_4OS_2$: C 62.23; H 5.70; N 13.20 %. Found: C 62.59; H 5.89; N 13.43 %. ^{1}H NMR δ, ppm, *Hz*: 0.98 (d, 6H, *J* = 6.7, CH(C$\underline{H}_3$)$_2$); 2.15–2.33 (m, 3H, C$\underline{H}$(CH$_3$)$_2$, 2-CH_2), 2.55 (s, 3H, SCH_3); 2.71 (d, 2H, *J* = 7.2, CHC$\underline{H}_2$); 2.98 (t, 2H, *J* = 7.5, 3-CH_2); 3.56 (t, 2H, *J* = 7.6, 1-CH_2); 4.74 (d, 2H, *J* = 5.6, NHC$\underline{H}_2$); 6.25–6.32 (m, 2H, 3,4-CH_{fur}.); 7.37 (dd, 1H, *J* = 1.7, 0.8, 5-CH_{fur}); 7.98 (br t, 1H, *J* = 5.7, NH).

***N*-Benzyl-4-isobutyl-9-(methylthio)-2,3-dihydro-1*H*-cyclopenta[4',5']pyrido [3',2':4,5]thieno[3,2-*d*]pyrimidin-7-amine (2q).** Yield 86%; mp 76-78°C. Anal. Calcd for $C_{24}H_{26}N_4S_2$: C 66.32; H 6.03; N 12.89 %. Found: C 66.64; H 6.21; N 13.13 %. ^{1}H NMR δ, ppm, *Hz*: 0.98 (d, 6H, *J* = 6.7, CH(C$\underline{H}_3$)$_2$); 2.15–2.33 (m, 3H, C$\underline{H}$(CH$_3$)$_2$, 2-CH_2); 2.52 (s, 3H, SCH_3); 2.70 (d, 2H, *J* = 7.2, CHC$\underline{H}_2$); 3.00 (t, 2H, *J* = 7.5, 3-CH_2); 3.56 (t, 2H, *J* = 7.6, 1-CH_2); 4.76 (d, 2H, *J* = 5.9 , NHC$\underline{H}_2$); 7.16–7.41 (m, 5H, Ph); 8.08 (t, 1H, *J* = 5.7, NH).

4-Isobutyl-9-(methylthio)-*N*-(pyridin-2-ylmethyl)-2,3-dihydro-1*H*-cyclopenta-[4',5']pyrido[3',2':4,5]thieno[3,2-*d*]pyrimidin-7-amine (**2r**). Yield

73%; mp 181-183 °C. Anal. Calcd for $C_{23}H_{25}N_5S_2$: C 63.42; H 5.78; N 16.08%. Found: C 63.77; H 5.98; N 16.31 %. ^{1}H NMR δ, ppm, *Hz*: 0.98 (d, 6H, *J* = 6.7, CH(C<u>H</u>$_3$)$_2$); 2.15–2.33 (m, 3H, C<u>H</u>(CH$_3$)$_2$, 2-CH$_2$); 2.47 (s, 3H, SCH$_3$); 2.72 (d, 2H, *J* = 7.2, CHC<u>H</u>$_2$); 3.01 (t, 2H, *J* = 7.5, 3-CH$_2$); 3.56 (t, 2H, *J* = 7.6, 1-CH$_2$); 4.86 (d, 2H, *J* = 5.8, NHC<u>H</u>$_2$); 7.20 (ddd, 1H, *J* = 7.5, 4.7, 1.0, 5-CH-C$_5$H$_4$N); 7.38 (ddd, 1H, *J* = 7.6, 1.1, 0.9, 3-CH-C$_5$H$_4$N); 7.68 (ddd, 1H, *J* = 7.9, 7.4, 1.8, 4-CH-C$_5$H$_4$N); 8.10 (t, 1H, *J* = 5.8, NH); 8.51 (ddd, 1H, *J* = 4.8, 1.8, 0.9, 6-CH-C$_5$H$_4$N).

4-Isobutyl-9-(methylthio)-*N*-(pyridin-3-ylmethyl)-2,3-dihydro-1*H*-cyclopenta-[4',5']pyrido[3',2':4,5]thieno[3,2-*d*]pyrimidin-7-amine (2s). Yield 77%; mp 109-111°C. Anal. Calcd for $C_{23}H_{25}N_5S_2$: C 63.42; H 5.78; N 16.08%. Found: C 63.72; H 5.97; N 16.33 %. ^{1}H NMR δ, ppm, *Hz*: 0.98 (d, 6H, *J* = 6.7, CH(C<u>H</u>$_3$)$_2$); 2.15–2.33 (m, 3H, C<u>H</u>(CH$_3$)$_2$, 2-CH$_2$); 2.53 (c, 3H, SCH$_3$); 2.71 (2H, d, *J* = 7.2, CHC<u>H</u>$_2$); 3.00 (t, 2H, *J* = 7.5, 3-CH$_2$); 3.56 (t, 2H, *J* = 7.6, 1-CH$_2$); 4.75 (d, 2H, *J* = 5.9, NHC<u>H</u>$_2$); 7.23 (dd, 1H, *J* = 7.9, 4.9, 5-CH-C$_5$H$_4$N); 7.76 (dt, 1H, *J* = 7.8, 2.0, 6-CH-C$_5$H$_4$N); 8.15 (t, 1H, *J* = 5.9, NH); 8.40 (dd, 1H, *J* = 4.8, 2.0, 4-CH-C$_5$H$_4$N); 8.60 (t, 1H, *J* = 2.0, 2-CH-C$_5$H$_4$N).).

4-Isobutyl-9-(methylthio)-*N*-(2-phenylethyl)-2,3-dihydro-1*H*-cyclopenta[4',5']-pyrido[3',2':4,5]thieno[3,2-*d*]pyrimidin-7-amine (2t). Yield 85%; mp 83-85°C. Anal. Calcd for $C_{25}H_{28}N_4S_2$: C 66.93; H 6.29; N 12.49 %. Found: C 67.29; H 6.51; N 12.73 %. ^{1}H NMR δ, ppm, *Hz*: 0.99 (d, 6H, *J* = 6.7, CH(C<u>H</u>$_3$)$_2$); 2.15–2.33 (m, 3H, C<u>H</u>(CH$_3$)$_2$, 2-CH$_2$); 2.58 (c, 3H, SCH$_3$); 2.70 (d, 2H, *J* = 7.2, CHC<u>H</u>$_2$); 2.99 (t, 2H, *J* = 7.2, C<u>H</u>$_2$Ph); 3.03 (t, 2H, *J* = 7.5, 3-CH$_2$); 3.56 (t, 2H, *J* = 7.6, 1-CH$_2$); 3.69–3.81(m, 2H, NHC<u>H</u>$_2$); 7.10–7.31 (m, 5H, Ph); 7.55 (t, 1H, *J* = 5.7, NH).

***N*,*N*-Diethyl-4-isobutyl-9-(methylthio)-2,3-dihydro-1*H*-cyclopenta[4',5'] pyrido-[3',2':4,5]-thieno[3,2-*d*]pyrimidin-7-amine (2u).** Yield 81%; mp 121-123°C. Anal. Calcd for $C_{21}H_{28}N_4S_2$: C 62.96; H 7.04; N 13.99 %. Found: C 63.28; H 7.24; N 14.21 %. ^{1}H NMR δ, ppm, *Hz*: 0.98 (d, 6H, *J* = 6.7, CH(C<u>H</u>$_3$)$_2$); 1.35 (t, 6H, *J* = 7.0, (CH$_2$C<u>H</u>$_3$)$_2$); 2.15–2.33 (m, 3H, C<u>H</u>(CH$_3$)$_2$, 2-CH$_2$); 2.54 (s, 3H, SCH$_3$); 2.70 (d, 2H, *J* = 7.2, CHC<u>H</u>$_2$); 2.99 (t, 2H, *J* = 7.5, 3-CH$_2$); 3.57 (t, 2H, *J* = 7.6, 1-CH$_2$); 3.80 (q, 4H, *J* = 7.0, N(C<u>H</u>$_2$CH$_3$)$_2$).

2-[[4-Isobutyl-9-(methylthio)-2,3-dihydro-1*H*-cyclopenta[4',5']pyrido [3',2':4,5]-thieno[3,2-*d*]pyrimidin-7-yl](methyl)amino]ethanol (2v). Yield 88%; mp 144-146°C. Anal. Calcd for $C_{20}H_{26}N_4OS_2$: C 59.67; H 6.51; N 13.92%. Found: C 60.02; H 6.70; N 14.18 %. ^{1}H NMR δ, ppm, *Hz*: 0.98 (d, 6H, *J* = 6.7, CH(C<u>H</u>$_3$)$_2$); 2.15–2.33 (m, 3H, C<u>H</u>(CH$_3$)$_2$, 2-CH$_2$); 2.55 (s, 3H, SCH$_3$); 2.71 (2H, d, *J* = 7.2, CHC<u>H</u>$_2$); 2.99 (t, 2H, *J* = 7.5, 3-CH$_2$); 3.50 (s, 3H, NCH$_3$); 3.58 (t, 2H, *J* = 7.6, 1-CH$_2$); 3.71–3.78 (m, 2H, NHC<u>H</u>$_2$CH$_2$OH); 3.83–3.90 (m, 2H, NHCH$_2$C<u>H</u>$_2$OH); 4.56 (br, 1H, OH).

2-{Ethyl[4-isobutyl-9-(methylthio)-2,3-dihydro-1*H*-cyclopenta[4',5']pyrido-[3',2':4,5]thieno[3,2-*d*]pyrimidin-7-yl]amino}ethanol (2w). Yield 79%; mp 137-139°C. Anal. Calcd for $C_{21}H_{28}N_4OS_2$: C 60.54; H 6.77; N 13.45 %. Found: C 60.85; H 6.94; N 13.68 %. ^{1}H NMR δ, ppm, *Hz*: 0.98 (d, 6H, *J* = 6.7, CH(C<u>H</u>$_3$)$_2$); 1.30-1.41

(m, 3H, $CH_2C\underline{H}_3$); 2.15–2.33 (m, 3H, $C\underline{H}(CH_3)_2$, 2-CH_2); 2.55 (s, 3H, SCH_3); 2.71 (d, 2H, *J* = 7.2, $CHC\underline{H}_2$); 3.00 (t, 2H, *J* = 7.5, 3-CH_2); 3.58 (t, 2H, *J* = 7.6, 1-CH_2); 3.71-3.86 (m, 4H, $C\underline{H}_2C\underline{H}_2OH$); 3.91 (q, *J* = 7.0, 2H, $C\underline{H}_2CH_3$); 4.51 (br, 1H, OH).

Procedure for the synthesis of compound 4. To an ice-cold solution of compound **1** (2 *mmol*) in glacial acetic acid (35 *mL*), a solution of sodium nitrite (276 *mg*, 4 *mmol*, dissolved in the least amount of water) was added dropwise under stirring in an ice-bath at 5°C. The reaction mixture was maintained at room temperature for 12 *h*, and then water (50 *mL*) was added. The resulting crystals were filtered off, washed with water, dried, and recrystallized from a mixture of ethanol/dichloromethane (1:3).

7-Azido-4-isobutyl-9-(methylthio)-2,3-dihydro-1*H*-cyclopenta[4',5']pyrido-[3',2':4,5]thieno[3,2-*d*]pyrimidine/10-isobutyl-5-(methylthio)-8,9-dihydro-7*H*-cyclopenta-[4',5']pyrido[3',2':4,5]thieno[2,3-e]tetrazolo[1,5-*c*]pyrimidine (4A/T). Yield 88%; mp 148–149°C; IR ν/cm^{-1} ($CHCl_3$): 2155, 2138 (N_3). Anal. Calcd for $C_{17}H_{18}N_6S_2$: C 55.11; H 4.90; N 22.68 %. Found: C 54.79; H 5.08; N 22.92 %. ^{1}H NMR δ, ppm, *Hz*: 0.98 (d, 3.6H, *J* = 6.6, $CH(C\underline{H}_3)_2$);1.02 (d, 2.4H, *J* = 6.6, $CH(C\underline{H}_3)_2$); 2.21–2.38 (m, 3H, 8-CH_2 and $C\underline{H}(CH_3)_2$); 2.65 (s, 1.8H, SCH_3); 2.94 (s, 1.2H, SCH_3); 2.73 (d, 1.2H, *J* = 7.1, $CHC\underline{H}_2$); 2.77 (d, 0.8H, *J* = 7.1, $CHC\underline{H}_2$); 3.03 (t, 1.2H, *J* = 7.5, 9-CH_2); 3.08 (t, 0.8H, *J* = 7.5, 9-CH_2); 3.56 (t, 1.2H, *J* = 7.6, 7-CH_2); 3.64 (t, 0.8H, *J* = 7.6, 7-CH_2).

Procedure for the synthesis of compound 5. A mixture of compound **4** (1 *mmol*) and pyrrolidine (5 *mL*) was refluxed for 5 *h*. The reaction mixture was cooled, water (25 *mL*) was added, and the separated crystals were filtered off, washed with water, dried, and recrystallized from ethanol.

4-Isobutyl-7,9-dipyrrolidin-1-yl-2,3-dihydro-1*H*-cyclopenta[4',5']pyrido [3',2':4,5]-thieno[3,2-*d*]pyrimidine (5). Yield 73%; mp 218–220°C. ^{1}H NMR (δ, ppm, *Hz*: 0.98 (d, 6H, = 6.6, $CH(C\underline{H}_3)_2$); 1.95-2.00 (m, 4H, 2CH_2, C_4H_8N); 2.02-2.07 (m, 4H, 2CH_2, C_4H_8N); 2.14–2.30 (m, 3H, 2-CH_2, $C\underline{H}(CH_3)_2$); 2.68 (d, 2H, *J* = 7.1, $CHC\underline{H}_2$); 2.96 (t, 2H, *J* = 7.5, 3-CH_2); 3.56 (t, 2H, *J* = 7.6, 1-CH_2); 3.56-3.62 (m, 4H, $N(CH_2)_2$); 3.83-3.88 (m, 4H, $N(CH_2)_2$). ^{13}C NMR (75 MHz, DMSO/CCl_4, 1/3) δ: 22.2 (2CH_3); 24.2 (CH_2); 24.7 ($(CH_2)_2$); 25.0 ($(CH_2)_2$); 27.7 (CH); 29.8 (CH_2); 31.8 (CH_2); 44.1 (CH_2); 45.8 ($(NCH_2)_2$); 46.7 ($(NCH_2)_2$); 101.41; 134.2; 150.2; 155.9; 157.0; 158.1.

Procedure for the synthesis of compound 6. A mixture of compound **4** (1 *mmol*) and 2-aminoethanol or morpholine (5 *mL*) was refluxed for 5 *h*. The reaction mixture was cooled, water (50 *mL*) was added, and the separated crystals were filtered off, washed with water, dried, and recrystallized from ethanol. Yield 71%.

The physico-chemical data of obtained compound **4** in all aspects were identical with those of the same earlier synthesized compound and described in reference [9].

Procedure for the synthesis of compound 7. A mixture of compound **4** (370.5 *mg*, 1 *mmol*) and morpholine (2.2 *mmol*) in ethanol (10 *mL*) was refluxed for 15 *h*. The reaction mixture was cooled, water (25 *mL*) was added, and the separated crystals were filtered off, washed with water, dried, and recrystallized from ethanol.

7-Azido-4-isobutyl-9-morpholin-4-yl-2,3-dihydro-1*H*-cyclopenta[4',5']pyrido[3',2':4,5]thieno[3,2-*d*]pyrimidine (7). Yield 70%; mp 194–196 °C; IR ν/cm^{-1}: 2131 (N_3). Anal. Calcd for $C_{20}H_{23}N_7OS$: C 58.66; H 5.66; N 23.94 %. Found: C 58.39; H 5.81; N 23.73 %. ^{1}H NMR δ, ppm, *Hz*: 0.98 (d, 6H, *J* = 6.6, $CH(C\underline{H}_3)_2$); 2.19–2.33 (m, 3H, 2-CH_2, $C\underline{H}(CH_3)_2$); 2.70 (d, 2H, *J* = 7.1, $CHC\underline{H}_2$); 3.00 (t, 2H, *J* = 7.5, 3-CH_2); 3.51 (t, 2H, *J* = 7.6, 1-CH_2); 3.72-3.77 (m, 4H, $N(CH_2)_2$); 3.81-3.86 (m, 4H, $O(CH_2)_2$). ^{13}C NMR (75 MHz, DMSO/CCl_4, 1/3) δ: 22.2 ($2CH_3$); 24.0 (CH_2); 27.7 (CH); 29.7 (CH_2); 31.7 (CH_2); 40.0 ($N(CH_2)_2$); 44.4 (CH_2); 68.5 ($O(CH_2)_2$); 106.8; 121.4; 135.0; 150.5; 155.5; 159.0; 159.3; 159.4; 160.7.

9-(ՄԵԹԻԼԹԻՈ)ԹԻԵՆՈ[3,2-D]ՊԻՐԻՄԻԴԻՆԻ ՆՈՐ ԱՄԻՆՈԱԾԱՆՑՅԱԼՆԵՐԻ ՍԻՆԹԵԶԸ և ԱԶԻԴ-ՏԵՏՐԱԶՈԼԱՅԻՆ ՀԱՎԱՍԱՐԱԿՇՌՈՒԹՅՈՒՆԸ

Է. Կ. ՀԱԿՈԲՅԱՆ

Աշխատանքում նկարագրված է ցիկլոպենտա[4',5']պիրիդո[3',2':4,5]թիենո[3,2-d]պիրիմիդինի նոր ամինոածանցյալների սինթեզը համապատասխան 7-քլորթիենո[3,2-d]պիրիմիդինի հիման վրա: Ուսումնասիրված է ազիդ-տետրազոլային տաուտոմերիան 10-իզոբուտիլ-5-(մեթիլթիո)-8,9-դիհիդրո-7H-ցիկլոպենտա[4',5']պիրիդո[3',2':4,5] թիենո[2,3-e]տետրազոլո[1,5-c]պիրիմիդինում: Պարզվել է, որ եթե մեթիլթիո խմբի ներմուծումը պիրիմիդինային օղակ հավասարակշռությունը չեղում է դեպի ազիդային ձևը, իսկ ամինային խմբի ներմուծման դեպքում այն ամբողջովին տեղաշարժվում է դեպի ազիդային ձևը:

СИНТЕЗ НОВЫХ АМИНОПРОИЗВОДНЫХ 9-(МЕТИЛТИО)ТИЕНО[3,2-*d*] ПИРИМИДИНА И АЗИДО-ТЕТРАЗОЛЬНОЕ РАВНОВЕСИЕ

Э. К. АКОПЯН

В работе описан синтез новых 7-аминопроизводных циклопента[4',5']пиридо-[3',2':4,5]тиено[3,2-*d*]пиримидина на основе соответствующего 7-хлортиено[3,2-*d*]пиримидина. Исследована азидо-тетразольная таутомерия в 10-изобутил-5-(метилтио)-8,9-дигидро-7*H*-циклопента[4',5']пиридо[3',2':4,5]тиено[2,3-*e*]тетразоло[1,5-*c*]пиримидине. Выявлено, что, если введение метилтиогруппы в пиримидиновый цикл сдвигает равновесие в сторону азидной формы, то при введения аминогруппы равновесие полностью перемещается в сторону азидной формы.

REFERENCES

[1] *Litvinov V.P.* // Russ. Chem. Bull., 2005, v. 54, p. 864.

[2] *Taltavull J., Serrat J., Gracia J., Gavalda A., Andres M., Cordoba M., Miralpeix M., Vilella D., Beleta J., Ryder H., Pages L* // J. Med. Chem,, 2010, v. 53, p. 6912.

[3] *Reichelt C., Ludwig A., Schulze A., Daghish M., Leistner S., Krödel A., Heinicke J.* / US Patent 8,058,285 B2, 2011.

[4] *Shah T., Singh N., Goyal R., Dev A., Chhabria M., Shishoo C.* // Pharmacology Communications, 1995, v. 5, p 253.

[5] *Agarwal A., Louise-May S., Thanassi Jane A., Podos S. D., Cheng J., Thoma C., Liu C., Wiles J. A., Nelson D.M., Phadke A.S., Bradbury B.J., Deshpande M.S., Pucci M.J. //* Bioorg. Med. Chem. Lett., 2007, v. 17, p. 2807.

[6] *Deev S.L., Shenkarev Z.O., Shestakova T.S., Chupakhin O.N., Rusinov V.L., Arseniev A.S //* J. Org. Chem,, 2010, v.75, p.8487.

[7] *Abu-Eittah R.H., El-Kelany K.E* // Spectrochim. Acta A: Molecular and Biomolecular Spectroscopy, 2012, v. 99, p. 316.

[8] *Sirakanyan S.N., Spinelli D., Geronikaki A., Kartsev V.G., Panosyan H.A., Ayvazyan A.G., Tamazyan R.A., Frenna, V., Hovakimyan A. A//* Tetrahedron, 2016, v. 72, p.1919.

[9] *Sirakanyan S.N., Spinelli D., Geronikaki A., Kartsev V.G., Hakobyan E.K., Stepanyan H.M., Zuppiroli L., Hovakimyan A.A. //* Curr. Org. Chem., 2017, v. 21, № 13, p. 1227.

[10] *Lioux T., Gosselin G. Mathe Ch.* // Eur. J. Org. Chem,, 2003, p. 3997.

[11] *Lakshman M.K., Singh, M.K., Parrish D., Balachandran R., Day B.W.* // J. Org. Chem,, 2010, v. 75, p. 2461.

[12] *Mekheimer, R. A.*// J. Chem. Soc. Perkin Trans. 1, 1999, p. 2183.

[13] *Hirota K., Maruhashi K., Kitarnura N., Asao T., Senda Sh. //* J. Chem. Soc., Perkin Trans. 1 1984, p. 1719.

[14] *Stanovnik B., Tišler M.* // Tetrahedron, 1969, v. 25, p. 3313.

[15] *Abu-Zied Kh M., Gaafar A.M., Aly A.S. //* Phosphorus, Sulfur and Silicon, 2007, v. 182, p. 447.

ՀԱՅԱՍՏԱՆԻ ՀԱՆՐԱՊԵՏՈՒԹՅԱՆ ԳԻՏՈՒԹՅՈՒՆՆԵՐԻ
ԱԶԳԱՅԻՆ ԱԿԱԴԵՄԻԱ
НАЦИОНАЛЬНАЯ АКАДЕМИЯ НАУК РЕСПУБЛИКИ АРМЕНИЯ
NATIONAL ACADEMY OF SCIENCES OF THE REPUBLIC OF ARMENIA

Հայաստանի քիմիական հանդես
Химический журнал Армении **71, №4, 2018** Chemical Journal of Armenia

UDC 615.322:582.998.1

ROUND-LEAVED WINTEGREEN (PYROLA ROTUNDIFOLIA) AS A VALUABLE MEDICINAL PLANT RAW MATERIAL

S. A. DADAYAN[a,b], L. A. STEPANYAN[a], A. S. DADAYAN[a,b], M. B. GASOYAN[a], H. R. PETROSYAN[b], A. S. POGHOSYAN[a] and A. O. TSATURYAN[a,b]

[a]Scientific and Production Center "Armbiotechnology" NAS RA
14, Gyurjyan Str., 0056, Yerevan, Armenia
[b]Yerevan State University, Institute of Pharmacy
1, A. Manoukyan Str., Yerevan, 0025, Armenia
E-mail: slavik_dadayan@yahoo.com

The phytochemical and mineral composition of BAS of round-leaved wintergreen (Pyrola rotundifolia) growing in the Lori Region of Armenia has been studied. It is established that the plant extracts are rich in a wide range of pharmacologically active and antioxidant (AO) substances, in particular, arbutin, tannins, naphthoquinones, triterpenoids, organic acids, micro- and macroelements, etc. The plant extracts were found to contain 10 amino acids and 20 vital micro-and macroelements.

On the basis of the research carried out, extracts and broths of *round-leaved wintergreen* can be recommended as a source of amino acids, as well as a preventive and corrective agent when insufficiency or imbalance of macro- and microelements in tissue- and cellular structures in various pathological processes of the body. Extracts of wintergreen can be used as an environmentally friendly source of arbutin in urinary tract infections (UTI) and antioxidants against early aging.

Fig. 1, tables 3, references 18.

Phytotherapy is one of the most ancient sciences. Its history began more than six thousand years ago [1]. Already at the earliest stages of mankind development, herbs were not only a source of human nutrition, but also a remedy for the treatment of diseases. The mildness of the action of most plant preparations and the absence of toxic manifestations with their use (which is related to their naturalness, proximity to the human body) allow us to assume their significant importance in the prevention of various diseases. The undoubted merit of some species of medicinal plant raw materials is also the variety of biologically active substances that are capable of providing the polyvalence of pharmacological effects.

In modern life, it is impossible to avoid the development of various diseases including urological, the share of which is 10-12% in the total structure of morbidity of the world population [2]. Uncomplicated urinary tract infections are one of the most frequent diseases in women of reproductive age. According to statistics, annually 150 million cases of acute cystitis are registered in the world [3]. This high incidence testifies to the urgency and necessity of searching for safe, effective, side-effects free drugs to which phytotherapeutic means primarily belong.

In this regard, one of the promising plants is round-leaved wintergreen. The traditional areas of this plant spread are forests in the temperate zones of the Northern Hemisphere (from the Arctic to Mexico and the Himalayas). The plant grows well in the Russian Federation (Altai Territory) and Transcaucasian republics; specifically, as a wild plant it grows in the forest landscapes of the Lori Region. It is a perennial herb of the Pyroleae family with a long branched creeping rhizome, from the nodes of which additional roots and aboveground sprouts spread. Medicinal raw materials are the leaves of the wintergreen, its flowers, stem that contain a large amount of BAS (iridoids, tannin, phenol, naphthoquinone, triterpenoids, ericoline, chymaphylin), organic acids, micro- and macroelements, resins, essential oils, glycosides, etc.

It is known that the composition and properties of plant raw materials of the same biological species can vary significantly depending on the place of their growth, time of collection, methods of processing and other factors [4-7]. In this regard, prior to the use of this raw material for medicinal purposes, or as a source of AO, it is necessary to study the properties of extracts of plant raw materials growing in a given geographical area.

Hence, study of the qualitative and quantitative composition of biologically active substances (BAS) of round-leaved wintergreen growing in the Lori Region of Armenia is of great interest.

Purpose and objectives of the study. The purpose of the present study is investigation of the phytochemical composition of BAS of round-leaved wintergreen, which provides a wide range of pharmacological effects of the plant.

Experimental Part

Materials and methods

Collection and preparation of raw material. Raw material (leaves, stems and flowers of wintergreen) was collected in June-August 2017 in the forest landscapes in the vicinity of Vanadzor city, far from highways and settlements. The raw material was dried to an air-dry state in a drying chamber at 313*K*, packed in paper bags and stored at room temperature. To obtain the extract, the dried raw material was ground in a ceramic mortar to a powdery state (particle size ≤ 1 *mm*) and passed through a sieve with holes 1 *mm* in diameter.

Determination of moisture, ash content, extra active substances in the analyzed samples was carried out according to the standard procedures [8]. The results of studies are presented in Table 1.

The amino acid, macro-, microelement composition of the plant was studied, the amount of BAS of the phenolic origin (flavonoids, tannins arbutin, vitamin P, vitamin C) displaying the highest physiological and therapeutic activities was determined.

For quantitative determination of arbutin, 5 *g* (exact weight) of the crushed leaves of wintergreen was placed in a 100 *ml* flask, 50 *ml* of water was poured and the whole was boiled for 5 *min*. The extract was filtered into a 100 ml volumetric flask [9]. 25 ml of water was poured into the flask with raw material and boiled for 20 *min*, after which the extract was filtered into the same flask; the raw material was transferred to a filter and washed twice with 10 *ml* hot water, connecting the rinsing water to the filtrate. Then 3 *ml* of a solution of basic lead acetate was added to the extract, mixed and after cooling, was adjusted with water to a mark. The flask was placed in a boiling water bath until the precipitate was completely coagulated. The hot liquid was filtered into a dry flask. To remove the excess of the basic lead acetate, 0.8 *g* of sodium sulfate was added. The solution was filtered (solution A). 0.08 *g* of sodium sulfacyl was dissolved in 10 *ml* of water, 10 *ml* of 0.1*N* hydrochloric acid was added and the volume was adjusted to 100 *ml* (solution B). 2 *ml* of solution B, 2 *ml* of a 0.02% water solution of sodium nitrite were introduced into a test tube, left for 3 *min.* Then 0.5 *ml* of solution A, 0.04 *ml* of a 10% water solution of sodium hydroxide were added, the volume was adjusted to 6 *ml* with water and kept in a warm water bath for 1 *min.* After 20 *min*, the optical density was measured on a UV1800PC spectrophotometer at 490 *nm* wavelength.

The quantitative content of arbutin is calculated by the formula: X% = D x 0.938 x 6 x100/E x a x b, where D is the optical density of the test solution (D = 1.0501); 0.938 - conversion factor for anhydrous arbutin; 6 – total volume of the test solution, *ml*; 100 – volume of a volumetric flask, *ml*; E – specific absorption index of arbutin at a wavelength of 490 *nm*, equal to 221.5; a – weight of raw material (a = 0.5 *g*); b – extraction volume taken for analysis (b = 0.5 *g*).

The results are inserted in the formula:

$$X\%=1.0501\times0.938\times6\times100/22.5\times0.5\times0.5=10.67\%$$

For the quantitative analysis of flavonoids, anthocyanins, carotenoids, rutin, sugars, spectrophotometry methods were used [10-12]. The amount of vitamin C, carboxylic acids and tannins was determined by a titrimetric method [8]. The results are shown in Table 1.

Table 1

The quantitative content of biologically active substances in the extract of round-leaved wintergreen

Moisture,%	7.2
Extractive substances, %	28.59
Arbutin, *mg*%	10.67
Flavonoids, %	1.23
Anthocyanins, %	0.085
Rutin, *mg*%	22.59
Vitamin C, *mg*%	235.72
Carboxylic acids, %	2.35
Tannins, in terms of tannin, %	19.55
Water-soluble polysaccharides	11.25
Carotenoids, in terms of β-carotene, *mg* %	24.128

Determination of the elemental composition was carried out by atomic emission spectrometry with inductively coupled plasma, using the IRISIntrepid spectrometer (ThermoElectron, USA). The sample weights were preliminary held in a muffle furnace at 450-500^{o}C for 4 *h*. After cooling, the ash residue was treated twice with 5 *ml* of 6N HCL with slow evaporation in a water bath. The residue was dissolved by heating in 0.1N HCl and filtered off [13]. The content of chemical elements in the leaves of round-leaved wintergreen is shown in Table 2.

Table 2

The content of chemical elements in the samples of round-leaved wintergreen growing in the Lori Region (in *mg/kg* of absolutely dry raw material)

Macro-microelements	Certain indicators *mg* / *kg*	Macro-microelements	Certain indicators *mg* / *kg*
Fe	124.26	Mn	1.594
Cu	4.75	Co	<0.0047
Zn	8.05	Se	1.389
Ca	8857.4	Cd	0.052
Mg	8324.74	V	0.795
K	13158.3	Cr	0.596
Na	603.12	Ni	0.0413
Al	162.38	Pb	<0.0046
P	398.25	As	0.723
S	352.38	Si	211.02

Qualitative and quantitative analysis of free amino acids (Table 3 and Figure) was carried out using the amino acid analyzer Nexera X2 (Shimadzu, Japan).

Table 3

The content of free amino acids in hydrolysate of round-leaved wintergreen

Amino acids	L-Asp	L-Glu	L-Ser	L-His	Gly	L-Thr	L-Arg	L-Ala	L-Leu	L-Lys
Content of amino acids in terms of dry raw material *mg*/*g*	4.47	4.768	2.384	1.788	7.505	2.09	2.98	2.95	2.98	2.98

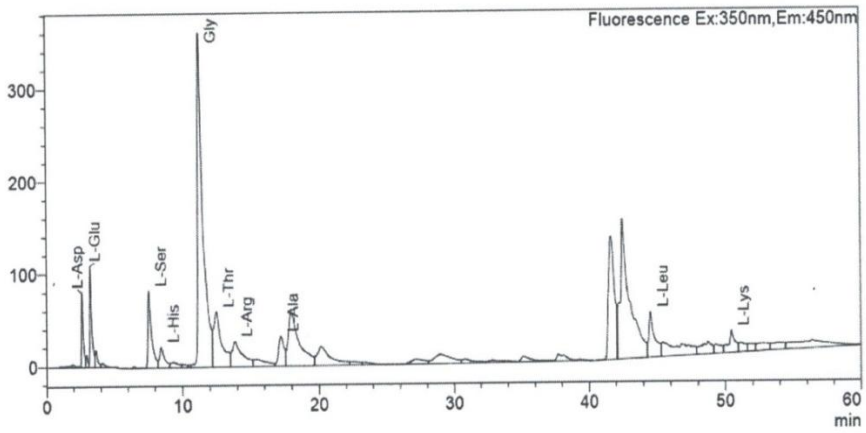

Fig. Chromatogram of free amino acids in the aboveground part of wintergreen.

The device sensitivity is 0.1 *μmol*. The calculation was carried out by comparing the peak areas of the samples under study with the peak areas of a standard amino acid mixture (Sigma, USA). Preparation of the test samples for amino acid analysis was performed as follows: a sample (5 *g*) of the herb dried at 60°C was placed in a 50 *ml* round-bottomed flask made of heat-resistant glass, 20 *ml* of *6N* HCl was added, the flask was closed with a stopper and fixed with a steel clamp. Hydrolysis of the dry sample was carried out in a vacuum drying chamber at 110°C for 22 *h*. After hydrolysis, the contents of the ampoule were cooled, filtered, evaporated and recrystallized from a solution of C_2H_5OH/H_2O = 1/1. After repeated filtration and drying, the amino acid mixture was dissolved in a citrate buffer pH 2.2 [14]. The content of free amino acids in the aboveground part of wintergreen is given in Table 3 and Figure.

To determine the antioxidant activity of wintergreen, to 1 *g* (exact weight) of the raw material 50 *ml* of 30% ethyl alcohol is poured and extracted with a reflux condenser for 30 *min*. Then, the contents of the flask are filtered through a paper filter, cooled and the volume of extraction is adjusted to 50 *ml* with 30% alcohol. 8 *ml* of freshly boiled and cooled distilled water, 1 *ml* of a 20% solution of sulfuric acid, 1 *ml* of 0.05 *N* solution of potassium permanganate are introduced into a 50 *ml* beaker. The whole is mixed and titrated with a 30% alcohol infusion of wintergreen

from a microburette (volume 1 *ml* with a fission rate of 0.01 *ml*) until the pink color disappears. For the control experiment, about 0.0500 *g* (exact weight) of quercetin (FS 42-1290-79) is dissolved in 40 *ml* of ethanol, transferred to a 100 *ml* volumetric flask, made up to the mark with alcohol and stirred. 8 *ml* of freshly boiled and cooled distilled water, 1 *ml* of a 20% solution of sulfuric acid, 1 *ml* of a 0.05 *N* solution of potassium permanganate are mixed into a 50 *ml* titration beaker. The whole is mixed and titrated from a microburette (volume 1 *ml* with a division value of 0.01 *ml*) with a quercetin solution until the disappearance of the pink color. 1 *ml* of a 0.05 *N* solution of potassium permanganate corresponds to 0.25 *mg* of quercetin.

The calculation of the indicator of the antioxidant activity (AOA, which corresponds to concentration of BAS of a reducing nature in terms of quercetin (in *mg/g*), is carried out according to the formula: $B=C_k x V_k x V_o/V_x x m$, where B is the concentation of BAS of the reducing nature of the object under study, used for titration of 1 *ml* of 0.05 *N* potassium permanganate solution, *mg/g*; C_k – the concentration of quercetin in the solution used for the titration of 1 *ml* of 0.05 *N* potassium permanganate solution, *mg/g* (0.5 *mg*/*ml*); V_k – the volume of quercetin solution, spent on titration of 1 *ml* of 0.05 *N* solution of potassium permanganate, *ml* (1.4 *ml*); V_o – the volume of the investigated solution, *ml* (50 *ml*); V_x – the volume of the solution of the object under study, spent on the titration of 1 *ml* of 0.05 *N* solution of potassium permanganate, *ml* (0.4 *ml*); m is the mass of the sample of the object under study, *g* (1*g*).

$$B = 0.5 \times 1.4 \times 50/0.4 \times 1 = 87.5 \ mg/g$$

Thus, the total amount of BAS of a reducing nature in terms of quercetin in 1 *ml* or 1 *g* of the drug was determined.

According to the results obtained, during the titration in the case of quercetin, the consumption was more (1.4 *ml*) than with the extract of wintergreen (0.4 *ml*), which indicates that the wintergreen extract can be treated as an effective preventive means against antioxidant aging of the body [15].

Results and discussion

The research results of the elemental composition of the leaves of round-leaved wintergreen show the availability of 20 elements. Round-leaved wintergreen contains vital macroelements (Na, K, Ca, Mg), essential (Fe, Cu, Zn, Mn, Cr, Se, Co) and conditionally essential microelements (As, Ni, Cd) that ensure proper operation of the main systems of the body (muscle – participate in the process of muscle contraction, digestive and cardio-vascular).

According to [16], the content of cadmium in plants collected in environmentally friendly growing areas is 0.05-0.3, arsenic 1.0-5/0 *mg/kg*. The excess content of mercury is considered to start from 1.0 *mg/kg*. On the whole, the level of concentrations of the investigated elements in the researched extracts of

round-leaved wintergreen is within the range of background values, which makes it possible to classify this plant as ecologically pure [17,18].

As a result of the performed study, 10 free amino acids were found in the hydrolysate (Table 2). The presence of such an amount of amino acids provides a wide range of pharmacological effect of this phytopreparation.

From Table 2 it follows that the content of glycin, which has a positive effect on the CNS, prevails in round-leaved wintergreen. The plant is also rich in glutamic and aspartic acids. Among the numerous functions of these acids, the most significant are the regenerating and immunomodulating with a simultaneous beneficial effect on the hormonal status of the body. As follows from Table 3, the leaves of wintergreen contain a lot of tannins, vitamin C, rutin that have a bactericidal, anti-inflammatory, antioxidant effect. From a medical point of view, arbutin is valuable. Arbutin has an antiseptic property; it is used in chronic kidney diseases and purulent inflammation of the bladder and urinary tract, in inflammation of the prostate gland, chronic pyelonephritis, cystitis, urolithiasis.

High antioxidant activity of wintergreen extracts can be explained by the fact that the investigated extracts contain multifunctional BAS with the presence of easily oxidizable functional groups (for example, -SH, $(CH_3)_2CH$-), which bind free radicals formed in living organisms relatively faster.

Thus, preliminary studies of round-leaved wintergreen (Pyrola rotundifolia) growing in forest landscapes of the Lori Region have shown that it contains various classes of biologically active substances ensuring a wide range of pharmacological effect of the plant: immunomodulating, anti-inflammatory, wound healing, antioxidant, etc.

ԿԼՈՐԱՎՈՒՆ ՏԱՆՁԱՏԵՐԵՎԸ ՈՐՊԵՍ ՀԵՌԱՆԿԱՐԱՅԻՆ ԴԵՂԱԲՈՒՍԱՅԻՆ ՀՈՒՄՔ

Ս. Ա. ԴԱԴԱՅԱՆ, Լ. Ա. ՍՏԵՓԱՆՅԱՆ, Ա. Ս. ԴԱԴԱՅԱՆ, Մ. Բ. ԳԱՍՈՅԱՆ, Ն. Ռ. ՊԵՏՐՈՍՅԱՆ, Ա. Ս. ՊՈՂՈՍՅԱՆ և Ա. Ն. ԾԱՏՈՒՐՅԱՆ

Հետազոտվել է Լոռու մարզում հավաքված կլորավուն տանձատերևից ստացված էքստրակտների (ԿԱՆ, ազատ ամինաթթուներ, հանքային տարրեր և այլն) ֆիտոքիմիական բաղադրությունն ու հանքային կազմը: Էքստրակտների թթվային հիդրոլիզատում հայտնաբերվել են սպիտակուցային ծագման 10 ազատ ամինաթթուներ, իսկ ատոմա-էմիսիոնային սպեկտրոմետրիայի եղանակով պարզվել է, որ բույսի վերգետնյա օրգաններում առկա են 20 հանքային տարրեր, որոնցից ծանր մետաղների (Co, Cd, Cr, V, Ni, Pb, As և այլն) պարունակությունը գտնվում են էկոլոգիապես մաքուր բուսահումքերի համար նախատեսված պահանջների կամ ղրանց ֆոնային արժեքների տիրույթում:

Հետազոտվել է նաև կլորավուն տանձատերևից ստացված թուրմերի և էքստրակտների հակաօքսիդանտային ակտիվությունը, համեմատելով այն հայտնի հակաօքսիդանտային նմուշի՝ կվերցետինի նույնանուն տվյալների հետ: Պարզվել է, որ Լոռու մարզի Վանաձորի տարատածաչրջանի սաղարթախիտ անտառների լանդշաֆտներից հավաքված կլորավուն տանձատերևի հակաօքսիդանտային ակտիվությունը մոտ 3 անգամ գերազանցում է հայտնի հակաօքսիդանտ կվերցետինի հատկությանը:

Ստացված արդյունքների հիման վրա հետազոտված կլորավուն տանձատերև բուսահումքը կարելի է առաջարկել, որպես օրգանիզմների հակաօքսիդանտային ծերացման դեմ պայքարի արդյունավետ կանխարգելման էկոլոգիապես մաքուր միջոց: Բուսահումքից պատրաստված թուրմերն ու էքստրակտները կարելի է կիրառել նաև մարդու օրգանիզմի տարբեր ախտաբանական պրոցեսների՝ հյուսվածքային և բջջային կառուցվածքներում առաջացող մակրո- և միկրոտարրերի անբավարարության կանխարգելման նպատակով:

Իսկ արքուտինի մեծ քանակության առկայությունը հնարավորություն է ընձեռում նաև այդ բուսահումքերի հալենային պատրաստուկներն օգտագործել նաև միզասեռական օրգանների բորբոքումների կանխարգելման նպատակով:

ГРУШАНКА КРУГЛОЛИСТНАЯ В КАЧЕСТВЕ ПЕРСПЕКТИВНОГО ЛЕКАРСТВЕННОГО СЫРЬЯ

С. А. ДАДАЯН[а,б], Л. А. СТЕПАНЯН[а], А. С. ДАДАЯН[а,б], М. Б. ГАСОЯН[а], А. Р. ПЕТРОСЯН[б], А. С. ПОГОСЯН[а] и А. О. ЦАТУРЯН[а,б]

Изучены фитохимический и минеральный составы экстрактов (БАВ, свободные аминокислоты, минеральные элементы и др.) грушанки круглолистной, собранной в Лорийском марзе Республики Армения.

В кислотном гидролизате экстрактов обнаружены 10 свободных белковых аминокислот. С помощью атомно-эмиссионной спектрофотометрии установлено, что в органах надземной части растения присутствуют 20 минеральных элементов, в том числе тяжелые металлы (Co, Cd, Cr, V, Ni, Pb, As и др.), содержание которых соответствует требованиям, предъявляемым к экологически чистым растениям, или находится в пределах фоновых значений.

Изучена также антиоксидантная активность настоев и экстрактов грушанки круглолистной по сравнению с аналогичными значениями известного антиоксиданта – кверцетина. Установлено, что антиоксидантная активность образцов ГРУшанки круглолистной, отобранных из ландшафтов густолиственных лесов в окрестностях г. Ванадзор Лорийского марза, почти в три раза превышает таковую кверцетина.

На основании полученных результатов исследований биомассу грушанки круглолистной можно рекомендовать в качестве эффективного антиоксидантного средства, предупреждающего преждевременное старение. Настои и экстракты растения также можно применять для профилактики и коррекции недостатка или дисбаланса макро- и микроэлементов в тканевых и клеточных структурах при различных патологических процессах в организме человека.

В тоже время присутствие в грушанке круглолистной большого количества арбутина позволяет использовать галеновые препараты растения в качестве противовоспалительного средства при заболеваниях мочеполовых органов.

REFERENCES

[1] *Карпеев А.А.* // Традиц. мед., 2012, № 2, с. 51.

[2] https://www.monographies.ru/ru/book/section?id=5665

[3] *Savas L, Guvel S, Onlen Y.* // West Indian Med., 2006, v. 55, p. 188.

[4] *Варданян Л.Р., Шутова А.Г., Айрапетян С.А., Варданян Р.Л., Агабеков В.Е., Решетников В.Н.* // Доклады АН Беларуси, 2013, т. 57, №5, с. 72.

[5] *Дмитриева Г.Ю.* Автореф. дисс «Влияние экологических факторов на содержание в растениях некоторых антиоксидантов» канд. биол. наук, Калининград, 2009, 25 с.
[6] *Zheng W.F., Liu T., Xiang X.Y., Gu Q.* // Acta pharmaceutica Sinica, 2007, v.42, №7, p. 750.
[7] *Liu C., Zhao C., Pan H.H., Kang J., Yu X.T., Wang H.Q., Li B.M., Xie Y.Z., Chen R.Y.* // J. of Natural Products, 2014, v.77, №1, p.35.
[8] ГОСТ 24027.2-80.
[9] Патент РФ RU2327145C2. //RU Grant 2008.
[10] Гост 4565-79.
[11] Гост13496.17-95.
[12] *Пермякова М.А.* / Молодежь и наука: сборник материалов X Юбилейной Всероссийской научно-технической конференции студентов, аспирантов и молодых ученых с международным участием, посвященной 80-летию образования Красноярского края, Красноярск, Сиб. федер. ун-т., 2014.
[13] *Хавезов И., Цалев Д.* Атомно-абсорбционный анализ. Л., Химия, 1983, 144 с.
[14] Практическая химия белка. / под ред. Дарбе А., М., Мир, 1989, 623 с.
[15] Патент РФ № 2170930. 2001.
[16] *Кабата-Пендиас А., Пендиас Х.* Микроэлементы в почвах и растениях. М., Мир. 1989, 440 с.
[17] *Кощеев А.К.* Дикорастущие съедобные растения в нашем питании. М., Пищевая промышленность, 1981, 256 с.
[18] *Мальгин М.А., Пузанов А.В., Ельчинникова О.А.* // Сиб. эколог. журн., 1995, с. 510.

ՀԱՅԱՍՏԱՆԻ ՀԱՆՐԱՊԵՏՈՒԹՅԱՆ ԳԻՏՈՒԹՅՈՒՆՆԵՐԻ
ԱԶԳԱՅԻՆ ԱԿԱԴԵՄԻԱ
НАЦИОНАЛЬНАЯ АКАДЕМИЯ НАУК РЕСПУБЛИКИ АРМЕНИЯ
NATIONAL ACADEMY OF SCIENCES OF THE REPUBLIC OF ARMENIA

Հայաստանի քիմիական հանդես
Химический журнал Армении **71, №4, 2018** Chemical Journal of Armenia

UDC 547.854

NEW THREE-DIMENSIONAL HETEROCYCLIC CLUSTER. BIS-BENZO[4′,5′]IMIDAZO[2′,1′: 6,1]PYRIDO[2,3-d]PYRIMIDINES, SYMMETRICALLY LINKED BY A TRIARYLMETHANE LINKER

Modern methodology for finding new compounds for introduction into medical and industrial chemistry implies, among other approaches, the synthesis of chemical compounds of a fundamentally new design. In this report, we describe the synthesis of substituted bis-benzo[[4′,5′]imidazo-[2′,1′:6,1]pyrido[2,3-d]pyrimidines, in which two tetracyclic skeletons are symmetrically linked by a triarylmethane linker.

The design of the synthesized large molecule has a unique three-dimensional structure (Fig.1), which makes it interesting in terms of studying the affinity for various biomolecules and photophysical, chelating properties, and can be used for detection of nitro-containing explosives and ecotoxins, as well as fluorescent biomarkers in biomedical investigations.

The synthesis was carried out according to the following Scheme:

Scheme

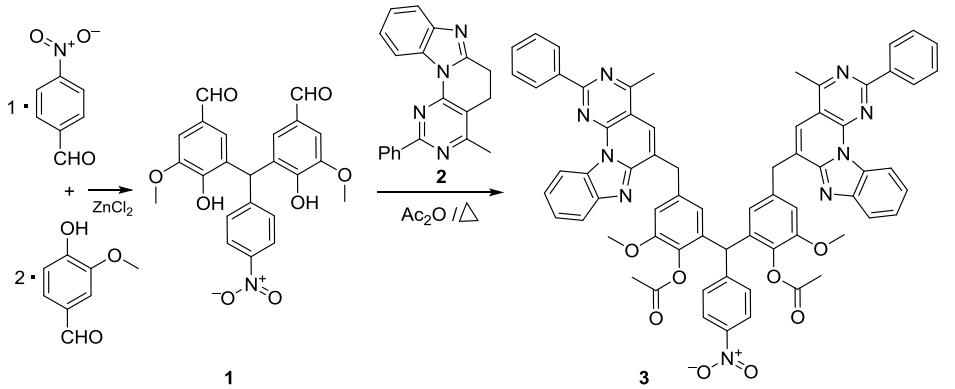

The initial dialdehyde of the triarylmethane series **1** was obtained by the interaction of 4-nitrobenzaldehyde and vanillin in a ratio of 1/2 in the presence of $ZnCl_2$ according to the method described in the literature [1]. However, in the cited work, the author was unable to establish the exact structure of the isomer of the synthesized compound, limiting himself only to the correct assignment of compound

1 to the triarylmethane derivative, in which aldehyde groups are present in the vanillin moiety.

We have established that two molecules of 4-hydroxy-3-methoxybenzaldehyde react on the carbonyl group of an electron-deficient 4-nitrobenzaldehyde (electrophile) in the presence of $ZnCl_2$ to form a single isomer in which the introduced group is in the *meta*-position to the formyl and *ortho*-position to the hydroxyl groups of the vanillin moiety. This is in accord with the orientation rule for substituents in the aromatic ring in the Friedel-Crafts reaction. Dialdehyde **1** is put into the interaction with 4-methyl-2-phenyl-5,6-dihydrobenzo[4',5']imidazo[2',1',6,1] pyrido-[2,3-d]pyrimidine (**2**) [2] in a molar ratio of 1/2 by boiling in acetic anhydride according to the previously described method [3] with the formation of bis-derivative **3**. As in the case of condensation of tetracycle **2** with aromatic and heterocyclic aldehydes in acetic anhydride [3] the reaction proceeds exclusively on the methylene group 6 of the heterocycle, followed by a 1,3-prototropic shift and the formation of 6-arylmethyl derivative **3**.

The structure of the synthesized compounds **1,3** was proved by ^{1}H NMR spectroscopy.

Visualization in the form of a ball and stick model, optimization of the three-dimensional structure and analysis of the geometry of the molecule (Figure) were carried out in the Chem3D 16.0 program, the ChemOffice software.

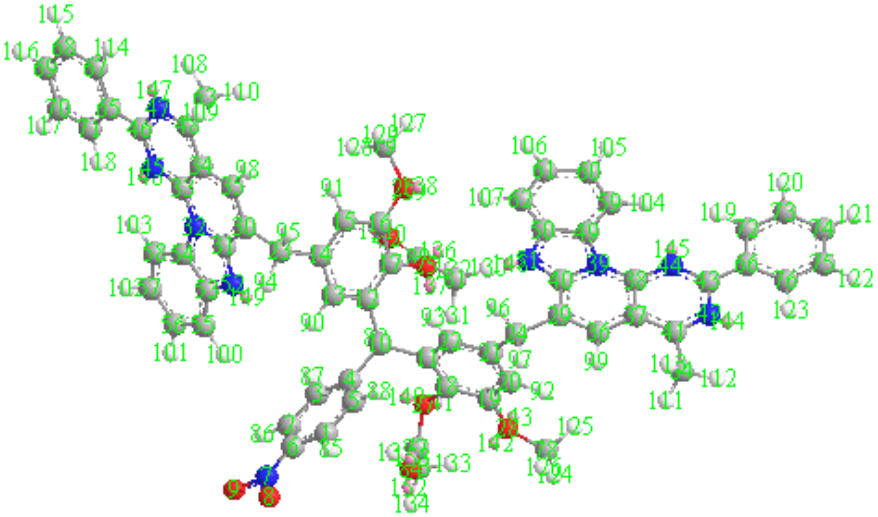

Figure. Ball and stick model of compound **3** after optimization of the three-dimensional structure.

The nearest contacts are presented only for hydrogen atoms: H(127)-Lp(152), H(112)-Lp(149), H(127)-H(135), N(74)-H(135), N(76) -H(131), N(76)-H(128), N(74)-H(127), N(50)-H(123), H(112)-H(119), N(52)-H(119), N(50)-H(117), N(52)-H(112), C(12)-H(93), C(35)-H(92), C(29)-H(91), C(4)-H(90), O(33)-H(89), C(3)-H(89), O(9)-H(86), O(8)-H(85).

The research was carried out at Russian–Armenian (Slavonic) University and supported by the funds allocated under the subsidy of the Ministry of Education and Science of the Russian Federation to finance research activities at Russian–Armenian (Slavonic) University, as well as with the financial support of the State Committee of Science of the Ministry of Education and Science of the Republic of Armenia within the framework of the scientific project No. 18T-1D249

Experimental part

The IR spectra were recorded on a Nicolet Avatar 330 spectrometer from samples dispersed in mineral oil. The ^{1}H NMR spectra were measured on a VarianMercury-300 spectrometer at 300 *MHz* using tetramethylsilan as internal reference. Thin-layer chromatography was performed on Silufol UV-254 plates in hexane – dichloroethane – ethanol / 1-1-1 system; spots were visualized by treatment with iodine vapor. Elemental analysis was carried out on an automated EA Eurovector elemental analyzer (Italy).

[(4-Nitrophenyl)-di-(2-hydroxy-3-methoxy-5-formylphenyl)]methane (1). Prepared according to the described method [1]. Yield 48%, mp 275-276°C from AcOH (lit. 276°C [1]), R_f 0.60. IR spectrum, ν, 3208 (OH), 1676 (CO), 1607, 1592 (C=C–C=N). ^{1}H NMR spectrum (DMSO-d_6 / CCl_4: 1/3), δ, ppm, *Hz*: 3.94 s (6H, OMe); 6.26 brs (1H, CH); 6.92 brd (2H, J = 1.8, H-6.6′ C_6H_3); 7.31-7.36 m (2H, H-2.6 C_6H_4); 7.33 d (2H, J = 1.8, H-2.2 ′ C_6H_3); 8.11-8.16 m (2H, H-3.5 C_6H_4); 9.63 s (2H, CHO); 9.67 br (2H, OH).

{(4-Nitrophenyl)-bis-[2-acetoxy-5-[(4-methyl-2-phenylbenzo[4′,5′]imidazo [1′,2′:1,6]-pyrido-[2,3-d]pyrimidin-6-yl)]methyl-3-methoxy]phenyl}methane (3). A solution of 1.18 *g* (0.005 *mol*) of dialdehyde **1** and 3.12 *g* (0.01 *mol*) of 4-methyl-2-phenylbenzo[4′,5′]imidazo[2′,1′: 6,1]-pyrido[2,3-d] -pyrimidine (**2**) in 40 *ml* of acetic anhydride was heated under reflux for 24 hours, evaporated to half the volume and left overnight in the cold. The precipitated product was filtered and dried. Yield 64.8%, yellow-green crystals, mp 320-322°C (DMF), R_f 0.75. IR spectrum, ν, $см^{-1}$: 1770, 1675 (CO), 1594 (C=C–C=N). ^{1}H NMR spectrum (DMSO-d_6), δ, ppm, *Hz*: 2.17 s (6H, 2 • Me); 2.24 brs (6H, 2 • Me); 3.54 brd (2H, J = 14.7 CH_2^a); 3.74 s (6H, 2 • Me); 4.02 d (2H, J = 14.7 CH_2^b); 5.85 s (1H, CH); 6.95 brs (2H, H-5); 7.15-7.20 m (4H, 2•$H^{2,6}$ C_6H_2); 7.25 ddd (2H, J = 8.2,7.3,1,1.0 C_6H_4);7.37-7.43 m (6H, Ar); 7.47-7.54 m (4H, Ar); 7.85 brd (2H, J = 8.0 C_6H_4); 8.04-8.08 m (4H, *ortho*-C_6H_5); 8.22-8.26 m (2H, C_6H_4NO2); 8.31 brd (2H, J = 8.2 C_6H_4). Found %, C 72.62; H 4.48; N 11.52. $C_{67}H_{51}N_9O_8$. Calculated,%: C 72.49; H 4.63; N 11.35.

ՆՈՐ ԵՌԱՉԱՓ ՀԵՏԵՐՈՑԻԿԼԱՅԻՆ ԽՐՉԻԿ. ԲԻՍ-ԲԵՆԶՕ[4', 5']ԻՄԻԴԱԶՕ[2',1':6, 1]ՊԻՐԻԴՈ[2,3-D]ՊԻՐԻՄԻԴԻՆ՝ ՀԱՄԱՉԱՓՈՐԵՆ ԿԱՊՎԱԾ ԵՌԱՐԻԼՄԵԹԱՆԱՅԻՆ ԿԱՄՐՋԱԿՈՎ

Ա. Ա. ՀԱՐՈՒԹՅՈՒՆՅԱՆ, Հ. Ա. ՓԱՆՈՍՅԱՆ, Գ. Տ. ՂՈՒԿԱՍՅԱՆ և Գ. Հ. ԴԱՆԱԳՈՒԼՅԱՆ

4-Նիտրոբենզալդեհիդի և 4-հիդրօքսի-3-մեթօքսիբենզալդեհիդի կոնդենսման արդյունքում սինթեզված [(4-նիտրոֆենիլ)-դի-(2-հիդրօքսի-3-մեթօքսի-5-ֆորմիլ)]մեթանը փոխազդեցության մեջ է դրվել 4-մեթիլ-2-ֆենիլ-5,6-դեհիդրոբենզո[4',5']-իմիդազո [2',1',6,1]պիրիդո[2,3-d]պիրիմիդինի հետ և ստացվել է ((4-նիտրոֆենիլ)-բիս-[2-ացետօքսի-5-[(4-մեթիլ-2-ֆենիլբենզո[4',5']իմիդազո[1',2':1,6]-պիրիդո[2,3-d]պիրիմիդին-6-իլ)]մեթիլ-3-մեթօքսի]ֆենիլ)մեթան: Սինթեզված միացությունների կառուցվածքը հաստատվել է ՄՄՊ 1H սպեկրալ եղակով:

СИНТЕЗ БИС-БЕНЗО[4 ', 5']ИМИДАЗО[2 ', 1': 6, 1]ПИРИДО[2,3-d]ПИРИМИДИНА, СИММЕТРИЧНО ПОДКЛЮЧЕННОГО ЧЕРЕЗ ТРИАРИЛМЕТАНОВЫЙ ЛИНКЕР

А. А. АРУТЮНЯН, Г. А. ПАНОСЯН, Г. Т. ГУКАСЯН и Г. Г. ДАНАГУЛЯН

Конденсацией 4-нитробензальдегида с 4-гидрокси-3-метоксибензальдегидом синтезирован 4-нитрофенилметил-3,3’-бис(4-гидрокси-5-метоксибензальдегид), взаимодействием которого с 4-метил-2-фенил-5,6-дигидробензо[4',5']имидазо [2',1',6,1]пиридо[2,3-d]пиримидином получен бис-бензо[4′,5′]имидазо[2′,1′: 6,1] пиридо[2,3-d]пиримидин. Строение синтезированных соединений подтверждено ЯМР ^{1}H спектроскопией.

REFERENCES

[1] *Rogoff M* .// Ber., 1902, v. 35, p. 1961.
[2] *Harutyunyan A.A* .// Chem. J. Armenia, 2012, v. 65, №2, p. 257.
[3] *Harutyunyan A.A., Ghukasyan G.T., Danagulyan G.G.* // International Conference “100 Years of Development of Chemistry: From Synthesis of Polyethylene to Stereodivergence». May 16–18, 2018, Perm, Russia, p. 69.

[1] Russian-Armenian (Slavonic) University
[2] The Scientific Technological Center of Organic and Pharmaceutical Chemistry NAS RA[2]
26, Azatutyan Str., Yerevan, 0014, Armenia.
E-mail: harutyunyan.arthur@yahoo.com

A. A. HARUTYUNYAN [1,2]
H. A. PANOSYAN [2]
G. T. GHUKASYAN [1,2]
G. G. DANAGULYAN [1,2]

ANNUAL INDEX OF AUTHORS

Вниманию авторов!

Подробную информацию о ***«Химическом журнале Армении»,*** *содержание номеров журнала в графической форме и аннотации статей, годовые авторские указатели, а также развернутые правила для авторов можно получить в сети Интернет по адресу:* ***http://chemjournal.sci.am*** *и* ***www.flib.sci.am***

ПРАВИЛА ДЛЯ АВТОРОВ

Общие положения

К публикации **в «*Химическом журнале Армении*»** принимаются материалы, содержащие результаты оригинальных исследований, оформленные в виде **полных статей, кратких сообщений и писем в редакцию.**

Журнал публикует работы **по всем направлениям химической науки**, в том числе по общей и неорганической химии, физической химии и химической физике, органической химии, металлоорганической и координационной химии, химии полимеров, химии природных соединений, биоорганической химии и химии материалов.

Статьи, предлагаемые к публикации в разделе биоорганической химии, должны быть посвящены получению новых потенциально биологически активных соединений, в том числе и выделенных из природных объектов. **При описании новых веществ, обладающих значительной (в сравнении с применяемыми в медицине лекарствами) биологической активностью,** статья может содержать результаты биологических исследований, включающие ссылки на использованные методы изучения биологической активности, информацию о типе использованных биообъектов, активности и токсичности синтезированных препаратов в сопоставлении с соответствующими показателями применяемых в медицине лекарств.

В заключении следует привести краткий аргументированный вывод о связи между структурой и биологической активностью исследованных соединений. Опубликованные материалы, а также материалы, представленные для публикации в других журналах, к рассмотрению не принимаются.

Авторские обзоры должны представлять собой обобщение и анализ результатов цикла работ одного или нескольких авторов по единой тематике.

Полные статьи принимаются объемом до 12 страниц, объем **краткого сообщения** — не более 5 страниц машинописного текста. **Письма в редакцию** должны содержать изложенные в краткой форме научные результаты принципиально важного характера, требующие срочной публикации. Редакция оставляет за собой право сокращать статьи независимо от их объема.

Для публикации статьи авторам необходимо представить в редакцию следующие материалы и **документы:**

1) направление от организации (в 1 экз.);

2) экспертное заключение (для граждан РА) (в 1 экз.);

3) подписанный всеми авторами текст статьи, включая аннотацию, таблицы, рисунки и подписи к ним (все в 2-х экз.);

4) графический реферат (в 2-х экз.);

Статья должна быть написана сжато, аккуратно оформлена и тщательно отредактирована. Не допускается дублирование одних и тех же данных в таблицах, в схемах и рисунках.

Автор несет полную ответственность за достоверность экспериментальных данных, приводимых в статье.

Все статьи, направляемые в редакцию, подвергаются рецензированию и научному редактированию.

Статья, направленная авторам на доработку, должна быть возвращена в исправленном виде **вместе с ее первоначальным вариантом** в максимально короткие сроки. К переработанной рукописи необходимо приложить **письмо от авторов**, содержащее ответы на все замечания и комментарии и поясняющее все внесенные изменения**. Статья, задержанная на**

исправлении более двух месяцев или требующая повторной переработки, рассматривается как вновь поступившая.

Редакция посылает автору перед набором для проверки отредактированный экземпляр статьи и корректуру.

Структура публикаций

Публикация **обзоров, полных статей и кратких сообщений** начинается с индекса УДК, затем следуют заглавие статьи, инициалы и фамилии авторов, развернутые названия научных учреждений, полные почтовые адреса с индексами почтовых отделений, номера факсов и адреса электронной почты. Далее приводится краткая аннотация (не более 20 строк) с указанием конкретных результатов работы и вытекающих из них выводов.

В статьях **теоретического и физико-химического характера** приводятся сжатое введение в проблему и постановка задачи исследования, экспериментальная или методическая часть, обсуждение полученных результатов с **заключением**, а в статьях, **посвященных синтезу**, — общая часть (введение и задача исследования), обсуждение полученных результатов с **заключением** и экспериментальная часть. Рисунки с подрисуночными подписями и таблицы могут быть введены в текст. В **письмах в редакцию** аннотация на русском языке не приводится и разбивка на разделы не требуется; даются индекс УДК, название статьи, инициалы и фамилии авторов, название научных учреждений и их адреса, резюме на армянском и английском языках.

Графический реферат прилагается на отдельной странице (120×55 мм) и представляет собой **информативную иллюстрацию** (ключевую схему, структуру соединения, уравнение реакции, график и т.п.), отражающую суть статьи в **графическом** виде. Текст в графическом реферате допускается только в случае крайней необходимости, при этом следует избегать дублирования названия статьи и текста аннотации.

При несоблюдении указанных выше правил статья не принимается к публикации.

Пример оформления заглавия статьи, списка авторов, адресов учреждений, аннотации.

УДК.....

АСИММЕТРИЧЕСКИЙ СИНТЕЗ β-ГЕТЕРОЦИКЛИЧЕСКИ ЗАМЕЩЕННЫХ L-α-АМИНОКИСЛОТ

А. С. Сагиян,[а] Ю. Н. Белоконь[б] и К. Фишер [в]

[а] Ереванский государственный университет
Армения, 0025, Ереван, ул. А. Манукяна, 1
Факс: (374-10)559355 E-mail:sagysu@netsys.am
[б] Институт элементоорганических соединений
им. А. Н. Несмеянова Российской академии наук
Российская Федерация, 119991, Москва, ул. Вавилова, 28
Факс: (495) 135 6549. E-mail: yubel@ineos.ac.ru
[в] Институт органического катализа IFOK Университета г. Росток
Германия, Росток, Д-180055, Бухбиндер штрассе, 5-6
Факс: E-mail:

Разработан новый эффективный метод асимметрического синтеза β-гетероциклически замещенных L-α-аминокислот посредством присоединения 3-амино-1,2,4-тиадиазола и 5-меркапто-1,2,4-триазолов, содержащих различные заместители в положениях 3 и 4, к C=C связи Ni(II) комплекса с основанием Шиффа дегидроаланина и (S)-2-N-(N'-бензилпролил)аминобензофенона.

Примеры оформления графических рефератов

О взаимодействии N-алкилиминов с ацетоуксусным эфиром

М. С. Саргсян
С. С. Айоцян
А. Х. Хачатрян
А. Э. Бадасян
С. Г. Конькова

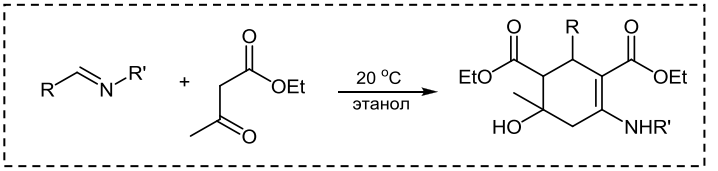

Хим. ж. Армении, 2011, т. 64, №4, с. 511

Кинетика высокотемпературного азотирования тантала в изотермических условиях

Ц. А. Адамян
Е. Н. Степанян
А. А. Чатилян
С. Л. Харатян

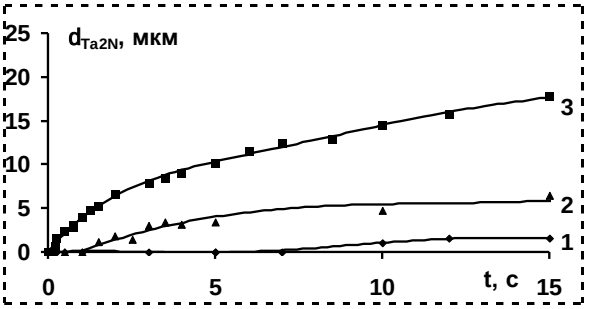

Хим. ж. Армении, 2011, т. 64, №3, с. 316

Оформление статей в «Химическом журнале Армении»

Текст статьи печатается **через 1.5 интервала** (без помарок и вставок) на белой бумаге стандартного размера (формат А4) с полями 3 см с левой стороны, 1.5 см с правой стороны, 2.5 см сверху, 2.5 см снизу, **размер шрифта — 12**.

Все страницы рукописи, включая список литературы и графический реферат, нумеруются.

Уравнения, схемы, таблицы, рисунки и ссылки на литературу нумеруются **в порядке их упоминания в тексте**.

Список цитируемой литературы должен включать ссылки на наиболее существенные работы по теме статьи. В тексте статьи должны быть упомянуты **все ссылки**, приведенные в списке литературы. В тексте **ссылки** на литературу даются в квадратных скобках и нумеруются **строго в порядке их упоминания**. Список литературы печатается на отдельной странице с указанием инициалов и фамилий **всех авторов**.

Список литературы должен быть оформлен следующим образом:

Книги: *Бучаченко А.Л., Вассерман А.М.* Стабильные радикалы. М., Химия, 1973, 58 с.

Статьи в сборниках: Ола *Дж., Фарук О., Пракаш Дж. К.С.* в кн: Активация и каталитические реакции алканов / под ред. К.М.Хилла. М., Наука, 1992, с. 39.

При цитировании переводных изданий после выходных данных русскоязычной версии в квадратных скобках необходимо указать выходные данные оригинального издания. Например: *Внутреннее вращение молекул.*/ под ред. В.Д.Орвилл-Томаса. М., Мир, 1974, 374 с. [*Internal Rotation in Molecules*, Ed. W. J. Orville-Thomas, Wiley, New York, 1974, 329 pp.].

Журналы: *Gal´pern E.G., Stankevich I.V., Chistyakov A.L., Chernozatonskii L.A.* // Chem. Phys. Lett., 1997, v.269, p.85.

При цитировании русскоязычного журнала, переводимого за рубежом, необходимо приводить ссылку и на англоязычную версию. Например: Лайков Д. Н., Устынюк Ю. А.// *Изв. АН, Сер. хим.,* 2005, с.804 [*Russ. Chem. Bull., Int. Ed.*, 2005, 54, 820].

Патенты: А.с. 9854 СССР // *Б.И.*, 1978, 61. или: US Pat. 55973 // *Chem. Abstrs*., 1982, **97**, 150732.

Диссертации: Ковалев Б.Г. Автореф. дисс. «....» доктора хим. наук. Город, институт, год, стр.

Программы: Sheldrick G. M., *SHELXL93, Program for the Refinement of Crystal Structure*, Göttingen University, Göttingen (Germany), 1993.

Банки данных: *Cambridge Structural Database System, Version 5.17*, 1999.

Ссылки на неопубликованные результаты и частные сообщения даются исключительно в виде сносок, а в списке литературы не приводятся и не нумеруются. При цитировании неопубликованных работ и частных сообщений необходимо представить разрешение от лица, на чьи данные приводится ссылка.

Памятка для авторов

Для максимального **сокращения сроков публикации** редакция просит авторов обратить особое внимание на **оформление статьи**.

Общие положения

Материалы, представляемые в редакцию:

 фамилия, имя, отчество и координаты лица, с которым редакция должна вести переписку (почтовый адрес, номер телефона, номер факса, адрес электронной почты). Фамилия автора, ответственного за переписку, должна быть отмечена звездочкой.

 направление от организации

 экспертное заключение (для граждан РА)

 текст статьи, аннотации на русском, английском и армянском языках на отдельных страницах (либо в тексте), рисунки и таблицы (все в 2 экз.)

 графический реферат

 последовательность расположения частей статьи (кроме писем в редакцию):

 индекс УДК

 название статьи

 автор(ы)

 развернутое название научной организации

 почтовый адрес с индексом

 факс

 адрес электронной почты

 аннотация

 собственно текст статьи

 введение

 постановка задачи

для статей физико-химической тематики:

 экспериментальная часть

 обсуждение полученных результатов с заключением

для статей, посвященных синтезу:

 обсуждение полученных результатов с заключением

 экспериментальная часть

 благодарности

 список литературы

В экспериментальной части должны быть представлены **доказательства строения и чистоты** всех новых соединений, источники использованных **нетривиальных реагентов** или **методики их получения**, а также условия **дополнительной** подготовки реагентов и растворителей.

Для всех синтезированных соединений следует дать **названия по номенклатуре** IUPAC. Металлоорганические комплексы могут быть названы по системе *Chemical Abstracts*.

Все **таблицы**, **схемы**, **рисунки**, **соединения и ссылки на литературу** должны нумероваться строго в порядке упоминания в тексте.

На осях графиков должны быть указаны **наименования** и **единицы измерения** соответствующих величин.

Рисунки спектров не должны быть выполнены от руки.

Все используемые **аббревиатуры** и **сокращения** должны соответствовать приведенному в Правилах для авторов списку или расшифровываться при первом упоминании.

Данные рентгеноструктурного исследования следует представлять в виде рисунка(ков) молекулы (с пронумерованными атомами) или кристаллической упаковки и таблиц, содержащих **необходимые** геометрические характеристики молекул (**основные** длины связей, валентные и торсионные углы).

Для основного текста статьи обязательно использование шрифта Unicode, желательно Times New Roman, для греческих букв — шрифт Symbol.

Символы переменных физических величин (например, температура — *T*), единицы их измерения (K), стереохимические дескрипторы (*цис*, *Z*, *R*), локанты (*N*-метил), буквенные (но не цифровые) символы при обозначении групп симметрии должны быть напечатаны *курсивом* (*C2v*, но не *C2v*).

В списке литературы должны использоваться только стандартные сокращения названий журналов.

CONTENTS

ԲՈՎԱՆԴԱԿՈՒԹՅՈՒՆ

СОДЕРЖАНИЕ